

Investigations into the Mechanical Properties of Insect Cuticle

Eoin E. Parle

B.A.I., B.A.



A thesis submitted to the University of Dublin in partial fulfilment of the requirements for the
degree of

Doctor of Philosophy

in

Mechanical and Manufacturing Engineering

September 30th 2015

Supervised by Professor David Taylor

Declaration

I declare that this thesis has not been submitted as an exercise for a degree at this or any other university and it is entirely my own work unless otherwise indicated.

I agree to deposit this thesis in the University's open access institutional repository or allow the library to do so on my behalf, subject to Irish Copyright Legislation and Trinity College Library conditions of use and acknowledgement.

A handwritten signature in blue ink that reads "Eoin Parle". The signature is written in a cursive style with a blue highlight effect.

Eoin Parle

September 30th, 2015

Acknowledgements

I would like to thank my supervisor Professor David Taylor for offering me the opportunity to undertake this Ph.D. Throughout the past three years he always took the time to provide me with his expertise, experience, knowledge and assistance. I have learned much from him over the last three years that will hopefully stand me in good stead in the future for a fruitful research career.

I would also like to thank Dr. Jan-Henning Dirks for his expert assistance and advice on all things biological. He has been a source of inspiration for me during my first three years in academia, and continues to be a source of knowledge and assistance whenever needed.

Peter O'Reilly's assistance in the use of the machines in the workshop and the lab, and advice on the design and manufacture of the miniature rigs necessary for conducting my tests is greatly appreciated. Likewise the speedy manufacture and delivery of these rigs from Mick Reilly, Sean, JJ and Gabriel was very helpful.

Thank you to students Hannah Larmon, Simona Herbaj, and Fiona Sheils for their assistance in carrying out portions of the testing under my supervision.

The zoology department – namely Peter Stafford, Martyn Linnie and Alison Boyce deserve many thanks for allowing me to house and rear my insects in the basement of their facility.

Thanks also to all staff in the Centre for Microscopy Analysis (CMA) Heath Bagshaw, Neal Leddy, and especially Clodagh Dooley who has helped out enormously on all things microscopy related.

On a personal note, I would like to thank my wife Olivia for her constant support, patience, reassurance and enthusiasm over the course of this Ph.D. and indeed, in everything I do. Without her, this Ph.D. would never have been completed on time. Thanks also to my son John-Luc for being such a great source of enjoyment, perspective and motivation over the last 8 months.

Many thanks also to my parents John and Bernadette for their unfailing support, interest and encouragement over the years, especially to my mam for her proofreading, and likewise to my brothers Cormac and Padraig for all of their assistance in proofreading my Ph.D. thesis. I hope I can return the favour someday!

Summary

Insect cuticle is a composite material comprised of chitin fibres embedded in a protein matrix. It performs a wide variety of functions across class Insecta, and as such displays a wide bandwidth of material properties. This is achieved by varying the amounts and orientations of the fibres, the constituents of the proteins, and their degree of cross-linking and hydration. Many previous studies into the mechanical properties of insect cuticle have focussed on the insect tibia and have characterised such properties as strength, toughness, hardness, stiffness and fatigue. This Ph.D. builds on previous work by investigating how various tibia properties such as its geometry, its strength, stiffness and failure mode can be influenced by a number of different factors. I have examined insect cuticle from a fracture mechanics and material science point of view. In all studies, a cantilever bending load was applied to tibiae to replicate bending forces experienced *in vivo*. A sensitive 5 N load cell recorded applied force, and tibia dimensions were analysed using SEM photographs. From these reliable, repeatable calculations for stress, strain and stiffness were obtained.

When investigating how biomechanical factors have influenced the adaptation of tibia cuticle in several different insect tibiae, I found that they must endure higher forces during emergency behaviour than during normal locomotion such as walking and running. Comparing the failure strengths of each leg with the stresses endured *in vivo* allowed me to estimate safety factors for each leg. These were relatively high (6 – 7) for normal locomotion, but much lower (1.5 – 4) for more strenuous activities. This implies that the legs operate close to their structural limit during such activities.

I also found that the age of the adult locust can have a profound effect on the tibia properties. Its thickness increases at a rate of 1.8 μm / day for the first 20 days (approx.) after moulting, after which cuticle deposition rates reduce to approx. 0.4 μm / day. This is accompanied by a rapid increase in strength and stiffness over the same time period, after which both properties remain relatively constant. After moulting, and when the cuticle is thin (high radius / thickness ratio), the

legs are inclined to fail by local buckling. This in itself is an incentive to grow thicker and become stiffer. Once the cuticle reaches a certain thickness, buckling is no longer the primary failure mode (as shown by the predictive calculations). The legs will now fail due to material failure (fracture / yielding). This is not a failure mode that can be avoided by the addition of more material, hence the significant decrease in deposition rate after this point.

I have examined the phenomenon of local elastic buckling of the tibiae of several insect species including the desert locust hind-leg and mid-leg, the American and Death's head cockroaches, the stick insect and the bumblebee using predictive equations from the literature and FE modelling. I found that such predictions matched my experimental results closely, implying that this type of analysis could prove useful for predicting failures of other insect tibiae in the future, or indeed thin-walled tubular structures of any kind – including those with a non-circular cross-section, or with specialisations such as ridges or fins seen on the stick insect.

When examining how the insect responds to injury, I discovered the importance of the deposition of new cuticle underneath an incision in the repair process. This helps to reinforce the tibia structure, and restore its strength to acceptable levels. A tibia showing repair recovered on average 66% of its original pre-injury strength compared to the corresponding value of 33% for an injured leg showing no repair. This patch of new cuticle is also vital in preventing cracks from growing from the injury. I have confirmed that the deposition of new cuticle in response to injury is targeted to the injury site, and that the rate of deposition here closely matches that seen immediately post-moult. Deposition rates in other areas (including beside the injury) remained at normal levels for a mature adult – implying that the injury itself is a stimulus for the local resurrection of the accelerated growth rate observed after moulting.

I also examined how the insect responds to minor or material level damage. I observed how the living cuticle can recover completely from high stress cyclic loading, regaining its stiffness completely, and showing no difference in failure strength or stiffness to legs (from the same insects) which had not been cycled. Tibiae removed from the insect showed no such recovery,

implying that the processes at work may be governed by the living cells of the insect as opposed to being a passive material phenomenon.

I have detailed all of the above in this thesis, and have proposed possible theories explaining the behaviours observed. The more studies carried out on this interesting material, the more thought-provoking results are discovered. I believe that this thesis has shed some light on various factors that influence the mechanical properties of insect cuticle, and together with previous work, goes some way to building a more complete understanding of this versatile material.

Table of Contents

Declaration.....	i
Acknowledgements.....	ii
Summary.....	iii
List of Figures.....	x
List of Tables.....	xiii
Publications and Presentations	xiv
Chapter 1: Introduction.....	1
1.1 Insects	1
1.2 Cuticle.....	2
1.2.1 Microstructure	4
1.2.2 Layers within the Cuticle.....	6
1.2.3 Epidermis, Basement Membrane and Hemolymph.....	9
1.2.4 Pore Canals	9
1.2.5 Proteins.....	11
1.2.6 Sclerotization.....	11
1.3 Moulting and Growth	12
1.3.1 Cuticle Growth.....	15
1.4 Function	16
1.4.1 Sensory Capabilities of the Tibia	20
1.5 Mechanical Properties.....	21
1.6 Composite Materials	24
1.6.1 Failure of composites	28
1.7 Failure of Tubes	29
1.8 Biomechanics.....	34
1.8.1 Walking and Running	34
1.8.2 Forces	35
1.8.3 Jumping	36
1.9 Insect Wound Healing Response	39
1.9.1 How does the insect's immune system work?	40
1.9.2 Coagulation.....	41
1.9.3 Melanization	41
1.9.4 Cell Migration	43
1.9.5 Summary.....	45

1.9.6	Mammal wound healing response	46
1.9.7	Similarities.....	47
1.9.8	Differences.....	47
1.9.9	Comments on Injury Response	48
1.10	Bone Adaptation.....	48
1.11	Summary and Conclusions	50
Chapter 2: Objectives and Methods		52
2.1	Objectives of this thesis.....	52
2.2	Materials, Methods and Calculations.....	55
2.2.1	Insects.....	55
2.2.2	The Tibia	56
2.2.3	Experimental Procedure.....	56
2.2.4	Measurements	59
2.2.5	Calculations.....	59
2.2.6	Assumptions.....	62
Chapter 3: Biomechanical factors in the adaptations of insect tibia cuticle		66
3.1	Abstract.....	66
3.2	Introduction	66
3.3	Materials & Methods	69
3.3.1	Insects.....	69
3.3.2	Mechanical Testing, Measurements and Calculations	69
3.3.3	Statistics.....	71
3.3.4	Biomechanics.....	71
3.4	Results.....	75
3.4.1	Mechanical Properties.....	76
3.4.2	Biomechanics.....	77
3.4.3	Factor of Safety.....	78
3.5	Discussion.....	79
3.6	Conclusion	85
Chapter 4: Buckling failures in insect exoskeletons		86
4.1	Abstract.....	86
4.2	Introduction	86
4.3	Methods	87
4.4	Results.....	90
4.4.1	Buckling Predictions	92
4.5	Discussion.....	97
4.6	Conclusions	101

Chapter 5: Cuticle growth rates: their purpose and effect on tibia structural properties in the desert locust.....	102
5.1 Abstract.....	102
5.2 Introduction	103
5.3 Materials And Methods.....	104
5.4 Experimental Procedure.....	104
5.5 Results.....	105
5.6 Discussion.....	109
5.6.1 Purpose for deposition.....	117
5.6.2 Stimulus for deposition	118
5.7 Conclusions	121
5.8 Future Work	121
Chapter 6: Bridging the gap: targeted cuticle deposition restores mechanical strength to wounded insect tibiae.....	123
6.1 Abstract.....	123
6.2 Introduction	124
6.3 Materials and Methods	126
6.3.1 Insects.....	126
6.3.2 Experimental Procedure.....	127
6.3.3 Testing	129
6.4 Results.....	132
6.4.1 Thickness Results:	135
6.4.2 Cuticle Deposition Rates:	135
6.5 Discussion.....	136
6.5.1 Apparent Fracture Toughness	140
6.5.2 What stops repair?	141
6.5.3 Thickness Results	142
6.5.4 Cuticle Deposition Rates:	143
6.6 Conclusions	144
6.7 Future Work	145
Chapter 7: Self-healing properties of insect cuticle.....	146
7.1 Abstract.....	146
7.2 Introduction	146
7.3 Materials and Methods	147
7.3.1 Insects.....	147
7.3.2 Experimental Setup.....	147
7.3.3 Calculations.....	148

7.4	Results.....	149
7.5	Discussion.....	153
7.5.1	Energy.....	153
7.5.2	Stiffness	155
7.5.3	Control Experiments.....	157
7.5.4	Applying a load increases the stiffness.....	157
7.5.5	Hydration regulation mechanism of the locust is controlled centrally	157
7.6	Conclusion	158
	Conclusions.....	159
	Future Work	162
	References.....	166

List of Figures

FIGURE 1.1: FEMALE ADULT DESERT LOCUST (<i>SCHISTOCERCA GREGARIA</i>), PHOTO BY E. PARLE.	2
FIGURE 1.2: THE HIERARCHICAL STRUCTURE OF LOBSTER CUTICLE. (FABRITIUS ET AL., 2009).....	4
FIGURE 1.3: EPIDERMAL CELL AND A GLANDULAR UNIT WITH A GLAND CELL (CHAPMAN, 2013)	5
FIGURE 1.4: SECTION THROUGH THE INTEGUMENT (CHAPMAN, 2013)	6
FIGURE 1.5: STACKING HEIGHTS VISIBLE IN LOBSTER CUTICLE (FABRITIUS, SACHS ET AL., 2009)	8
FIGURE 1.6: CUTICULAR LAYERS STAINED WITH MALLORY TRICHROME (KLOCKE AND SCHMITZ, 2011).	8
FIGURE 1.7: HELICOIDALLY ARRANGED CHITIN MICROFIBERS CONTAINING PORE CANALS (CHAPMAN, 2013).....	10
FIGURE 1.8: SEM PHOTO OF LOCUST TIBIA CUTICLE SHOWING PORE CANALS AND MICRO-FIBRES (SEM PHOTO BY E. PARLE)	10
FIGURE 1.9: INSECTS EMERGING FROM EXUVIUM (BY E. PARLE AND BY P. BALSON).....	12
FIGURE 1.10: THE VARIOUS STAGES OF MOULTING. (CHAPMAN, 2013, SNODGRASS, 2015).	14
FIGURE 1.11: CUTICLE PRODUCTION DURING THE MOULTING PROCESS (CHAPMAN, 2013)	14
FIGURE 1.12: BEFORE DURING AND AFTER MOULTING (BERNAYS, 1972; CHAPMAN, 2013).....	15
FIGURE 1.13: SECTIONS FROM HIND TIBIA OF THE LONG-HORNED GRASSHOPPER (<i>DECTICUS VERRUCIVORUS</i>) (NEVILLE, 1965)..	16
FIGURE 1.14: THE ANATOMY OF THE SEGMENTED LEG (CHAPMAN, 2013)	16
FIGURE 1.15: INTRINSIC MUSCLE GROUPS AND THE SENSORY SYSTEM OF THE INSECT LEG (CHAPMAN, 2013)	17
FIGURE 1.16: VARIOUS JOINT TYPES (CHAPMAN, 2013)	19
FIGURE 1.17: WING JOINT OF A GRASSHOPPER (CHAPMAN, 2013)	19
FIGURE 1.18: TWO TIBIA BASED SENSING DEVICES (CHAPMAN, 2013)	21
FIGURE 1.19: STIFFNESS V DENSITY PLOT FOR NATURAL MATERIALS (VINCENT AND WEGST, 2004).	22
FIGURE 1.20: PORE REINFORCED CIRCUMFERENTIALLY BY FIBRES (CHEN ET AL., 2002).....	26
FIGURE 1.21: THE HIERARCHICAL STRUCTURE OF BONE AND BAMBOO (MORTENSEN, 2006).....	26
FIGURE 1.22: LOADING COMPOSITE STSTRUCTURES	27
FIGURE 1.23: FAILURE MODES OF A TUBE LOADED IN BENDING (TAYLOR AND DIRKS, 2012)	30
FIGURE 1.24: PREDICTIVE FAILURE STRENGTHS OF LOCUST TIBIA (TAYLOR AND DIRKS, 2012).....	33
FIGURE 1.25: GROUND REACTION FORCES FOR A DEATH’S HEAD COCKROACH HIND LEG. (FROM WWW.DAILYMAIL.CO.UK)	35
FIGURE 1.26: THE GROUND REACTION FORCE IN THE VERTICAL DIRECTION FOR <i>P. AMERICANA</i> RUNNING EXCLUSIVELY ON ITS HIND LEGS (FULL AND TU, 1991)	35
FIGURE 1.27: THE EXTENSOR AND FLEXOR MUSCLES (HEITLER, 2012)	36
FIGURE 1.28: TIBIA MOTION DURING JUMPING (HEITLER, 1977).....	37
FIGURE 1.29: DETAILED INTERNAL STRUCTURE OF TIBIA-FEMORAL JOINT (BENNET-CLARK, 1975)	37
FIGURE 1.30: VIDEO MICROGRAPH SLIDES ANIMATING THE LOCUST JUMP (HEITLER, 2012)	38
FIGURE 1.31: CELL MIGRATION INTO EXCISION WOUND (WIGGLESWORTH, 1937)	43
FIGURE 1.32: LINES OF PRINCIPAL AND SECONDARY LOADING STRESSES AND A CROSS SECTION OF AN ADULT FEMUR SHOWING TRABECULAE ORIENTED TO CLOSELY MATCH THESE (WOLFF, 1870)	50
FIGURE 2.1: A HEALTHY FEMALE ADULT DESERT LOCUST SPECIMEN (PHOTO BY E. PARLE.).....	55
FIGURE 2.2: THE EXPERIMENTAL SETUP	57
FIGURE 2.3: THE EXPERIMENTAL RIG.....	58
FIGURE 2.4: THE LOADING REGIME FOR A CANTILEVER BEAM	60
FIGURE 2.5: STRESS V STRAIN OR “LOADING CURVE” FOR A TYPICAL SAMPLE.....	62
FIGURE 2.6: SEM PHOTOS ILLUSTRATING THE VARIATION IN CROSS-SECTIONAL SHAPE	63
FIGURE 2.7: CIRCULAR AND ELLIPTICAL CROSS-SECTIONS.....	63
FIGURE 3.1: THE ANATOMY OF THE ISOPOD CRUSTACEAN <i>IDOTEA WOSNESENSKII</i> (ALEXANDER ET AL., 1995).....	67

FIGURE 3.2: THE INSECTS EXAMINED. (PHOTO (A) FROM WWW.BUGABOPESTCONTROL.COM, PHOTO (B) BY E. PARLE, PHOTO (C) FROM WWW.DAILYMAIL.CO.UK)	69
FIGURE 3.3: ANSYS REPRESENTATION OF TIBIA AS A HOLLOW CIRCULAR CYLINDER.....	70
FIGURE 3.4: EMERGENCY TYPE BEHAVIOUR: (PHOTOS FROM HEITLER (2012), WWW.SHUTTERSTOCK.COM (PHOTO BY NICO TRAUT) AND FROM KAAE (2015)).	73
FIGURE 3.5: FORCE RESOLUTION FROM HORIZONTAL AND VERTICAL “GROUND REACTION FORCES” INTO BENDING AND COMPRESSION FORCES.	73
FIGURE 3.6: SHOWING HOW BENDING AND COMPRESSIVE FORCES DIFFER BASED ON THE ANGLE OF THE TIBIA RELATIVE TO THE GROUND.....	74
FIGURE 3.7: SEM IMAGES OF CROSS SECTIONS OF THE LOCUST HIND-LEG, LOCUST MID-LEG, AMERICAN COCKROACH HIND-LEG AND DEATH’S HEAD COCKROACH HIND-LEG.	75
FIGURE 3.8: THE LOADING CURVE FOR A TYPICAL SAMPLE OF EACH INSECT TIBIA	76
FIGURE 3.9: EXPERIMENTALLY MEASURED MECHANICAL PROPERTIES.....	77
FIGURE 3.10: STRIDE FREQUENCIES FOR <i>BLABERUS</i> AND <i>PERIPLANETA</i> (CHAPMAN, 2013).	81
FIGURE 4.1: EXPERIMENTAL SET UP AND A TYPICAL FORCE / DISPLACEMENT CURVE	88
FIGURE 4.2: SEM PHOTOGRAPHS OF CROSS SECTIONS OF INSECT TIBIAE	90
FIGURE 4.3:SEM AND CORRESPONDING FE MODEL OF THE STICK INSECT LEG, SHOWING A BUCKLING FEATURE IN ONE OF THE LONGITUDINAL RIDGES	92
FIGURE 4.4: EXPERIMENTAL RESULTS FOR BENDING STRESS AT FAILURE AND THE PREDICTIONS USING FEA AND CALLADINE’S FORMULA.	92
FIGURE 4.5: EXAMPLES OF FE SIMULATIONS OF BUCKLING EVENTS	93
FIGURE 4.6: RESULTS FROM FE SIMULATIONS OF CIRCULAR TUBES WITH AND WITHOUT FINS	94
FIGURE 4.7: EXPERIMENTAL DATA FOR A STICK INSECT TIBIA AND THE RESULTS OF A FINITE ELEMENT SIMULATION OF A MODEL OF THE SAME TIBIA.....	95
FIGURE 4.8: EXPERIMENTAL DATA FOR A BEE TIBIA AND THE RESULTS OF A FINITE ELEMENT SIMULATION OF A MODEL OF THE SAME TIBIA.....	97
FIGURE 4.9: THE BARK OF A MATURE TREE SHOWING LONGITUDINAL RIDGES (PHOTO FROM CAROLINA NATURE WEBSITE).....	99
FIGURE 4.10: SPINES ON LOCUST HIND-LEG, LOCUST MID-LEG, AMERICAN HIND-LEG AND DEATH’S HEAD HIND-LEG	99
FIGURE 5.1: 5TH INSTAR LOCUSTS AND NEWLY MOULTED ADULTS	1044
FIGURE 5.2: MICROCT IMAGES OF LOCUST TIBIA CUTICLE AT 3, 12 AND 56 DAYS AFTER MOULTING AND SKETCHES TO ILLUSTRATE THE GROWTH OF CUTICLE OVER TIME (JENSEN AND WEIS-FOGH, 1962)	1055
FIGURE 5.3: CUTICLE THICKNESS AND TIBIA RADIUS AS A FUNCTION OF THE DAYS SINCE THE FINAL MOULT	1066
FIGURE 5.4: BENDING MOMENT TO CAUSE FAILURE AS A FUNCTION OF CUTICLE THICKNESS	1066
FIGURE 5.5: STRESS TO CAUSE FAILURE AND STIFFNESS AS A FUNCTION OF CUTICLE THICKNESS	1077
FIGURE 5.6: FAILURE STRENGTH AS A FUNCTION OF CUTICLE THICKNESS AND PREDICTION FOR ELASTIC BUCKLING FAILURES OBTAINED FOR EACH SAMPLE.....	1088
FIGURE 5.7: PREDICTED STRESS TO FAILURE AS A FUNCTION OF EXPERIMENTAL STRESS TO FAILURE.....	1088
FIGURE 5.8: INITIAL STAINING TESTS	1122
FIGURE 5.9: INITIAL GRAPH PLOTTING MEASUREMENTS TAKEN OF TOTAL CUTICLE THICKNESS, EXOCUTICLE THICKNESS AND ENDOCUTICLE THICKNESS.	1122
FIGURE 5.10: THE PREDICTION OF BUCKLING STRENGTH, THE MATERIAL FRACTURE STRENGTH, THE COMBINATION OF FRACTURE AND BUCKLING, AND THE EXPERIMENTAL VALUES AS A FUNCTION OF R/T	1144
FIGURE 5.11: PLOTTING FAILURE STRENGTH AND JUMPING STRESS AND SAFETY FACTOR (THE RATIO OF THE TWO) AS A FUNCTION OF CUTICLE THICKNESS.....	1166
FIGURE 5.12: A LOCUST WITH BOTH TIBIAE PERMANENTLY DEFORMED	1177

FIGURE 5.13: THICKNESS, STRENGTH AND STIFFNESS OF 1ST LEG REMOVED COMPARED TO THE 2ND (REMAINING) LEG.....	1200
FIGURE 6.1: TIMING OF WOUND RESPONSES FOR DROSOPHILA LARVAE FOLLOWING A PUNCTURE WOUND (FROM GALKO AND KRASNOW (2004))	1257
FIGURE 6.2: THE CUTTING RIG FOR PERFORMING INCISIONS.....	1279
FIGURE 6.3: PHOTOS OF SAMPLES SHOWING INCREMENTAL CUT DEPTHS USED.....	12830
FIGURE 6.4: THE TESTING RIG USED SHOWING A FAILURE OCCURRING AT THE POINT OF INCISION.	1291
FIGURE 6.5: CROSS SECTION OF THE TIBIA SEPARATED INTO WOUNDED DORSAL AREA (T1), THE VENTRAL (T2) AND SIDES (T3) OF THE TIBIA, ALSO SHOWING THE CUT LENGTH (L) AND THE INJURED AREA (SHADED RED).	1302
FIGURE 6.6: THE INCISION AND THE ARC LENGTH OF THE INCISION (2A) USED IN MY CALCULATIONS FOR APPARENT FRACTURE TOUGHNESS, AND THE INCLUDED ANGLE.	1313
FIGURE 6.7: CROSS SECTIONS OF TIBIA AT THE POINT OF INCISION (ORIGINAL INCISION SHOWN BY THE DASHED LINE).....	1335
FIGURE 6.8: RESULTS FOR FAILURE STRENGTH, BENDING MOMENT TO CAUSE FAILURE, APPARENT STIFFNESS AND APPARENT FRACTURE TOUGHNESS	1344
FIGURE 6.9: CUTICLE THICKNESS T1, T2 AND T3 FOR THE INJURED AND NOT REPAIRED, INJURED AND REPAIRED, AND UNINJURED CONTROL LEGS FROM A PREVIOUS STUDY.	1355
FIGURE 6.10: CUTICLE THICKNESS AS A FUNCTION OF TIME SINCE INJURY FOR VARIOUS ZONES FOR ALL SAMPLES DISPLAYING REPAIR AND CUTICLE DEPOSITION RATES POST INJURY COMPARED TO DEPOSITION RATES OBSERVED IN THE UNINJURED CONTROL SAMPLES IN THE IMMEDIATELY POST MOULT MODELLING PERIOD, AND THE LATER DORMANT PERIOD.....	1355
FIGURE 6.11: TWO POSSIBLE FAILURE MODES FOR A SPECIMEN WITH A DEFECT, YIELDING AND FRACTURE AS A FUNCTION OF FLAW OR CRACK SIZE.	13840
FIGURE 6.12: THE TWO POSSIBLE FAILURE MODES FOR MY SAMPLES	1391
FIGURE 6.13: LONGITUDINAL SECTION OF UNTESTED TIBIAE 30 DAYS AFTER INJURY. INCISION IS DENOTED BY DOTTED LINE AND ARROW, ONE SHOWING NO REPAIR, THE OTHER SHOWING SIGNIFICANT REPAIR	1413
FIGURE 7.1: RIG FOR HOUSING THE LOCUST FOR DURATION OF THE EXPERIMENT.....	1477
FIGURE 7.2: TYPICAL TEST GRAPH PLOTTING STRESS AGAINST STRAIN.....	14949
FIGURE 7.3: LOADING ENERGY REQUIRED TO DEFORM TIBIA BY 1MM AT A RATE OF 5MM/MIN FOR EACH CYCLE OF THE TESTS	1500
FIGURE 7.4: AVERAGE ENERGIES REQUIRED FOR LOADING AND UNLOADING ALL TIBIAE FOR EACH CYCLE OF THE TESTS.....	1500
FIGURE 7.5: SAMPLE OF INDIVIDUAL STIFFNESS VALUES FOR LIVING CUTICLE	1511
FIGURE 7.6: SAMPLE OF INDIVIDUAL YOUNG’S MODULUS VALUES FOR CUTICLE POST REMOVAL	1522
FIGURE 7.7: AVERAGE STIFFNESS RESULTS FOR LIVING AND DEAD CUTICLE	1522

List of Tables

TABLE 1.1: RECENTLY PUBLISHED VALUES FOR MECHANICAL PROPERTIES OF INSECT CUTICLE	23
TABLE 1.2: GROUND REACTION FORCES MEASURED FOR DIFFERENT INSECTS	38
TABLE 1.3: A BRIEF INDEX OF SOME OF THE PREVIOUS RESEARCH INTO INSECT WOUND HEALING, THE INSECT EXAMINED, METHODS USED, AND SUBJECT INVESTIGATED.....	40
TABLE 2.1: DIFFERENCES CAUSED BY ELLIPTICAL AND CIRCULAR CROSS SECTIONS.....	64
TABLE 3.1: GROUND REACTION FORCES PREVIOUSLY MEASURED FOR DIFFERENT INSECTS	71
TABLE 3.2: RELEVANT DIMENSIONS FOR LOCUST MID-LEGS (N = 26), AMERICAN COCKROACH (N = 17) AND DEATH'S HEAD COCKROACH (N = 10), FOR MASS READINGS N = 10 FOR ALL SPECIMENS. MEASUREMENTS FOR LOCUST HIND LEGS (IN ALL TABLES) ARE FROM DIRKS AND TAYLOR (2012).....	76
TABLE 3.3: EXPERIMENTALLY MEASURED MECHANICAL PROPERTIES	77
TABLE 3.4: <i>IN VIVO</i> STRESSES EXPERIENCED BY THE TIBIA OF EACH INSECT WHEN WALKING, RUNNING, AND DURING EMERGENCY BEHAVIOUR (JUMPING, WEDGING AND RIGHTING). UNDERLINED NUMBERS ARE DIRECT CALCULATIONS BASED ON DATA FROM THE LITERATURE. FIGURES IN ITALICS ARE ESTIMATES FROM SCALING UP / DOWN THESE NUMBERS.....	78
TABLE 3.5: SAFETY FACTORS OF INSECT TIBIAE FOR VARIOUS SITUATIONS. RELEVANT STRESS TO CAUSE FAILURE IS DIVIDED BY <i>IN VIVO</i> APPLIED STRESS TO OBTAIN THE SAFETY FACTOR.	79
TABLE 4.1: EXPERIMENTAL VALUES AND PREDICTIONS FOR STRENGTH AND STIFFNESS.....	91
TABLE 6.1: SUMMARY OF LAYERS OF AN INSECT EXOSKELETON AND THEIR IMMUNE FUNCTIONS (CHAPMAN, 2013)	1244
TABLE 6.2: THE FOUR STAGES OF WOUND HEALING, THEIR PURPOSE, AND WHAT HAPPENS IF ANY ONE STAGE IS ABSENT. INFORMATION GATHERED FROM WIGGLESWORTH (1937), LAI-FOOK (1966); LAI-FOOK (1968), LOCKE (1966), ROWLEY AND RATCLIFFE (1976); ROWLEY AND RATCLIFFE (1978), DILLAMAN AND ROER (1980), WRIGHT (1987), LAI, CHEN ET AL. (2001), GALKO AND KRASNOW (2004), DUSHAY (2009) AND BELACORTU AND PARICIO (2011).....	1255
TABLE 6.3: AVERAGE VALUES FOR FAILURE STRESS, (APPARENT) STIFFNESS AND BM TO FAILURE FOR EACH TIME PERIO.....	1322

Publications and Presentations

This work has been presented as follows:

Publications:

Parle, E., Herbaj, S., Sheils, F., Larmon, H., and Taylor D., (2016). Buckling Failures in Insect Exoskeletons. *Journal of Bioinspiration and Biomimetics*. (In press).

Parle, E., Dirks, J-H., and Taylor D. (2016) Bridging the gap: wound healing in insects restores mechanical strength by targeted cuticle deposition. *Journal for the Royal Society Interface* (in press).

Parle, E., Larmon, H., and Taylor, D. Biomechanical factors in the adaptations of insect tibia cuticle. *PLoS One* (under review)

Parle, E., Dooley, C., O'Neill, M and Taylor, D., Insect cuticle growth rates: their purpose and effect on tibia structural properties in the desert locust (in preparation).

Parle, E. and Taylor, D., (2013). The Self-Healing Properties of Insect Cuticle. *Journal of Postgraduate Research*, Trinity College Dublin, 12: 90-111.

Dirks, J.-H., Parle, E., and Taylor, D. (2013) Fatigue of insect cuticle. *Journal of Experimental Biology*. 216(10), 1924-1927.

Conference Papers:

Bridging the gap: wound healing in insects restores mechanical strength by targeted cuticle deposition

- BINI (Bioengineering in Ireland), 2016, Galway, Ireland (*Oral Presentation*)

Age-related changes in the stiffness of insect cuticle

- BINI (Bioengineering in Ireland), 2016, Galway, Ireland (*Oral Presentation*)

Insect cuticle growth rates: their purpose and effect on tibia structural properties in the desert locust.

- Joint Symposium of IMS (Irish Mechanics Society) and ISSEC (Irish Society for Scientific & Engineering Computation) 2015, University College Dublin, Ireland (*Oral Presentation*)

How cuticle growth affects the mechanical properties and failure mode of an insect's tibia:

- ICOMBT (International Conference of Mechanics of Biomaterials and Tissues) 2015, Waikoloa Marriot Resort, Hawaii, USA (*Oral Presentation*)

Measuring locust tibia cuticle layers to study mechanical properties and repair:

- ICOMBT (International Conference of Mechanics of Biomaterials and Tissues) 2015, Waikoloa Marriot Resort, Hawaii, USA (*Oral Presentation*)

Biomechanical factors in the evolution of insect tibia cuticle:

- SEB (Society of Experimental Biology) 2015, Clarion Congress Hotel, Prague, Czech Republic (*Oral Presentation*)

Buckling failures in insect legs:

- SEB (Society of Experimental Biology) 2015, Clarion Congress Hotel, Prague, Czech Republic (*Oral Presentation*)

Self-Healing Properties of Insect Cuticle:

- WCB (World Congress of Biomechanics) 2014, Hynes Convention Centre, Boston, USA (*Poster Presentation*)
- SEB (Society of Experimental Biology) 2014, Manchester University, Manchester, UK (*Oral Presentation*)
- Sir Bernard Crossland Symposium, 2014, NUIG, Galway, Ireland (*Poster and Oral Presentation*)

Fatigue Properties of Insect Cuticle:

- ICOMBT (International Conference of Mechanics of Biomaterials and Tissues) 2013, Sitges, Barcelona, Spain (*Poster Presentation*)
- SEB (Society of Experimental Biology) 2013. Valencia Conference Centre, Valencia, Spain (*Oral Presentation*)
- BINI (Bioengineering in Ireland) 2013. Johnstown, Co. Meath, Ireland (*Poster Presentation*)

Chapter 1: Introduction

1.1 Insects

Early arthropods walked (or crawled) the Earth up to 540 million years ago. They have evolved to conquer every environment from the equatorial jungles and deserts to the frozen poles. The success of insects is owed to their diversity, their sheer abundance (due to high reproduction rates), and their ability to fly. Though most live on land, insects were the first animals to take to the air, and there are also many aquatic species. Of the 1.5 million (approx.) animal species that have been scientifically identified, two-thirds are arthropods such as crustaceans, arachnids, myriapods and insects. Vertebrates in comparison account for less than 3% of all species. Insects account for a substantial 75% of all animals on Earth. In some environments, ants alone account for 25% of the total animal biomass present.

Insects are crucial in almost every ecosystem imaginable. Their eating habits help maintain and recycle plant matter – termites alone remove more plant material from the African savannah than every herd of wildebeest, zebra, and other ungulate combined. Other insects are vital for disposal of leaf litter, dung and animal carcasses, returning valuable nutrients to the soil. Bees and other insects pollinate the vast majority of flowering plants, without which fruit, vegetables and flowers would simply not exist. Without insects, the world would look very different. The loss of bees alone could apparently cause the extinction of up to 25% of all life on Earth. Insects also provide a vital role at the bottom of many food chains. Practically all birds (and smaller vertebrate species) survive on a diet of insects – a single swallow chick may consume as many as 200,000 flies, beetles and other insects before leaving the nest.

Insects can also be a pest. Some are parasitic (often to other insects). Others can transmit disease to plants and animals resulting in crop failures, plagues and diseases such as malaria. Plagues of insects can devour crops and destroy wooden structures.

Insects such as the desert locust (Figure 1.1) have been used extensively in genetic, physiological and evolutionary studies, leading to many important discoveries. Other studies have examined

some of the properties of the light, versatile, durable cuticle material that forms their insect bodies.



Figure 1.1: female adult desert locust (*Schistocerca gregaria*), photo by E. Parle.

1.2 Cuticle

The exoskeletons of insects are composed of a material known as cuticle, which consists of fibres of chitin embedded in a matrix of proteins. Other arthropods such as crabs and lobsters are also largely composed of cuticle, which is reinforced with mineral particles. This versatile material makes up not only the arthropod's exoskeleton, but its tendons, mandibles, wings and even its eyes, performing a wide variety of functions and exhibiting a very wide range of material properties (Vincent and Wegst, 2004).

Although one of the most abundant natural materials on the planet, there has been relatively little research carried out on its mechanical properties (such as strength, stiffness, fatigue and toughness). Less still has been carried out on various factors which can affect and influence these properties. The focus of this Ph.D. is to build on previous studies by investigating some of these factors such as growth, maturity, injury and biomechanics to provide a more complete picture of the mechanical properties of this material. The work is largely experimental in nature coupled with some finite element modelling to examine failure modes. In this introductory chapter I

review much of the literature currently published that is relevant to my studies. I begin by giving a brief review of insect cuticle itself – its microstructure, macrostructure, constituents, how it is deposited by the insect, and several factors that can affect its properties. In order to grow, most insects and arthropods need to moult, and the properties of the cuticle are altered significantly before, during and after moulting. How the moulting process and the continued growth of the cuticle after moulting influence the mechanical properties of insect cuticle is the focus of the study described in Chapter 5. Cuticle comprises the majority of the insect, and its mechanical properties can vary widely from place to place on a single insect to tailor to varied particular functions and purposes (e.g. hard mandibles for chewing, flexible joints for moving). I review some of these functions and some recently published data on the mechanical properties of insect cuticle such as strength, stiffness, toughness and fatigue.

Insect cuticle is a naturally occurring composite material. I examine and explain the importance of composite materials and why they are desirable for use by engineers. The part of the insect which I examine in my Ph.D. is the tibia, which is essentially a thin-walled tube. I review various failure modes of thin-walled tubes and several papers that examine the failure of naturally occurring tubular structures. This literature is relevant to my study on the buckling of insect tibiae in Chapter 4.

The insect tibia can be subjected to various applied forces *in vivo* during normal locomotion and emergency behaviour. I review the biomechanics of such behaviour in locusts and cockroaches, which I will later use to calculate stresses experienced by these insect legs and their safety factors in Chapter 3. I also carry out an extensive review of the insect wound healing response which is relevant to the studies on major and minor damage repair described in Chapters 6 and 7 respectively.

1.2.1 Microstructure

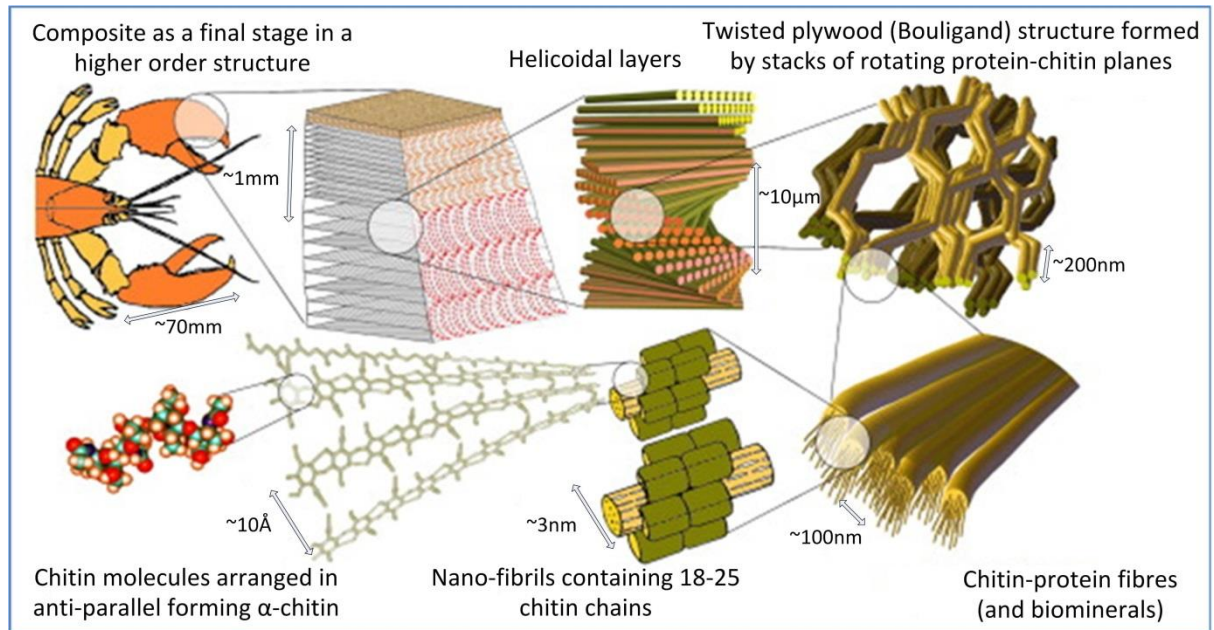


Figure 1.2: the hierarchical structure of lobster cuticle. (Fabritius et al., 2009)

The main component of cuticle is chitin, which is the second most abundant organic material on the planet (after cellulose). Chitin is a polysaccharide molecule which is a linear polymer of β -1,4-linked N-acetylglucosamine. These long molecules of chitin (contributing 20 - 50% of the dry weight of the insect cuticle (Chapman, 2013)) are the building block of the insect body, just as cellulose is for a plant. They are arranged in anti-parallel (parallel, but oriented in opposite directions) to form α -chitin. The nano-fibrils in cuticle have a high aspect ratio, being 2-5 nm in diameter and $0.3\mu\text{m}$ long (Chapman, 2013). Each contains about 20 single chitin chains that are embedded in a protein matrix. Fibres in each layer are uniformly parallel and their orientation changes in successive layers in a helicoidal fashion (Chen et al., 2004), or layers with helicoidally arranged microfibrils may alternate with layers in which the microfibrils are uniformly oriented (this is visible in cockroaches and locusts (Neville, 1963)). This hierarchical structure is shown in Figure 1.2. Jensen and Weis-Fogh (1962) observed parallel lamellae of chitin ($0.2\mu\text{m}$ thick) "glued" together by sheets of the protein resilin ($0.3\mu\text{m}$ thick). The helicoidal arrangement may vary, as will the "stacking height" – the number of layers (or thickness of cuticle) in which the preferred fibre direction changes through 180° . In the water bug *Hydrocirus*, the stacking height is 25 layers or 160nm (Mortensen, 2006). The alternating layer system seen in locusts and

cockroaches is determined by the individual insect's exposure to light and dark. Cuticle deposited at night is arranged helicoidally (and is lamellate – i.e. contains several layers), while cuticle laid down during the day is unidirectional (and non-lamellate). The layered arrangement can be disrupted by artificially altering the environmental conditions in which the insect is kept – e.g. exposing the insect to constant light will induce production of non-lamellate cuticle only (Neville, 1965).

All cuticle is derived from the epidermal cells. Plaques at the tips of protrusions from the cells (called microvilli) are thought to be the site of chitin fibre secretion (Chapman, 2013). Actin filaments connected to the plaques may help orientate the chitin-synthesising machinery. Different classes of cells (such as those in Figure 1.3 (a) and (b)) are involved in producing different components of the cuticle. Some cells (class 1) produce new cuticle, some (class 2) have no contact with the cuticle at all and others (class 3) produce the cement on the outer surface of the cuticle.

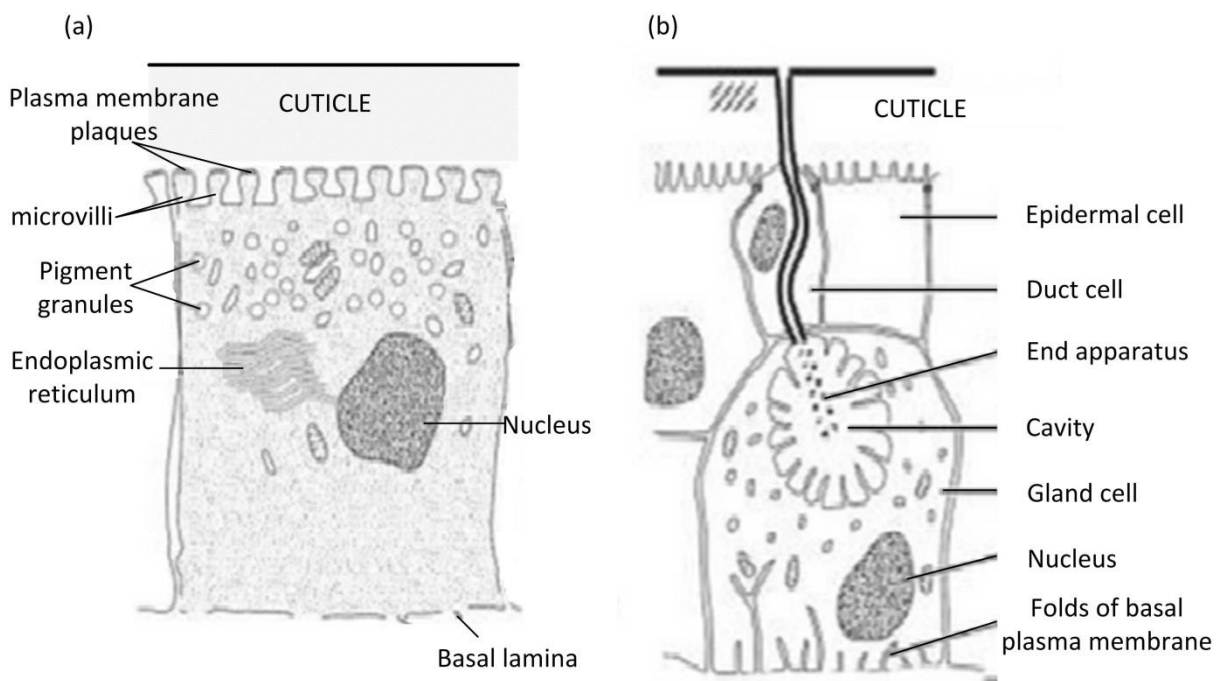


Figure 1.3: (a) a typical epidermal cell during the intermolt period. Cuticle is secreted at the plasma membrane plaques on the tips of the microvilli. This is a class 1 cell (lacks a duct to the exterior). (b) a class 3 glandular unit with a gland cell that is connected to the exterior via a duct formed by a duct cell. (Chapman, 2013)

1.2.2 Layers within the Cuticle

There are two distinct layers within the cuticle – the thin outer layer called the Epicuticle and the thicker Procuticle layer beneath.

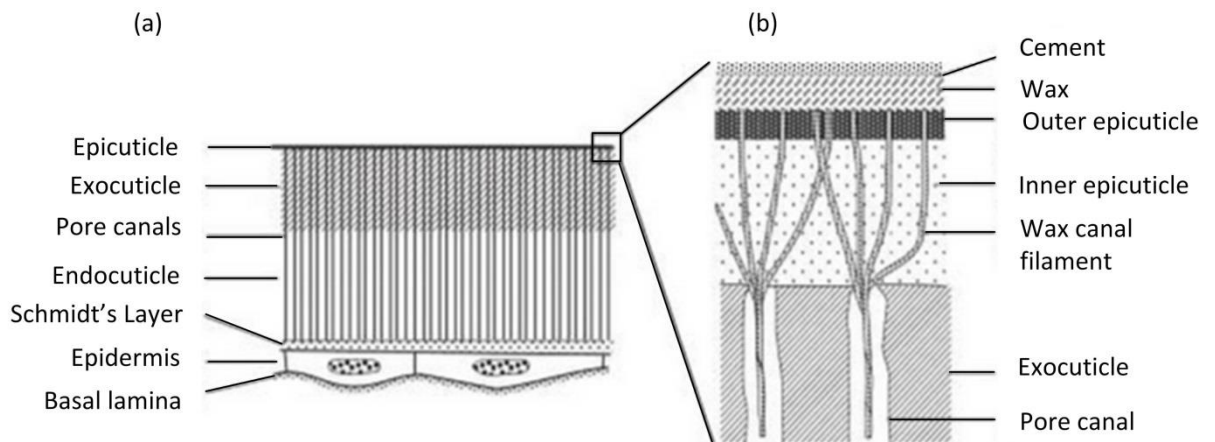


Figure 1.4: (a) section through the integument (or exoskeleton) of a mature insect showing the cuticular layers, the epidermis and the basal lamina, and (b) section through the epicuticle at greater magnification. (Chapman, 2013)

1.2.2.1 The Epicuticle

The Epicuticle is a thin (1 – 4 μm), waxy outer layer which contains little or no chitin, is inextensible once hardened, and forms the limit of possibility of growth of the insect. It can contain up to 4 distinct sub-layers (Figure 1.4 (b)).

The outermost “cement layer” is a protective hard shell not present in all insects, consisting of a very thin layer of mucopolysaccharides and lipids. It is the only layer not made from the epidermis, but is instead made by secretions from dermal glands by means of gland ducts through the procuticle (see Figure 1.3 (b)). The lac insect (*Kerria lacca*) yields such quantities of this substance to be used commercially as “shellac” – used as a tough clear wood finish, and a salon treatment for nails.

The “wax / lipid layer” is produced by epidermal cells and contains fatty acids, hydrocarbons and alcohols. This can be seen as the “greasy” surface of the cockroach, is usually a hydrophobic surface, and is crucial in protecting against water loss due to evaporation in dry atmospheres, as well as resistance to invasion by pathogens. Bees can produce this wax in vast quantities,

especially when they have an adequate supply of honey (which provides the necessary chemicals for producing the wax). Flat scales are produced from this wax to form the bee's honeycomb.

The "outer layer" and "inner layer" (just outside the Procuticle) are formed from tanned lipoproteins that are stabilized by molecular cross-links, and are distinct from one another in some insects. This material is sometimes called sclerotin or cuticulin, and has an important function in the moulting process (see Section 1.3).

1.2.2.2 The Procuticle

Beneath the Epicuticle, the (outer) exocuticle and (inner) endocuticle form what is commonly referred to as the procuticle (Figure 1.4 (a)). This is the layered biocomposite – a protein matrix reinforced with chitin fibres – which provides the bulk of the structure and mechanical properties to the cuticle. The two layers are very similar, as both contain relatively equal amounts of fibrous chitin and proteins. The degree of crosslinking or "tanning" distinguishes the exocuticle from the endocuticle. The exocuticle has a more highly cross-linked protein matrix, and is therefore harder and more dense. Endocuticle is usually the thickest layer of the cuticle and is more tough and flexible. The exocuticle is usually fully formed when the insect moults, while the endocuticle is formed thereafter from secreted chitin molecules laid down in parallel filaments arranged in thin layers. Exocuticle is absent or minimised at joints to allow flexible movement. Distinct growth layers can be seen as a daily banded pattern under a microscope (Neville, 1965).

In some areas, another layer of mesocuticle is present between the exocuticle and endocuticle. This is effectively a "transition zone" between the two. Both the degree of tanning and the packing of the layers seen in mesocuticle fall between that of the exocuticle and the endocuticle. (Klocke and Schmitz, 2011). Mesocuticle is absent in the locust hind tibia (Neville, 1965). These layers can be distinguished histologically by staining with Mallory Trichrome Stain (Klocke and Schmitz, 2011). Exocuticle, which does not readily stain, appears faint yellow or amber, mesocuticle appears red and endocuticle blue (see Figure 1.6). The layers can also be differentiated by their stacking heights (Figure 1.5), which will be considerably smaller in

exocuticle compared to endocuticle, most probably caused by the larger rotation angle of the fibres (Fabritius, Sachs et al., 2009).

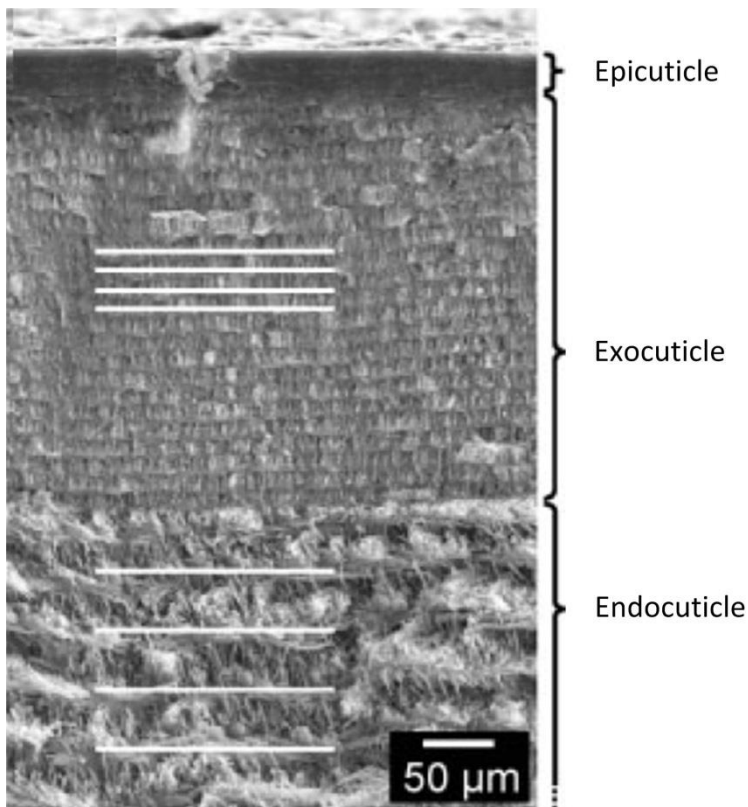


Figure 1.5: the different stacking heights visible in the layers of lobster cuticle (Fabritius, Sachs et al., 2009)

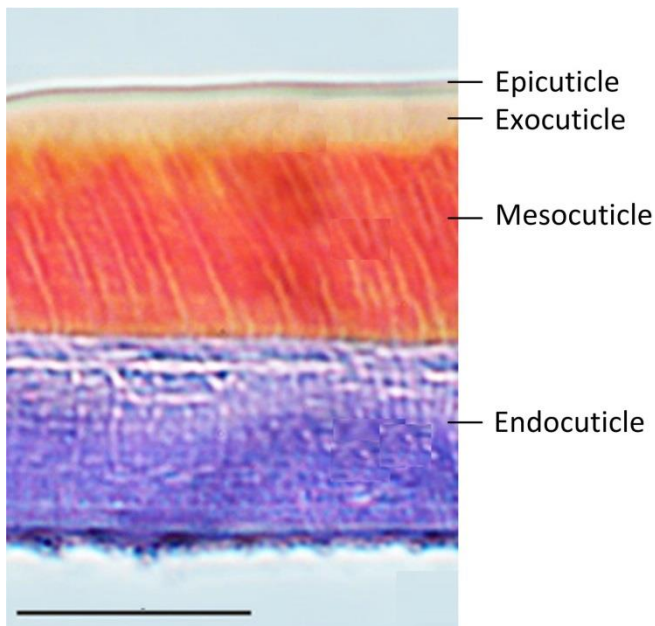


Figure 1.6: cuticular layers of the locust sternum stained with Mallory Trichrome stain, showing exo-, meso- and endocuticle (Klocke and Schmitz, 2011).

1.2.3 Epidermis, Basement Membrane and Hemolymph

Underneath the procuticle lies the epithelium or epidermis – a single layer of living cells which are the only living part of the integument. It is used for secretion, absorption, protection, transport and detection of sensation. Most significantly, the cells secrete thin layers of endocuticle daily and larger amounts when replacing the cuticle during moulting (or when the insect is injured). Together with a thin layer of connective tissue called the basement (or basal) membrane, the epidermis provides a barrier between the a-cellular cuticle and the blood of the insect (known as the hemolymph). This is the liquid in which nutrients, cells, proteins, fats, sugars, enzymes and other chemicals and minerals are stored and distributed around the insect's body. The basement membrane is formed from GAGs (glycoaminoglycans) and proteins similar to collagen, and regulates the flow of molecules to and from the internal organs and glands. It also acts as a selectively permeable membrane to allow nutrients and other molecules to be transported from the hemolymph to various parts of the integument when required (e.g. when injured (Lai-Fook, 1968)).

1.2.4 Pore Canals

Pore canals such as those visible in Figure 1.8 have a diameter of 1 μm or less and run at right angles to the surface from the epidermis through the extracellular cuticle material to the inner epicuticle. The pores are flattened in a plane parallel to the fibre orientation in each layer (see Figure 1.7) – leading to a twisted ribbon form due to the helicoidal arrangement of the layers. These canals contain tubular filaments arising from the plasma membrane of the epidermal cell. At the epicuticle, these filaments diverge and extend to the surface of the outer epicuticle. The epidermis, basement membrane and pore canals are most active during moulting (ecdysis).

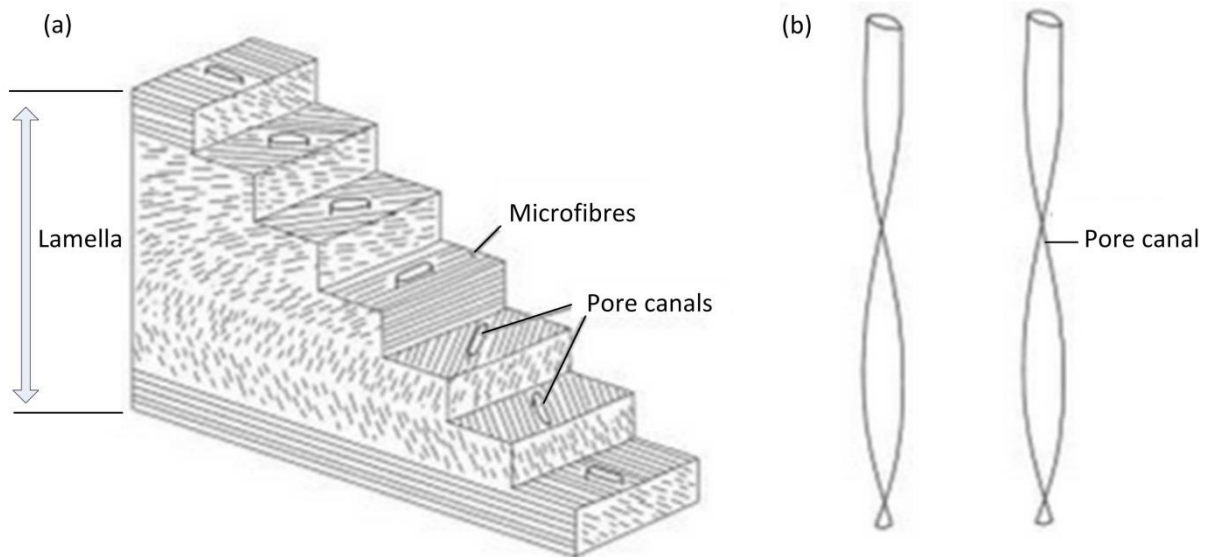


Figure 1.7: (a) section of a single “stack” of cuticle with helicoidally arranged chitin microfibrils containing pore canals which are flattened in the plane parallel to the fibres, leading to the twisted ribbon structure shown in (b). (Chapman, 2013)

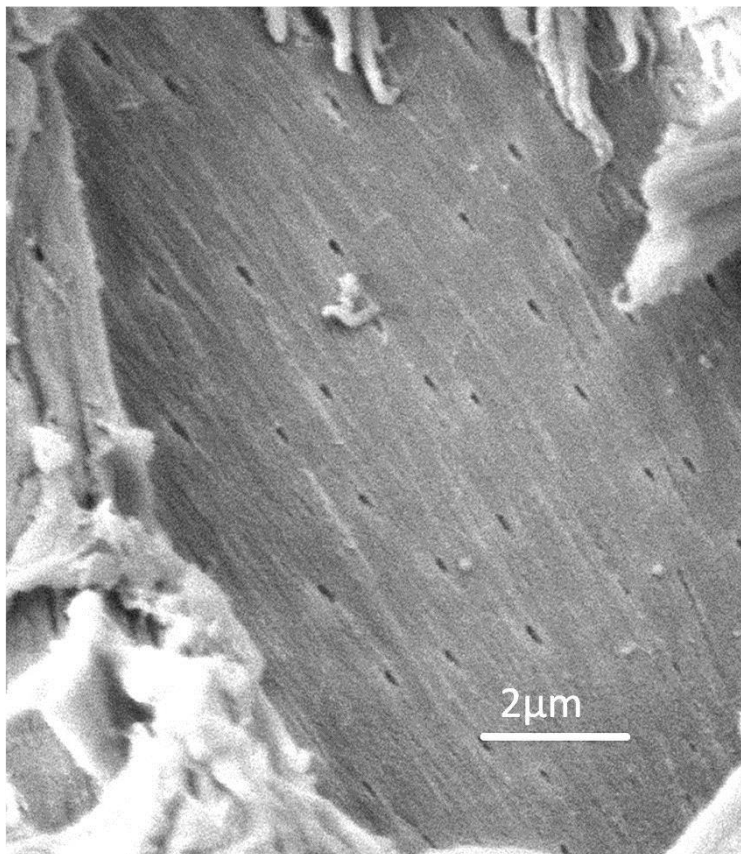


Figure 1.8: SEM photo of locust tibia cuticle showing pore canals and micro-fibres. The pores are flattened in the same direction as the long axes of the fibres (SEM photo by E. Parle)

1.2.5 Proteins

Proteins are very specific to the types of cuticle. Two well established protein groups include the RR1 cuticle protein which is associated with soft or flexible cuticle found in membranes and joints, and the RR2 protein found in stiff, hard cuticle. Various proteins occur at different stages of insect development, or in different body parts of an individual insect. Some proteins may occur in almost pure form in areas where they are needed – e.g. the rubber-like resilin for wing articulation and hinged muscle connections (see Figure 1.16). Different proteins can have a dramatic effect on the mechanical properties of the cuticle regardless of its state of sclerotization. Proteins can be related to various functions such as pigmentation and immune responses as well as structural (e.g. the highly hydrophobic apidermins) or cuticle modifying (e.g. deacetylases EC3.5.1.41). The physiochemical properties can be altered by changing the degree of deacetylation, which can vary a great deal between different insect species and body parts. Complete deacetylation of chitin yields chitosan (a homopolymer consisting exclusively of glucosamine (Chapman, 2013)). Chitosan has antibacterial properties, so this process may also provide some protection against bacterial invasion. Chitosan's antibacterial properties, as well as its biocompatible and bioresorbable properties make it a very desirable material in the field of bioengineering. It is currently used in wound dressings and dissolvable sutures (Fernandez and Ingber, 2012; Baxter et al., 2013)

1.2.6 Sclerotization

Secondary stabilization of the cuticle is achieved by sclerotization (or tanning) – the means by which the cuticular proteins become cross-linked (Pryor, 1940). The process is complex, involving the oxidation of N-acetyldopamine and N- β -alanyldopamine to the corresponding *o*-quinones. These products may then be further modified and become linked to histidine and lysine residues in the cuticular proteins, and may also become attached to the chitin fibrils (Andersen et al., 1996; Andersen, 2010). Put simply, covalent bonds are formed between protein molecules (and possibly between chitin and protein) forming a stable three dimensional network structure. The increase in bond-density leads to a decrease in hydration and a hardening (and sometimes darkening) of

the cuticle. As exocuticle is more heavily sclerotized than endocuticle, it contains less water (12% compared to 40-70%, (Vincent and Wegst, 2004; Muller et al., 2008)). The extent of sclerotization has a profound effect on the mechanical properties of the cuticle (Mortensen, 2006).

1.3 Moulting and Growth

Due to the inextensible nature of most cuticles, the growth of the insect is limited. For the insect to grow in size, the cuticle must be shed and replaced. This sequence of events is called moulting. It involves apolysis and ecdysis, and is outlined in Figures 1.10 and 1.11.



Figure 1.9: (a) an adult locust and (b) an adult cicada emerging from an “old cuticle” shell or exuvium. Photo (a) by E. Parle, photo (b) by P. Balson (copied from www.pinterest.com)

Apolysis is the separation of the cuticle of the insect from the epidermis. This allows an enzyme to be secreted from the epidermis which seeps in under the “old” cuticle. The enzyme remains inactive until such a point as the insect is ready to moult – i.e. “new” cuticle has formed underneath it. The outer epicuticle (cuticulum) is secreted first, with the inner epicuticle being secreted afterwards. Once this is complete, production of procuticle begins. Chitin microfibrils are

produced as outlined earlier accompanied by synthesis of proteins (some from the epidermis, some from the hemolymph). The new procuticle will be soft and wrinkled (Figure 1.12). The enzyme is then activated, and the old cuticle is semi-digested, making it weaker and easier to break through (and providing a source of food for the moulting insect). Only unsclerotized cuticle can be resorbed and digested during moulting, making the process more economical for soft-cuticle larva such as maggots as most of the material can be conserved. Some insects may eat their exuviae to maximize conservation of the cuticle.

The new cuticle is expanded (by gulping air / increasing blood or fluid pressure), which cracks the old cuticle along lines of weakness determined by the digestion process (Figure 1.10 (e)). Eventually the new insect emerges and sheds the exuvium (Figure 1.9). Upon emerging, the new cuticle is soft, pliable and pale before becoming fully expanded (Andersen, Peter et al., 1996). The outermost layer of the epicuticle (cement layer) is then secreted from dermal glands through gland ducts in the Procuticle. Just prior to sclerotization, the molecules used for tanning (catechols dopa and dopamine) are formed and transported to the cuticle via pore canals (Pryor, 1940). Sclerotization occurs alongside or shortly after moulting. Cross links are formed, the water content decreases dramatically in a few hours (from 70% to 40% for locust femur cuticle (Andersen, Peter et al., 1996)) and the cuticle becomes harder and darker. This process may take only last for 0-12 hours (Hepburn and Joffe, 1974), or up to 3 days (Chapman, 2013).

Immediately post-moult, the cuticle becomes much harder (Muller, Olek et al., 2008) and stiffer (from 0.85 ± 0.17 GPa to 4.6 ± 0.7 GPa (Katz and Gosline, 1994)) due to the rapid sclerotization and dehydration (Hepburn and Joffe, 1974; Vincent and Hillerton, 1979; Vincent, 1980). At this stage, almost all of the exoskeleton is comprised of exocuticle (Neville, 1963). The tanning process continues over the next three days and endocuticle is laid down rapidly, both of which lead to an increase in flexural stiffness (Hepburn and Joffe, 1974; Katz and Gosline, 1994).

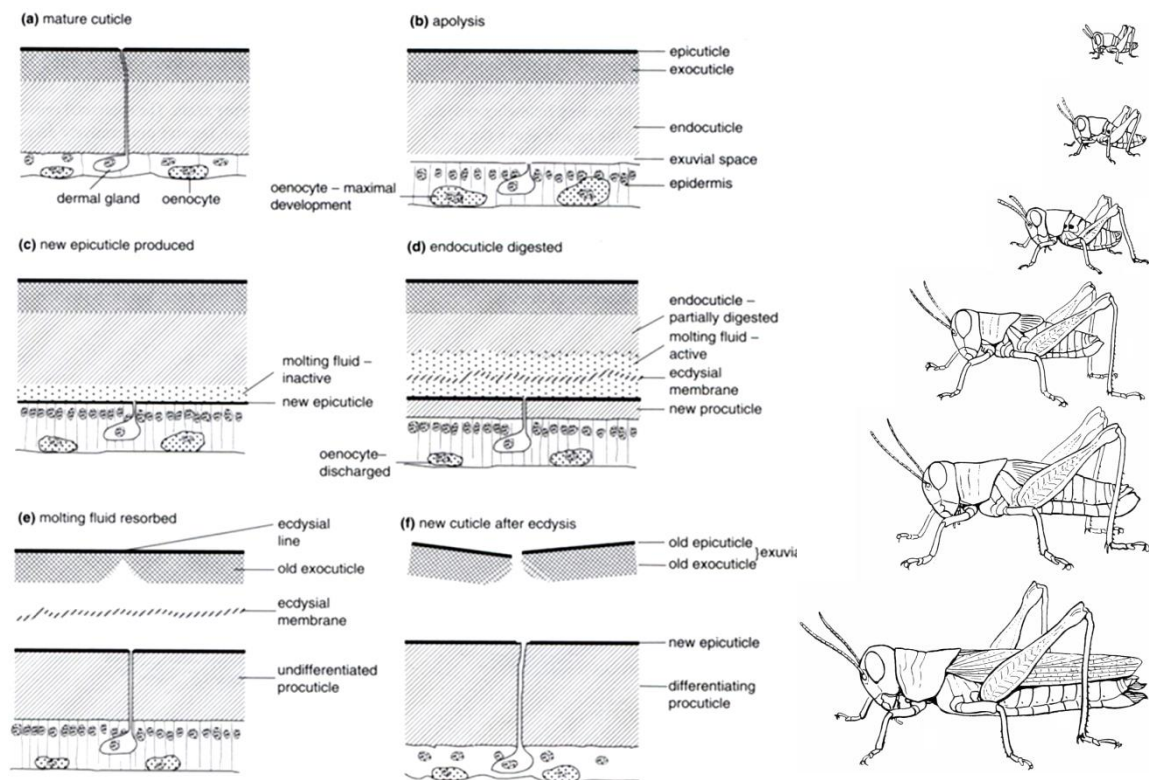


Figure 1.10: the various stages of moulting. (a) mature cuticle. (b) apolysis begins as the epidermis separates from the cuticle, microvilli are disintegrated from the cuticle and plasma membrane plaques are internalized. (c) molting fluid is produced, new microvilli and plasma membrane plaques are formed and new epicuticle is secreted. (d) the old endocuticle is partially digested when the molting fluid is activated, and new procuticle is deposited. (e) all the old endocuticle is digested and resorbed, only the old epicuticle holds the old cuticle shell together along the ecdysial line, new cuticle become thicker. (f) the old cuticle breaks along the ecdysial line, the exuvium is shed, the new cuticle differentiates due to sclerotization, and the epidermal cells return to their original state (Chapman, 2013). Image on right shows the six stages or instars of the grasshopper – only the adult has wings suited for flying (Snodgrass, 2015).

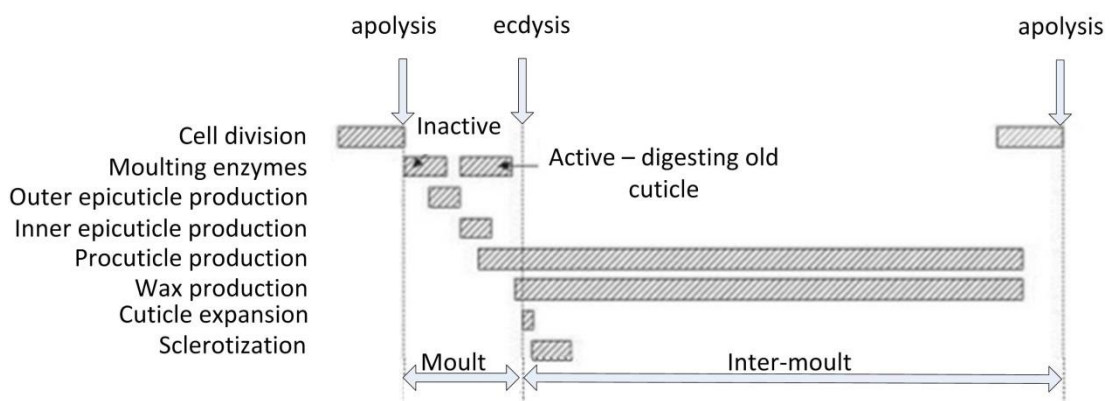


Figure 1.11: the sequence of events of cuticle production and the timings of the secretions of the various layers during the moulting process (and afterwards). Some timings may differ between species. (Chapman, 2013)

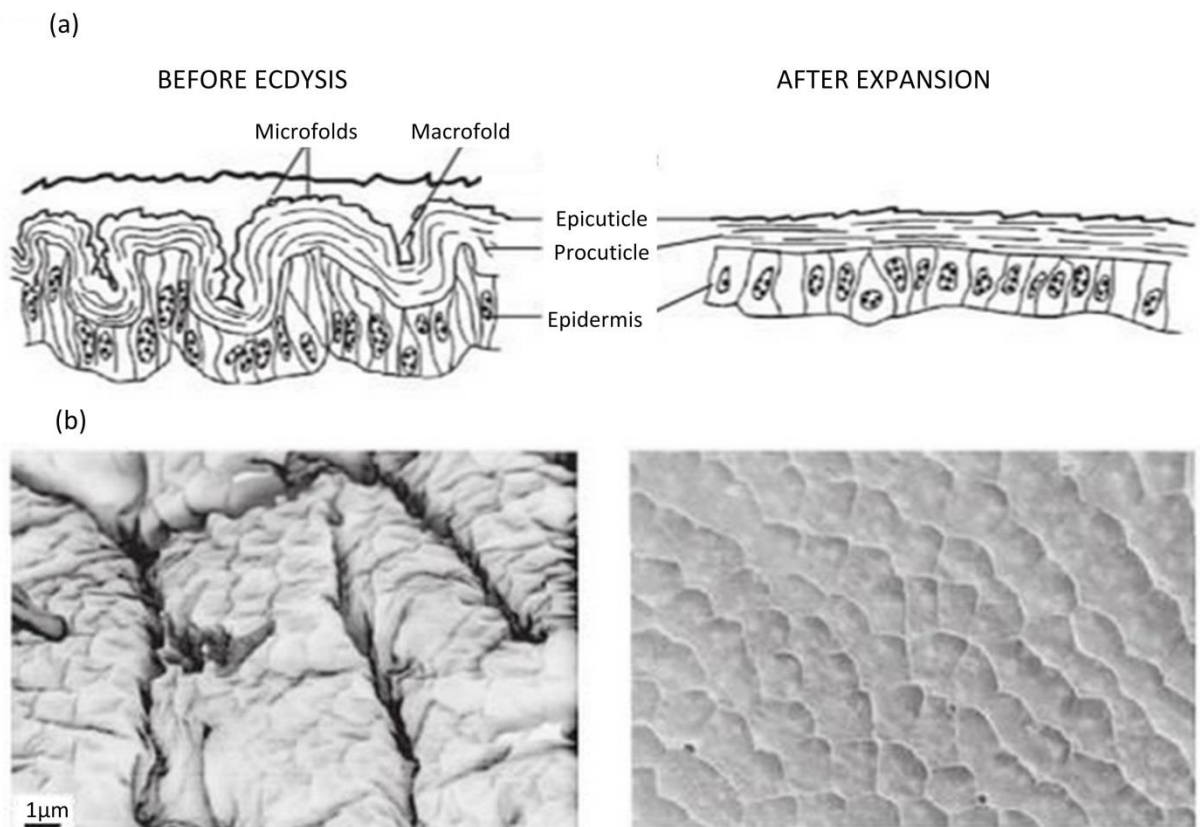


Figure 1.12: (a) cross sections through the integument, (b) SEM images of the cuticle surface. Before ecdysis, the new cuticle displays micro and macro folds, and 30 minutes later (after expansion but before sclerotization) no macro folds are visible, and micro folds have almost disappeared also. The outline of each epidermal cell that produced each patch of cuticle is visible (Bernays, 1972; Chapman, 2013)

1.3.1 Cuticle Growth

From this point on the overall thickness of the cuticle gradually increases for several weeks by deposition of further layers of endocuticle on the inner surface, orchestrated by the epidermal cells, in such a fashion that the number of days since the last moult can be counted (much like the rings on a tree trunk, see Figure 1.13 (Neville, 1963))

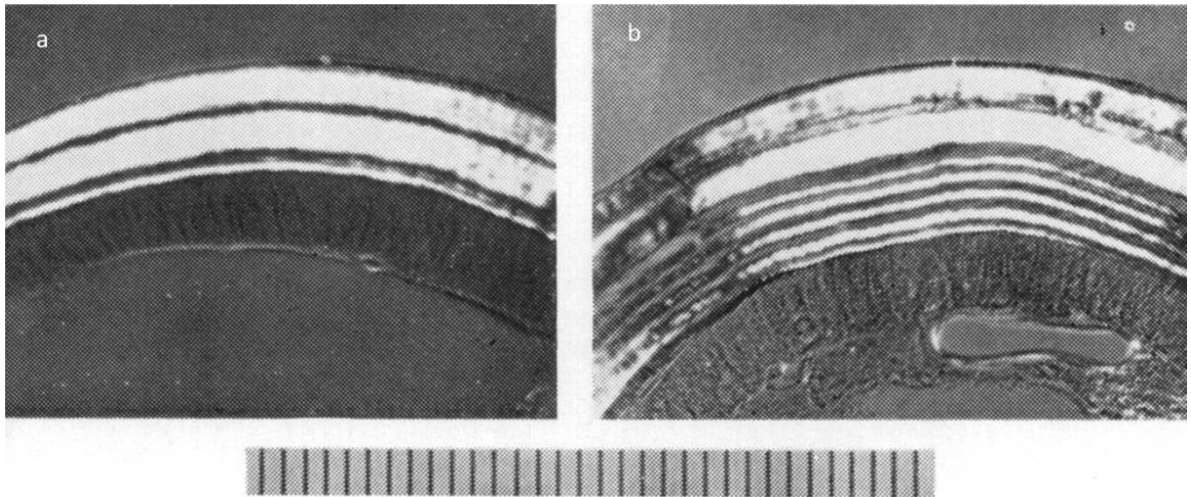


Figure 1.13: Sections from hind tibia of the long-horned grasshopper (*Decticus verrucivorus*) (a) shows the right-hand hind tibia removed one day after moulting, showing thick exocuticle, and a pair of layers (light and dark) of endocuticle. (b) shows the left-hand hind tibia of the same insect four days later. The exocuticle is the same as (a), but there are now 5 pairs of growth layers in the endocuticle. Scale: 1 division = 10 μ m. From Neville (1965).

1.4 Function

The skeleton of any animal is required to be stiff and strong, but also contributes significantly to the weight and energy usage. It can be assumed that evolution will tend to produce skeletal parts which are sufficient to provide locomotion and other physical activities while minimizing resource investment by not being too large and heavy.

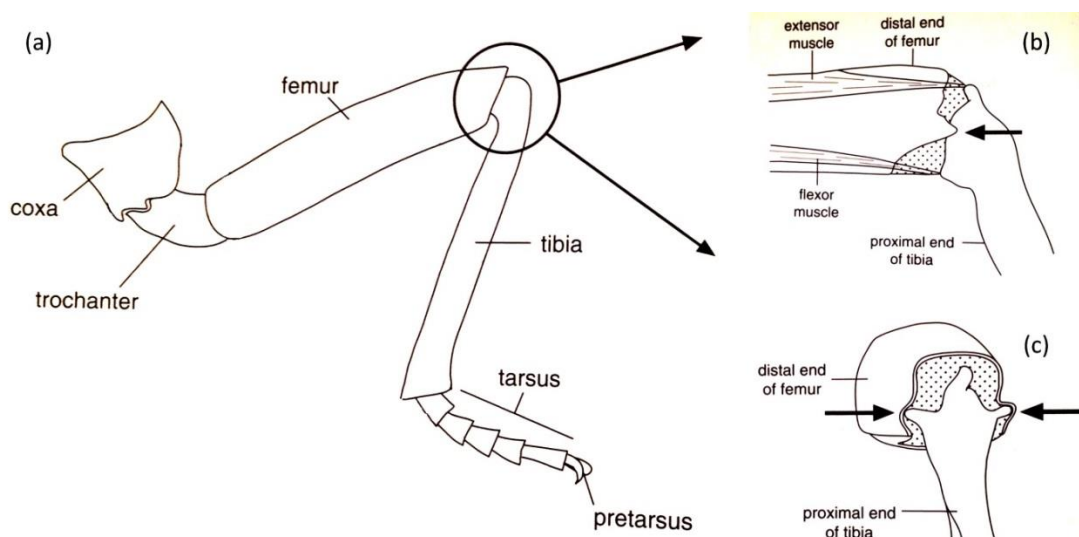


Figure 1.14: the anatomy of the segmented leg (a) with details of tibia-femoral (knee) joint (b) and (c) with points of articulation shown by arrows. Also shown in (b) is the extensor and flexor muscles which can pull the tibia in either direction about its articulation point. (Chapman, 2013)

The insect leg is a segmented structure consisting of the coxa, trochanter, femur, tibia, tarsus and pretarsus (shown in Figure 1.14). Unlike the endoskeleton of mammals, muscles and tendons are contained inside the insect bones (exoskeleton) as pictured in Figure 1.14 and 1.15 (a). Other features on the legs include hairs, hair plates and campaniform sensilla, all of which are part of the insect's sensory system (described in more detail later, and pictured in Figure 1.15 (b)).

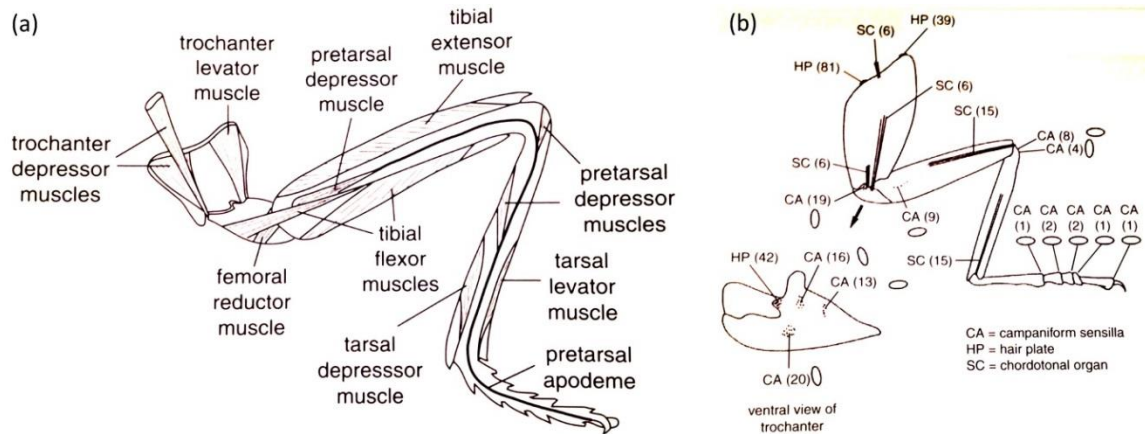


Figure 1.15: diagrams showing the intrinsic muscle groups (a), and the sensory system (b) of the insect leg. Numbers in brackets show number of sensilla in each group. Ellipses show orientations of campaniform sensilla. (Chapman, 2013)

Terrestrial locomotion, such as running and walking, is the primary function of most insect legs (other uses include jumping, grasping, digging, swimming and grooming). The biomechanics involved in such motion has been well researched (Section 1.8). Motor patterns seem to be coordinated centrally in tandem with sensory feedback from the terrain on which the insect travels. Strains are monitored by mechano-sensing organs (campaniform sensilla) on the legs. The viscoelastic nature of the cuticle found in the insect legs may also provide some stability during fast movements. Even standing still requires muscular activity. Forces – such as those experienced by a gust of wind – tending to change the angle of the leg segments (e.g. tibia-femur angle) are opposed by a muscular reflex. In the case of the femur-tibia joint, a tendency to reduce the angle is opposed by the extensor (Figure 1.14 (b)), and a tendency to increase the angle is opposed by the flexor.

The insect exoskeleton is not only a support and attachment for muscles, but is also used in feeding (mandibles), locomotion and reproduction. It provides the insect with a defence against

entrance or penetration of chemicals, fungi or disease, and a barrier against the exit or evaporation of water from within due to its surface chemistry. Its tough shell can also protect against predators. The exoskeleton will determine the shape, size and classification of the insect. It also lines the trachea, lines and protects the hindgut and foregut and forms the wings in adult insects. The tubular shape of the legs is a very economical use of material, providing great strength and relative lightness (compared to the endo or internal skeleton of vertebrates). Insect flight is made possible by the formation of the very light, rigid structures from which their wings are made.

Countless specialisations can be observed across insect species. In order to fulfil such a wide variety of functions, insect cuticle displays an enormous bandwidth of material properties (Vincent and Wegst, 2004). The mechanical properties of the cuticle hinge on the interaction of a number of variables – the amounts and orientation of the chitin fibres, the constituents and the degree of sclerotization within the protein matrix. Harder, stiffer cuticles tend to have low chitin content (15-30% dry weight) and high protein content (70-85%) together with a low (12%) water content. Softer flexible cuticles tend to have a roughly 50% chitin / protein mix (dry weight) and a high water content (40-75%). Different proteins (e.g. resilin) and the texture and orientation of the microfibrils can also give the cuticle different properties independent of the degree of hardening or cross-linking (Andersen, Peter et al., 1996). The shape of the cuticle itself can also contribute to rigidity. Metals and minerals can also be used to increase hardness (e.g. zinc reinforcement of the mandibles of the caterpillar (Fontaine et al., 1991)).

High stiffness, hardness or strength is not always desirable. Flexible membrane joints such as those in Figures 1.16 and 1.17 provide freedom of movement (together with muscles to provide fine control). The need for lubrication in many joints is completely eliminated due to such configurations. Soft extensible unsclerotized cuticle facilitates movement (by changes in body form) for many larval insects, and also permits growth without moulting (e.g. caterpillars). Altering the water content in cuticle can also modify its properties *in vivo*. A small percentage reduction during normal development in soft maggot cuticle can lead to a ten-fold increase in

stiffness. Conversely, the cuticle can be plasticized (e.g. *Rhodnius* taking a blood meal). Increasing the water content of its cuticle from 26% to 31% can decrease stiffness from 219 MPa to 10 MPa, enabling a stretching action that can increase the insect's body surface area four-fold, allowing it to consume a large meal. This is also reversible as the meal is digested and fluid is excreted.

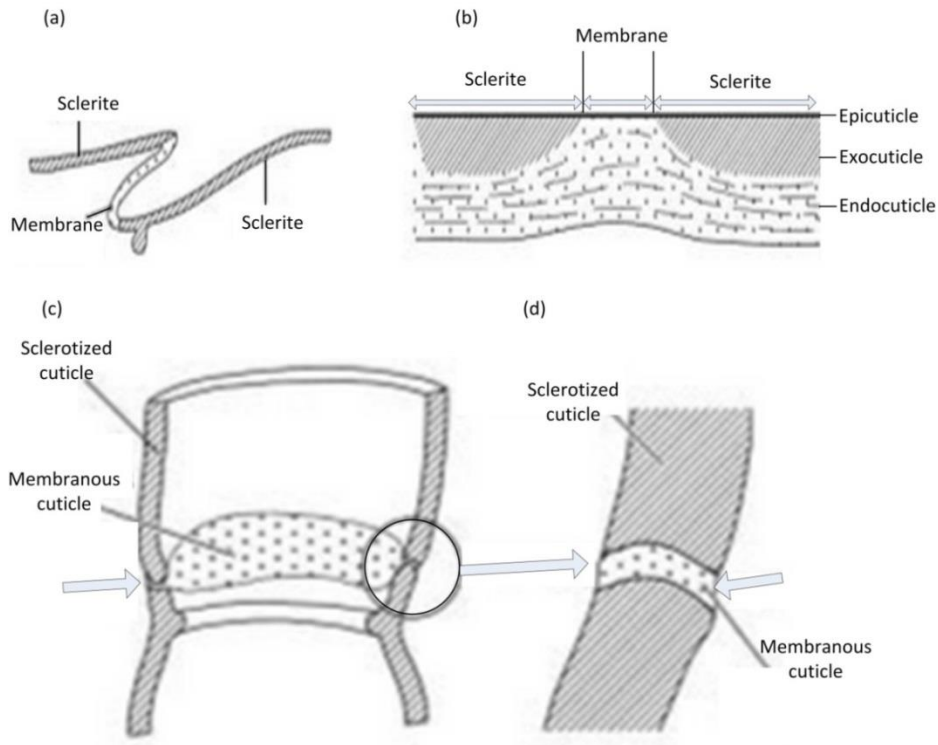


Figure 1.16: flexible (membranous) cuticle enables articulation at various joint types in the insect. (a) shows the arrangement of the intersegmental membrane (b) shows another membranous connection similar to (a). (c) and (d) show an intrinsic articulation found in most leg joints (point of articulation indicated by arrows) (Chapman, 2013)

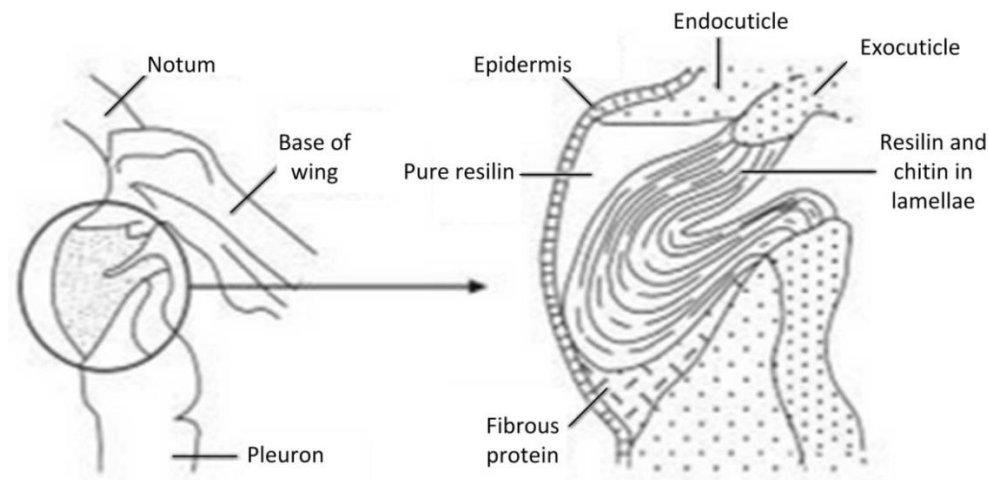


Figure 1.17: another joint, this time a section through the thoracic wall and wing base of a grasshopper, showing the position of the wing hinge, and the arrangement of endocuticle, exocuticle, layered chitin and resilin and the pad of pure resilin. (Chapman, 2013)

1.4.1 Sensory Capabilities of the Tibia

An extensive range of sensory receptors are present on insect legs (shown in Figure 1.15 (b)). These include hairs, spines, adhesive pads, and campaniform sensilla (among others). Some of these provide information on the relative positions of the leg segments (proprioceptors), while others are mechanoreceptors or chemoreceptors. Hair plates for proprioception are usually located next to joints on locusts, stick insects and cockroaches. Hair-like structures are anchored in a socket within the cuticle (see Figure 1.18 (a)). Protruding from the cuticle, the hairs allow movement by external stimulus such as touch or a gust of wind. Even a movement due to a very small force is amplified by the length of the hair (acting like a lever). The displacement of the hair within the socket triggers a neural stimulation. Such sensing organs ensure the insect responds in an appropriate manner when a certain part of its leg is touched.

Campaniform sensilla (Figure 1.18 (b)) are oval in shape and can monitor strains in the cuticle, being sensitive to compression along their short axis. They are most responsive to bending (the primary loading regime of the tibia). Stresses applied to the cuticle cause deformations in the campaniform sensilla, stimulating neural transmissions which in turn trigger appropriate reflex responses in muscles to alleviate the applied stresses (a negative feedback loop). These sensilla are often grouped together and can be oriented similarly or differently to monitor strains in different directions. For example on the proximal end of the tibia of *Periplaneta*, some are oriented parallel with the long axis of the leg, and others at right angles to it. An individual group can thus monitor both magnitude and direction of any applied force. They act as strain gauges or load sensors, and can respond to forces applied by the insect's own muscles, or external forces. Many are oriented at right angles to the direction of principal stress. Their structure can vary widely depending on their position. They can be found grouped beside joints, singly under spines on each leg (in some orthopteroid insects – such as cockroaches, locusts, crickets and stick insects), on the base of the antennae and on veins close to the wing base – all areas which are sensitive to stresses.

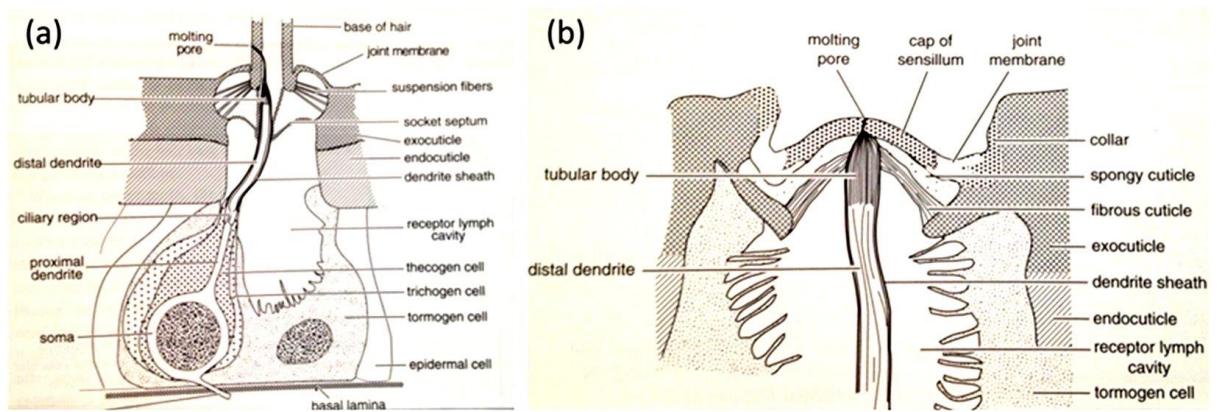


Figure 1.18: two tibia based sensing devices: (a) hair and (b) campaniform sensilla. (Chapman, 2013)

1.5 Mechanical Properties

Research into the material properties of insect cuticle has been somewhat limited compared to what has been done on vertebrate bones. Various techniques have been employed on a range of different insects and various body parts. Strength and elasticity have been established (Jensen and Weis-Fogh, 1962; Dirks and Taylor, 2012a), as have hardness and stiffness of various body parts (Hillerton et al., 1982; Muller, Olek et al., 2008; Sun et al., 2008). More recently, fracture toughness and fatigue properties have been published by our research group (Dirks and Taylor, 2012a; Dirks and Taylor, 2012b; Dirks et al., 2013). Different techniques employed include nano-indentation, tensile testing of whole tibia or of excised sections, and three-point and cantilever bending tests.

Stiffness (Young's Modulus, E) of insect cuticle has been shown to range from roughly 1 kPa to several GPa (see Figure 1.19, (Vincent and Wegst, 2004)) depending on the type of cuticle tested. This wide bandwidth of stiffness is achieved while keeping the density of the material more or less constant. Low density gives cuticle a lightness which is another attractive attribute, minimizing the weight that must be carried by the insect while walking and flying. Various factors such as fibre amount and orientation, degree of crosslinking, degree of hydration, etc. have been experimentally shown to affect the materials stiffness, hardness, toughness and strength (Schoberl and Jager, 2006; Muller, Olek et al., 2008; Dirks and Durr, 2011; Klocke and Schmitz, 2011; Dirks and Taylor, 2012a). Many older publications tested dried specimens. Often this was a necessary artefact of the tests due to preparation time, embedding etc. required. Later studies

established the profound effect that water has as a modulator of material properties in cuticle (Enders et al., 2004; Barbakadze et al., 2006; Schoberl and Jager, 2006; Vincent, 2009; Klocke and Schmitz, 2011; Dirks and Taylor, 2012a). For a particular cuticular structure; size, shape, the proteins and the fibre amounts and orientation are fixed. Permanent control of its material properties is dictated post-moult by the degree of cross-linking. The degree of hydration is the only variable that can be altered *in vivo* to achieve a more transient control of the material properties (Hillerton, 1984). The degree of cross-linking will also dictate the degree of hydration possible.

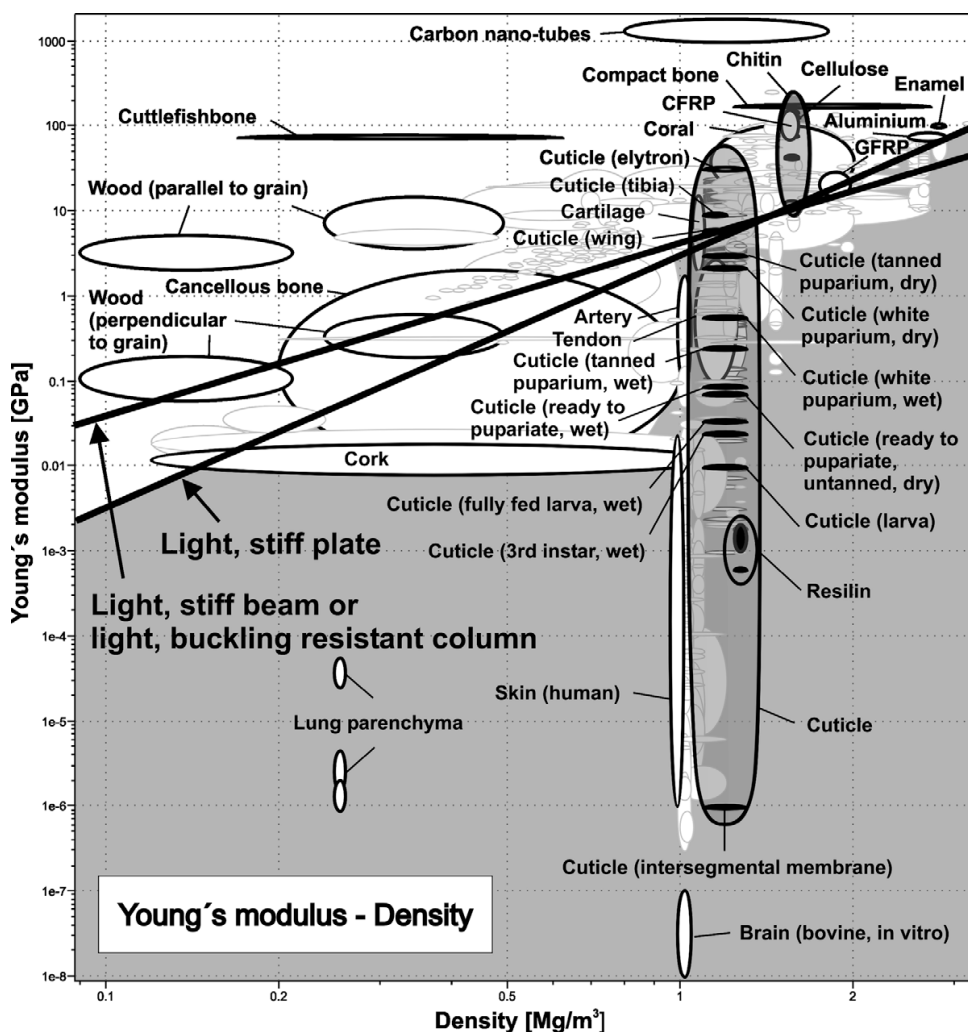


Figure 1.19: wide ranging stiffness observed in different types of insect cuticle from 1kPa to over 50 GPa (while the density remains between 1 and 1.4 Mg/m³). From Vincent and Wegst (2004).

Some basic material properties from more recent studies on the adult desert locust are outlined in Table 1.1

Property	Result	Researcher
E	3.05 GPa	Dirks and Taylor (2012a)
σ_{bending}	72.05 MPa	Dirks and Taylor (2012a)
σ_{tensile}	78 – 257 MPa (femur)	Hepburn and Joffe (1974)
K_{ic}	4.12 MPaVm	Dirks and Taylor (2012a)
G_c	5.56 kJ/m ²	Dirks and Taylor (2012a)
Hardness	0.05-0.15 GPa (sternum)	Klocke and Schmitz (2011)
Fatigue Limit (10 ⁵ cycles)	61.7 MPa (tibia) 14.3 MPa (wings)	Dirks, Parle et al. (2013)

Table 1.1: recently published values for stiffness, strength (bending and tensile), fracture toughness (K_{ic}), work of fracture (or strain energy release rate) G_c , hardness (tested by nano-indentation normal and transverse to the fibre orientation), and the fatigue limit. All data relates to fresh cuticle from mature adult desert locusts, specifically the tibia (unless otherwise stated).

Insect tibia cuticle can exhibit some quite extraordinary properties. Its stiffness is relatively low (3 GPa when fresh, upwards of 9 GPa when dry (Jensen and Weis-Fogh, 1962)) compared to other natural biocomposites such as cortical bone (14 GPa) and wood (11 GPa when tested along the grain (Engineering Toolbox Website, 2015)) and much less than structural materials such as steel (200 GPa) and aluminium (70 GPa). Its failure strength is also comparable to that of human cortical bone (100 – 120 MPa tested in tension), and aluminium (95 MPa).

Although sclerotized cuticle is very hard, it is not indestructible, and extensive wear has been observed on mandibles and the tibiae / tarsus of several burrowing insects such as desert harvester ants (Johnson et al., 2011).

Fracture toughness is a measure of a material's defect tolerance. The work of fracture (G_c) describes how much energy is required to form new surfaces during crack propagation. For both properties, the higher the number, the more difficult it is for a crack to propagate from an existing defect in the material. Its low stiffness coupled with its high fracture toughness combine to give cuticle a very high work of fracture value, making cuticle one of the toughest natural composites explored to date, much tougher than bone, and more similar to materials found in antlers and horns in vertebrates (Dirks and Taylor, 2012a)

This tolerance for defects no doubt contributes significantly to its remarkable fatigue properties. Fatigue is a measure of the durability of a material when cyclic loads less than the material's strength are repeatedly applied. Various parts of the insect exoskeleton must endure countless cyclic loads during normal locomotion. Extended periods of running / walking (locusts often walk with high intensity for up to 2 hours continuously (Moorehouse et al., 1978)) and vast migratory journeys undertaken (sometimes across thousands of kilometres) imply that legs and wings of insects must be extremely durable. Dirks, Parle et al. (2013) showed that the locust leg and wing can withstand up to 100,000 cycles while operating at 76% (61.7 MPa) and 46% (14.3 MPa) of their failure strengths respectively. Mammalian bone can resist fatigue failure to a certain extent by continuous repair – a process known as remodelling carried out by bone cells (Taylor and Lee, 2003). Insect cuticle performs on par with human cortical bone despite this process being absent – another indication that the body parts tested are highly durable, and that the fitness of the insect can be maintained despite the endurance of continuous cyclic loads.

These desirable properties are undoubtedly related to the composite nature of the material. Composite materials can often enjoy “the best of both worlds” in terms of material properties such as stiffness, lightness, toughness and fatigue.

1.6 Composite Materials

Composite materials consist of fibres (or particles) embedded in a matrix – in the case of insect cuticle: chitin fibres embedded in a protein matrix. The two materials are generally quite different. Usually a stiff fibre is used to reinforce a less stiff (or sometimes brittle) matrix, enabling the composite to better withstand compressive, tensile, shear and flexural loads. The matrix binds the fibres together, often protecting them from damage or wear due to mechanical abrasion or environmental corrosion. The matrix effectively isolates individual fibres, allowing them to act as separate entities. The fibres can be aligned in certain directions in order to better resist applied stresses. Loads applied to the composite can be transferred to the fibres (which bear most of the load), depending on the quality of the interfacial bond between matrix and fibres. A ductile matrix

slows / stops crack growth (even cracks originating from brittle or broken fibres), increasing the material's toughness. Conversely a brittle matrix depends on ductile fibres to trap cracks. Thinner, shorter fibres tend to contain fewer flaws.

Man-made composite materials can often be used to great effect for structural applications. For example – in aerospace, reducing weight by reducing material density can be preferable to increasing stiffness. This is achieved by using light, strong, stable fibres to reinforce some of the lighter engineering metals and alloys. Carbon fibres can be added to glass to reduce weight and reduce brittleness by allowing some plastic deformation at areas of high stress concentration (crack tips and defects or features in the glass). Metals can be reinforced with ceramic particles to improve strength, stiffness, hardness, creep and fatigue properties, increase wear and abrasion resistance and also increase the operating temperatures that the material can endure (such materials are commonly used in pumps, piston sleeves and engines). Essentially, composites can enjoy the benefits from material properties of both matrix and composite, thus functioning more effectively or efficiently than either would individually.

Naturally occurring composites include wood, bone, antler and horn. They often exhibit a similar hierarchical structure to insect cuticle (see Figure 1.21). Specifically, they all consist of long-chain polymer type molecules (chitin, collagen, cellulose, or keratin) which are grouped together to form micro-fibrils. These are grouped together to form larger fibres or fibrils which are embedded in a protein matrix. Layers of this material can be arranged in different manners to best resist forces experienced by the material (some such arrangements are shown in Figure 1.21 – note the similarities to Figure 1.2). Composites such as wood and bamboo are widely used in the construction industry due to their wide availability and desirable mechanical properties such as high strength, stiffness and toughness. Potential points of weakness and stress concentration are often reinforced by the fibres in naturally occurring biocomposites. The fibrous structure is oriented such that the material adjacent to these areas is given extra protection against potential damage or crack initiation. Features such as spiracles and sensors on insects form holes through the cuticle. Fibres are not interrupted by these holes, instead they are arranged around the holes

(see Figure 1.20) to reinforce the area, so the hole does not act as a stress concentration (Vincent and Wegst, 2004).

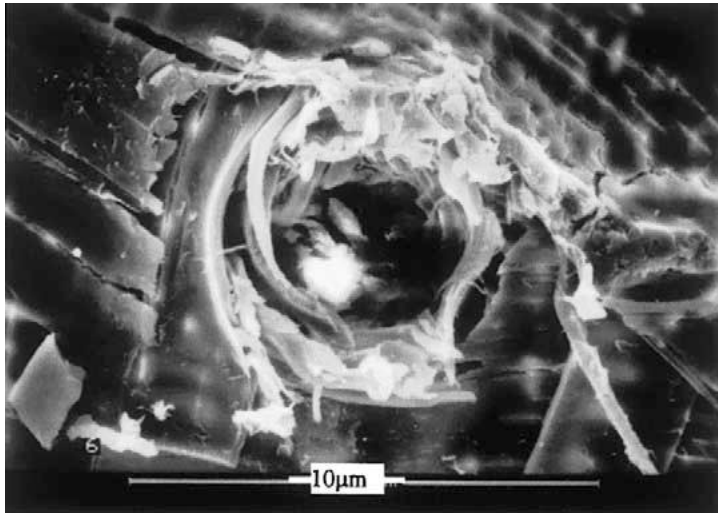


Figure 1.20: A pore or hole used as a transport channel is reinforced circumferentially by fibres (Chen et al., 2002)

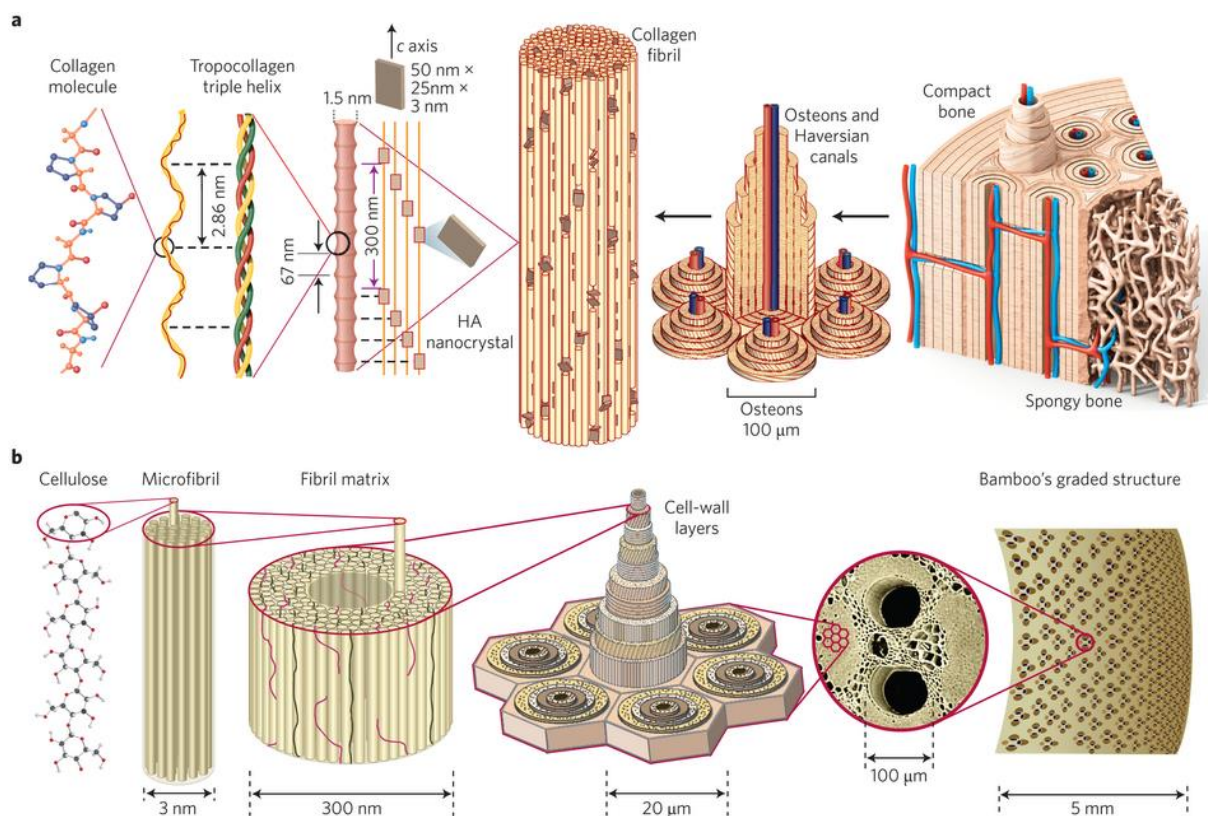


Figure 1.21: (Mortensen, 2006) the hierarchical structure of bone and bamboo. Note the similarities to that of insect cuticle (see Figure 1.2)

Composites behave differently and display different mechanical properties based on the applied load and orientation of the reinforcing fibres. Looking at the simplest model of unidirectional fibre (F) embedded in matrix (M), under uniaxial load P:

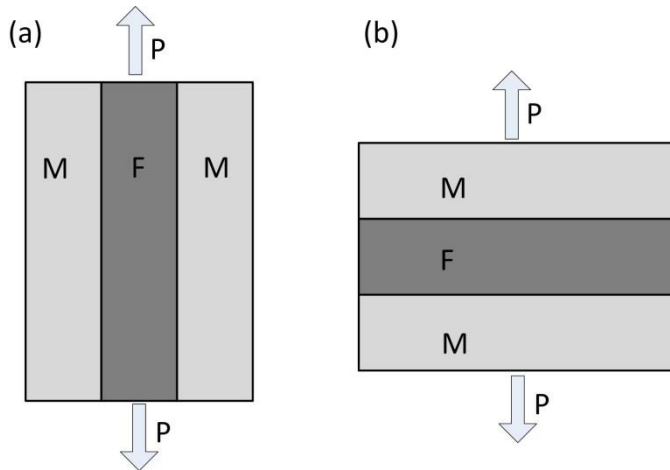


Figure 1.22: simplified examples of the two extremes of loading conditions possible for a fibre (F) matrix (M) composite structure

When loaded longitudinally (Figure 1.22 (a)), the composite will exhibit a higher stiffness than when loaded transversely (Figure 1.22 (b)). The fibres are better positioned to resist the applied loads as both the fibre and matrix will experience the same strain. Under transverse loading, the fibres can be said to be “poorly positioned” as the matrix can experience more strain than the fibres and the composite will usually fail due to matrix cracking – i.e. the composite properties are dictated by the matrix properties.

The stiffness of individual chitin fibres has been empirically estimated to range between 70-90 GPa (Wainwright et al., 1976; Ker, 1977; Hillerton, 1984). Stiffness of matrix proteins can be established by tensile testing cuticle with unidirectional fibres in a direction normal to the fibre direction (as in Figure 1.22 (b)). A stiffness of 2.7 MPa was established for the protein matrix of the inextensible locust intersegmental membrane (Hepburn and Chandler, 1976) and for *Calliphora* larval cuticle (Vincent, 1980). Similar analysis on *Schistocerca* tibial extensor apodeme (tendon) revealed a chitin fibre stiffness of 86 GPa and a matrix stiffness of 0.12 GPa. This shows that fibre stiffness is similar in stiff and pliant cuticles while the protein properties can differ

significantly. Therefore, the overall properties are dictated by the amount and orientation of fibres, and the type of protein.

It is a misconception that the stiff chitin fibres provide the hardness to cuticle, as pliant cuticle always contains more chitin than stiffer cuticle. The locust tibial extensor apodeme is 100 times stiffer than the locust intersegmental membrane, yet only has one third of the chitin content (Tychsen and Vincent, 1976; Ker, 1977). In stiffer cuticle, the chitin fibres act as the main load bearer, allowed to do so due to the stable inter-matrix and fibre-matrix bonds (which transfer the load to the fibrils) caused by the cross-linking seen in those cuticles. More pliant cuticles are less heavily cross-linked, so these bonds are not quite so fixed (they are more labile), meaning the load cannot be transferred as readily. In this case, the chitin fibrils contribute to the stiffness as a high aspect ratio filler (Hillerton, 1984).

1.6.1 Failure of composites

When the fibre is stronger than the matrix (as is the case for cuticle), matrix cracking or damage can be localised and arrested by the adjacent fibres (Daniel, 2006). As load is increased, adjacent fibres may break (if oriented similarly). These localised failures can eventually coalesce to produce catastrophic failure. Various loading conditions such as longitudinal or transverse compression or tension can bring about different mechanisms of failure. Most fibre matrix composites are weakest in transverse tension (as shown in Figure 1.22 (b)). Fibres may buckle under compression or fracture under tension. The matrix may also experience cracking or de-bonding from the fibres. During normal locomotion such as walking, running and jumping, the primary mode of loading for insect legs is bending (Sutton and Burrows, 2008), so a combination of these loads will be experienced at different zones in the tibia. Applying a cantilever bending load will put one side of the tibia under compression, and one under tension (outlined in Section 2.2.4).

The failure of an individual layer or group of layers in a laminate composite material usually does not imply total failure of the laminate. As failure begins, the intact layers must shoulder the stress previously experienced by the failed layers, which is possible due to different fibre orientations within the layers. Complex stress redistribution is at work here. For this reason, an alternating

fibre orientation is a distinct advantage over a unidirectional fibre orientation. A variety of fibre orientations affect the fundamental strength of each lamina, depending on load direction. The exact stacking sequence will affect the overall stiffness. Depending on what loads are to be applied, man-made composites can be designed to act or even to fail in the safest manner possible. This way, repairs may be easier to carry out, and catastrophic failures or irreparable damage may be minimized, and lower safety factors can be used.

Locust tibia cuticle displays an alternating unidirectional / helicoidal stacking pattern in its layered composite structure. Unidirectional fibres are predominantly orientated parallel to the tibia axis (Neville, 1965). This makes the tibia stiffest in this direction according to the rule of mixtures – optimizing the tibia for resisting bending loads. Other natural biocomposites such as bamboo, bone and wood display similar properties. Often the direction of the fibres is optimized to resist the applied loads (e.g. fibres or “grains” in wood are usually parallel to the main axis in trees or bamboo to best resist wind induced bending loads).

On review of several various composite models (Voigt (Voigt, 1928), Reuss (Reuss, 1929), Hashin-Shtrikman (Hashin and Shtrickman, 1963) and Mori-Tanaka (Mori and Tanaka, 1973)), it was decided that composite theory would not be used as a tool for analysis of the tibia cuticle – no model could sufficiently capture the complexity of the material such as the variation in fibre orientations.

1.7 Failure of Tubes

Slender thin-walled hollow tubes can provide a high strength to weight ratio and reduce material or resource investment. They can be found in both artificial (e.g. aircraft, catheters) and natural (e.g. plant stems, bones, insect legs) structures.

Under load, a tube may suddenly collapse by buckling, a mode of failure which is notoriously difficult to predict at the design stage. Elastic buckling occurs at stresses less than the yield strength or fracture stress of the material and is characterised by a condition of instability with respect to deformation in some direction. It is dependent on both the material stiffness (Young’s

Modulus), and the geometry / morphology – or how the material is arranged in relation to the applied load. In Euler buckling, for example, a column loaded in axial compression becomes unstable with respect to transverse displacements. Applying a bending load to a tube (such as that applied naturally during normal locomotion to an insect leg) can also result in a buckling failure. In this case two different phenomena can occur, known as *local buckling* and *ovalisation buckling* (Figure 1.23). Local buckling can arise in any thin plate structure experiencing compressive stress: out-of-plane displacements occur giving rise to localised kinks in the plate. In ovalisation buckling an initially circular tube becomes oval in shape as a result of applied bending loads, effectively reducing the second moment of area I . This type of deformation becomes unstable at a critical bending moment (Brazier, 1927), leading to a catastrophic loss of stiffness. The radius, thickness and stiffness of the tube to be loaded will all be factors in determining the stress to cause a buckling failure.

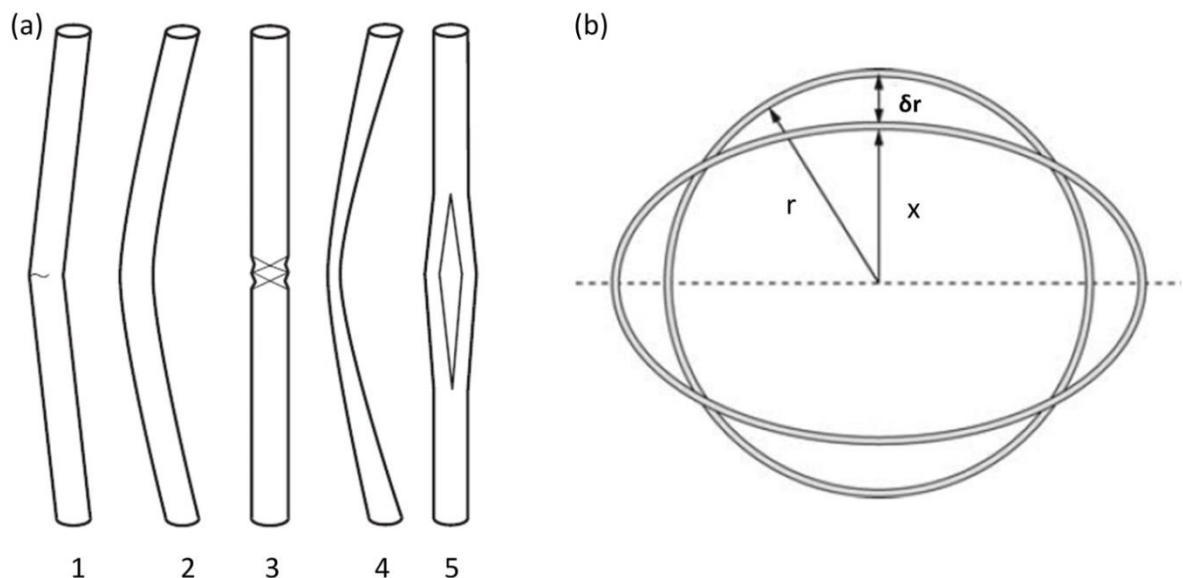


Figure 1.23: (a) some of the possible failure of modes a tube loaded in bending (Taylor and Dirks, 2012): 1 = fracture, 2 = Euler buckling, 3 = local buckling, 4 = ovalisation, 5 = splitting. Often 3 and 4 occur together. The point where ovalisation is most pronounced becomes a weak-point or instability which causes local buckling in the structure. (b) shows the cross section of the ovalisation of a tube in bending. The original radius r is reduced by δr to minor axis of the ovalised section x (Wegst and Ashby, 2007)

Even for the relatively simple case of a tube of circular cross section and constant wall thickness, loaded in pure bending, it is difficult to accurately predict the onset of buckling. Analytical

solutions often differ significantly from experimental results: e.g. (Timoshenko and Gere, 1961) and (Rees, 1997). For a tube of radius r and thickness t made from a material with Young's modulus E and Poisson's ratio ν , the critical bending moment M_b for both local buckling and ovalisation buckling can be described by the following equation:

$$M_b = \frac{\alpha r t^2 E}{\sqrt{1-\nu^2}} \quad (1.1)$$

Assuming a Poisson's ratio of 0.3, maximum stress in the tube at this bending moment is given by:

$$\sigma_b = \beta E \frac{t}{r} \quad (1.2)$$

- Obtained from using the flexure formula:

$$\circ \quad \sigma = \frac{M_b * r}{I} \quad (1.3)$$

- And assuming a thin-walled tube ($t \ll r$), the second moment of area can be simplified to:

$$\circ \quad I = \pi r^3 t \quad (1.4)$$

The constants in equations 1.1 and 1.2, α and β , have been assigned different values by different workers in the past. For example several textbooks (Timoshenko and Gere, 1961) quote a value of $\beta = 0.605$. However NASA conducted an extensive investigation, comparing theoretical and experimental data for a wide range of tube dimensions and materials (NASA, 1968). They proposed that this constant should be lower, and should vary with r/t , having a value of 0.525 for $r/t = 10$ (the lowest r/t value considered), decreasing slightly to 0.500 for $r/t = 20$. Wade et al. (2006) developed a computer simulation for a tube in pure bending: they predicted that local buckling would occur before ovalisation buckling and found a value of $\beta = 0.542$ for $r/t = 10$. Calladine proposed a much lower value of 0.313 in his analysis, which predicted local buckling whilst taking account of the change in shape caused by ovalisation (Calladine, 1983). Thus even for this relatively simple case the literature gives values for the critical buckling load which vary by almost a factor of 2. For more complex cases it may be appropriate to use finite element analysis (FEA). A simple linear elastic analysis will not predict buckling. Many commercial FE packages have special routines for detecting elastic instability. Alternatively, it may be possible to simulate

buckling by using the facility of FE packages to accommodate large deflections using iterative analysis to detect geometric nonlinearities, i.e. non-linear force-deflection relationships which occur due to significant changes in the shape of the body during loading.

Many naturally occurring tubular structures such as plant stems, bamboo and insect legs tend to be orthotropic – that is, their strength and stiffness are greater parallel to the main axis than circumferentially. These tubes are much stiffer and stronger in bending than equivalent tubes made from isotropic material (same properties in all directions) – usually due to the fibre direction being parallel to the tibia axis. Wegst and Ashby (2007) showed that orthotropic tubes containing fibres parallel to the main axis often fail in compression by fibre buckling at a stress which is lower than the tensile stress.

For some combinations of geometry and material properties σ_b will be higher than the yield strength or fracture stress of the material, in which case failure will occur by yielding or fracture before elastic buckling. For stresses close to this critical value, the two modes of buckling and yielding/fracture may interact. It can be shown that an optimal strength to weight ratio is achieved when these two modes of failure are equally likely. Wegst and Ashby (2007) developed this analysis for the case of materials with orthotropic mechanical properties and applied it to plant stems.

Taylor and Dirks (2012) applied the same approach to two arthropod limb segments, the hind tibia of the locust and the merus of the blue crab, showing in both cases that the r/t ratio was close to the predicted optimum value. The technique involved plotting predictions for different failure modes (Figure 1.24), and comparing to experimental values. The point where two failure modes intersect gives an r/t ratio that is optimized for resisting both failure modes. For example, in Figure 1.24 (a), the normalized bending moment is plotted as a function of r/t . The r/t value of 7.2 is the point of intersection of buckling and fracture. At this value, failure is just as likely to occur by buckling as by fracture, therefore the structure is optimized to resist bending. The value

of 29 is the point of intersection for Euler buckling and local buckling, therefore this is the optimal r/t value for resisting axial compression (Figure 1.24 (b)).

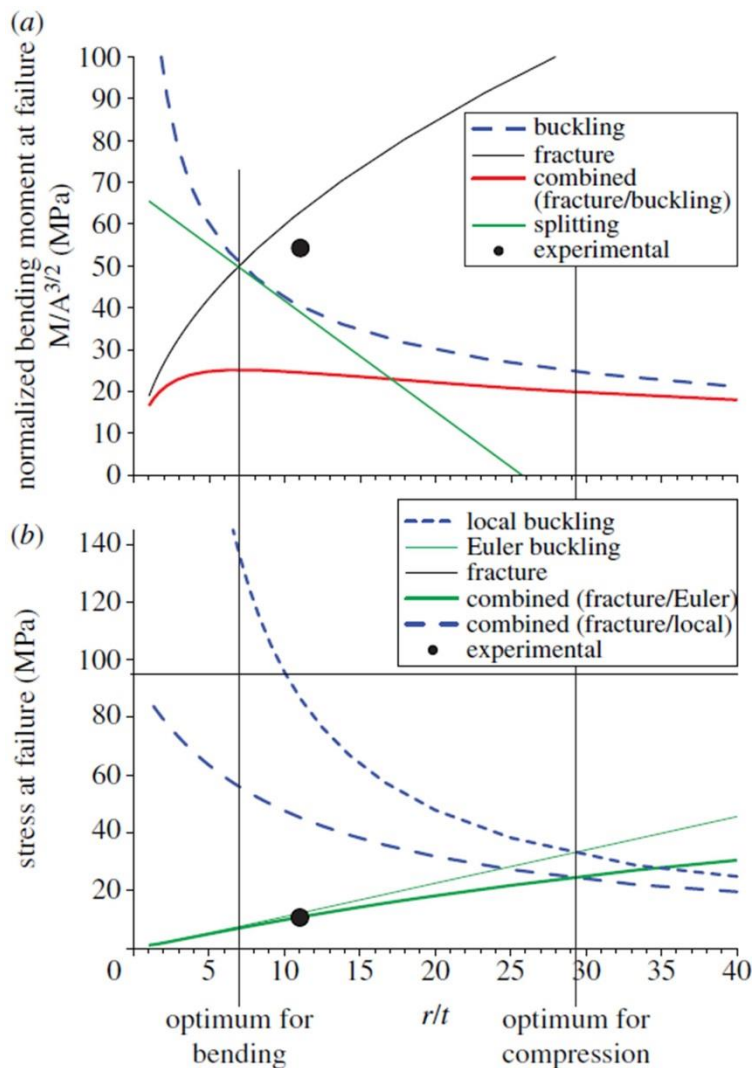


Figure 1.24: (Taylor and Dirks, 2012). Predictions for the locust tibia loaded in bending (a) and axial compression (b). Vertical lines show optimum values to resist each type of load. Experimental data points (black dots) show the r/t value for the locust leg lies much closer to the bending prediction than the compression. In bending, the leg is stronger than predicted (dot lies over buckling prediction, but under fracture). In compression, the failure stress is well predicted.

Apart from this paper, there has been no work published on buckling failures of insect cuticle, though one review mentions the fact that some body parts have ridges which might resist Euler buckling (Vincent and Wegst, 2004). The primary mode of loading for insect legs is bending, as a result of ground reaction forces during normal daily activities (explained in Section 1.7). As such, understanding the possible failure modes of the leg due to these bending loads is biologically relevant.

1.8 Biomechanics

1.8.1 Walking and Running

When walking and running, six-legged insects commonly use an alternating tripod gait. The right-front, right-hind and left-middle legs contact the ground at approximately the same time during a stride, and this alternates with the left-front, left-hind and right-middle legs. This gait has been characterised as a running or bouncing gait despite the lack of an “aerial” phase (Full and Tu, 1990; Full and Tu, 1991). Similar to mammalian running bipeds or trotting quadrupeds (Cavagna et al., 1964; Cavagna et al., 1977), there is interplay of potential energy due to gravity and horizontal kinetic energy as the insect’s centre of mass undergoes repeated accelerations and decelerations with each step, even when travelling at a constant average velocity. Each leg pair (front pair, middle pair, hind pair) performs a unique function during hexapedal locomotion in the forward propulsion of the insect’s centre of mass, and each displays a different ground reaction force pattern (Full et al., 1991). The legs of most insects (at least, the ones examined in this thesis) are positioned laterally instead of underneath the body, like birds or mammals. This leads to the production of horizontal and lateral forces 2-4 times larger (when compared to vertical forces) than those experienced in mammals and birds. This actually works to the insects’ advantage, reducing joint moments and total muscle force required for movement (Full, Blickhan et al., 1991).

Gait can change depending on the velocity of the insect (or stride frequency). The American cockroach (*Periplaneta americana*) employs the tripod gait similar to the Death’s Head cockroach (*Blaberus discoidalis*) when moving at speeds less than 1.0 m/s (Full and Tu, 1991). When travelling faster, it uses four legs (hind and mid-legs only), and at top speeds exclusively uses its hind legs for propulsion. This cockroach can move at speeds of up to 1.5 m/s (or 50 body lengths per second), its stride frequency approaching wing-beat frequencies during flight (25 Hz, Delcomyn (1971)). At these speeds it is probably not necessary to use all six legs. At all speeds, the pattern of ground reaction force is consistent. The insect accelerates its centre of mass upwards, forwards and to one side during each step irrelevant of the number of legs used.

1.8.2 Forces

Recording three dimensional ground reaction forces (such as those shown in Figure 1.25) is crucial for biomechanical analysis.

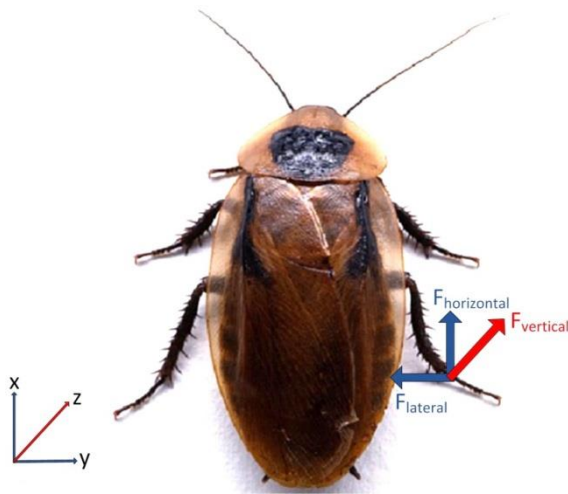


Figure 1.25: ground reaction forces for a death's head cockroach hind leg: $F_{\text{horizontal}}$ (in the x direction), F_{lateral} (in the y direction), and F_{vertical} (in the z direction). Photo from www.dailymail.co.uk

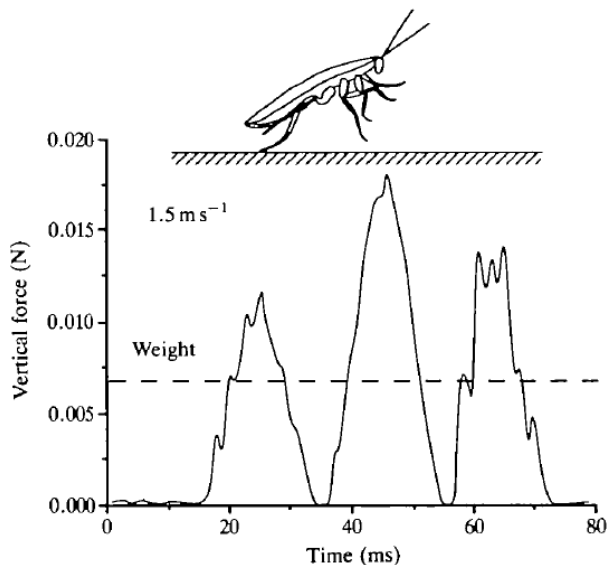


Figure 1.26: from Full and Tu (1991): the ground reaction force in the vertical direction for *P. americana* running exclusively on its hind legs. Areas showing a zero force indicate an aerial phase. Cockroaches running in this manner elevated their body with their head angled upwards (at 23°)

A variety of techniques have proved successful for performing accurate measurements for ground reaction forces on such small animals. These include custom built miniature force platforms used to gather data such as that shown in Figure 1.26, (Full and Tu, 1990; Full and Tu, 1991) combined with video analysis (Reinhardt et al., 2009) and photoelastic force platforms (Full et al., 1995)

among others. Ground reaction forces expressed in the x, y and z directions (horizontal, lateral and vertical respectively) can be resolved using basic vector mathematics to obtain a resultant force experienced by the leg:

$$F_{resultant} = \sqrt{F_x^2 + F_y^2 + F_z^2} \quad (1.5)$$

1.8.3 Jumping

Locusts, grasshoppers, fleas and other insects employ a complex mechanism for performing their jumps. A spring-like device is used to store the energy of a flexed muscle. This energy is then transmitted to the tibia, pushing against the ground with high speed and force, catapulting the insect into the air with forces equal to many times its mass (Bennet-Clark, 1975). The source of power for this push comes from the contraction of muscles inside the leg – namely the extensor and flexor apodemes (similar to muscles or tendons). These are used during walking to move the tibia about its pivot (Figure 1.27).

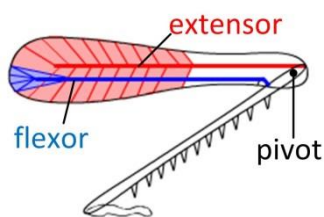


Figure 1.27: the extensor muscle and tendon (red), flexor muscle (blue), and the pivot about which the tibia moves relative to the femur (Heitler, 2012)

The process of jumping (photographed in Figure 1.30) is outlined in Figure 1.28. Firstly the flexor muscle is contracted to draw the tibia toward the femur (1.28 (b)). The large extensor muscle is contracted slowly (to achieve maximum force), transferring energy to the semi-lunar process (Figure 1.28 (c)). Its composition of heavily sclerotized cuticle and the protein resilin allows it to act like a coiled spring (or an archer’s bow). The flexor also remains contracted to keep the tibia in position. Then there is a “trigger relaxation” of the flexor (Figure 1.28 (d)), which allows rapid and forceful extension of the tibia. The energy for the jump is built up slowly by muscle contraction, stored in the semi-lunar process, and released very quickly. This is enabled by “Heitler’s Lump”,

which acts as a catch to hold and release the flexor apodeme. The anatomy of the locust tibia-femoral joint is shown in more detail in Figure 1.29.

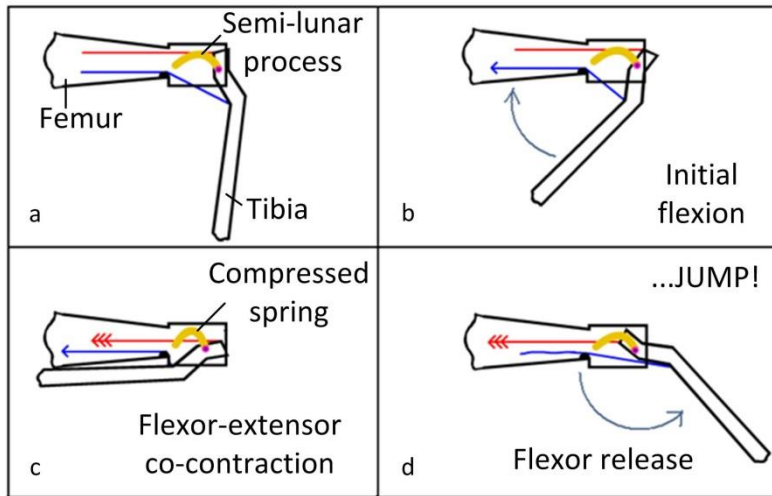


Figure 1.28: tibia motion during jumping (Heitler, 1977)

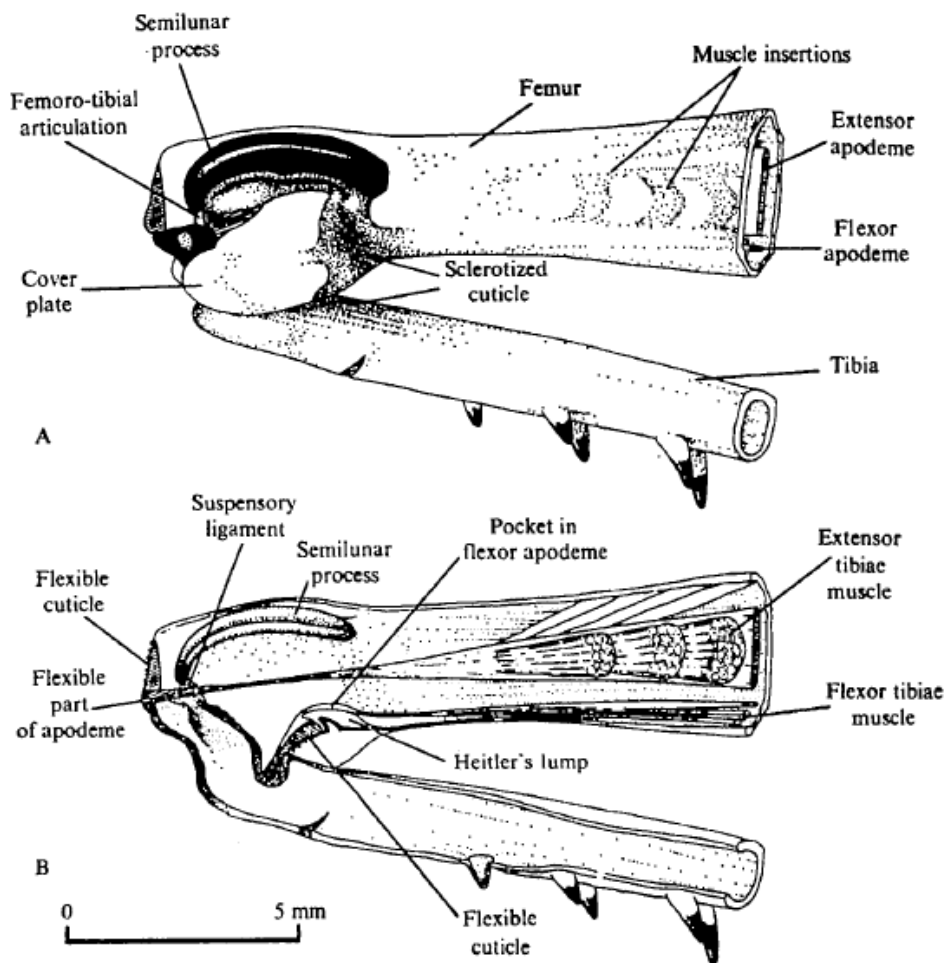


Figure 1.29: from Bennet-Clark (1975): detailed internal structure of tibia-femoral joint

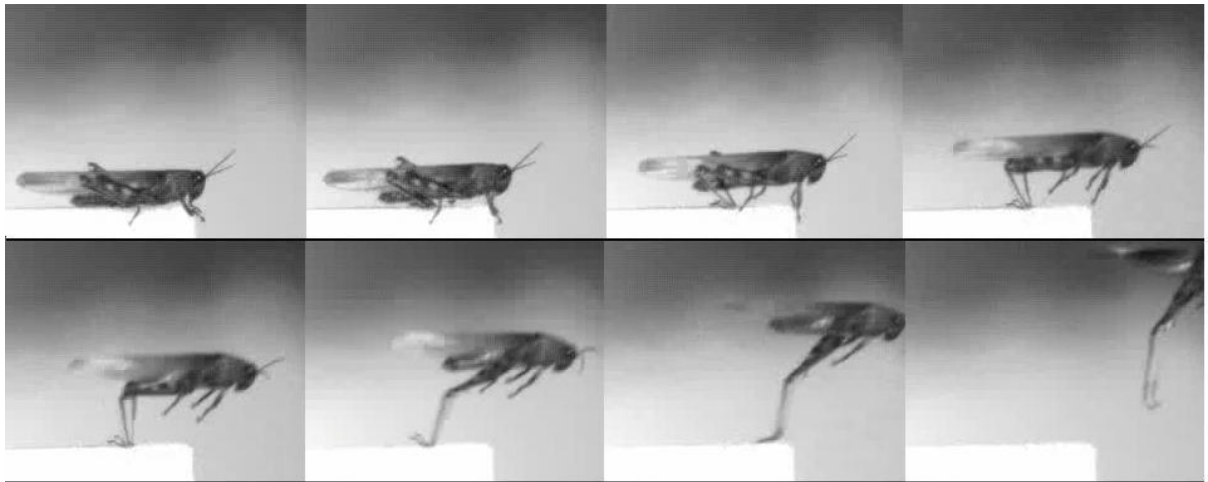


Figure 1.30: video micrograph slides animating the locust jump (Heitler, 2012)

Ground reaction forces have been measured for the locust jump (Bennet-Clark, 1975). Similar measurements have also been carried out on other so-called “emergency behaviour” which is more seldom performed behaviour such as righting (when overturned, (Full, Yamauchi et al., 1995)) and wedging (squeezing through a small crevice, Full and Ahn (1995)). Table 1.2 shows that the ground reaction forces for emergency behaviours are far greater than those for normal running / walking.

<i>Insect</i> (Source)	Activity	Ground Reaction Force (N)
<i>P. americana</i> (Full and Tu, 1991)	Running	0.015 _{vertical} 0.003 _{horizontal}
<i>B. discoidalis</i> (Full, Blickhan et al., 1991)	Walking	0.011 _{vertical} 0.005 _{horizontal}
<i>B. discoidalis</i> (Full, Yamauchi et al., 1995)	Righting	0.142 _{vertical} 0.034 _{horizontal}
<i>B. discoidalis</i> (Full and Ahn, 1995)	Wedging	0.18 _{resultant}
<i>S. gregaria</i> (Taylor and Dirks, 2012)	Jumping	0.15 _{resultant}

Table 1.2: ground reaction forces measured for different insects

Cuticle of various body parts is customized to suit a particular function. That of the tibia must be durable enough to withstand countless cyclic forces during running and walking without succumbing to a fatigue failure, and must also possess sufficient static strength to withstand forces experienced during emergency behaviour.

1.9 Insect Wound Healing Response

The ability to heal wounds is essential for the survival of any animal. The processes involved in wound healing in mammals and arthropods have been studied extensively. Much research has been done into the roles played by chemistry, biology and genetics in the wound healing of insects (summarized in Table 1.3). Mammals can heal broken bones and repair broken skin, restoring the structural and functional properties of the material to their pre-injury state (Li et al., 2007). Unlike mammal tissue, cuticle is acellular and is not vascularized. Instead, it relies on a network of pore canals to connect it to the hemolymph through the epidermis and basal membrane. How do these function in response to an injury? To understand the factors that could contribute to restoring the mechanical strength and stability of the insect exoskeleton (and insect cuticle in general) after wounding, it is necessary to study the processes involved in wound healing in detail.

Author	Insect Studied	Methods Used	Subject Investigated
Wigglesworth (1937)	<i>Rhodnius Proxilus</i>	Light microscopy	Robust wound healing response, cell migration
Locke (1966)	<i>Rhodnius proxilus</i>	Implanting of inert objects into the cuticle	Migration of epidermis over an implant
Lai-Fook (1968)	<i>Rhodnius Proxilus</i>	Light microscopy and electron microscopy	Wound response without breach of epidermis (using sandpaper)
Rowley and Ratcliffe (1978)	<i>Galleria mellonella</i> (Wax moth)	Histological techniques	Wound reaction steps for first 72 hours after wounding
Dillaman and Roer (1980)	<i>Carcinus maenas</i> (green crab)	SEM observations	Deposition of material over 69 days following puncture wound
Wright (1987)	<i>Drosophila melanogaster</i> (fruit fly)	Genetic and chemical review	Melanisation in response to infection
Marmaras et al. (1996)	<i>Ceratits capitata</i> (Mediterranean fruit fly)	Cellular and biochemical analyses. Incubated cuticular proteins with E. coli, dopamine and tyrosine	Defense reactions in relation to melanization and sclerotization
Lai et al., (2001)	<i>Armigeres subalbatus</i> (mosquito larvae)	SEM observations	Mechanism of coagulation and melanization

Galko and Krasnow (2004)	<i>Drosophila melanogaster</i> (larvae)	Puncture wounds, genetic mutations, live imaging and genetic tools	Cellular events and genetic requirements of epidermal wound healing
Belacortu and Paricio (2011)	<i>Drosophila melanogaster</i>	Live imaging and genetic tools	Effect of suppressing genetic pathways on different wound healing processes. Especially epithelial repair

Table 1.3: a brief index of some of the previous research into insect wound healing, the insect examined, methods used, and subject investigated.

1.9.1 How does the insect's immune system work?

Insects may lack the elements necessary for the adaptive immune response of vertebrates (Breugelmanns et al., 2008) but they do exhibit their own unique immune systems (Marmaras, Charalambidis et al., 1996). The first line of defence for any arthropod is the physical barrier of its integument (Rowley and Ratcliffe, 1978). Cuticle itself is relatively stiff, strong and tough (Vincent and Wegst, 2004; Dirks and Taylor, 2012a) and provides a physical obstacle which prevents potentially infectious organisms from penetrating into the body cavity (Dunn, 1991). The surface of the epicuticle prevents adhesion required for fungal and bacterial colonization and is also impregnated with antibacterial and antifungal lipids and peptides (Breugelmanns, Van Soest et al., 2008). The integument is most easily (and most often) breached post-molt when tanning is incomplete and the cuticle is still soft (Rowley and Ratcliffe, 1978). When pathogens manage to breach through the cuticle, a second line of defence is initiated in the form of cellular reactions (namely the hemocytes, (Lackie, 1988)). This defence can include formation of larger aggregates for encapsulation (phagocytosis) of foreign bodies such as parasites and pathogens. The hemolymph also carries various non-cellular (humoral) products that protect the insect against infection (Chapman, 2013). These can be almost undetectable in uninfected insects, but increase vastly in response to infection by bacteria or mechanical wounding. If the physical integrity of the cuticle is interrupted; three "classic" steps are always induced in both insects and other arthropods such as crabs (Sewell, 1955). These are hemolymph coagulation, melanisation, and cell migration (Chapman, 2013).

1.9.2 Coagulation

The first step in any wound healing process is coagulation. Coagulation in all animals can be defined as the formation of an insoluble matrix in the blood that stops bleeding (hemostasis), assists wound healing and protects against infection. Few similarities have been found between coagulation processes in different insect species, and even the same species at different life stages can exhibit different coagulation characteristics (Dushay, 2009). For example, mosquito (*Armigeres subalbatus*) hemolymph clotting involves filamentous filopodia interconnecting with cytoplasmic strands to form a network coagulum resulting in wound closure (Lai et al., 2001), while locust larvae form a plasma matrix to which hemocytes attach themselves (Dushay, 2009). Indeed, plasma and hemocytes seem to be one common factor in coagulation for insects, and clotting tends to take place quite rapidly (which is why it is so difficult to study). What is happening at a molecular level during coagulation in any insect is far from being well understood, and the process is quite different from that of the clotting of vertebrate blood, although the purpose is the same for both classes of animal.

A scab will not form unless the cuticle is breached (e.g. a pinch wound will not result in a scab (Galko and Krasnow, 2004)) which suggests that contact with the air may be a cause for this reaction. Experimentally, any blood which escapes to the surface dries in air to form a scab or plug, which is composed of debris such as necrotic cells (damaged by wounding), and coagulation products (Nakamura et al., 1976; Barwig, 1985; Geng and Dunn, 1988; Scherfer et al., 2004). In some larger insects with hard cuticles, the hemolymph may be under less than atmospheric pressure, and so the insect does not bleed noticeably when injured (Dushay, 2009). In this case, coagulation is not necessary for stemming blood loss, but is functionally important in wound healing and prevention of infection. Clots of larger insects tend to form as a soft “primary” clot which is then melanized (increasing its mechanical strength).

1.9.3 Melanization

A melanization or sclerotization reaction (often both occur together) is the second stage of the insect wound healing response, and it occurs in conjunction with or immediately after

coagulation. *Sclerotization* or “tanning” (outlined in Section 1.2.6) refers to the normal cross-linking of cuticular proteins in the matrix containing the chitin fibres. It usually involves hardening, darkening and (to some degree) desiccation of the cuticle, and occurs shortly after moulting. *Melanisation* is a reaction that leads to the synthesis of a brown-black insoluble humoral material known as melanin, which is involved in encapsulation of foreign bodies and parasites, blood clotting, wound healing and cuticle sclerotization.

The synthesis of melanin forms toxic intermediary compounds which are thought to kill invading microorganisms.

Although neither melanization nor sclerotization are completely understood, they are similar in many respects. ProPO (prophenoloxidase), tyrosine and p47 are biologically activated molecules which play an important role in both processes in *Ceratitis capitata* (Marmaras, Charalambidis et al., 1996). These non-cellular materials cross-link with proteins such as LPS (lipopolysaccharide) during sclerotization and during wound healing. DDC (dopa decarboxylase) is another important enzyme not only for sclerotization and melanization, but also for immune responses (Marmaras, Charalambidis et al., 1996). In the locust, protease inhibitors (PI) in the hemolymph prevent the unwanted activation of the cross-linking process *in vivo* unless required. They also inhibit invading pathogenic fungi and thus prevent the degradation of the insect cuticle and / or internal tissues (Dushay, 2009).

Unlike coagulation, melanization of the cuticle can also occur when the epidermis is not breached (Lai-Fook, 1966). Superficial damage (e.g. abrasions using fine emery paper Lai-Fook (1968); Johnson, Kaiser et al. (2011)) to the surface of the insects' integument can result in the cuticle adjacent to the damaged area becoming more heavily sclerotized (often darkening in colour also). This is attributed to a reactant(s) supplied from the hemolymph through the epidermis via pore canals to the wound site in response to the injury. The reactants only become active (or are catalysed) upon arriving at the injury site. Pore canal filaments are also thought to be the line of communication of disturbances in the epicuticle to the epidermis. The epidermis and basal membrane actively control the number and type of molecules that cross from the hemolymph

into the cuticle when required (e.g. in response to injury (Lai-Fook, 1968)). This control is maintained even when a large imbalance is produced in the hemolymph experimentally. The control only breaks down when the epidermis is permanently damaged.

In the open circulatory system of insects, when wounded, the coagulation and melanisation of the hemolymph is used to seal wounds, limit fluid loss and entrap potentially harmful microbes at wound sites (in horseshoe crabs, their clots kill bacteria (Bergner et al., 1997)). The melanised scab also acts as a scaffold across which the epidermis can migrate.

1.9.4 Cell Migration

The third step in wound repair is the repair of the epidermis, which continues after the clot has formed and melanised; the clot itself acting as a scaffold to enable this repair. When a section of the insect's integument is removed, epidermal cells adjacent to the wound will elongate and migrate into the excised region from all sides, clearing debris (see Figure 1.31). This usually occurs within 48 hours. The epidermis will even migrate around the edges of a foreign body (such as an impermeable implant of glass or Teflon, (Locke, 1966)). Activation is most pronounced around areas suffering the most injury (e.g. at corners of an excision). The lack of continuity of the epidermis seems to be the cause of growth (cell movement and cell division) – this does not cease until the continuity of the epidermis has been restored and a normal cell density has been established (4-5 days).

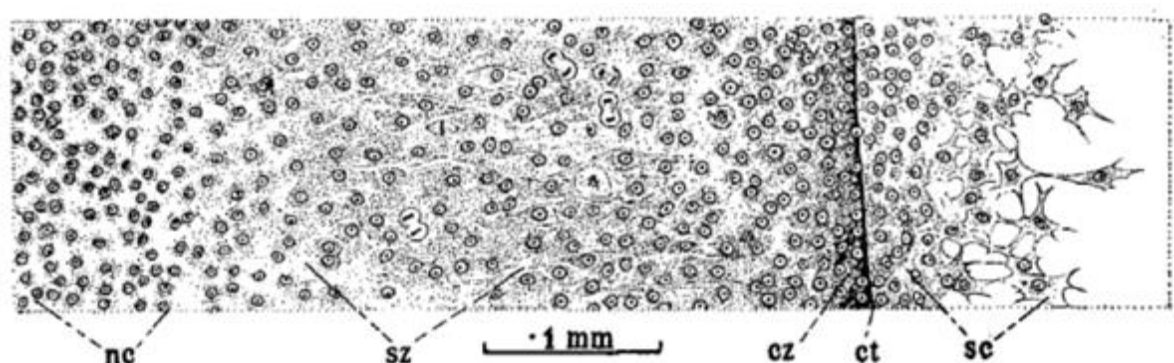


Figure 1.31: from Wigglesworth (1937): the epidermis of adult cuticle 4 days after an excision of about 1mm square. ct = margin of excised area, cz = zone of congested cells along the cut margin; nc = normal unchanged cells; sc = cells spreading over the excised area; sz = zone of sparse activated cells, many undergoing division.

Only when its continuity is restored can the epidermis begin to secrete new cuticle, maintaining the integrity of the surface. Newly deposited cuticle is continuous with old cuticle at the wound margin and does not seem to be sclerotized or differentiated into separate exo and endo cuticles – only endocuticular material is deposited. All new-formed tissues (with the exception of nerves) that arise during regeneration in arthropods are derived from the epidermis. This demonstrates how important its restoration is to the survival of the animal.

1.9.4.1 Stimulus for cell migration

No difference in the amount of migration and aggregation of cells has been observed when comparing a simple incision to an excision of several millimetres (Wigglesworth, 1937). This suggests the scale of the injury is unknown to the neighbouring cells – only that there is a connection missing which was previously present. The actual stimulus for the cells to migrate may come from a lack of some diffusible chemical that the epidermal cells normally get from their neighbour. When the neighbouring cells are removed, it prompts the epidermis to grow and migrate. Migration only occurs in the presence of hemocytes, suggesting the migration could be regulated by a factor produced by the hemocyte (Bohn, 1975).

These responses are coordinated, and each stage performs a discrete function of the well-orchestrated wound healing process. The absence of any one stage will ultimately hinder the effectiveness of any later stages, but their activation is not coupled or dependent on one another. They are under separate genetic controls, each of which can be suppressed without stopping another (Belacortu and Paricio, 2011). The absence of a scab usually results in a chronic wound as there is no scaffold for the epidermal cells to migrate across/through. Suppressing the gene necessary for the formation of “crystal cells” used for melanisation in *Drosophila* showed that only 15% survived after 24 hours (Galko and Krasnow, 2004). Inactivation of the JNK pathway through gene suppression stops the epidermis migration (but does not affect scab formation or melanization) which also results in a chronic wound (Galko and Krasnow, 2004).

1.9.4.2 Hemocytes

These cells (residing in the hemolymph) play a vital role in the healing of wounds and infection prevention throughout all life stages of the insect. They include:

- The *prohemocyte* – a stem cell from which other hemocytes are derived
- The *granulocyte* (or granular cell). This releases intracellular granules when activated (as part of a “degranulation process”) which help form clots and encapsulate foreign bodies. (Rowley and Ratcliffe, 1976)
- The *plasmatocyte* (strongly adherent and can spread across foreign surfaces). These are the most active cells in the repair of an integumental wound (Lai-Fook, 1966). Necrotic cells and tissue damaged during wounding are encapsulated by a multi-layered sheath of plasmatocytes (Rowley and Ratcliffe, 1978).
- Plasmatocytes contain granules which become less dense in response to wounding. The granules behave as “storage products” whose contents provide a precursor material to the deposition of new cuticle material – i.e. tissue formation. Conversely, the granulocyte may convert material (necrotic cells, debris etc) taken up from the wound into a storage granule.

Plasmatocytes and granulocytes appear to be the only two cells responsible for defence reactions such as wound healing, nodule formation, encapsulation and, to a lesser extent, hemolymph coagulation in the wax moth (Rowley and Ratcliffe, 1978). Some hemocytes do not circulate in the insect’s system, but pool and join to epithelial tissues. These can be released on demand into circulation when required (e.g. following an immune challenge). This process can be followed by proliferation and / or differentiation (Breugelmans, Van Soest et al., 2008).

1.9.5 Summary

If the insect epidermis is damaged, a clot forms using components from the hemocytes and plasma. A gel is released from granulocytes, which stabilizes the clot by means of melanization

within 24 hours of injury. The epidermal cells then migrate over the clot to repair the wound. New cuticle can be secreted when the epidermis is restored.

In some larvae (*Drosophila*, Galko and Krasnow (2004)), the scab may be absorbed, debris cleared and the exterior of the animal is almost indistinguishable from before the injury (this process is similar to bone remodelling that takes place in mammals). For juvenile insects, all trace of injury may vanish completely between one moult and the next (Locke, 1966), but for adults, the injury cannot be healed completely.

1.9.6 Mammal wound healing response

The response to tissue damage or injury in mammals also involves three classic phases (inflammation, fibroplasia and maturation (Broughton and Rohrich, 2005))

1.9.6.1 Inflammation (0-6 hours)

The response will depend on the stimulus (physical injury / infection etc.). There is a cellular and vascular response to clean the wound of necrotic / damaged tissue / foreign material (this involves collagen degradation), followed by rapid formation of a blood clot at the injury site (this prevents infection, accelerates wound healing, stops bleeding and releases growth factors).

1.9.6.2 Fibroplasia or proliferation (day 2-4)

Beneath the clot, the damaged epithelium spreads across the wound gap in order to restore tissue integrity (Martin, 1997; Singer and Clark, 1999). Epithelial cells on the boundary of the injury are seen to flatten, orient themselves towards the wound centre and migrate across the wound, prompting their neighbours to do the same. Damaged blood vessels are restored (angiogenesis) in order to supply oxygen and nutrients to cells involved with rebuilding the affected tissue (Greenhalgh, 1998). Granulation tissue is formed, and collagen and fibronectin are secreted. This stabilizes the area and increases the wound tensile strength as the wound contracts.

1.9.6.3 Maturation (remodelling)

The lines of tension applied to the area determine the alignment of the collagen. A process of remodelling occurs as unnecessary cells are eliminated by apoptosis (Haslett, 1992; Hinz, 2007) and more stable and permanent crosslinks are established based on the mechanical environment (Broughton and Rohrich, 2005). The wound stabilises as its tensile strength increases more. The remaining scar is the “memory of the wound” (Belacortu and Paricio, 2011) in adult organisms.

1.9.7 Similarities

Closing the epidermal gap left by an injury is the most important step for any animal. In both mammals and insects, re-establishing epithelial integrity using a clot is how the healing process begins. The clot, irrelevant of its constituents performs the same function – sealing the wound and providing a scaffold or substratum for the epidermal cells to migrate across / through. In both circumstances, the surrounding epidermal cells orient towards the wound site and migrate through this clot in a similar manner (by extending cell processes and then their cell bodies into the plug until epidermal continuity is re-established). During the “homeostatic regeneration” phase, inflammatory cells are recruited to the wound site. Fibroblasts for mammals and plasmatocytes and granulocytes for insects are used to the same effect – clearing necrotic tissue, forming granulation tissue and secreting new material. Older and damaged cells are removed (by apoptosis), and replaced. These new cells integrate into the pre-existing tissue.

For most adult insects, this part of the process is absent. The scab remains permanent, never being broken down or degraded further into cuticle tissue resembling its surroundings. Some larvae have no such trouble which perhaps shows that juvenile insects possess an ability to remodel and regenerate that adults do not. Other larvae (or juveniles) retain a scab or scar, but only until their next moult.

1.9.8 Differences

The composition of the clots differ (different coagulogens (Nakamura, Iwanaga et al., 1976; Belacortu and Paricio, 2011)). Inflammation and cell recruitment to the area is much more

pronounced in mammals. There are of course a myriad of other differences depending on the chosen insect (as these also differ significantly from one another).

1.9.9 Comments on Injury Response

Examining the processes across vertebrates and arthropods, it is obvious that there are far more similarities than differences (Galko and Krasnow, 2004). Both involve inflammation, cell proliferation and a maturation of sorts. The many parallels between them in terms of fundamental cellular and molecular responses which would suggest that wound healing is an ancient process that evolved before the divergence of the two classes.

1.10 Bone Adaptation

Mammalian bones experience a process of “modelling” as they grow, which forms skeletal elements so they have the appropriate shape, mass and morphology as the animal ages into adulthood (Baron and Kneissel, 2013). This is a slow process in which bone resorption and formation occur in an uncoupled manner in response to mechanical loading. Mammalian bones are also subject to a constant process of “remodelling” (Taylor and Lee, 2003): a mechanism of balanced resorption and formation (tissue turnover) in a healthy individual. Stresses applied during normal daily activities cause micro-cracks to form in our bones (Burr and Martin, 1993) which would undoubtedly lead to their catastrophic failure were it not for the remodelling process. This damage initiates the process, which involves three types of cells. Osteocytes act as “mechano-sensor” cells which alert the body to the presence of a crack (Burr, 2000). Osteoclasts are drawn to the site of injury or damage, and essentially clear the area of damaged material, preparing it for the third type of bone cell – osteoblasts – to lay down new bone matrix, which is then mineralised, restoring the original mechanical properties of the bone. This process of remodelling is essentially one of maintenance and occurs constantly on all of our bones throughout the course of our lives, and is also the final stage in the healing of a major injury such as a bone fracture.

Both of these processes allow living bone to adapt to applied mechanical loads while maintaining structural integrity. Wolff's law (Wolff, 1892) describes this relationship (Lee and Taylor, 1999) suggesting that bone in a healthy person or animal will adapt to the loads under which it is placed. Bone can self-regulate to gain maximum strength in response to applied loads, while minimizing weight (Roux, 1881). Trabeculae can be oriented within a bone in response to the principal stresses experienced when loaded (see Figure 1.32) Bone placed under excessive stress can increase in density and mass (e.g. the radius and humerus of the dominant arm of a professional tennis player (Jones et al., 1977) or baseball pitcher (King et al., 1969) compared to their other arm). Conversely, astronauts experiencing extended periods of weightlessness (or patients with extended bed rest, (Weinreb et al., 1989)) can display a reduction in bone mass and density.

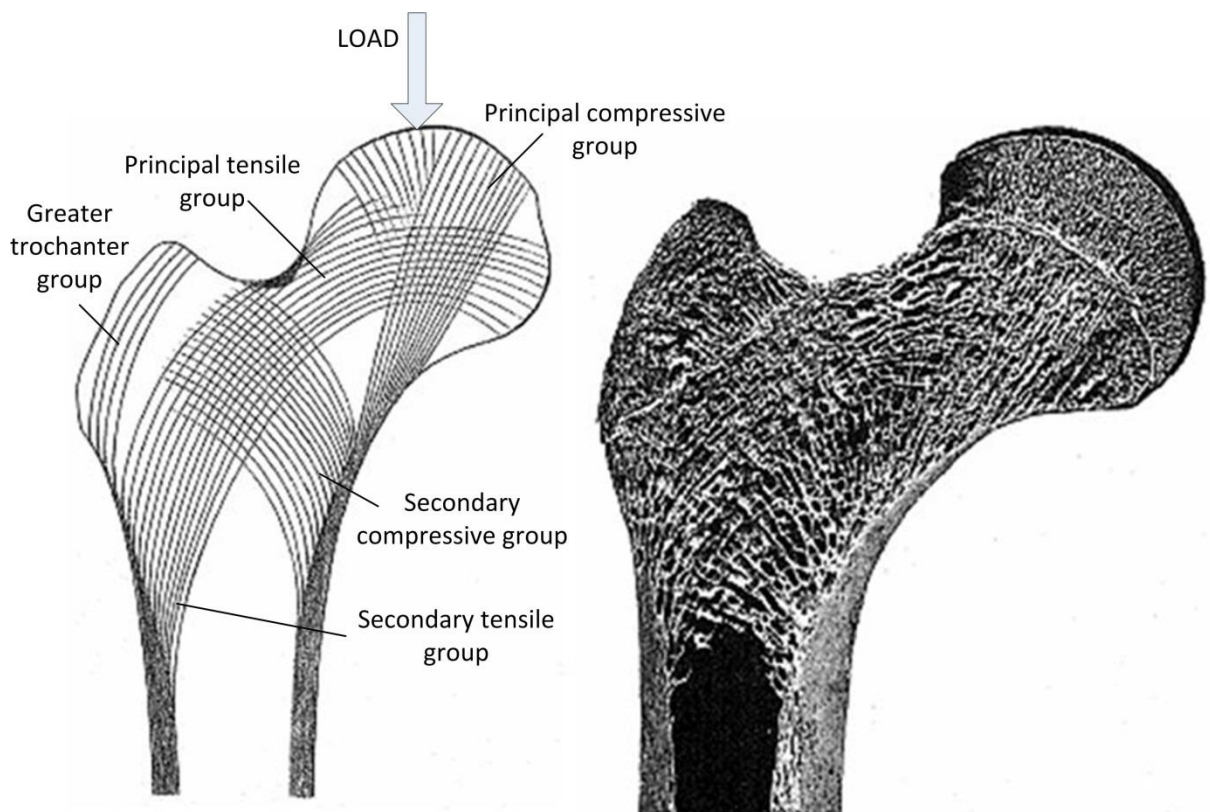


Figure 1.32: a sketch from Wolff (1870) of the lines of principal and secondary stresses experienced in response to normal loading (left), and a cross section of an adult femur showing trabeculae oriented to closely match these

1.11 Summary and Conclusions

This introductory chapter has highlighted some of the previous studies that have been carried out on insects. Their integument comprises of an exoskeleton which consists of a material called cuticle. Chitin fibres are embedded in a protein matrix, and layers of this material are deposited by the insect on a daily basis. The hierarchical composite nature of cuticle is similar to many other composites evident in the natural world such as bone, wood, bamboo, horn and antler. As their exoskeleton is rigid, it must be shed during the moulting process in order for the insect to grow. After moulting, the new cuticle is soft and pliant, and must be sclerotized or tanned (bonding of proteins with each other and with the chitin fibres) in order to become rigid. This material is known as exocuticle. As the insect ages, it deposits layers of endocuticle (similar to exocuticle, but less tanned) internally in such a manner that the number of days since the previous moult can be counted much like the rings on a tree.

Cuticle must perform a vast variety of functions, and the exoskeleton of an insect can contain countless specializations across an individual, across insect stages, and across the class Insecta. As such, cuticle displays a wide bandwidth of material properties which are determined by several factors: the amount and orientation of the chitin fibres, the constituents and degree of cross-linking and hydration of the protein matrix, the relative amounts of exo- and endocuticle, and the shape of the structures themselves. Many of these material properties have been investigated previously by a wide variety of researchers over the last century (including our own research group). Methods of investigation have differed, as have insects used and properties examined. Some properties investigated recently include cuticle strength, stiffness, toughness, hardness and fatigue.

The tibiae of different insects are exposed to different loading regimes depending on their daily activities. The ground reaction forces experienced by the legs of insects due to the biomechanics of normal locomotion such as running and walking have been studied and quantified, as have those of more extreme situations known as “emergency behaviour”, which includes jumping for a

locust, and wedging (squeezing through a small crevice) and righting (when overturned) for a cockroach.

Insect wound healing has also been studied extensively from a biological, cellular and genetic point of view. The process is quite similar to the mammal wound healing response, in that both involve the clotting of blood (hemolymph for the insect) to seal the wound to protect it from the external environment and to stem the loss of blood and moisture, followed by a hardening (melanisation) of the clot, and a migration of epidermal cells across or through it, to form a continuous layer. Lastly, tissue continuity is restored. In the case of the adult insect, the wound remains unhealed, but new cuticle is deposited beneath the wound once epidermal continuity is restored.

Chapter 2: Objectives and Methods

2.1 Objectives of this thesis

Despite its abundance as a natural material, relatively few investigations into the mechanical properties of insect cuticle have been carried out previously (in comparison to equivalent studies on mammals). Of these, very few have focussed on factors that can influence the mechanical properties of insect cuticle. This is the primary objective of this thesis.

Firstly, I aimed to investigate how the biomechanics of various insect species could influence not only mechanical properties such as strength and stiffness, but also the geometry of different insect legs. Is the material arranged specifically to resist applied forces (similar to bone trabeculae in mammals)? Is all tibia cuticle of the same strength and stiffness? The hind-leg of a locust must endure very high stresses while jumping compared to its mid-legs which are only used for walking or balancing. A cockroach uses its legs for scurrying, but must sometimes right itself or squeeze through small holes or crevices. How are these different loading regimes accounted for by the relevant species (namely the desert locust, the American cockroach and the Death's Head cockroach)? Are they reflected in the geometry or the strength and stiffness of the legs? Is the material arranged differently morphologically to best resist *in vivo* forces? Are the legs "built for purpose"? Determining this would involve investigating the mechanical properties and geometries of legs from various insect species and in various positions, and researching the biomechanical forces and stresses experienced by these legs. Comparing failure strengths to applied stresses could also yield interesting results regarding the safety factors of these tibiae. This examination is described in Chapter 3.

Having examined how cuticle can be adapted across different species or from leg to leg on a single insect, I then wanted to investigate how these factors influence the failure mode of the tibiae. Insect tibiae are essentially hollow tubes that experience bending during normal locomotion. Such structures are vulnerable to buckling failures under bending, so I wanted to discover if local buckling was taking place. This is notoriously difficult to predict as it occurs at stresses less than the yield strength of the material due to an instability which causes a sudden deformation or

kinking. Drawing on data from Chapter 3 and investigating some different insect tibiae (namely the stick insect and the bumblebee), I aimed to see if these buckling failures could be predicted using mathematical predictions and finite element analysis (FEA). I also wanted to examine some of the specializations seen in the tibiae, and their contribution to the buckling strength of the leg. Chapter 4 describes this explorative study.

The next factor I wanted to investigate was the growth of the tibia cuticle over the life of the adult insect. Although insect cuticle is acellular, it grows and changes as the insect ages. A newly moulted insect is comprised mainly of exocuticle – a strong, stiff material. This is reinforced gradually by the inward growth of the softer, more pliant endocuticle. Previous studies have theorised that the exocuticle bears most of the stress in this structure, while the endocuticle essentially acts as a shock absorber or crack stopper. As it comprises the bulk of the cuticle in a mature adult tibia, I did not believe this to be the case, and wanted to investigate its contribution to the properties of the tibia structure. Did it have any mechanical significance to the strength, stiffness or failure mode of the tubular structure of the tibia, or was it deposited purely for biological reasons? Why does the insect employ this graded two-tier structure and what could the possible triggers for starting and stopping its deposition be? This is all investigated in Chapter 5.

Although the wound healing response of insects has been studied extensively, not a single published study investigates its effectiveness at restoring structural integrity to injured cuticle. Is the response effective at restoring the original pre-injury strength and stiffness to the material (as is the case for mammal tissue healing)? Is the deposition of new endocuticle under the wound a response that is triggered by the injury, or just the result of normal endocuticle growth (a natural occurrence throughout the life of the insect)? What is the composition of the new material? Is this deposition specifically targeted to be preferential in the area adjacent to the wound? If so, this would represent an intelligent system as opposed to a passive phenomenon. These questions are examined in Chapter 6.

The wound healing processes of insects and mammals show many similarities. Does insect cuticle share any commonalities with mammals with respect to bone modelling and remodelling? Are

there similar processes occurring at some level in insects, specifically in their “bones” or exoskeletons? Having examined how the insect recovers from major (or macro) damage in Chapter 6, I aimed to investigate its capabilities at recovering from minor (micro) damage at a material level. To test this hypothesis, I planned to apply cyclic forces until I observed plastic deformation. Deformation should be accompanied by a reduction in loading energies and a reduction in stiffness of the cuticle material. This may all be recoverable if the living insect is allowed a period of rest in between successive tests. Identical tests would have to be carried out on cuticle *ex vivo* to ensure that any recovery could be attributed to the living insect as opposed to being a passive material phenomenon. This study is described in Chapter 7.

2.2 Materials, Methods and Calculations

2.2.1 Insects

All insects used were kept in a controlled 12h (35°C) / 12h (20°C) day / night cycle and fed with fresh plants and dried cereals *ad libitum*. Faeces and corpses were removed daily. Locusts (such as the one pictured in Figure 2.1) were originally obtained from Reptile Haven (Fishamble St., Dublin 2), but these did not tend to be long-lived (perhaps due to the presence of parasites). For this reason, insects were ordered from Blades Biological Ltd (Cowden, Edenbridge, Kent, UK, <http://www.blades-bio.co.uk>). Storage tanks and lamps for heat and light were also purchased from this supplier.



Figure 2.1: a healthy female adult desert locust specimen, photo by E. Parle.

2.2.2 The Tibia

Owing to the great variation in material properties seen across various insect stages and body parts, a single body part or appendage which would display minimal variation and be comparable between species was chosen for examination. The hind tibia fulfilled these requirements. Most experiments were performed on adult female desert locusts (*Schistocerca gregaria*). Other hind-tibiae tested include two types of cockroach, stick insects, and bees. The mid-leg of the locust was also tested.

The hind tibia is a specimen that has been researched to some extent in terms of biomechanics and material properties. The locust hind-tibia (Figure 2.2, from Jensen and Weis-Fogh (1962)) provides an ideal specimen for study. Its form can be assumed to be that of a hollow circular cylinder, its variation from a straight line does not exceed 0.3mm. It is relatively large compared to other insect tibiae, readily available, and is reasonably easy to handle (it is not overly delicate). The bulk of the tibia is filled with a large trachea or hollow (Bennet-Clark, 1975). Muscles within are few and small, contributing nothing to the material properties of the tibia. As in previous studies (Dirks and Taylor, 2012a; Dirks and Taylor, 2012b; Dirks, Parle et al., 2013) irregularities caused by the specialised double row of spines reinforcing the dorsal side have been ignored. The specialised



Figure 2.2: the desert locust hind tibia

buckling region observed (Bayley et al., 2012) can also be ignored as this part of the tibia was always embedded in dental cement during testing.

2.2.3 Experimental Procedure

Although several different tests were carried out on various insect legs in the separate studies over the course of this Ph.D., the basic testing procedure was almost always the same. The experimental setup is shown in Figure 2.3.



Figure 2.3: the experimental setup. 1: the Zwick tensile / compression testing machine. 2: the manual control panel. 3: the 5 N load cell. 4: the computer equipment for controlling the Zwick machine. 5: the graphical user interface of the TextExpert software displaying force-displacement curves. 6: USB microscope for monitoring / photographing samples during tests. 7: the display and user interface of the USB microscope.

The insect legs were tested to failure in bending by applying a cantilever load using a tensile-compression testing machine (Zwick / Roell Z005, Ulm, Germany), a 5 Newton load cell, and a testing rig similar to that pictured in Figure 2.4 (c). I chose cantilever bending as a loading mode which can be conveniently applied experimentally and in FEA and which places limb segments in a state of stress close to pure bending (Taylor and Dirks, 2012).

It has been shown (Dirks and Taylor, 2012a) that the properties of insect cuticle can change dramatically when the material is allowed to become desiccated (dry out). These effects have been observed on a locust tibia within 20 minutes of removal from the insect. For this reason, all tests were carried out within 10-15 minutes after removing the tibia. All legs were removed from insects under sedation by cutting just below the tibia-femoral (knee) joint. Immediately after this, the leg was set in fast hardening cold-cure acrylic dental cement (Simplex ACR308, Kedment,

Swindon, UK). This secured the leg in place, and effectively eliminated the “buckling region” observed in locusts (Bayley, Sutton et al., 2012), making the cuticle being tested more uniform. These tests reflect the primary mode of loading for insect legs – bending due to ground reaction forces during normal locomotion such as walking and jumping (Sutton and Burrows, 2008). Variations were made to the cubes which housed the dental cement, and to the indenter / pointer used for applying the load to the various different insect legs. For example, the bee tibia was much shorter than the locust or stick insect, so a flattened and blunted hypodermic needle was used to apply the force instead of the pointer shown in Figure 2.4 (c). A shallower well in the aluminium cube (to be filled with dental cement) was also used for shorter legs.

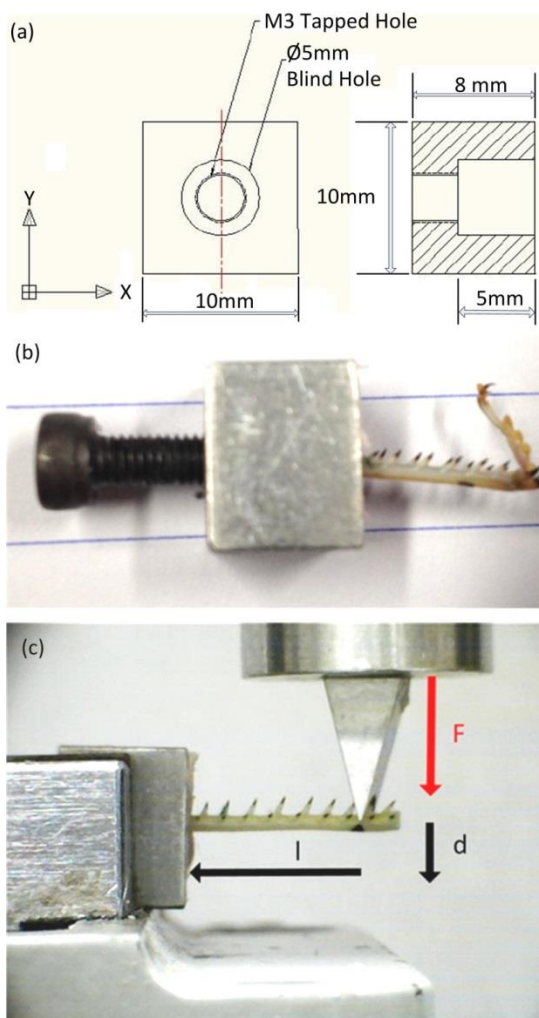


Figure 2.4: (a) technical drawing for manufacture of the experimental rig, (b) a locust tibia set in a well of dental cement inside this rig, (c) the cube is clamped in place and a cantilever load (F) is applied at distance (l) from the fixed end. Displacement (d) is also recorded. Once the test is finished, the M3 screw (shown in (b)) can be turned to pop out the dental cement and the tested specimen, which is then fixed and preserved.

Specimens were clamped in place and displacement was increased at a rate of 5 mm/min. Measurements of the cantilever length (l) were taken, and readings for force (F) and displacement (d) were recorded using TestXpert software. After failure was observed (characterised by a sudden drop in load), samples were removed from the rig and fixed using a 3.7% glutaraldehyde solution for 24 hours, after which they were preserved in a 70% ethanol solution.

2.2.4 Measurements

For my calculations to be accurate, it was necessary to measure the dimensions of each tibia individually. These can vary dramatically depending on the age and the condition of the insect, so an average value would not suffice. To measure these dimensions (radius and thickness), several cross-sectional slices were taken from each tibia tested. These were mounted using carbon cement, and gold-coated. Samples were photographed using an SEM (Zeiss Ultra Plus SEM, 5kV; Oberkochen, Germany) and measurements were taken using Fiji software (an Open Source Image Processing package based on ImageJ). 10-20 measurements for radius and thickness were taken for each sample using the Fiji software. Final thickness values used in calculations were averages of these values. Initial microCT images taken (see Figure 5.2 (a)) were of poor resolution and therefore not used for my final measurements.

2.2.5 Calculations

Applying engineering beam theory to the insect leg, one side of the leg will be under compression while the other side is under tension with a neutral axis (N/A) running down the middle where the stress is zero. Shear and bending moments will be induced within the tibia as shown in Figure 2.5.

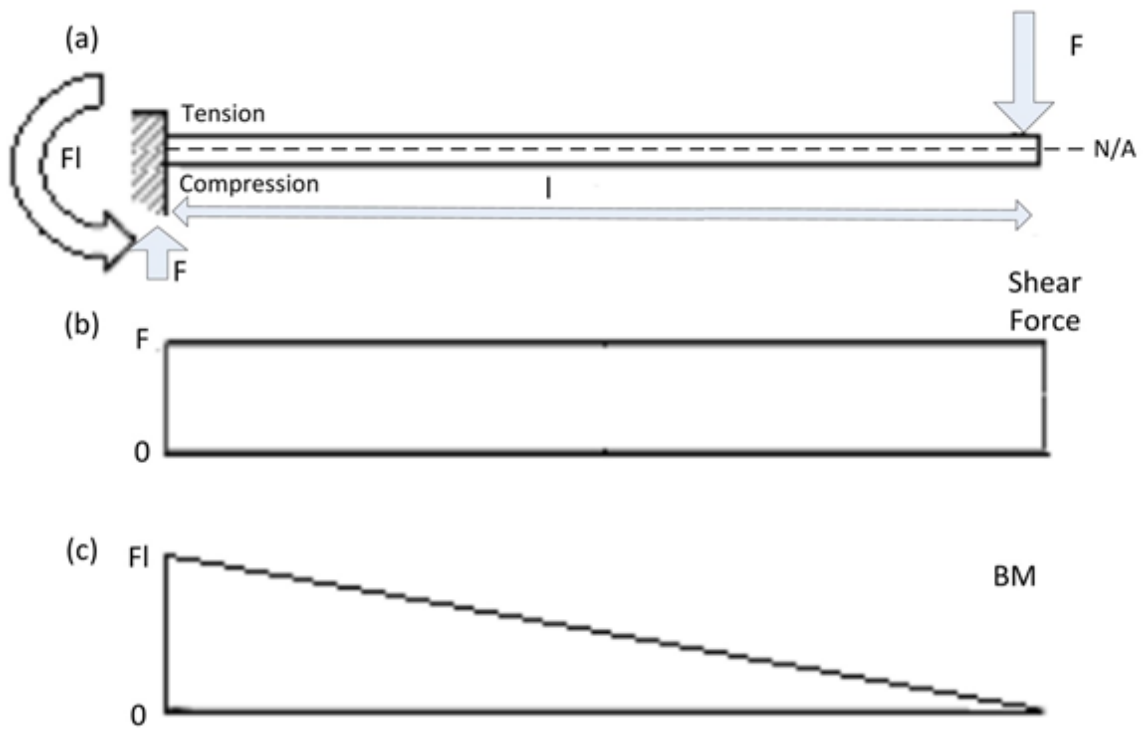


Figure 2.5: the loading regime for a cantilever beam showing applied force, induced shear force and bending moment (BM)

The maximum bending moment will be experienced at the fixed end:

$$M = Fl \tag{2.1}$$

Where:

- F = force applied
- l = length of cantilever

The flexure formula (2.2) was used to determine the maximum stress in the beam:

$$\sigma = \frac{My}{I} \tag{2.2}$$

Where:

- M = max bending moment
- y = distance from neutral axis (maximum at the top and bottom edges of the beam)
- I = moment of inertia of the beam

For the insect tibia:

$$\sigma = \frac{Flr}{I} \tag{2.3}$$

Where:

- F = applied force recorded during test
- r = average radius of the tibia
- $I = \frac{\pi}{4}(r^4 - (r - t)^4)$ – the second moment of area of the tibia (2.4)
- t = average cuticle thickness

Young's Modulus can be calculated using:

$$E = \frac{Fl^3}{3dl} \quad (2.5)$$

Where:

- d = deflection of the cantilever recorded during test.

Therefore strain can be calculated using:

$$\varepsilon = \frac{3dr}{l^2} \quad (2.6)$$

From:

$$E = \frac{\sigma}{\varepsilon} \quad (2.7)$$

The failure strength was assumed to be the maximum stress endured by the tibia during the test (dashed line in Figure 2.6). Stiffness (or Young's Modulus, E) of the samples was estimated using the value of the slope of the linear region of the loading curve (solid line in Figure 2.6). For some samples, the elastic regime was non-Hookean (i.e. non-linear). In this case, the initial tangent modulus was used (Jensen and Weis-Fogh, 1962; Hepburn and Joffe, 1974).

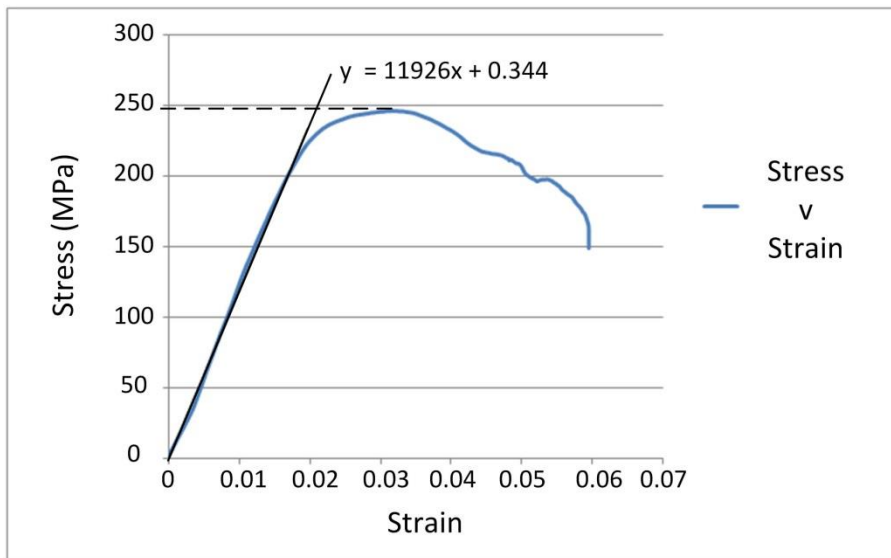


Figure 2.6: stress v strain or “loading curve” for a typical sample. The slope of the linear portion of the loading curve is used to estimate Young’s Modulus or stiffness (in this case, 11926 MPa, or 11.9 GPa). The max stress experienced was assumed to be the failure strength (in this case, 244 MPa).

Variations to these methods and calculations pertinent to each individual study are detailed in the relevant chapters.

2.2.6 Assumptions

Similar to many studies carried out in the past, (Dirks and Taylor, 2012a; Dirks, Parle et al., 2013) my calculations assume that the insect tibiae have the form of a hollow circular cylinder with a uniform cross-section, with uniform material throughout.

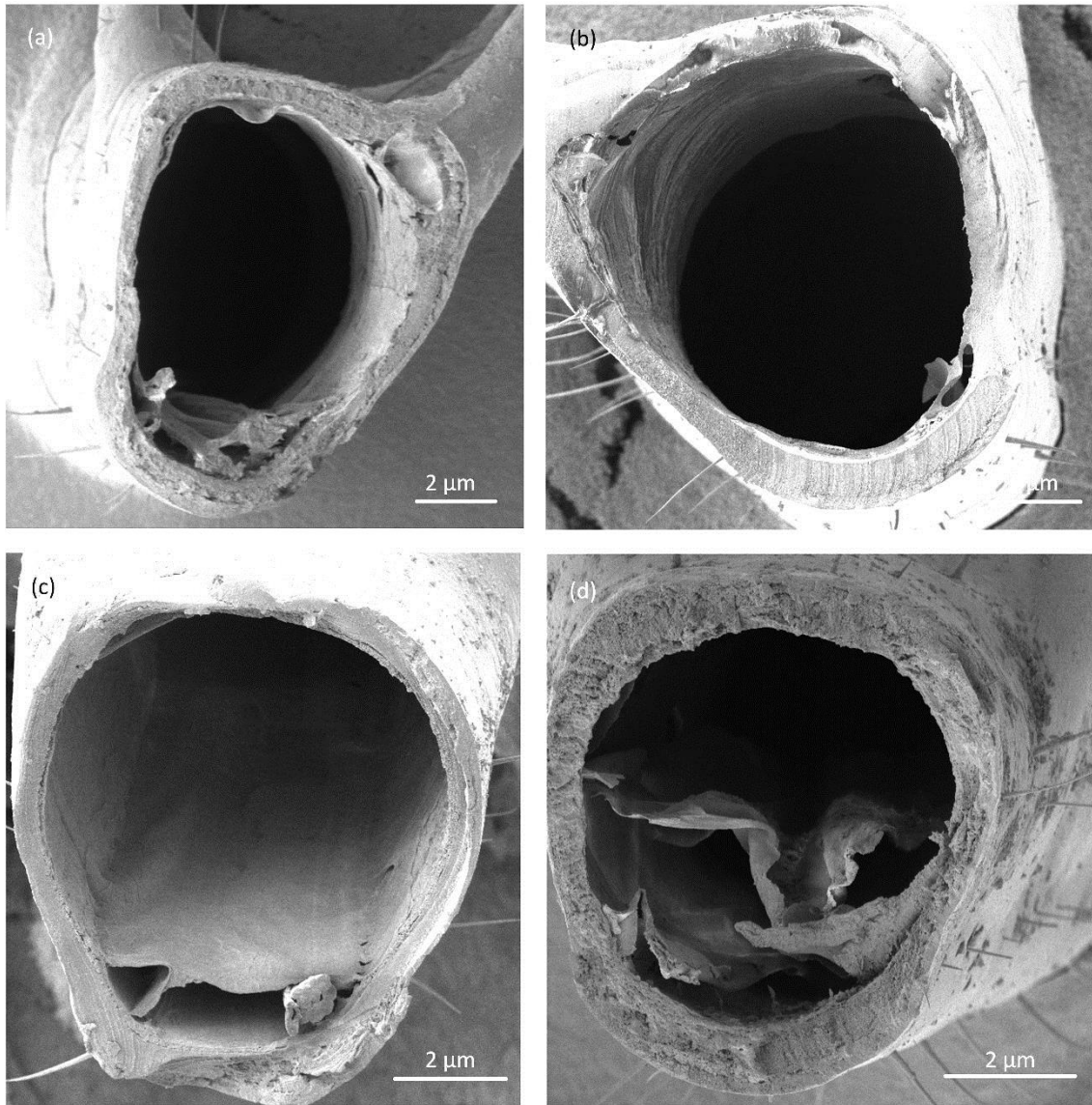


Figure 2.7: SEM photos of some locust tibiae illustrating the variation in cross-sectional shape. Some were more slightly elliptical in shape (a) and (b), while others were more circular (c) and (d).

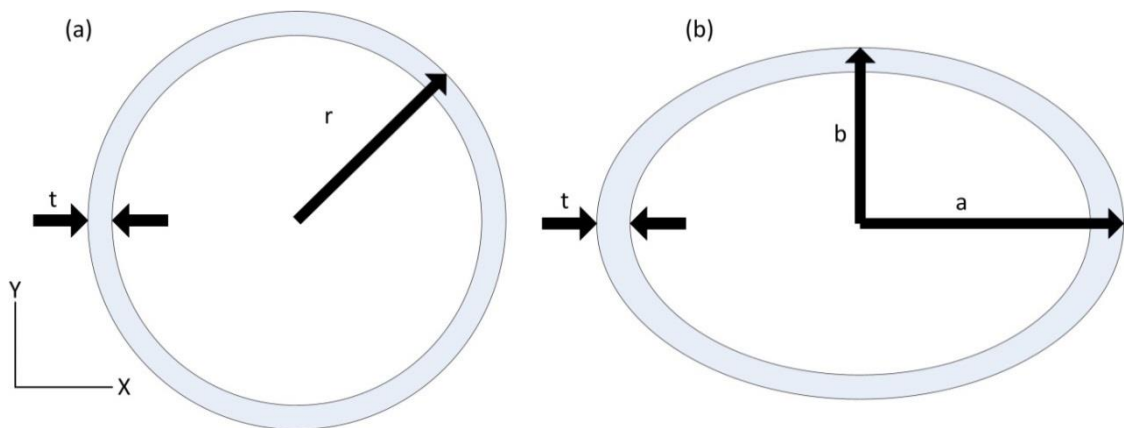


Figure 2.8: (a) circular annulus of radius r , thickness t . (b) elliptical annulus of major and minor radius a and b respectively, and thickness t .

For each sample, average values for its radius and thickness were calculated and used in the flexure formula (equation 2.3) to calculate the applied stress. These assumptions are not 100% accurate, as some samples were slightly more elliptical in nature (see Figure 2.7), which would affect the stress calculations as outlined in Table 2.1 (dimensions for calculations shown in Figure 2.8)





	Circle	Ellipse
Radius	0.5 mm	0.55mm (a) 0.45mm (b) 0.5 mm (average)
Thickness	0.08 mm	0.08 mm
Cross-sectional area	0.2312 mm ²	0.2312 mm ²
I (moment of inertia)	0.0247 mm ⁴	$I_x = 0.0207 \text{ mm}^4$  $I_y = 0.0286 \text{ mm}^4$ 
$\sigma = \frac{Flr}{I}$ (for $Fl = 1 \text{ Nmm}$)	20.2 MPa	19.2 MPa, loaded thus:  21.8 MPa, loaded thus: 

Table 2.1: differences caused by elliptical and circular cross sections.

Table 2.1 shows that the average radius and thickness assumption gives an accurate cross-sectional area calculation, but that the moment of inertia will vary slightly depending on the loading direction. All samples were loaded in the direction of the long-axis (the strongest direction of the elliptical tube), meaning that my stress calculations were a slight overestimation (20.2 MPa compared to 19.2 MPa in the example above). These calculations show that a deviation of 10% from the circular cross section (the upper-bound of deviations observed) only leads to a slight variation in stress (<8%). This was deemed acceptable, as all samples were tested in the same direction to keep the results as comparable as possible. It was deemed beyond the scope of this

study to try and accurately model the exact shape (and hence the exact moment of inertia) for each sample tested, as there were simply too many tests carried out.

Predictive methods for estimating failure stresses (outlined in relevant chapters) also assumed a circular cross section of the tested specimens. These predictions also assumed a uniform cross-section and uniform material throughout. The accuracy of these predictions to my experimental values ($\pm 10\%$) in itself may be justification enough for the assumptions made (see Chapter 4).

Chapter 3: Biomechanical factors in the adaptations of insect tibia cuticle

3.1 Abstract

Being among the most diverse groups of animals on Earth, insect cuticle exoskeletons vary greatly in terms of their size and shape. As such, they are subjected to different applied forces during daily activities. I examined and tested the tibiae of three different insect species: the desert locust (*Schistocerca gregaria*), American cockroach (*Periplaneta americana*) and Death's Head cockroach (*Blaberus discoidalis*). I found that they varied not only in geometry (length, radius and thickness) but also in material quality (Young's modulus).

The strength of the tibia, defined as the stress to cause failure when loaded in bending, was not found to vary significantly. This strength will depend on both geometry and material properties. I analysed the forces that each tibia would experience *in vivo* during various activities, and estimated a factor of safety: the ratio of failure strength to *in vivo* stress. I found that the factor of safety was only slightly greater than 1.5 for the most strenuous activities, such as jumping or escaping from tight spaces. This work contributes to the discussion on how form and material properties have evolved in response to the mechanical functions of the same body part in different insects.

3.2 Introduction

Many natural materials exhibit mechanical properties that reflect their organism's way of life. Morphological (geometric) and material properties of natural structures can vary depending on forces they experience or uses to which they are put. Species of sea anemones from high-current and low-current areas have been shown to have the same material properties, but different geometries – essentially resulting in different mechanical properties (Koehl, 1977a; Koehl, 1977b). Similarly, pine trees from windy or sheltered areas also consist of the same material, but different geometries lend a stronger bending resistance to those exposed to windier conditions (Telewski and Jaffe, 1986). It is also possible for these natural materials to differ in both geometry and

material properties – as is the case for *Eisenia* (an upright alga) exposed to sheltered and high-current environments (Charters et al., 1969).

Studies carried out on the pleopods (forked swimming limbs) of isopod crustaceans (see Figure 3.1) showed that the measured bending stiffness of the first 2 pairs of pleopods (used for providing thrust when swimming) was an order of magnitude larger than the 4th and 5th pairs (used primarily for respiration). The anterior (front) pairs had thicker cuticles, and a greater modulus of elasticity – an example of very similar (almost identical) structures on the same animal having significantly different geometries and material properties (1st pair were 12.5 times stiffer than 5th pair) – both fit for their own individual purpose.

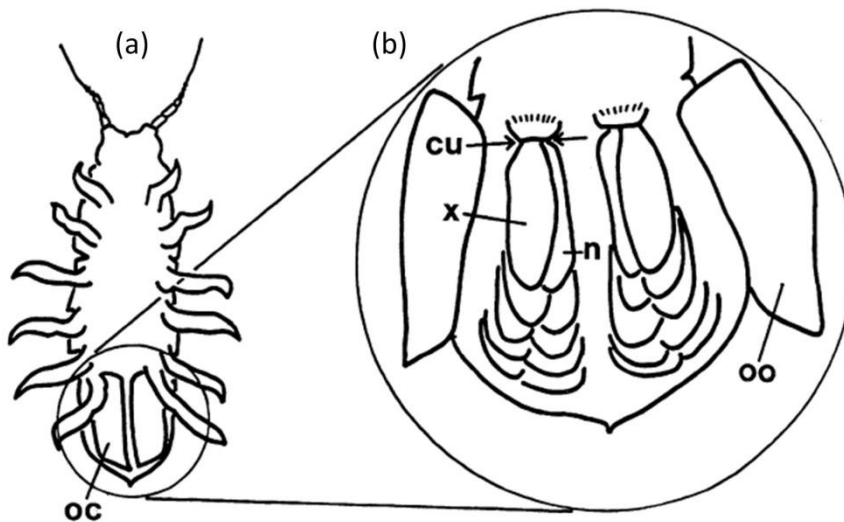


Figure 3.1: from Alexander et al. (1995): the anatomy of the isopod crustacean *Idotea wosnesenskii* (a) showing opercula closed (oc), and (b) showing opercula open (oo), the pleopods in their resting position, x = exopodite, n = endopodite, and location of cut (cu) for removal. These appendages are used for swimming and breathing. Specimens were tested using cantilever bending.

In a similar way, natural selection strives to optimize the skeleton and bone size of each animal species. Variables for optimization may include stiffness (Elastic Modulus), strength, toughness (material's ability to prevent crack growth), and fatigue strength. Bones of increased thickness can endure higher forces, but suffer an increase in weight. Instead, shape optimization (how the material is arranged) is often used to best resist the forces applied *in vivo*. Taylor and Dirks (2012) observed a radius to thickness ratio in locust hind tibia which was close to optimal to resist the

bending stresses applied during jumping. They also estimated that the force exerted during jumping was only slightly less than the failure force.

In engineering terms, a factor of safety defines the ratio of a structure's failure strength to the maximum applied stress which it experiences in use. Depending on how the structure is designed, used, examined and maintained, the safety factor can range from as little as 1.5 in, for example, aircraft fuselages and pressure vessels (Burr and Cheatham, 1995) to more than 100 in, for example, safety critical components in power stations. Mammalian bone has a factor of safety for static loads as low as 2-4 (Currey, 2002; Sabick et al., 2004). For long-term fatigue failure, the safety factor for mammalian bone is actually less than 1.0, failure being prevented by continuous self-repair (Taylor et al., 2007) due to the remodelling process. Apart from the case of mammalian bone, there has been little work done to investigate safety factors in biological structures: only a few researchers have addressed this matter for arthropod exoskeletons (Palmer et al., 1999; Taylor et al., 2000; McCullough, 2014).

Terrestrial locomotion such as running and walking is the primary function of most insect legs (other uses include jumping, grasping, digging, swimming and grooming). The biomechanics involved in such motion has been well researched. Insects apply forces to their skeletal parts in various activities, which can be categorised as either "normal behaviour" such as walking and running (and even standing still), or "emergency behaviour", which includes wedging (pushing through a small hole or crevice), righting (when overturned) and jumping to escape predators, or to take flight (pictured in Figure 3.4). The objectives for the present work were to measure the geometry, material stiffness and strength of a given body part – the tibia – in several different insects, and to combine this information with estimates of applied force to calculate safety factors for various activities.

3.3 Materials & Methods

3.3.1 Insects

The three species chosen for this study (shown in Figure 3.2) are relatively well researched in terms of biomechanics. I tested metathoracic (hind) tibiae of the American cockroach (*Periplaneta americana*) and the Death's Head cockroach (*Blaberus discoidalis*) and mesothoracic (middle) tibia of the desert locust (*Schistocerca gregaria*).



Figure 3.2: the insects examined: (a) American cockroach (*P. americana*), (b) the desert locust (*S. gregaria*), and (c) the Death's Head cockroach (*B. discoidalis*) Photo (a) taken from www.bugaboopestcontrol.com, photo (b) by E. Parle, photo (c) from www.dailymail.co.uk

I also used data on the hind legs of the desert locust (aged 14 days post moult) obtained in a previous study (Dirks and Taylor, 2012a). All are orthopteroid species, so are relatively closely related, but the three differ in size, shape and daily activities (walking, running, jumping), and as such, the stresses experienced by their tibiae *in vivo* was assumed to differ significantly also. All insects tested were adults at least 3 weeks post final moult. Insects from individual species were of the same sex (where possible). All animals were housed and cared for as outlined earlier (Section 2.2.1).

3.3.2 Mechanical Testing, Measurements and Calculations

All mechanical tests were performed as outlined previously (Section 2.2.3), using the same rigs and machines, and applying a cantilever bending load to failure. Measurements for leg dimensions were taken using SEM photos (Section 2.2.4). Whole body weight was obtained for insects before testing. Cross sectional area of the tibiae were calculated from measured dimensions using:

$$A = \pi(r^2 - (r - t)^2) \quad (3.1)$$

The same assumptions were made regarding shape of the tibiae (hollow tubes of circular cross section). In practice some tibiae vary from being perfectly circular, having an elliptical shape. Stress and strain were again calculated using (3.2, the flexure formula) and (3.3) respectively:

$$\sigma = \frac{Flr}{I} \quad (3.2)$$

$$\varepsilon = \frac{3dr}{l^2} \quad (3.3)$$

The above equations assume the length is much larger than the radius ($l/r > 20$, Young (1989)).

With some of the smaller specimens, this condition was not met. To correct my calculations for this geometrical deviance, I made individual computer models of a sample of these specimens using ANSYS (Workbench 14.0) finite element software (see Figure 3.3). Inputting the experimental dimensions and maximum applied forces for each leg to the model gave a correction factor for the failure stress experienced in the shorter legs (equation 3.4). Inputting the experimental Young's Modulus to the model, and comparing experimental and modelled deflections gave a correction factor for the Young's Modulus (equation 3.5).

$$CF_{Strength} = \frac{\sigma_{ANSYS}}{\sigma_{EXP}} \quad (3.4)$$

$$CF_{Stiffness} = \frac{d_{EXP}}{d_{ANSYS}} \quad (3.5)$$

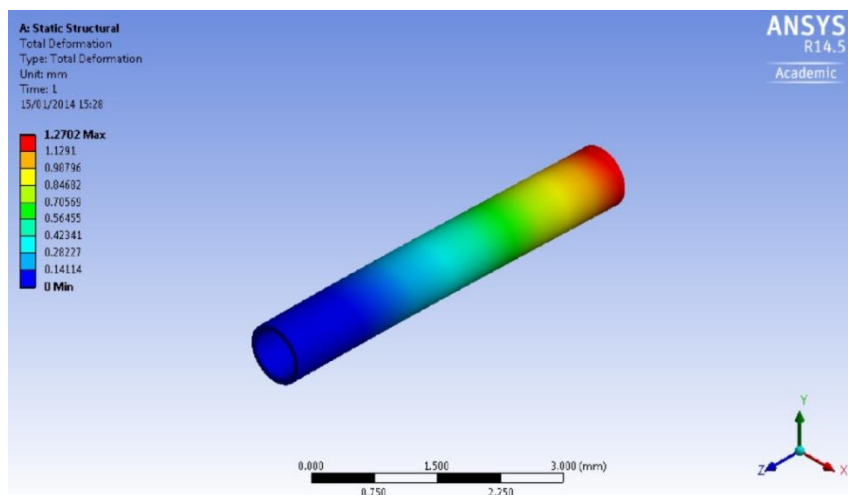


Figure 3.3: ANSYS representation of tibia as a hollow circular cylinder, fixed at the left hand side, with a force (max experimental force) in the negative y direction applied at the other end. Contours in the FE model show deflection. The experimentally determined stiffness was input as the material stiffness of the model. The ratio of ANSYS deflection (shown) to experimental deflection gave the Stiffness Corrector ($CF_{Stiffness}$). Similarly, the ratio of maximum compressive stress (ANSYS) to the max stress recorded

experimentally gave the Stress Corrector ($CF_{Strength}$). The experimental values for stiffness and strength were adjusted by these correction factors to give strength and stiffness values shown in Table 3.3 and 3.4.

3.3.3 Statistics

Statistical tests were performed using IBM's SPSS (Version 19). Univariate ANOVA tests were performed with Tukey-Kramer HSD (for unequal sample sizes) *post-hoc* tests to analyse significance between tibia groups with regards to strength and stiffness.

3.3.4 Biomechanics

In order to calculate the factor of safety for each tibia, ground reaction forces experienced *in vivo* were taken from previous literature and used to calculate stresses for each tibia, for various activities. Axial forces such as those produced by the insect's self-weight are very weak compared to those causing the tibia to bend. Taylor and Dirks (2012) used the previously published applied large extensor muscle force of 15 N and mechanical advantage of 50 (Bennet-Clark, 1975) to estimate a ground reaction force of 0.15 N per leg during the locust jump. They used this together with experimentally determined tibia dimensions (and equation 3.2) to obtain an estimate of the induced bending stress (42.2 MPa).

I used a similar approach to estimate bending stresses experienced in each tibia. Using ground reaction forces from the literature (outlined in Table 3.1) was the starting point for my *in vivo* stress calculations.

<i>Insect</i> (Source)	Activity	Ground Reaction Force (N)
<i>P. americana</i> Full and Tu (1991)	Running	0.015 _{vertical} 0.003 _{horizontal}
<i>B. discoidalis</i> Full, Blickhan et al. (1991)	Walking	0.011 _{vertical} 0.005 _{horizontal}
<i>B. discoidalis</i> Full, Yamauchi et al. (1995)	Righting	0.142 _{vertical} 0.034 _{horizontal}
<i>B. discoidalis</i> Full and Ahn (1995)	Wedging	0.18 _{resultant}
<i>S. gregaria</i> Taylor and Dirks (2012)	Jumping	0.15 _{resultant}

Table 3.1: ground reaction forces previously measured for different insects

Full and Tu (1991) experimentally determined the force on the American cockroach hind-leg while *running* at 0.92 m/s. This was scaled up by 1.38 to compensate for the larger average weight of my cockroaches. Full, Blickhan et al. (1991) determined the force on the Death's Head cockroach hind-leg while *walking* at 0.38 m/s.

No published data currently exists for the forces experienced by the locust mid-leg during walking. I estimated a value using two sets of data: the Death's Head cockroach mid-leg (Full, Blickhan et al., 1991) and the ant (*Formica polyctena*) mid leg (Reinhardt, Weihmann et al., 2009), scaling appropriately to allow for the difference in body weight. All three insects display the classic "tripod" walking gait. The resultant force values from these estimations were 12.9 mN (scaling from ant) and 7.8 mN (scaling from Death's Head cockroach). Ideally, the method of estimation would return two identical numbers, but as they are relatively similar, I deemed it satisfactory that an average of the two values would yield a rough approximation of the force experienced by the locust mid-leg.

For emergency activities of "wedging" and "righting" for the Death's Head cockroach I used data from Full and Ahn (1995) and Full, Yamauchi et al. (1995) respectively (numbers in Table 3.1). When a cockroach squeezes or "wedges" through a small slot, it thrusts its hind-legs alternately, which can produce a ground reaction force four times greater than body weight. Wedging and righting are a better way to gauge the maximum capacity of a single leg to generate force than running. Forces experienced during righting were up to 8 times higher than those experienced during running, and were even greater for wedging.

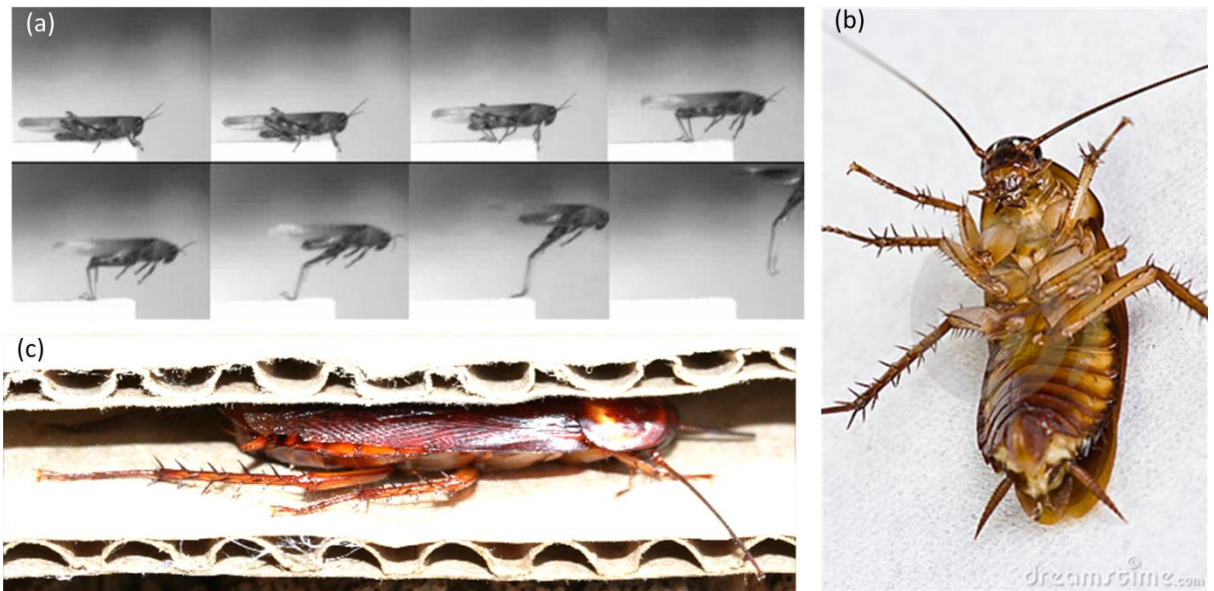


Figure 3.4: Emergency type behaviour: (a) a locust jumping from Heitler (2012), (b) an overturned Death’s Head cockroach attempting to right itself from www.shutterstock.com (photo by Nico Traut) (c) an American cockroach squeezing through a tight crevice from Kaae (2015).

In my cantilever bending tests, forces were applied at right angles to the tibia. Ground reaction forces in all previous literature mentioned above are expressed in terms of F_x and F_z : horizontal and vertical components of the force for an insect traversing a smooth level surface, as pictured in Figure 3.5(a). Not pictured is a lateral force, F_y also expressed in the literature and accounted for in my calculations. I resolved the ground reaction forces into pure compression (force component parallel to the tibia) and bending (force component perpendicular to the tibia) as shown in Figure 3.5(b), assuming a typical angle of 45° between the tibia and the ground. It was necessary to isolate the bending force for comparison to the applied bending loads in my tests.

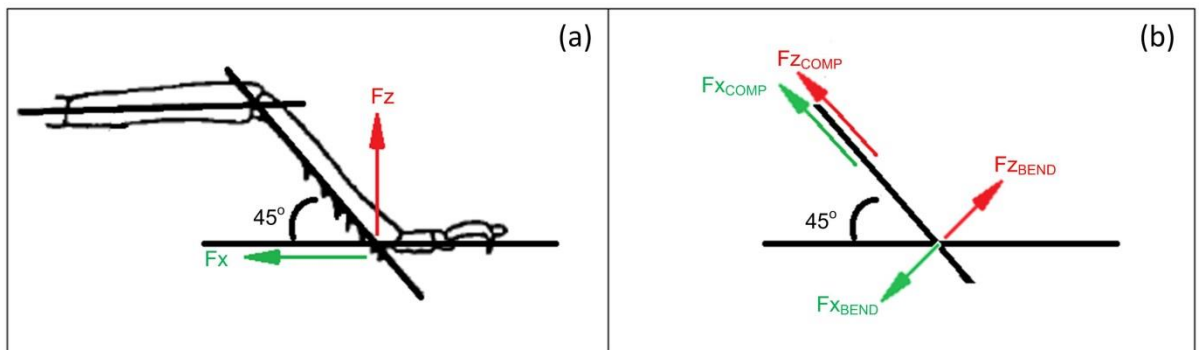


Figure 3.5: Force resolution from horizontal and vertical “ground reaction forces” into bending and compression forces.

Depending on the proportionate horizontal and vertical forces experienced, the tibia will experience different bending and compressive forces. These forces will also change depending on the angle the leg makes with the contact surface. An angle of 45° applies an equal bending and compressive force to the leg, (see Figure 3.6 – the point where the lines intersect). The magnitude of the force experienced at 45° always falls in the upper 70th percentile of maximum possible force, irrelevant of the proportionate ground reaction forces applied (in Figure 3.6, the force for a 45° angle is 12.7 mN compared to a max of 15.3 mN.) I therefore chose 45° as a good indicator of the max force experienced by the leg on a regular basis. The variation of force experienced with angle is beyond the scope of this study.

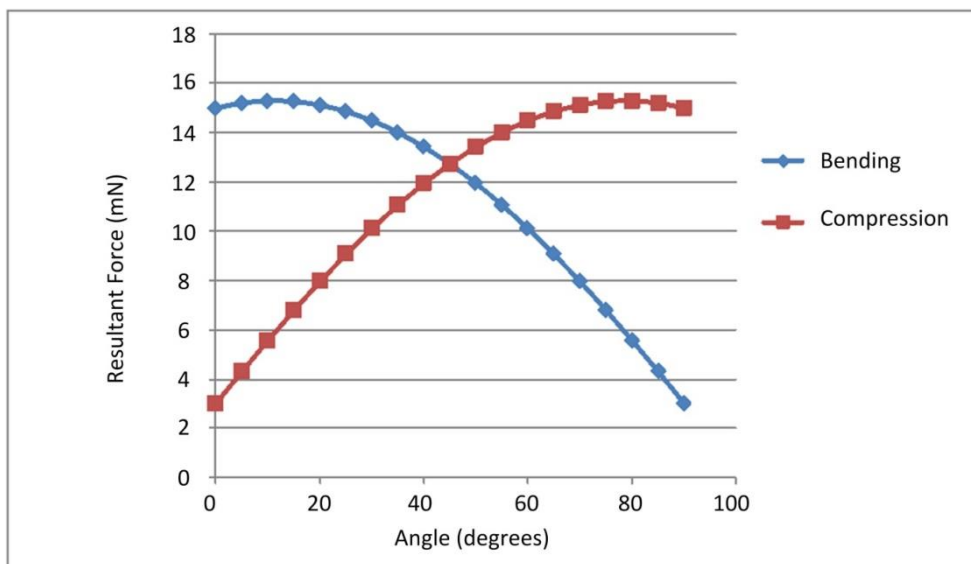


Figure 3.6: showing how bending and compressive forces differ based on the angle of the tibia relative to the ground. Data plotted are resultant forces for the running *P. americana* with $F_z = 15\text{mN}$, $F_x = 3\text{mN}$.

Having estimated the resultant bending force, the *in vivo* bending stress was calculated using the flexure formula (equation 3.2). Although compressive and bending forces may often be equal, compressive stresses ($\sigma = \frac{F}{A}$) can be ignored, as these are negligible compared to bending stresses ($\sigma = \frac{Flr}{I}$). Walking stresses were scaled up by a factor of 3 to estimate running stresses, and vice versa. This is a common approach in mammal biomechanics – forces experienced while running tend to be roughly three times greater than those experienced while walking (Whalen et al., 1988). Although insects differ in almost every way imaginable from mammals, their tripod gait

has been described as a running or bouncing gait (Full and Tu, 1990), similar to that of trotting quadrupeds or running bipeds (Cavagna, Saibene et al., 1964; Cavagna, Heglund et al., 1977).

3.4 Results

Figure 3.7 shows typical images of the cross sections of the four tibia types tested. Table 3.2 shows measured values of tibia dimensions and insect weight. There was relatively little variability (i.e. standard deviation) in dimensions within species for the tibiae examined. The locust mid-leg, though small in terms of length and radius, was found to be relatively thick-walled. The two locust tibiae have almost identical cross sectional areas despite having different radius and thickness values. Differences in insect weight for the three species are reflected in the cross sectional area of the tibia.

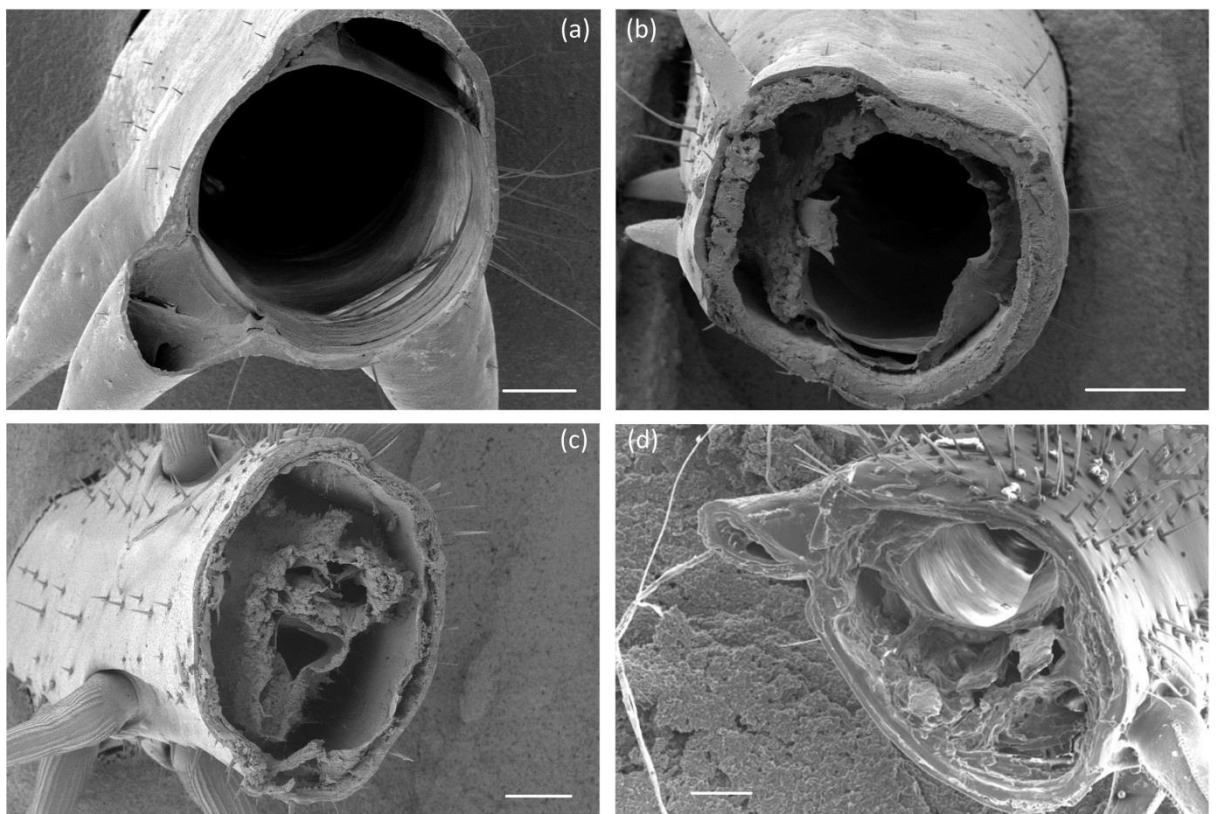


Figure 3.7: SEM images showing cross sections of the locust hind-leg (a), locust mid-leg (b), American Cockroach hind-leg (c) and Death's Head Cockroach hind-leg (d). All scale bars measure 200 μm .

	Radius (mm)	Thickness (mm)	Area (mm ²)	Length (mm)	Insect Weight (g)
Locust Hind-Leg	0.594 ± 0.04	0.054 ± 0.007	0.192	20.3 ± 4.8	1.55 ± 0.28
Locust Mid-leg	0.403 ± 0.04	0.086 ± 0.01	0.194	4.94 ± 0.3	1.55 ± 0.28
American Cockroach	0.409 ± 0.05	0.063 ± 0.02	0.149	5.98 ± 0.8	1.12 ± 0.21
Death's Head Cockroach	0.574 ± 0.06	0.076 ± 0.02	0.256	8.34 ± 1.3	3.36 ± 0.48

Table 3.2: Relevant dimensions (mean values ± one standard deviation) for locust mid-legs (n = 26), American cockroach (n = 17) and Death's Head cockroach (n = 10), for mass readings n = 10 for all specimens. Measurements for locust hind legs (in all tables) are from Dirks and Taylor (2012).

3.4.1 Mechanical Properties

Failure of the samples probably occurred by local buckling in the area adjacent to the fixation point which was under the greatest compressive stress (the bottom of the cantilever). Figure 3.8 shows typical stress/strain curves for the four types of tibia. Cuticle material stiffness (Young's Modulus) was obtained from the slope of the linear portion of the curve. Some samples behaved as a non-Hookean material (i.e. showed a non-linear loading curve). This implies some plastic and/or time-dependant (viscoelastic) deformation is occurring. For these, the initial tangent modulus was used to estimate Young's Modulus. Failure strength was defined as the maximum stress endured during a test: results are summarised in Table 3.3 (and graphed in Figure 3.9).

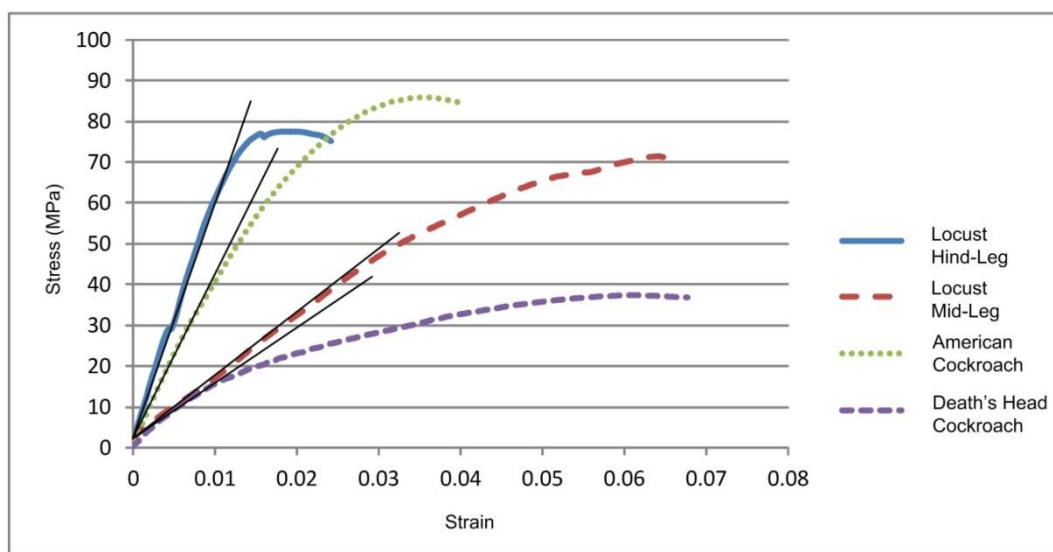


Figure 3.8: The loading curve (stress v strain graph) for a typical sample of each insect tibia. Shown is the initial linear slope of the loading curve which was used to estimate Young's Modulus (E). The max stress for each test was taken to be the failure strength of the tibia.

Initial univariate ANOVA analysis showed that difference in insect species and anatomical position significantly affected the stiffness but not the failure strength of the tibiae. Failure strength of the tibiae did not differ significantly ($P = 0.316$) among species. *Post-hoc* Tukey-Kramer HSD analysis (for unequal sample sizes) showed that the stiffness of the locust hind-leg differed significantly from the locust mid-leg ($P < 0.0001$) and the American cockroach leg ($P < 0.01$). No other difference in stiffness between the tibia types was significant ($P > 0.05$). This variation in the material's Young's Modulus indicates that different materials are present in these tibiae.

	Young's Modulus (GPa)	Failure Stress (MPa)	Failure Strain
Locust Hind-Leg	3.05 ± 0.6	72.05 ± 30.5	-
Locust Mid-leg	1.95 ± 0.65	88.51 ± 19.3	0.055 ± 0.02
American Cockroach	2.34 ± 0.72	82.06 ± 45.5	0.040 ± 0.02
Death's Head	2.72 ± 1.46	72.9 ± 19.8	0.036 ± 0.01

Table 3.3: Experimentally measured mechanical properties. Shown are mean values \pm 1 standard deviation.

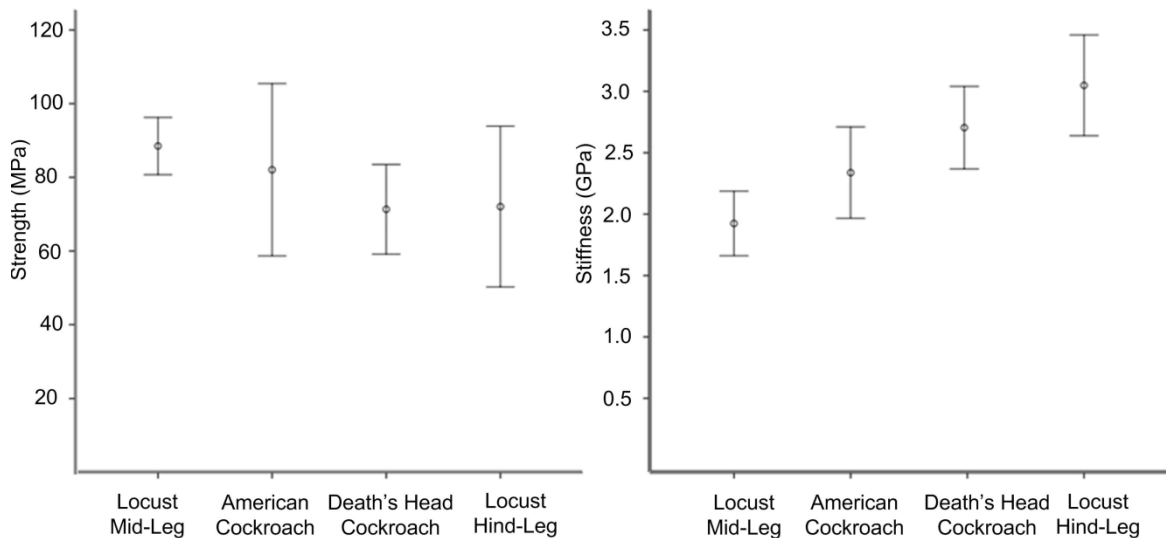


Figure 3.9: Experimentally measured mechanical properties with error bars showing a 95% confidence interval.

3.4.2 Biomechanics

Values for horizontal and vertical forces taken from the literature were resolved into applied bending forces as described earlier. This bending force was used together with average values of leg dimensions and the flexure formula (equation 3.2) to calculate the bending stresses shown in Table 3.4. It was only possible to find forces for either walking or running for each species (not

both). As such, running forces were scaled down by a factor of 3 to estimate walking forces, and vice versa. This is a common approach taken in mammalian biomechanics (Whalen et al., 1988). I believe this approach is acceptable, as a tripod gait is usually maintained at both speeds, and my calculations revealed that stresses experienced during walking were found to be quite similar across all insect species examined (likewise with running stresses), and was not greatly affected by insect weight. For the three cases of emergency behaviour for which data were available, jumping in the locust hind leg was found to generate the greatest amount of stress. Wedging and righting activities in the Death's Head cockroach gave rise to significantly higher stresses than normal walking and running activities.

	Walking Stress (MPa)	Running Stress (MPa)	Emergency Behaviour Stress (MPa)
Locust Mid-Leg	<i>2.15</i>	<i>6.45</i>	-
American Cockroach	<i>1.96</i>	<u>5.87</u>	-
Death's Head Cockroach	<u>1.89</u>	<i>5.67</i>	-
Locust Hind-Leg (jumping)	-	-	<u>42.2</u>
Death's Head Cockroach (wedging)	-	-	<u>23.29</u>
Death's Head Cockroach (righting)	-	-	<u>18.89</u>

Table 3.4: In vivo stresses experienced by the tibia of each insect when walking, running, and during emergency behaviour (jumping, wedging and righting). Underlined numbers are direct calculations based on data from the literature. Figures in italics are estimates from scaling up / down these numbers.

3.4.3 Factor of Safety

Table 3.5 shows estimates of the safety factor for each tibia under various loading conditions. The safety factor is obtained by dividing the failure strength by the applied stress. However, an insect tibia will be subjected to a large number of repeated cycles when walking and running, which may lead to a fatigue failure. Locusts have been recorded walking constantly for long periods of time (Moorehouse, Fosbrooke et al., 1978). They gradually build up their pace to a high intensity which

is sustained for up to 2 hours. The highest recorded stride frequency was 8 Hz, so experiencing almost 58,000 continuous cycles at a time is a regular occurrence for a locust. One can assume that the cockroaches would experience similar or greater numbers of sustained cycles based on their average stride frequencies of 14 Hz (Death’s Head) and 25 Hz (American). Previously, our research group found that a conservative estimate of the stress to cause fatigue failure after a large number of cycles in the locust hind tibia was approximately half the static failure strength (Dirks, Parle et al., 2013). So this factor has been applied in calculating the “relevant stress to failure” (for running stresses) in Table 3.5. Emergency behaviour (jumping, wedging, righting) would not be repeated often enough for fatigue failure to be an issue. For example Bennet-Clark (1975) showed that the locust cannot perform more than 10-20 jumps consecutively, and the cockroach’s wedging and righting actions are performed only infrequently (Full and Ahn, 1995; Full, Yamauchi et al., 1995). Therefore it can be assumed that the static strength is the “relevant stress to cause failure” in these cases.

	Relevant stress to cause failure (MPa)	<i>In vivo</i> applied stress (MPa)	Safety Factor
Locust Mid-Leg (<i>running</i>)	44.25	6.45	6.8
American Cockroach (<i>running</i>)	41.03	5.87	7.0
Death’s Head (<i>running</i>)	36.45	5.67	6.3
Locust Hind-Leg (<i>jumping</i>)	72.05	42.20	1.7
Death’s Head (<i>wedging</i>)	72.90	23.29	3.1
Death’s Head (<i>righting</i>)	72.90	18.89	3.9

Table 3.5: Safety factors of insect tibiae for various situations. Relevant stress to cause failure is divided by *in vivo* applied stress to obtain the safety factor.

3.5 Discussion

This work represents the first systematic study to compare dimensions, mechanical properties and *in vivo* stresses for the same body part in several different insects. I measured failure strength, defined as the stress to cause failure when the tibia was loaded in bending. This type of loading is relevant because the stresses caused by bending will certainly dominate owing to the relatively long, slender shape of the tibia and the off-axis forces it experiences *in vivo*. My results

show that the dimensions of the tibiae vary significantly, which is not surprising considering the different insect weights and different purposes to which the limbs are put. I also found that the cuticle material itself is different, having different Young's modulus values in all four cases. This implies differences in chitin fibre amount and orientation, or in the relative amounts of exocuticle and endocuticle.

The exact mode of failure is unclear. Taylor and Dirks (2012) proposed two possible modes for the locust hind tibia: tensile fracture and compressive buckling occurring adjacent to the fixation point of the cantilevered leg on the top and bottom respectively. Dirks, Parle et al. (2013) tested the same limb in cyclic loading and observed that fatigue failures occurred sometimes by tensile cracking and sometimes by compressive buckling. If local buckling is involved, then the stress at failure will depend not only on the material but also on the dimensions of the tibia. This helps to understand why the measured failure strengths of the four tibiae did not change in the same way as their Young's modulus values. In fact all of the tibiae had very similar strength values, showing no significant difference in my ANOVA analysis. More work was needed to establish the mode of failure and the factors, geometrical and material affecting it. This work is detailed in Chapter 4.

This analysis has some limitations: I assumed a simplified shape (hollow circular cylinder) for the cross section and used a linear elastic model, assuming no plastic deformation. In reality, the stress-strain curves (Figure 3.8) always showed a non-linear region before maximum stress, suggesting inelastic behaviour in the material, such as plastic deformation or sub-critical damage. This may be caused by either fracture or buckling or individual layers within the cuticle or delamination of the layers which eventually leads to the failure of the tibia. However, this area of non-linearity does not interfere with my assumptions, as the safety factors calculated for each insect imply that they are always operating within the linear region of the stress-strain curve.

The locust mid-leg and hind-leg have similar cross-sectional areas, but the locust hind-leg has a relatively more slender shape (larger radius, smaller thickness). Although both have similar failure strengths, the bending moment required to cause failure is significantly higher (35%) for the hind-leg (3.76 Nmm) than the mid-leg (2.79 Nmm). The hind-leg experiences greater bending moments

in vivo, enabled to do so by the superior material (as evidenced by the higher Young's Modulus). This indicates that cuticle composition and geometry can vary from leg to leg on a single insect to best resist the forces experienced *in vivo*.

The two cockroaches show some distinct physical differences. The Death's Head cockroach is much larger and heavier than the American (3.36 g compared to 1.12 g). This is reflected in the tibia geometries – the Death's Head tibia having a 20% larger radius and thickness (and a 50% larger cross-sectional area). One might expect material properties such as strength and stiffness to scale as a function of the insect's weight, but this is not the case. Although three times the weight of the American cockroach, the Death's Head cockroach hind-tibia displays no significant difference in strength or stiffness to the American. Why then does an insect which is so much smaller and lighter require material of the same strength and quality as a much larger one? I believe the reason to be that both insects experience very similar stresses when running and when walking. Both cockroaches display a similar walking gait, and their patterns of ground reaction force are described as being "not qualitatively different" (Full and Tu, 1991) even when the American cockroach abandons the tripod gait when running. Full's experiments measured forces experienced during "normal" (un-stimulated) locomotion – speeds of 0.98 m/s for the American cockroach, and 0.32 m/s for the Death's Head.

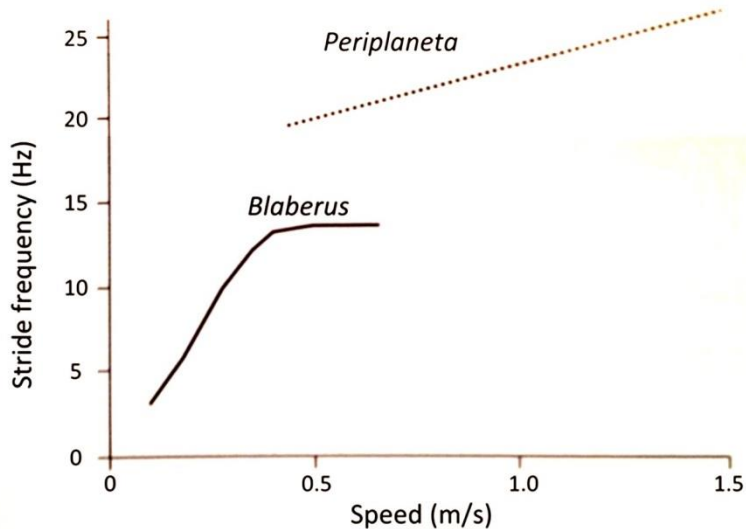


Figure 3.10: range of stride frequencies for *Blaberus* and *Periplaneta* plotted as a function of speed (Chapman, 2013).

Figure 3.10 shows that the Death's Head cockroach operates over a smaller range of speeds. Its stride frequency increases as its speed increases (until it reaches a max of 13Hz, after which increased stride length is used to increase its speed). *Periplaneta* shows relatively little change in stride frequency over a large range of speeds – stride length accounts for most of the increase in speed. It operates at frequencies close to wingbeat frequencies during flight.

This illustrates that the smaller American cockroach favours running, and can do so at maximum speeds of up to 1.0-1.5 m/s (or 50 body lengths per second (Full and Tu, 1991)), producing greater forces (and greater strain rates) in proportion to its body weight compared to that of the Death's Head cockroach. Maximum speeds for the Death's Head are less than half that found for the American. Also, the Death's Head is a more awkward runner (Full and Tu, 1991), apparently wasting more energy pitching and rolling than the American. This is why the stresses experienced by both insects' hind tibiae are so similar, and may also be the reason why the tibiae are so closely matched in terms of material strength and stiffness.

Biomechanics analysis has revealed safety factors which in some cases are very low, as small as 1.7 and 3.1 for adult insect tibiae. The locust has an extra specialization in the form of a buckling region close to the tibia-femoral joint. This area can deform plastically if unusually high forces are experienced, such as those observed when the tibia slips during a jump (Bayley, Sutton et al., 2012). The limb segments of these insects have evolved to operate at applied stresses which are very close to their limiting values. I allowed for the possibility of fatigue failure in common activities such as running, in which the leg is loaded many times, but even so it emerged that the lowest safety factors occurred during strenuous activities which are performed only occasionally, such as jumping and wedging. Although force measurements for wedging in American cockroaches could not be found, they are known to squeeze through gaps as small as 4 mm (Jayaram et al., 2013) while still maintaining a relatively high speed. One could speculate that a similar safety factor applies for performing such activities.

I calculated a safety factor of 6.8 for the locust mid-leg during running, but this is probably an underestimate because it assumed a high running speed of 0.92 m/s maintained for long periods:

flying could take preference when long distances must be travelled. It certainly seems that this tibia is much stronger than it needs to be, a finding which requires further work to explain. It may be possible that the mid-leg must also endure some “emergency behaviour” of its own (perhaps clinging to a surface during an attack or a windstorm). It would be useful to analyse the mid legs of other insects to gauge their safety factor for comparison. The mid leg also has to endure forces other than ground reaction forces that may influence its structure. Muscles in the locust front two legs are continuously active even when the locust is stationary (Chapman, 2013). Any force, such as a gust of wind that tends to change the angles between leg segments is opposed by a muscular reflex – in the case of the femur-tibia joint, the extensor and flexor muscles (mediated by the sensing organs such as the campaniform sensilla). This is known as the “postural position reflex”. These internally applied muscle forces may be more significant than the ground reaction forces experienced by these legs, possibly occurring quite frequently, which could be why they seem to be “distinctly over-built” (Katz and Gosline, 1992). Because of the specialization of its hind-leg for jumping, the locust also shows a very high variability in the stepping movement of its legs regarding the protraction / retraction phases (compared to the cockroach (Burns, 1973)), which could also lead to more unpredictable ground reaction forces when walking.

Some confirmation for these low safety factors comes from the work of Bennet-Clark (1975) who estimated a safety factor of 1.2 for the extensor apodeme (tendon) of locust hind leg during jumping. This was calculated in a similar manner, except that since the apodeme is loaded in tension, Bennet-Clarke used the tensile strength of the material. Palmer, Taylor et al. (1999) and Taylor, Palmer et al. (2000) estimated the safety factor for six species of predatory *Cancer* crabs (*Crustacea, Brachyura*) by comparing the exerted biting force to the breaking strength of their claws. These varied within and among the species depending on stage of development and wear, and ranged from 2 to 7. McCullough (2014) found the safety factor for the horn of the rhinoceros beetle (*Trypoxylus dichotomus*) to range from 3.5 to 10.3, which scaled with the inverse of the insect size.

All safety factors are average values. Since both the failure strength and the applied force have some variability associated with them, then even with a safety factor greater than 1.0 some failures would be expected to occur. There was quite a large variability in the measured failure strengths: the standard deviations were between 20% and 55% of their respective mean values, implying that it will quite often happen that the applied stress rises above the failure strength, causing failures of the tibia during jumping etc. A detailed probabilistic analysis, such as has been conducted for mammalian bones (Taylor, 2011) would require more information and is beyond the scope of this study. Taylor, Palmer et al. (2000) noticed a breakage frequency in natural populations of roughly 6% across six species of crab, while McCullough (2014) observed that 17% of the population of Rhinoceros Beetle tested showed some sign of injury, while 4% had severely damaged horns from battles with rivals. The limbs being tested in this study might be expected to evolve with rather high failure probabilities. This is the price of being light and economic in energy terms; sacrificing individual insects but making the species as a whole more viable. This would provide a very interesting topic for future research.

Later studies (such as that in Chapter 5) have shown that the figure of 72.05 MPa for the failure stress of a locust hind tibia (Taylor and Dirks, 2012) is not necessarily set in stone. The locusts used for Dirks' tests were 14 days after their final moult. As the insect grows and ages, the tibia cuticle also grows and matures – its strength increases steadily over the first 21 days post moult, eventually reaching an average strength of approximately 175 MPa. This implies that the factor of safety also increases as the insect ages (provided the applied jumping forces do not increase also). The safety factor of 1.7 for the locust hind leg during jumping may actually increase to closer to 4 (more similar to that seen in the Death's Head cockroach when wedging and righting) as the insect fully matures. It is accurate for locusts of the age and dimensions studied by Taylor and Dirks (2012). This is covered in more detail in Chapter 5.

3.6 Conclusion

This work has focussed on a single limb segment, the tibia, in two different positions and in three different species. I found significant differences not only in geometry but also in material quality, as measured by Young's modulus. The failure strengths of these tibiae when tested in bending were found to depend on both material quality and geometry, implying that the failure mode may be local buckling.

My biomechanics analysis revealed that the tibia is prone to failing not by fatigue during repetitive activities but by sudden fracture during emergency behaviour such as jumping and wedging. From an engineering perspective the legs seem to be slightly "overdesigned" for normal running and walking, but this is necessary to minimize failures from more strenuous activities. I estimated some very low safety factors, some less than 2.0, implying that evolution has operated to make these body parts only slightly stronger than they need to be. The tibia can be said to be a high-performance part having a slender form to give it low weight, and thereby having a significant risk of failure in use.

Chapter 4: Buckling failures in insect exoskeletons

4.1 Abstract

Thin-walled tubes loaded in bending are prone to failure by buckling. It is difficult to predict the loading conditions which cause buckling, especially for tubes of non-circular or asymmetrical cross section. I investigated the leg segments (tibiae) of two insect species: the stick insect (*Parapachymorpha zomproi*) and the bumblebee (*Bombus terrestris audax*), and compared these to work done previously on three other species: the desert locust (*Schistocerca gergaria*), American cockroach (*Periplaneta americana*), and Death's Head cockroach (*Blaberus discoidalis*). All tibiae were tested to failure in cantilever bending, and modelled using finite element analysis (FEA). The tibiae of the locust and the cockroaches were found to have an approximately circular cross-section. Their buckling loads were well predicted by linear elastic FEA, and also by one of the analytical solutions available in the literature for elastic buckling. The legs of the stick insect are also circular in cross section but have several prominent longitudinal ridges. One may assume that these ridges might protect the legs against buckling but this was not the case: the loads necessary for elastic buckling were not reached in practice because yield occurred in the material, causing plastic buckling. The legs of bees have a non-circular cross section due to a pollen-carrying feature (the corbicula). This was found not to significantly affect their resistance to buckling.

4.2 Introduction

The idea for this study evolved from the work described in the previous chapter. Having examined how geometry, stiffness and strength varied across tibiae (and three insect species), I wanted to know how exactly the legs were failing, and if I could predict these failures accurately for other insect legs based on what I already knew. Due to the applied bending load, and the thin-walled tubular structure of the leg, I assumed the dominant failure mode of the tibiae was one of buckling. The failure of thin-walled hollow tubes due to buckling (Section 1.7) is very difficult to predict. This chapter describes the collaborative effort of work done by myself and Prof. Taylor,

who conducted all of the FEA analysis detailed in this chapter. Data from the work outlined in Chapter 3 is also included here to give a more complete picture.

The primary mode of loading for insect legs *in vivo* is bending, as a result of ground reaction forces during activities such as walking and jumping (Sutton and Burrows, 2008). As such, analysis of failure modes due to bending (such as local buckling and ovalisation) are biologically relevant.

The objectives of this study were to investigate the failure of insect legs in bending using a combination of experimental testing and finite element analysis. I chose insects having a wide range of sizes, shapes and material properties, including cases in which the cross section is complex and cannot be modelled as a simple circular tube. I wanted to answer the following questions:

- Can FEA be used to predict the elastic buckling of tubes when loaded in bending?
- Can the buckling loads of insect legs be accurately predicted, either using FEA or using existing analytical solutions?
- Have insects evolved leg shapes which effectively resist failure by buckling?

Addressing these questions may provide insights that will help in the future design of engineering components and structures to resist buckling.

4.3 Methods

Mature insects having well developed exoskeletons following their final moult were used. The tibiae of two insect species were tested: the stick insect (*Parapachymorpha zomproi*) and the bumblebee (*Bombus terrestris audax*). In addition, I used data previously obtained for the hind tibia of the desert locust (*Schistocerca gregaria*, aged 14 days post moult (Dirks and Taylor, 2012a)), and data detailed in the previous chapter from the mid-leg of the locust (*Schistocerca gregaria*), and the hind legs of the American cockroach (*Periplaneta americana*) and Death's Head cockroach (*Blaberus discoidalis*). In total 110 leg samples were tested and photographed in the SEM. Experimental procedure, assumptions, measurements and calculations adhered to the protocol outlined in Section 2.2.

Experimental stress was again calculated using the flexure formula:

$$\sigma = \frac{F_{max} * l * r}{I} \quad (4.1)$$

The buckling strength of a thin-walled tube can be predicted using:

$$\sigma_b = \beta E \frac{t}{r} \quad (4.2)$$

Where β can vary depending on the source literature. Two previously published values were those of NASA (1968), where $\beta = 0.525$, and Calladine (1983), where $\beta = 0.313$. Calladine's prediction takes into account ovalisation and local buckling (outlined in Section 1.7). For the more complex leg-shapes (stick insect and bee), finite element analysis (FEA) was used to predict buckling loads.

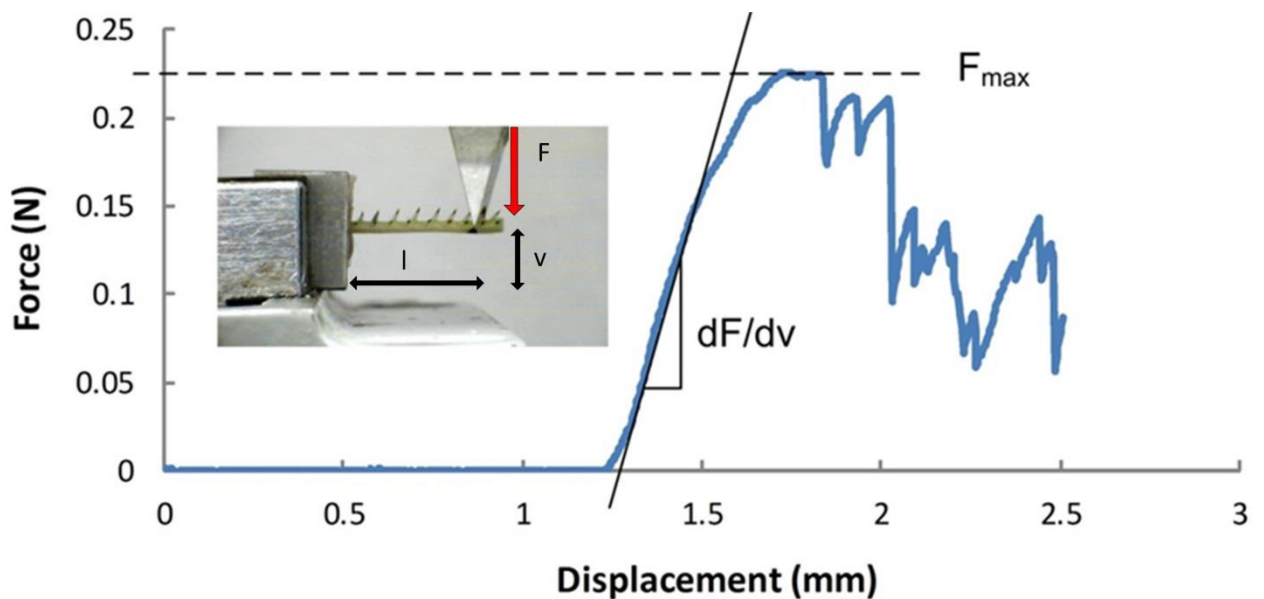


Figure 4.1: the same experimental set up as earlier was used for each insect tibia. Slight alterations in the holders and clamps were used for different legs (a more shallow well for the dental cement was used for shorter legs). A different pointer (a flattened, sanded hypodermic needle) was used for the bee legs which were too short to use the pointer pictured above. Also shown is a typical force / displacement curve. Once contact was made between the pointer and the sample the initial slope dF/dv was approximately constant, followed by a maximum force F_{max} after which the load-bearing capacity reduced. Young's modulus was calculated from the slope dF/dv (using equation (4.3)) and failure was defined as occurring at the maximum stress (calculated from F_{max} , using equation 4.1).

For samples with circular cross sections, Young's modulus E_l in the longitudinal direction was calculated from the slope of the initial, straight-line portion of the force-deflection curve (Figure 4.1) using the following equation:

$$E_l = \frac{l^3}{3I} \frac{dF}{dv} \quad (4.3)$$

For those limbs having non-circular shapes (the stick insect and bee, Figure 4.2 (b) and (c)) the experimental Young's modulus was not accurate (as the calculations assume a circular cross-section). Stiffness for these samples was found by making FE models, inputting experimental forces and stiffness, and comparing the predicted and experimental loading curves and deflections. All FEA was carried out by Professor David Taylor (my supervisor) using ANSYS software. Poisson's ratio was assumed to be 0.3. The "Large Deflections" option was used to model the nonlinear behaviour which is caused by locally high distortions that occur during buckling. The size of mesh elements and the number of iteration steps in the analysis were varied until convergence occurred. The cross section was assumed to be constant for the entire length of these tubes.

The buckling predictions (using equation 4.2 and the FEA) both assume that the material is linear elastic and isotropic. Anisotropy was incorporated as proposed by Wegst and Ashby (2007), by replacing E with $(E_l E_t)^{1/2}$ where E_l and E_t are the Young's modulus in the longitudinal and transverse directions respectively. E_t has never been measured for insect cuticle: following on from previous work (Taylor and Dirks, 2012a) I assumed a value equal to $E_l/2$. Thus applying a correction factor of $(\frac{1}{\sqrt{2}})$ to E in equation 4.2 accounted for anisotropy.

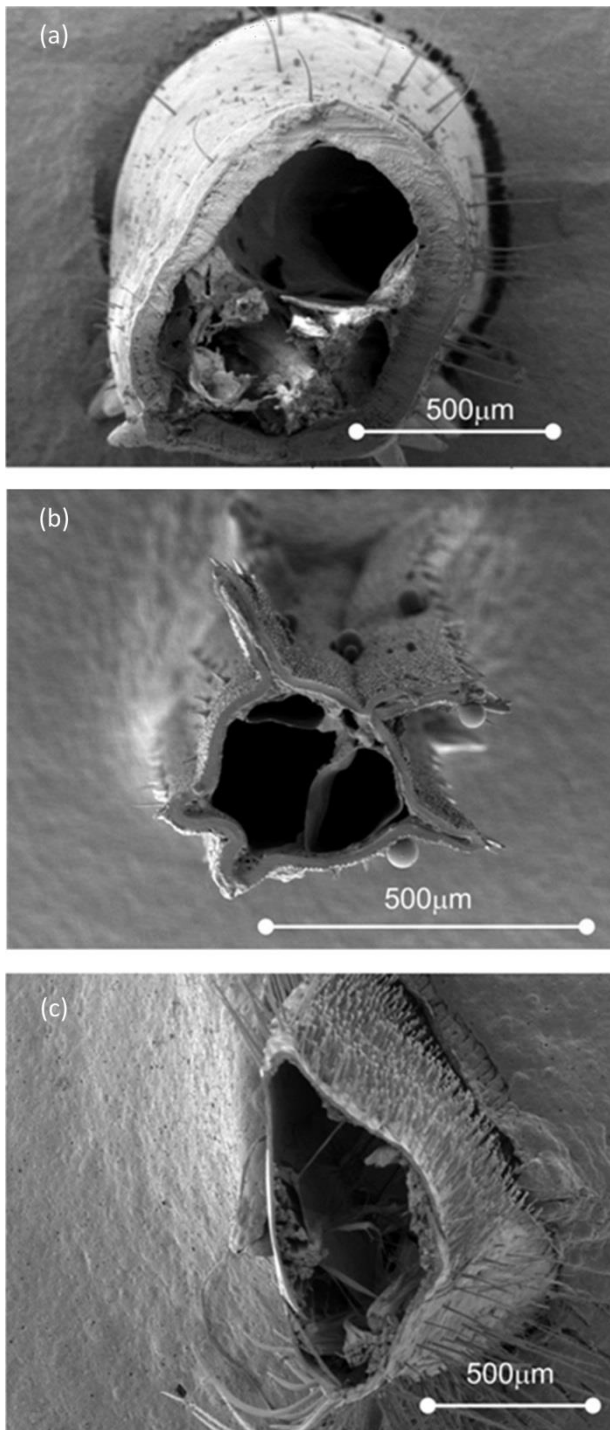


Figure 4.2: Scanning electron microscope photographs showing typical cross sections of insect tibiae. The locust and cockroach tibiae had approximately circular cross sections (typified here by the example of the locust mid leg, (a), cockroach tibia not pictured). The stick insect (b) had five prominent ridges running longitudinally along the leg. The bee (c) had one large, flat surface which is used for pollen collection.

4.4 Results

Table 4.1 shows the measured dimensions for each limb type. For the locust and cockroach limbs the r and t values are averages of readings taken around the circumference. For the stick insect

the longitudinal ridges were ignored when measuring r and t ; for the bee, the equivalent radius for a circular tube having the same cross sectional area was used.

	Number of samples tested	Radius r (mm)	Thickness t (mm)	Youngs modulus E (GPa)	Experimental failure stress (MPa)	Predicted buckling stress (FEA) (MPa)	Predicted buckling stress (Calladine) (MPa)
Locust	10	0.596 ± 0.04	0.054 ± 0.007	3.05	72.1 ± 30.1	72.3	61.2
Locust mid leg	26	0.403 ± 0.04	0.086 ± 0.01	1.95	88.5 ± 19.3	130.4	92.1
American Cockroach	17	0.410 ± 0.05	0.063 ± 0.02	2.34	82.1 ± 45.5	103.6	79.6
Death's Head Cockroach	10	0.574 ± 0.09	0.076 ± 0.02	2.72	72.9 ± 19.8	100.4	79.7
Stick Insect	33	0.155 ± 0.03	0.018 ± 0.006	5.5	116.0 ± 66.1	167.7	137.4
Bee	14	0.317 ± 0.05	0.023 ± 0.006	1.58	36.5 ± 31.2	30.2	25.4

Table 4.1: Experimental values and predictions – mean values \pm 1 standard deviation. E values were estimated using equation 4.3, assuming a circular cross section, except for the stick insect and bee, for which FEA was used. All stress values were calculated assuming a circular cross section: in the case of the stick insect the longitudinal ridges were ignored in the calculation.

The samples did not break during testing; in some cases a local buckling event was clearly visible after unloading (see Figure 4.3 (a)). Table 4.1 gives the estimated Young's modulus values based on the slope of the linear portion of the curve. Figure 4.4 shows the bending stress at failure calculated assuming a circular cross section, and, in the case of the stick insect, ignoring the presence of the longitudinal fins.

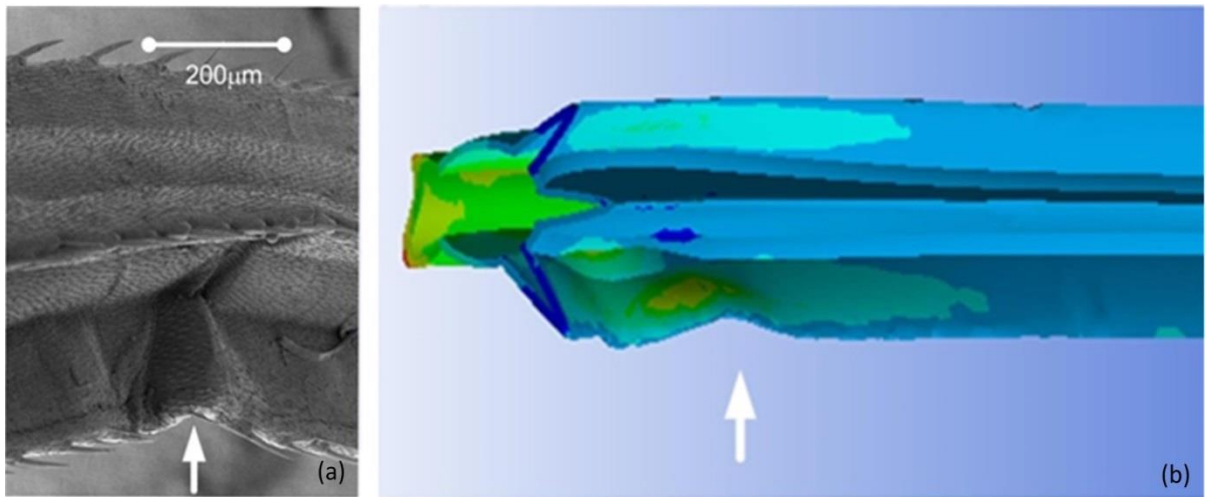


Figure 4.3: A scanning electron microscope image (a) and corresponding FE model (b) of the stick insect leg, showing a buckling feature in one of the longitudinal ridges (arrowed). Contours in the FE model show the Von Mises equivalent stress.

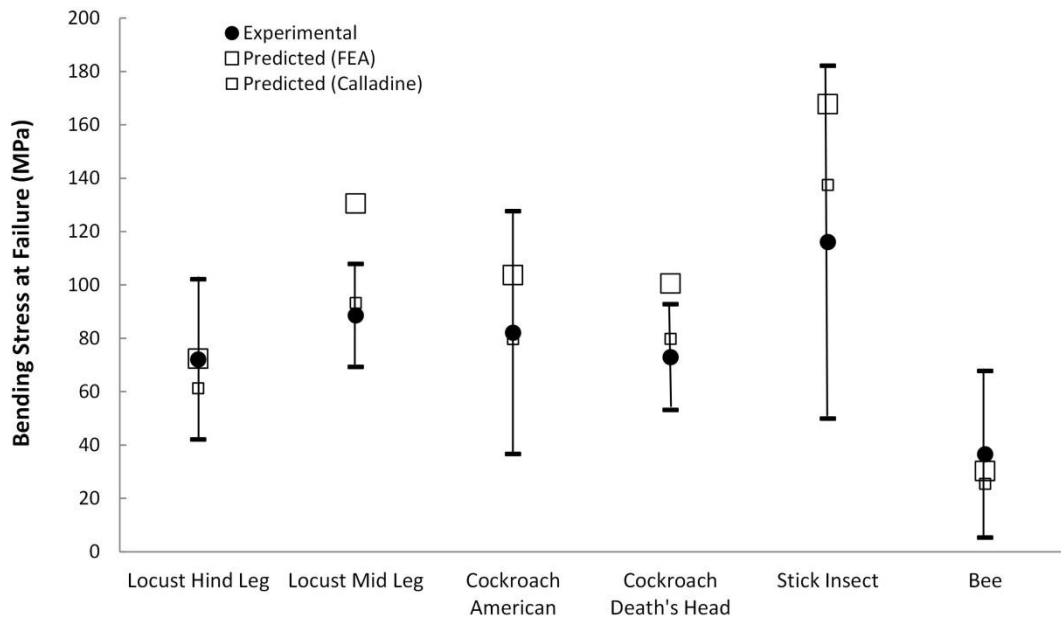


Figure 4.4: Experimental results for bending stress at failure (mean and standard deviation) and predictions using FEA and Calladine's formula. In all cases the stress is calculated assuming a circular tube of constant wall thickness. In the case of the stick insect the presence of the ridges is ignored.

4.4.1 Buckling Predictions

Buckling failures were successfully generated in the FE simulations. Figure 4.5 shows some examples. Figure 4.6 shows a comparison between FEA predictions and those using equation 4.2, for simple circular tubes having dimensions and material properties typical of those in the experimental samples. The tube thickness was kept constant at 0.06 mm whilst the radius was

varied from 0.3 mm to 1.2 mm, thus varying r/t from 5 to 20. Young's modulus was kept constant at 2 GPa. It can be seen that the FE predictions fell between those of Calladine and NASA, lying very close to the Calladine prediction at low r/t and somewhat higher at higher r/t . As seen in Table 4.1 and Figure 4.5, predictions made using Calladine and using FEA agree quite well with the experimental data, falling within one standard deviation in all but two cases. Overall the Calladine prediction is rather better: the average error being 14%.

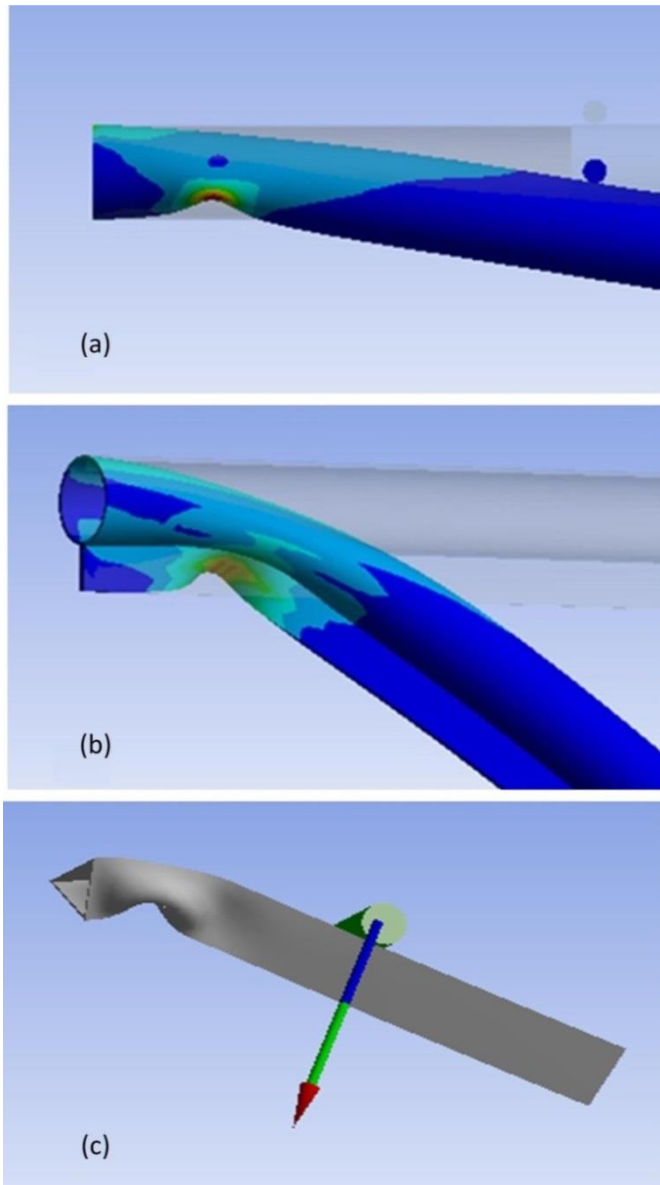


Figure 4.5: Examples of FE simulations of buckling events: the contours show Von Mises equivalent stress. Tubes were restrained at their left hand ends and subjected to cantilever bending by loading them through a small circular bar (shown in (c)), using a frictionless contact. (a): A side view of a circular tube, showing a buckling event occurring approximately one diameter from the fixed end. (b): A tube with a longitudinal fin: the fin has buckled sideways as a result of high compressive stresses. (c): The triangular model used for simulating buckling in the bee leg.

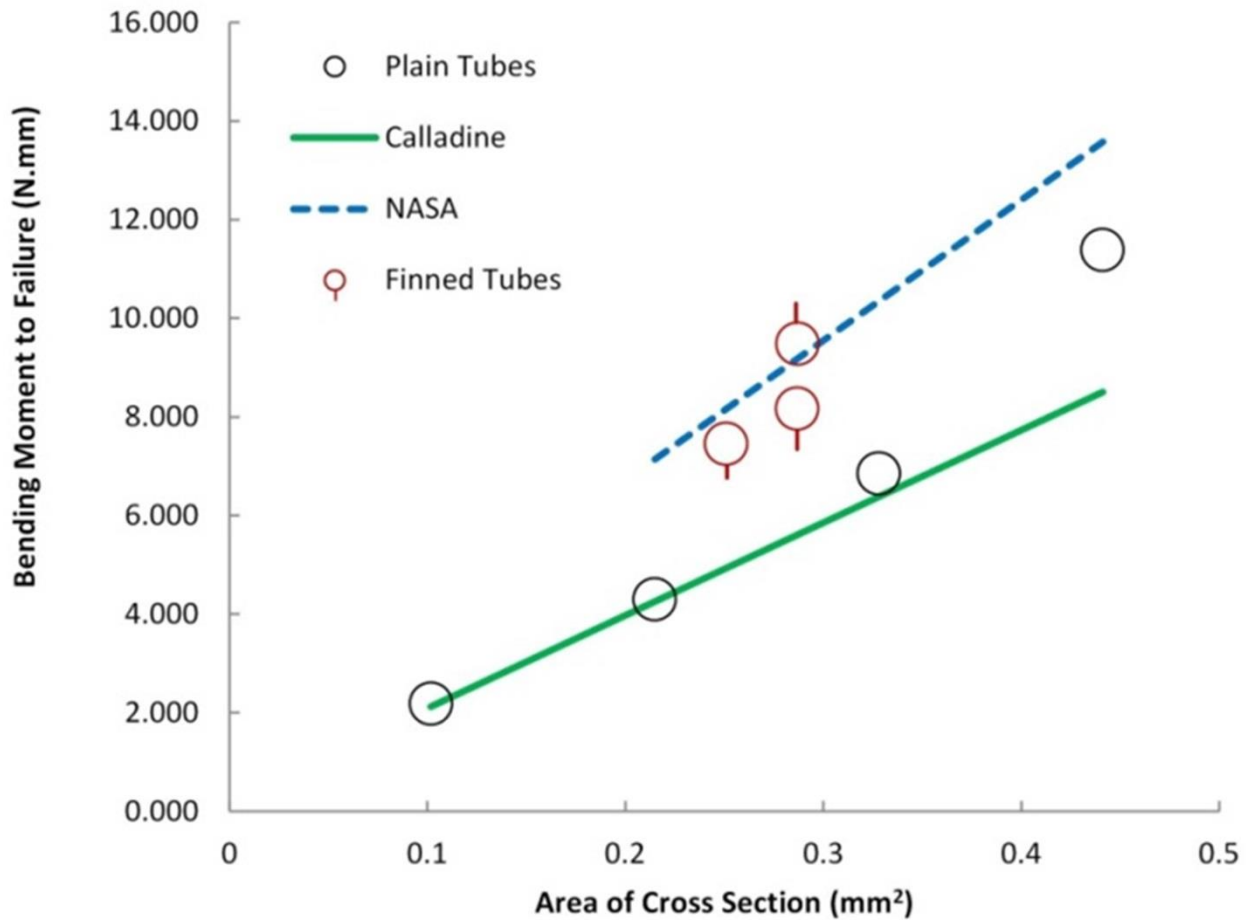


Figure 4.6: Results from FE simulations of circular tubes with and without fins. The tubes had dimensions typical of those found in the insect legs; r/t was varied from 5 to 20 keeping t constant. The bending moment at the onset of buckling is plotted as a function of the area of the cross section. Predictions according to NASA and Calladine are included. For the finned tubes the symbols indicate the length and location of the fin.

The effect of longitudinal ridges was investigated by making a number of models in which single fins were attached to circular tubes: these results are shown on Figure 4.6. Three different models were made: in two cases a fin of length equal to the tube radius was added on the top or bottom surface. The model with the fin on the bottom is shown in Figure 4.5 (b). In a third model a ridge of half the radius was placed on the bottom surface. By plotting the bending moment to failure as a function of the area of the cross section it is clear that all of these ridges are effective, increasing the strength of the tubes by about 40% above that of a circular tube of the same cross sectional area.

To further investigate the legs with non-circular cross sections – the stick insect and the bee – FE models were made to approximate the geometry of selected individual samples. Figure 4.3 shows a Finite Element model of a stick insect sample in which buckling occurred in one of the ridges, closely matching the experimental result. Figure 4.7 shows an example of one comparison made between experimental and simulated force/deflection curves. Choosing a Young's modulus of 7.7 GPa for the model in this instance gave a good match to the initial, elastic part of the stress strain curve but buckling failure was predicted to occur at a much higher force than found experimentally. Several such comparisons were made between experimental results and FE models to give the average stiffness value for the stick insect tibia shown in Table 4.1

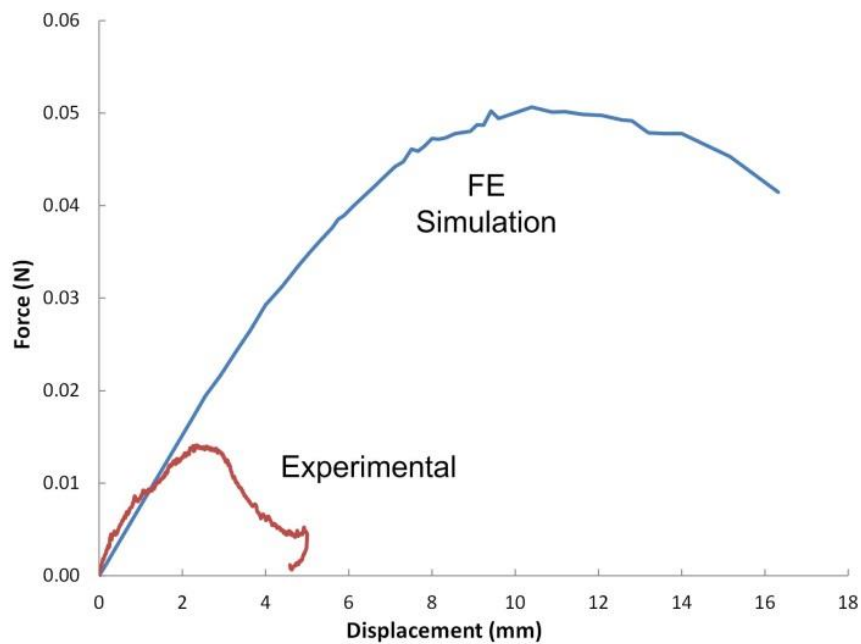


Figure 4.7: Experimental data for a stick insect tibia and the results of a Finite Element simulation of a model of the same tibia.

The average Young's modulus for all the stick insect samples tested was found to be 5.5GPa and the predicted buckling force was larger than the experimental value by a factor 2.57. The reason for this was revealed by examining the stresses which develop in the ridges (see Figure 4.3): at the experimental failure force, the maximum stress in the ridges is predicted to be 85MPa. This is likely to be similar to the yield strength of the material. The yield strength of insect cuticle has not

been accurately measured as yet, and there has been no previous work on the mechanical properties of cuticle from the stick insect. However two results exist for the tensile breaking strength of cuticle from locusts: 94.1MPa for the tibia of *Schistocerca gregaria* (Jensen and Weis-Fogh, 1962) and 78.5MPa for the hind plates of the femur of *Locusta migratoria migratorioides* (Hepburn and Joffe, 1974), so it seems reasonable that compressive yielding will occur in the stick insect cuticle at around 85MPa. This implies that failure is associated with yielding and plastic deformation in the ridges, ultimately leading to buckling (as see in Figure 4.3). Rather than elastic buckling, this is plastic buckling, confirmed by the permanent deformation visible in the SEM picture. Interestingly (as Figure 4.4 shows), the failure stress of the stick insect limbs can be predicted reasonably accurately by simply using the equation for a circular tube (equation 4.2) and ignoring the existence of the ridges. Of course in this case the stress value calculated is a nominal value, not an accurate reflection of the actual stresses. So a better way to express the accuracy of the prediction is in terms of the applied bending moment to failure, which can be predicted (ignoring the ridges) to be 1.8×10^{-4} Nm, compared to the experimental value of 1.53×10^{-4} Nm.

Bee leg samples were also analysed in the same way as outlined for the stick insect, making specific FE models (Figure 4.5 (c)) and comparing the force/deflection curves from the model and the experiment. As Figure 4.8 shows, by choosing a value for Young's modulus it was possible to achieve good predictions of both the stiffness (i.e. the initial slope of the force deflection curve) and the buckling load. In this way the average Young's modulus for the bee samples was determined to be 1.58GPa. As shown in Figure 4.4, the predicted nominal stress to failure (assuming a circular cross section of the same area and wall thickness) is slightly lower than the average experimental value, but the difference is small.

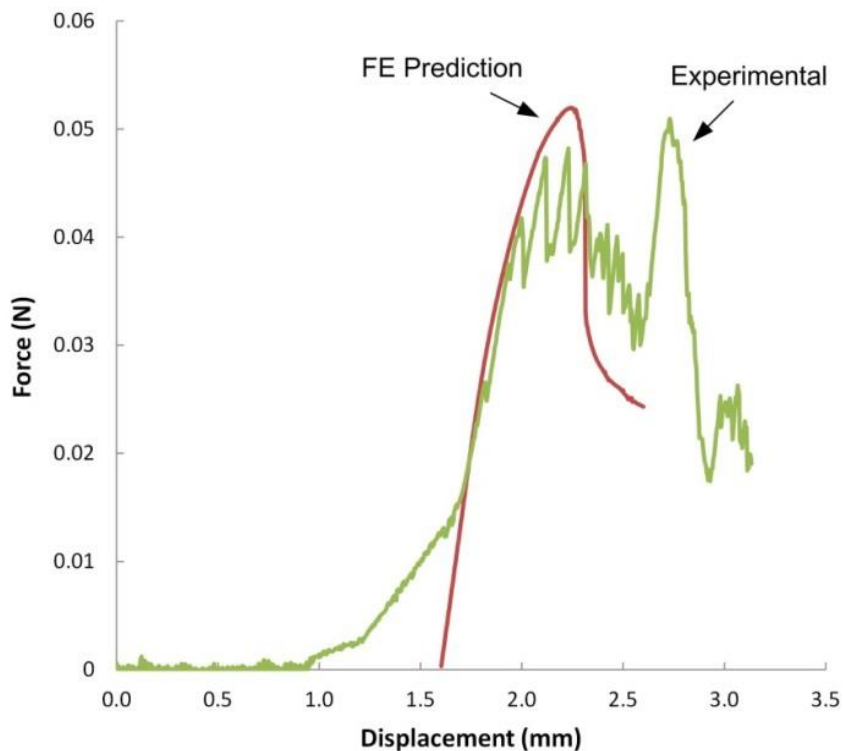


Figure 4.8: Experimental data for a bee tibia and the results of a Finite Element simulation of a model of the same tibia. The starting point for the FE simulation has been shifted along the displacement axis so that its initial linear portion corresponds with that of the experimental sample, ignoring an initial section with lower slope which is caused by the pointer settling onto the sample.

4.5 Discussion

This work has shown that buckling is the dominant mode of failure for the legs of a range of different insects. All these legs are made from chitin-based cuticle, but measurements of Young's modulus (Table 4.1) show that the material properties vary considerably from one species to another. This is undoubtedly linked to the amount and orientation of the chitin fibres, and the relative amounts of exocuticle and endocuticle present in the graded structure of the legs.

FE analysis of tubes with simple circular cross sections has shown that it is possible to predict buckling, with results comparable to those obtained from previous analytical solutions. For the range of r/t values tested, the predicted bending moment for buckling lies between the predictions of the Calladine (1983) and NASA (1968) formulae, being closer to Calladine. Rather than using FEA to find an instability condition, the large deflections facility was used. This is useful in cases where the force/displacement curve is non-linear as a result *not* of non-linear material

behaviour but rather due to geometric changes during loading, in this case the large local displacements of the tube wall in the region where buckling eventually occurs. The type of testing used – cantilever bending – gives a maximum bending moment at the fixed end of the sample, however buckling is prevented from occurring here by the restraint applied, so buckling occurs a short distance from the fixed end, approximately one diameter away (shown in Figures 4.3 (b) and 4.5 (a)).

FE analysis shows that adding a single fin to a circular tube increased the resistance to buckling significantly when compared to a circular tube having the same cross sectional area. This is not surprising since the fin was placed in the plane of bending. A slightly non-intuitive finding was that it is better to place the fin on the top surface, i.e. on the side experiencing tensile stress, rather than on the bottom surface where the buckling event actually occurs (see Figure 4.6).

These FE results would imply that the longitudinal ridges on stick insect legs have evolved to prevent buckling, however the experimental results suggest otherwise. Whilst this would be the case if the material behaved elastically (Figure 4.7) premature failure occurs, probably as a result of the onset of plastic deformation, causing a visible, permanent buckling event in one of the fins (Figure 4.3). This raises the question: “What is the purpose of these ridges?” Another possible mechanical purpose would be to increase stiffness: the legs of the stick insect are very long and slender, and will tend to deflect considerably even under forces which will not cause them to fail. Excessive deflection could prevent the legs from functioning correctly. The addition of these ridges increased the stiffness of the leg by approximately a factor of three. However, this is achieved at the expense of adding a considerable amount of material to the cross section (Figure 4.2 (b)). If the extra material were to be used instead to make a circular tube of larger radius, this would have increased the stiffness by about a factor of four. So it seems that the use of these ridges is not an optimal way of increasing stiffness. It is likely that they have evolved to serve some other purpose, perhaps not a mechanical one, possibly even to aid in the camouflage of the insect in the eyes of its predators. Longitudinal ridges are often observed in tree-bark, which is caused by splitting as the tree expands and grows (see Figure 4.9)



Figure 4.9: the bark of a mature tree showing longitudinal ridges. It may be possible that the purpose of the ridges visible on a stick insect's leg is to mimic this type of structure. (Photo from Carolina Nature website)

Although most are circular in cross-section, tibiae of the other insects examined also display specializations in the form of spines.

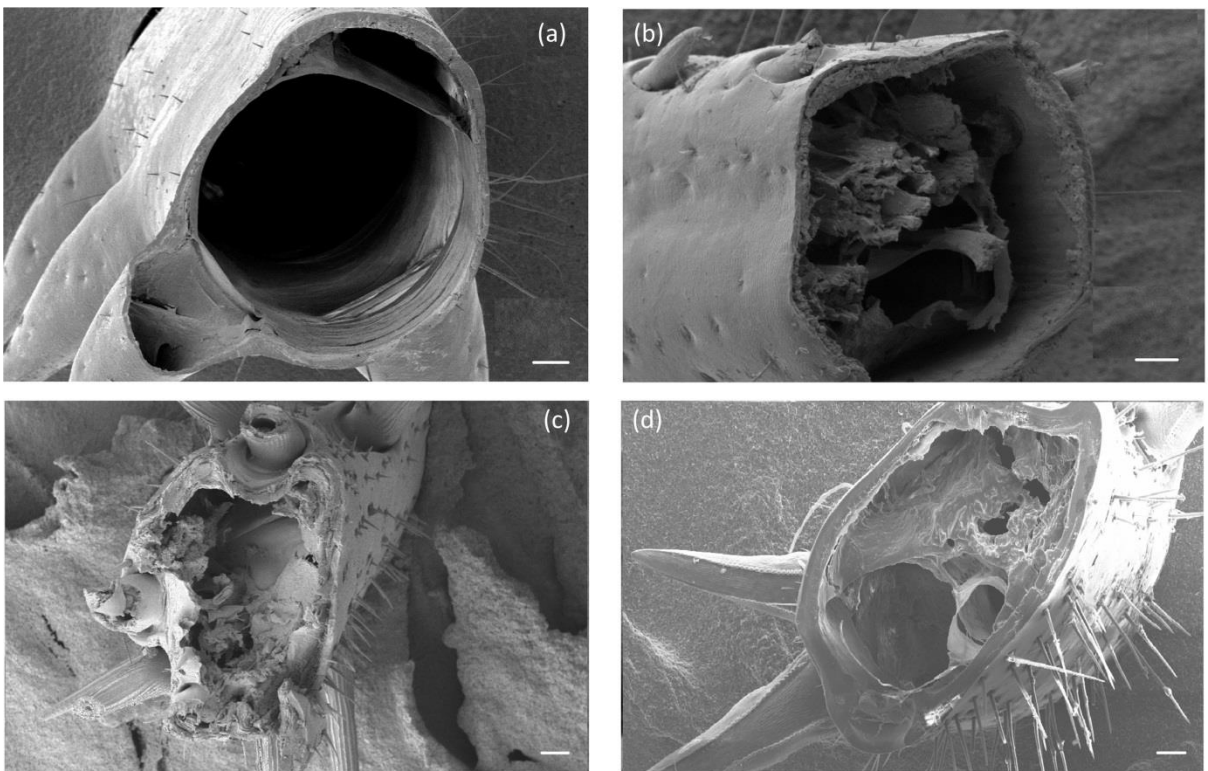


Figure 4.10: spines on locust hind-leg (a), locust mid-leg (b), American hind-leg (c) and Death's Head hind-leg (d). Scale bars measure 100µm.

Figure 4.10 shows that the arrangement of the spines differs from leg to leg. Both locust legs display a double row of "staggered" spines. The American and Death's Head cockroach have much

larger spines, oriented in a more random fashion. Some seem to be “embedded” into the cuticle, which may be a way of reinforcing a stress concentration that the base of the spine experiences when the tip contacts a surface during walking or running. It has been suggested that spines may serve a function in fighting off predators or rivals, and also that they reduce the “effective length” of the leg, reducing the chance of Euler buckling from occurring (Vincent and Wegst, 2004). It is also possible that these spines effectively increase the surface area that is in contact with the ground, perhaps enabling the insect to walk or run faster. All spines point in the opposite direction to that of walking, giving the impression that they are used for “pushing” the insect along, as it scurries across a surface.

The non-circular shape of the bee leg, having one large flat face, would appear to be disadvantageous as regards buckling, however this was not the case. Even though the leg was loaded with the flat side uppermost, thus giving it the smallest moment of inertia for the cross section, the bending moment required for buckling was very similar to that predicted for a circular cross section of the same area and thickness (see Figure 4.4) and this similarity was confirmed with an accurate FE model of this cross section. This shows that non-circular cross sections can be developed without sacrificing strength when buckling is the dominant failure mode.

A very simple formula, equation 4.2 with a constant $\beta = 0.313$ as proposed by Calladine, is able to give reasonably accurate predictions of the buckling strength for all insect legs tested, even though none of them are perfectly circular and some have very non-circular cross sections. In the case of the stick insect the longitudinal ridges were ignored in this calculation; the success of the Calladine formula in this case is clearly fortuitous since the mode of failure is not elastic buckling anyway. Finite element analysis using a non-linear material model would be needed to make accurate predictions. Apart from this case, elastic buckling was found to be responsible for all failures. These findings are useful because they help in understanding how these body parts have evolved, and what factors in the material properties and morphology are relevant. For example, the fact that failure occurs by elastic buckling rather than by plastic yielding or brittle fracture, means that the relevant material property is Young’s modulus, rather than the yield strength or

fracture toughness. It also informs the discussion regarding the geometry and dimensions of exoskeletal body parts: such parts will have relatively large diameters, compared to endoskeletons, which means that inevitably they will be quite thin-walled (to reduce weight), giving them the kinds of shapes for which buckling is a significant risk.

4.6 Conclusions

In this work, tests on the tibiae of several different species of insect showed that the mode of failure was buckling, a type of failure which is also common in engineering structures. Elastic buckling of circular tubes loaded in bending can be simulated using finite element analysis, using the “large deflections” mode. For the range of r/t values considered here the predictions are similar to those of Calladine, who incorporated ovalisation into a prediction of local buckling. The tibiae of locusts and cockroaches are approximately circular tubes of constant wall thickness. Cantilever bending causes elastic buckling which can be predicted using FEA, and even more accurately using Calladine’s formula (equation 4.2).

The tibiae of stick insects have prominent longitudinal ridges which would appear to be useful to increase stiffness and prevent buckling, however this turns out not to be the case because high stresses in the ridges cause failure by plastic buckling. This demonstrates how material properties and geometry can interact in complex ways, which must be taken into account when designing thin-walled tubes. The tibiae of bees have a triangular cross section featuring a large flat side for pollen collection. This does not significantly affect the bending moment to failure, showing that non-circular cross sections can be designed without compromising mechanical strength.

Insights into buckling prediction and prevention might be gained by studying this phenomenon in the exoskeletons of insects and other arthropods. Resistance to buckling depends on a combination of material properties and geometric factors and can be difficult to predict for components in engineering structures. The success of the FE approach in this study may prove very useful because it implies that FE modelling can also be used to investigate more complex cases such as tubes with fins and non-circular cross sections.

Chapter 5: Cuticle growth rates: their purpose and effect on tibia structural properties in the desert locust.

5.1 Abstract

It is commonly believed that after moulting, the inner Endocuticle is the only layer of the insect cuticle that grows, and does so as the insect deposits layers of the material on a daily basis. In this chapter, I examine the rate of this growth, and its effect on the mechanical properties and failure mode of adult locust (*Schistocerca gregaria*) hind tibiae. I experimentally tested these to failure using cantilever bending at several time intervals after their final moult, gathering information on failure strength, material stiffness and tibia dimensions. I found the rate of Endocuticle growth to initially be on average 1.8µm daily, dropping off to 0.3µm daily after approximately 21 days.

Similarly, the failure strength and stiffness of the tibia were both seen to increase as the thickness increased – more rapidly at first and then levelling off. As in the previous chapter, I have used Calladine's equation ($\sigma = \frac{0.313 \times E \times \text{thickness}}{\text{radius}}$) for predicting the elastic buckling strength, which provided a good fit for the experimental data for thinner samples, but not so for thicker (older) samples. I concluded that the thinner samples must be failing due to local buckling (which depends on geometry and stiffness), with the thicker ones failing due to reaching the ultimate (compressive or tensile) strength of the material during the tests. Compressive yielding or plastic buckling of the chitin fibres on the compressive side and a tensile yielding such as fracture or delamination on the tensile side may be competing and to some extent interacting to cause final failure (averaging 175.7 ± 31.5 MPa). As the insect matures and its tibia's thickness increases due to the addition of endocuticle, it becomes better equipped to resist a buckling failure. Once it reaches a certain thickness however, the addition of new material is not as urgent, which I believe is the reason that the rate of deposition slows down significantly.

Taylor and Dirks (2012) estimated an optimum r/t value for the locust tibia of 7.2 to resist the bending stresses experienced while jumping. This study proposes a new value of 10.25. Immediately after moulting, the cuticle is relatively thin, giving a large r/t value, which decreases as the insect ages and the cuticle thickens. The insect transitions through this optimum r/t value

approximately 12 days post moult (as opposed to 25 days by Taylor and Dirks' calculations). Reaching and passing beyond the optimal r/t value as quickly as possible is important for the fitness of the insect in avoiding buckling failures due to bending forces applied when jumping.

5.2 Introduction

After moulting, insect cuticle is initially soft, becoming much harder and stiffer over the next 1-3 days due to the sclerotization process (outlined in Section 1.2.6). At this point, the exoskeleton consists almost completely of exocuticle. Layers of endocuticle are deposited on a daily basis in such a fashion that the number of days since the last moult can be counted (much like the rings on a tree trunk, see Figure 1.13) (Neville, 1963).

The mechanical properties of the cuticle can depend on the interaction of several factors – the amounts and orientation of the chitin fibres, the constituents and the degree of sclerotization within the protein matrix. Hepburn and Joffe (1974) looked at the variation in mechanical properties of excised sections of the locust femur (in isolation) over short periods of time post-moult. In this chapter, I inspect the hind tibia of the adult desert locust (*Schistocerca gregaria*) at various stages post-moult. I examine the hind tibia as a structure, and how this changes and develops over time. All tests were carried out on insects more than three days after their final moult, so the exocuticle could be assumed to be totally sclerotized. According to current theory, the only variation to its tibia as the locust ages should be an increase in the amount of deposited endocuticle. What purpose does the endocuticle serve? Does it contribute to the material properties of the tibia at all or is it simply a biological phenomenon? Why does the insect employ this graded structure instead of having a uniform tibia? Wouldn't it be easier to just make its legs entirely from exocuticle? The main objective is to observe the rate of deposition of endocuticle over the adult life of the insect, and how it affects the overall mechanical properties of the insect leg such as the failure strength, the stiffness and the failure mode.

5.3 Materials And Methods

5th instar locusts (Figure 5.1 (a)) were kept in the same controlled environment outlined in (Section 2.2.1), and monitored daily. Newly moulted adults (Figure 5.1 (b)) were separated from juveniles every day in order to keep track of days since moult.

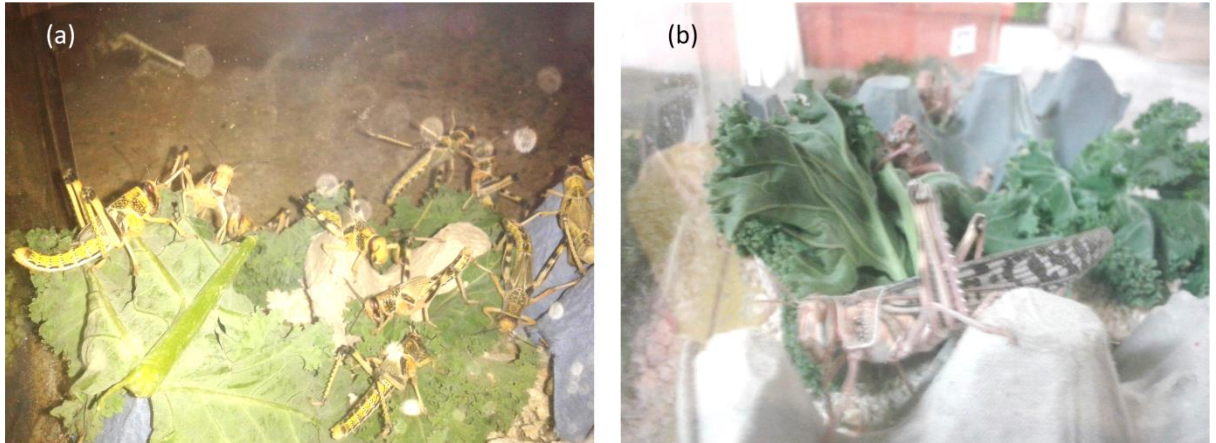


Figure 5.1: 5th instar locusts (a) and newly moulted adults (b)

5.4 Experimental Procedure

The experimental procedure, measurements and calculations were carried out as outlined in Section 2.2, using the rig shown in Figure 2.4. Initial microCT images taken (see Figure 5.2) were of poor resolution and therefore not used for the final measurements (SEM images used instead). Stress, strain and stiffness were all calculated as outlined previously.

As in the Chapter 4, I made predictions relating to the buckling strength of these tibiae using the formula:

$$\sigma = \frac{\beta * Et}{r} \quad (5.1)$$

Again:

$$\beta = 0.313$$

$$E = \frac{E_l}{\sqrt{2}} \text{ (due to the anisotropy of the cuticle)}$$

5.5 Results

Figure 5.2 illustrates the increase in thickness over time. The microCT images (a) show the same general trend as the sketches (b) (Jensen and Weis-Fogh, 1962).

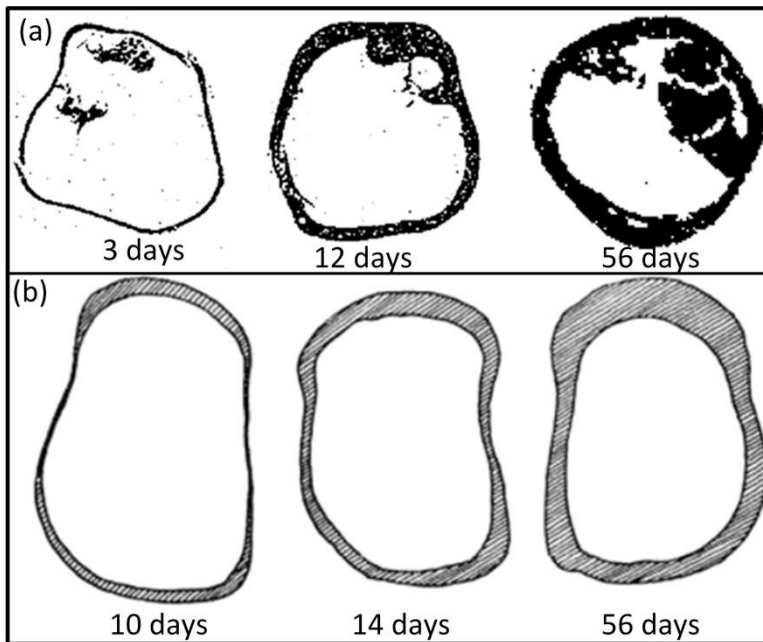


Figure 5.2: (a): microCT images of locust tibia cuticle at 3, 12 and 56 days after moulting. The tibiae at 3 days and 56 days are from the same insect (left and right legs respectively), and (b): sketches to illustrate the growth of cuticle over time (Jensen and Weis-Fogh, 1962). The tibiae at 10 days and 56 days are from the same insect (left and right legs respectively).

Figure 5.3 confirms what can be seen visually in Figure 5.2. The thickness is initially quite small (< 0.04 mm for up to 10 days). It increases rapidly at first, before plateauing after approximately 21 days. The radius can be seen to be constant throughout the life of the adult (between 0.4 and 0.5 mm). The slenderness ratio (r/t) can be seen to decrease as the insect ages. Initially the tibia is thin, so r/t is large (12-15). As the insect ages, the radius remains the same but the thickness increases, so r/t drops – sharply at first, then more gradually.

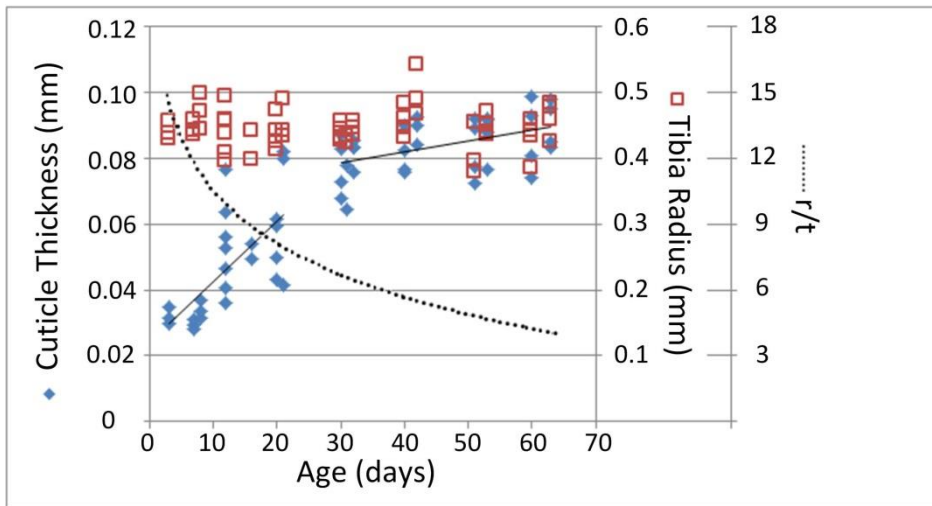


Figure 5.3: cuticle thickness and tibia radius as a function of the days since the final moult. Also plotted is the slenderness ratio or r/t value (dotted line).

Separating the data into samples less than or greater than 21 days old (Figure 5.3) shows that the initial rapid growth rate is on average $1.8 \mu\text{m}/\text{day}$, after which it reduces to an almost negligible $0.3 \mu\text{m}/\text{day}$ for the remainder of the adult's life. One of the main aims of this project is to observe how the material properties and behaviour change as a function of cuticle thickness (not age). Accordingly, I have divided the data into two groups: those thinner and those thicker than 0.06 mm – which was the average tibia thickness for insects 20-21 days after their final moult.

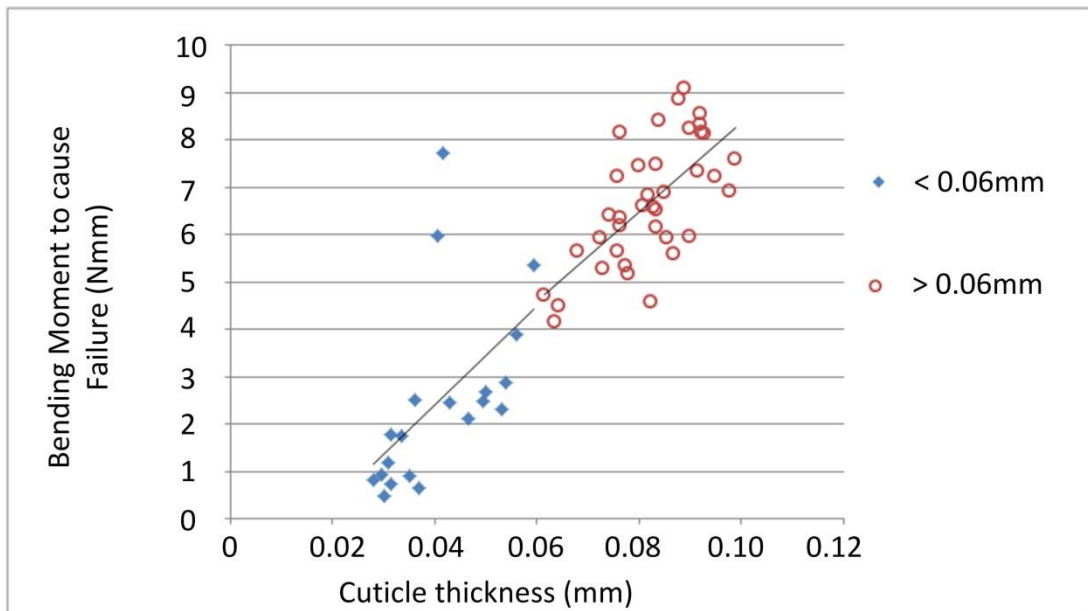


Figure 5.4: Bending moment to cause failure (max force * cantilever leg length) plotted as a function of cuticle thickness (separated into samples thinner than 0.06 mm and those thicker than 0.06 mm). Linear trend-lines are fitted to both groups.

Figure 5.4 shows how the bending moment required to cause failure increases as a function of cuticle thickness. The bending moment increases as the legs become thicker. The relationship is closely matched for both groups (slope of the lines are 103 (Nmm/mm) and 94 (Nmm/mm) for thinner and thicker samples respectively).

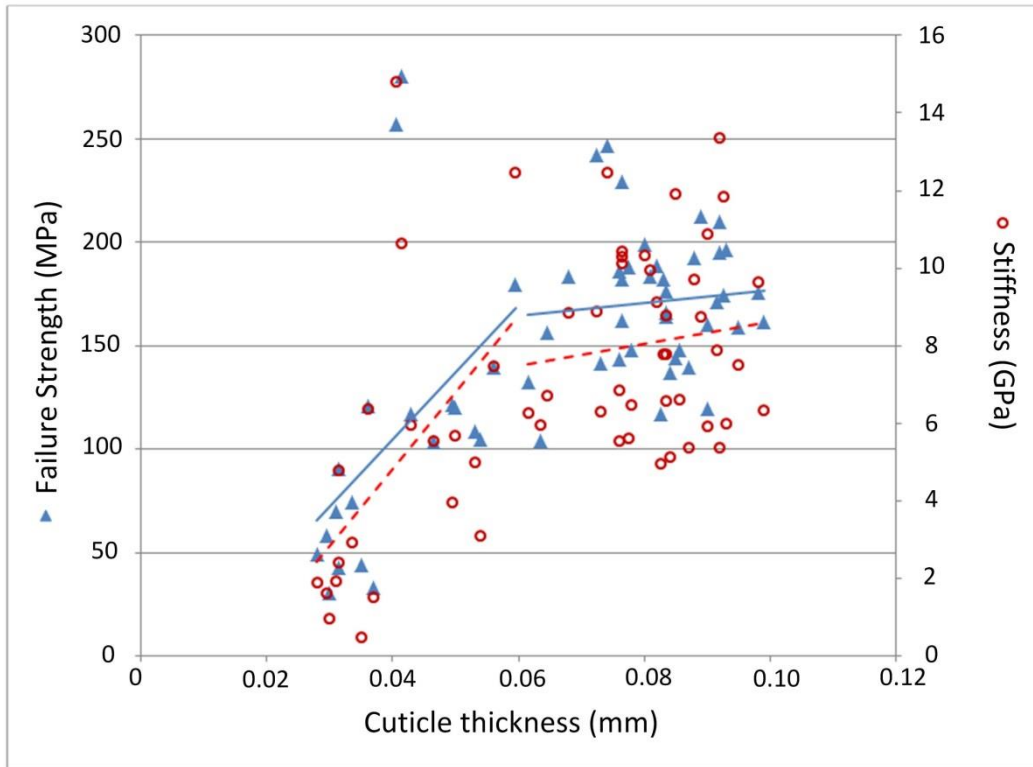


Figure 5.5: stress to cause failure and stiffness (Young’s Modulus, (E)) as a function of cuticle thickness. Data points are separated into two groups: those less than and greater than 0.06mm thick, with linear trend-lines fitted to each group; blue solid lines for strength, red dashed line for stiffness.

Figure 5.5 shows an initial rapid increase in failure strength and stiffness, with values levelling off after 21 days. The initial rate of increase for failure strength averages 3.26MPa/ μm growth, equating to an increase of approximately 5.87 MPa/day. The increase in stiffness averages 0.16 GPa/ μm , approximately 0.29 GPa/day initially. After 21 days, these rates are reduced to an almost negligible 0.31 MPa/ μm (0.09 MPa/day) and 0.029 GPa/ μm (0.0087 GPa/day) for failure strength and stiffness respectively.

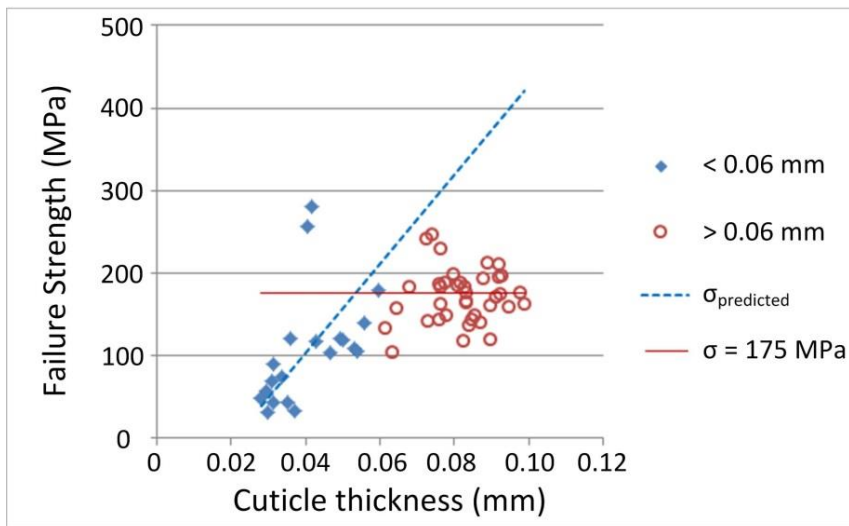


Figure 5.6: failure strength as a function of cuticle thickness for samples thinner and thicker than 0.06 mm. Prediction for elastic buckling failures obtained for each sample using equation (5.1), where E = experimentally determined Young's Modulus. Dotted line shows the trend for these predictions. Solid line shows line of constant stress (175 MPa).

Figure 5.6 shows that the predictive model for buckling failure (dotted blue line) closely matches the experimental results for the thinner samples, but is 2-3 times too great for thicker samples. The value for E (Young's Modulus) used in equation (5.1) for these predictions is the experimentally obtained stiffness. The experimental failure strength values for the thicker samples are clustered more closely around the line of constant stress (175 MPa).

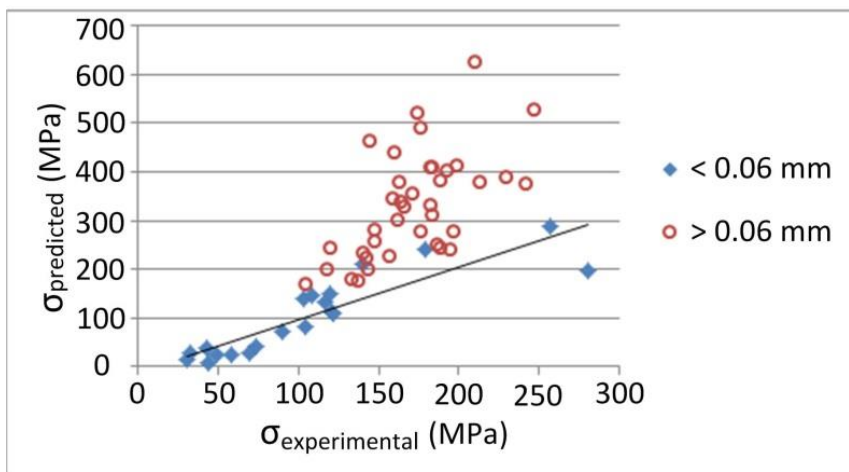


Figure 5.7: predicted stress to failure as a function of experimental stress to failure

If the predictions using equation (5.1) were perfectly accurate, then plotting the predicted stress as a function of the experimental stress should give a straight line, with a slope of 1. Figure 5.7 shows that samples thinner than 0.06mm are very closely clustered about this trend line (slope of

line is 1.09, $R^2 = 0.795$), but thicker samples are more widely scattered, with predictions 2-3 times greater than experimental values.

5.6 Discussion

Adult locusts accumulate mass for the first 4-7 days after moulting (Katz and Gosline, 1992), and continue to deposit endocuticle throughout the first 21 days following the moult (Neville, 1983). Dry cuticle weight of *Schistocerca* increases by a factor of 3.7 over the first 2-3 weeks post-moult (Weis-Fogh, 1952). The weight of chitin in the leg alone (and the wing) increases 5 times over the course of the first eight days post-moult (Candy and Kilby, 1962). Hepburn and Joffe (1974) measured an increase in thickness of 2.0 $\mu\text{m}/\text{day}$ over the first 14 days post-moult in the locust femur. My results are in close agreement with this. Figure 5.3 shows that the thickness of the cuticle increases rapidly at first (averaging 1.8 $\mu\text{m}/\text{day}$ for the first 21 days), the growth rate slowing down significantly after 21 days (to 0.3 $\mu\text{m}/\text{day}$), while the radius remains relatively constant across all age groups. This is well known and is supported by my microCT images (Figure 5.2 (a)) and the Jensen and Weis-Fogh (1962) sketches (Figure 5.2 (b)). What is the reason for this initial rapid increase in thickness, and why does it slow down so dramatically after 21 days?

Bending forces experienced in the locust tibia will dominate over axial compression due to the long slender shape of the leg and the off-axis forces experienced *in vivo*. Jumping induces the most severe loading in the locust hind tibia (Bennet-Clark, 1975; Sutton and Burrows, 2008). As the hind leg is loaded almost exclusively in bending while jumping, it will be prone to buckling failures in the early stages of the insect's adult life. I believe that the initial rapid (1.8 $\mu\text{m}/\text{day}$) deposition of cuticle serves to minimize buckling failures as quickly as possible. Once the leg is above a certain thickness (depending on the leg's stiffness and radius), unstable local buckling is no longer an issue, so the deposition of cuticle is not as important as it was originally. After this point, the continued deposition of cuticle is greatly reduced (to 0.3 $\mu\text{m}/\text{day}$).

The experimental data reinforces this theory. Figure 5.5 shows that failure strength increases rapidly (on average 5.87 MPa/day) for the first 21 days (until the leg is approximately 0.06 mm

thick). A thin walled tube (such as an insect tibia) loaded in bending is susceptible to a buckling failure (see Chapter 4), and these samples were seen to fail by local buckling (a kinking of the tibia adjacent to the fixation point was observed). The observed increase in failure strength therefore is actually an increase buckling strength (which depends on both the material quality (stiffness) and dimensions), which is undoubtedly linked to the rapid increase in thickness. Hepburn and Joffe (1974) carried out tensile tests on excised sections from locust femur found a similar rapid initial growth in endocuticle but saw that it contributed nothing to the overall tensile breaking strength of the excised sections, with forces to cause failure becoming constant after 2 days. My results contradict this finding. Figure 5.4 shows that the increase in thickness of the tibia leads to an increase in the bending moment required to cause failure across all samples, even continuing to do so after 21 days. My results also show that this extra material serves to structurally strengthen the leg as a whole, by helping to resist a buckling failure rather than increasing the actual material strength.

Although trying to determine the contribution of the endocuticle to the overall properties of the insect leg, it was necessary to analyse the tibia as a tube of a single material. The graded structure of the cuticle (hard, stiff outer exocuticle with pliant, tough inner endocuticle) leads to some complex load bearing situations. Indentation tests (Klocke and Schmitz, 2011) show that exocuticle can have a Modulus up to 3 times greater than endocuticle, and can be up to 4 times harder. Some have theorised that the exocuticle actually bears the vast majority of the strain, with the inner endocuticle merely acting as a “crack stopper” to better tolerate defects in the exocuticle. If this *was* the case, one would assume that the material would maintain the same strength and stiffness properties once the exocuticle layer is complete (the addition of new endocuticle only contributing a relatively small increase if any). Figure 5.5 shows that this is not the case, with strength and stiffness both being relatively small initially (when exocuticle dominates proportionally), but both increase dramatically as the new material is added. Figure 5.4 also shows that the increase in bending moment required to cause failure as more endocuticle is added continues throughout the life of the insect.

As material strength and stiffness are independent of thickness, one would also assume that adding a softer material to a stiffer one would cause the “average” or aggregate stiffness of the entire structure to decrease. Again, Figure 5.5 shows that this is not the case. The addition of the “softer” endocuticle definitely helps to increase the buckling strength of the tube-shaped tibia, but this does not explain the increase in stiffness.

This increase in stiffness observed over the first 21 days (Figure 5.5), implies that the material quality itself is also changing as the insect ages. The observed increase in stiffness will help the leg resist buckling failures (and also increase the material strength). Hepburn and Joffe’s (1974) tensile tests on excised sections of femur cuticle also showed a rise in stiffness but the contribution of endocuticle to the structural strength or stiffness remained unclear. They believed that the rise in stiffness may be due in part to a tanning process that is ongoing within the cuticle. Many previous studies have shown that the exocuticle takes up to 3 days to become fully sclerotized. It is also possible that some additional gradual tanning is taking place within the cuticle (Hepburn and Joffe 1974). It is unclear whether the entire endocuticle becomes slightly more tanned, or if the outermost endocuticle gradually becomes tanned exocuticle. It may also be possible that the exocuticle actually continues to get stiffer as the insect ages – the sclerotization process in the exocuticle could be continuing gradually for much longer than previously predicted. Our research group are currently undertaking some staining analysis on my tested specimens to determine this. By taking thin sections of the tibia using a cryo-micro-tome, and staining these with Mallory trichrome stain, one can distinguish the different layers from one another (exo, meso and endo cuticle layers are all stained different colours (Klocke and Schmitz, 2011)).

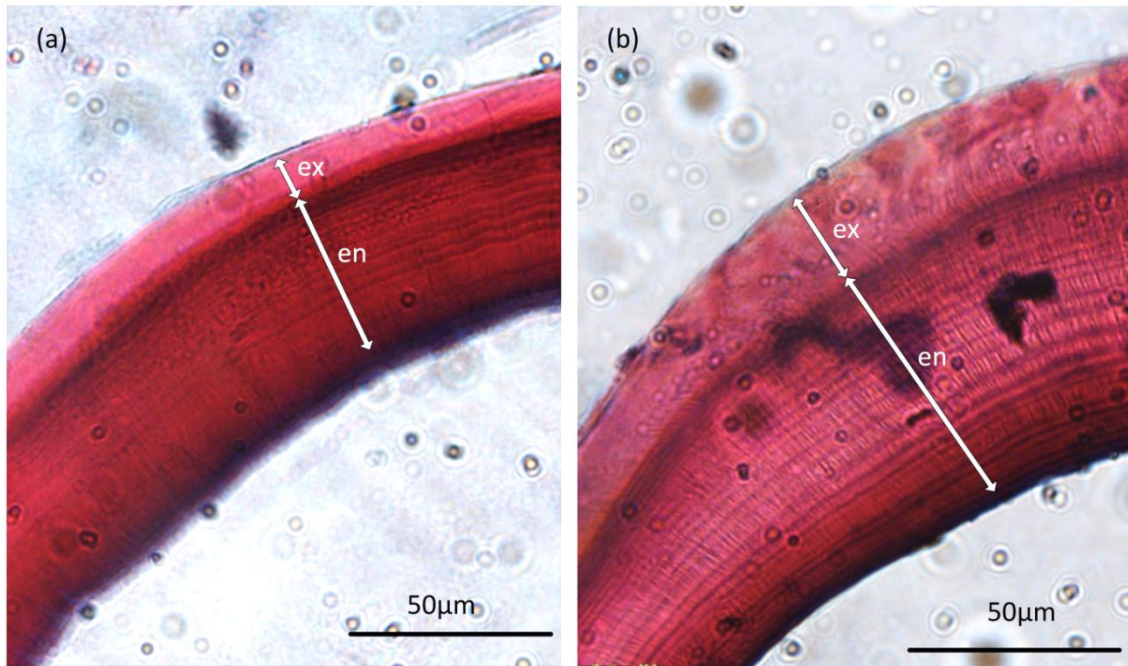


Figure 5.8: initial staining tests, ex = exocuticle, en = endocuticle, thickness of each indicated by arrows. (a) shows a section of cuticle 8 days post-moult (visible dark layers in the endocuticle). (b) shows a section 30 days post-moult. Total cuticle thickness for (a) and (b) is 56µm and 86µm, while exocuticle thickness for (a) and (b) is 12µm and 21µm respectively.

Figure 5.8 shows some stained samples. Notably, mesocuticle is absent in the locust tibia (Neville, 1965). Exocuticle has been stained a lighter shade of red, and endocuticle a darker purple / blue (our technique still requires some perfecting). The outer epicuticle is also visible as the thin outer line. Also visible are the alternating light and dark layers in the endocuticle showing the day / night cycle of deposition mentioned in Section 1.3.1).

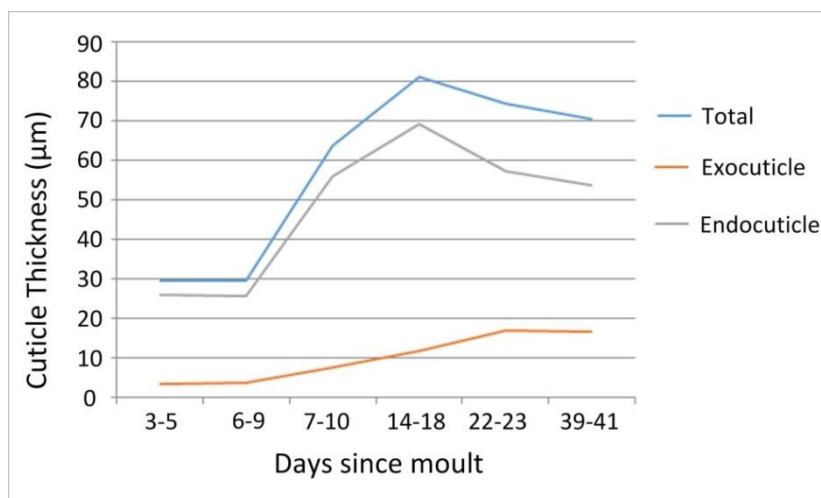


Figure 5.9: Initial graph plotting measurements taken of total cuticle thickness, exocuticle thickness and endocuticle thickness.

These tests are in the early stages, but they seem to support the theory that the exocuticle layer actually grows progressively over the insect's life, meaning that the outermost endocuticle could be gradually becoming sclerotized into exocuticle as the insect ages. In Figure 5.9, the thickness of the exocuticle increases at the expense of the endocuticle. This could be the reason for the observed increase in stiffness over the first 21 days post-moult. Figure 5.9 only plots one value for each timeframe. We are not sure what our staining tests will reveal, and many more similar staining tests on locusts of different ages would be required to get averages and to confirm this theory, but initial results seem promising.

In Figure 5.6, Calladine's equation (5.1) is used to predict the stress required to cause buckling for each of the samples. A linear trend line was fitted to this data. For the thinner (more slender) samples, these predictions match the experimental values quite closely, but predictions are 2-3 times above experimental values for thicker samples. The accuracy of the predictions is confirmed in Figure 5.7, where predicted buckling strength values are plotted as a function of experimental failure strength values. If my model matched my experiments perfectly, the slope of the line should be 1, and all data points should be on this line. The slope is actually 1.09, implying my predictions are reasonably accurate. All thinner samples (blue) are clustered closely around this line ($R^2 = 0.795$). Even the two "outliers" seen in Figure 5.6 (much higher failure strength than others) lie close to this line, showing that they too conform to the elastic buckling model. These tibiae may have sclerotized more quickly or to a greater extent, creating a material that was stronger and stiffer than the others, but still vulnerable to a buckling failure. The thicker samples do not lie near this line – again suggesting that these samples did not fail due to local elastic buckling. I believe that the thicker samples failed due to plastic (or permanent) buckling from reaching the material's ultimate strength during the test. The material (and therefore the leg) fails before reaching the predicted "buckling strength". This material failure may occur within the cuticle either through tensile fracture due to cracking or delamination, or through compressive collapse of individual layers – or a combination of both. Many of the samples fail at a stress below the lower of two modes, which may imply that there could be an interaction of failure modes

rather than one (buckling or fracture) acting in isolation – though this could also be due to some scatter inherent with testing biological specimens.

It has been suggested from analysis of several failure modes (including fracture and buckling) that the optimum r/t value for a locust tibia to resist bending stresses is approximately 7.2 (see Figure 1.24). I have plotted the progression of r/t as the insect ages in Figure 5.3 (dotted line). The value of 7.2 is reached when the insect is approximately 25 days old. This “optimum” value predicts when the leg is optimized to resist both buckling and material failure (i.e. is just as likely to fail due to one as the other). Initially, for the slender legs, the r/t value is much “greater” than optimal; the leg is more likely to fail by buckling (as the stress needed to cause buckling for these legs is much less than the material strength). As the insect grows, the legs will transition through the “optimal” r/t value for resisting bending, and will become “less” than optimal (or “overdesigned” from a buckling point of view). The dominant failure mode after this point will be a yielding of the material due to tensile fracture or compressive failure (instead of an unstable local buckling failure). This analysis complements my own findings that the leg initially suffers from buckling failure until it is thick enough for buckling not to be an issue.

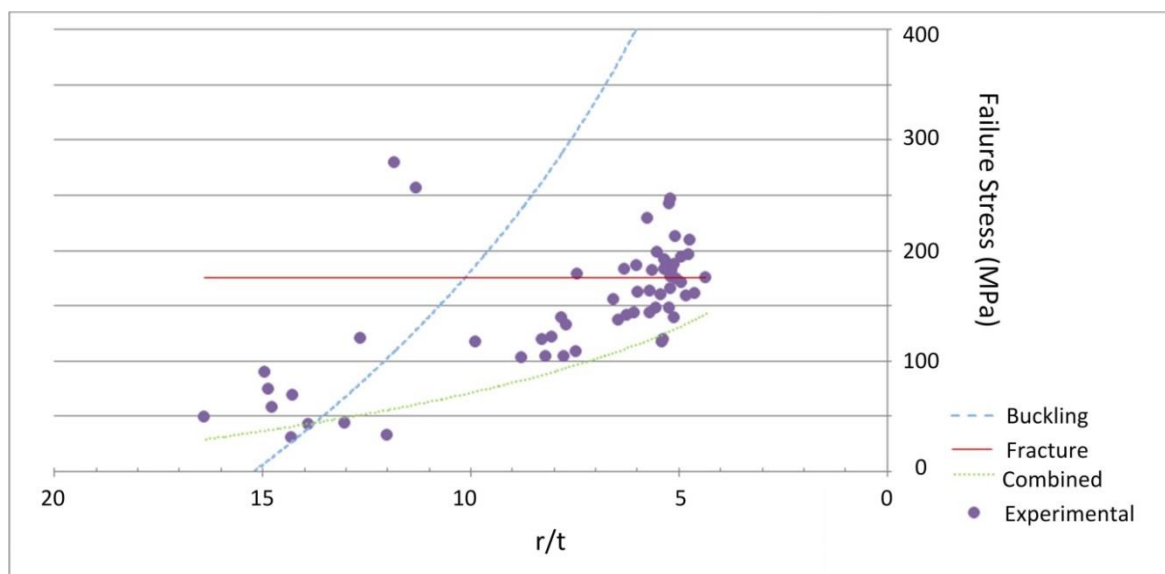


Figure 5.10: The prediction of buckling strength, the material fracture strength, the combination of fracture and buckling, and the experimental values as a function of r/t . I have assumed the “fracture strength” of the material to be constant (the average of all failure strengths for legs over 0.06 mm thick was 175 MPa). This value actually implies a failure of the leg by reaching the material strength, whether

by tensile fracture or compressive collapse (or both). X-axis values are plotted in reverse order to reflect how the r/t value changes (from left to right) throughout the life of the adult insect.

Plotting failure modes (in Figure 5.10) using a similar method to Taylor and Dirks (2012), shows how the experimental values compare to predictions. Most of my experimental values fail close to the lower of the two single failure modes, which is expected. The “combined” mode plotted here represents a lower bound for possible failure strength. This represents a situation where both buckling and fracture are occurring to the same extent simultaneously and is calculated by:

$$F_{total} = \frac{1}{\frac{1}{F_b} + \frac{1}{F_f}} \quad (5.2)$$

This graph also reveals an optimum r/t value of 10.25 (the crossover point between predicted buckling failure and material strength), meaning the locust would transition through the optimum r/t value approximately 12 days post-moult – much sooner than predicted using Taylor and Dirk’s optimum r/t value of 7.2.

Dirks and Taylor (2012a) calculated a value of 72.05 (\pm 30.5) MPa for the failure strength of a locust tibia 14 days after its final moult. These tests most likely give the buckling strength of the locust tibia at that particular age, as the locusts are not yet “fully mature”. This is confirmed by their thickness measurements 0.054 (\pm 0.007) mm of and their stiffness measurements of 3.05 (\pm 0.6) GPa, neither of which are as high as the values for the older insects shown in Figure 5.5. Using this figure of 72.05 MPa for the failure strength of the leg and using the jumping stress of 42.2 MPa yielded a safety factor of 1.7 (detailed in Chapter 3). Both calculations were carried out for locusts of the same age and tibia dimensions, so this safety factor is accurate for those locusts. It is unclear whether the ground reaction forces for jumping (and other locomotion) increase as the insect ages and becomes heavier (accumulating mass over the first 2-3 weeks of adult life (Weis-Fogh, 1952)).

Assuming that the force used to propel the insect (which is provided by the muscles via the semi-lunar process) is constant; the jumping stress induced will be much greater for more slender tibiae than thicker ones. For my samples, these jumping stresses are initially almost two-thirds

greater than the experimental failure strength values (75-80 MPa for the most slender legs).

Jumping stresses drop off rapidly as the leg gains thickness.

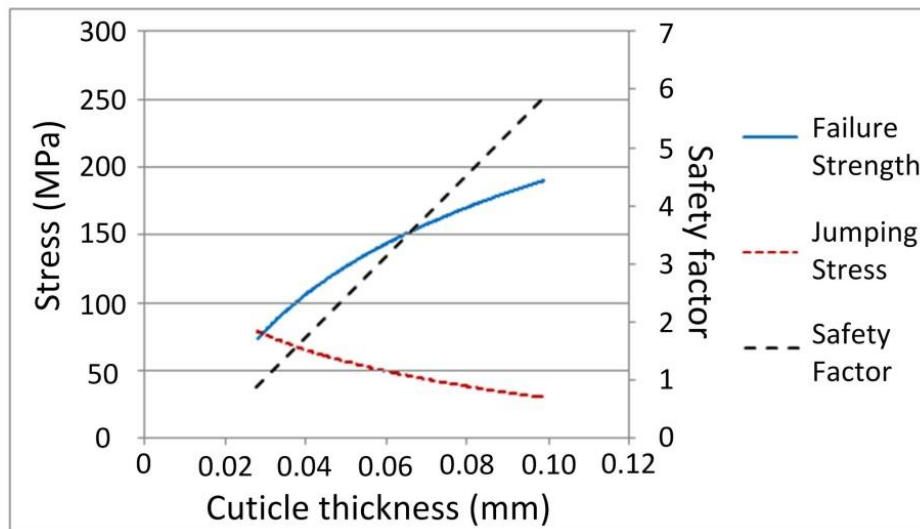


Figure 5.11: plotting failure strength and jumping stress as a function of cuticle thickness. Also plotted is the safety factor (the ratio of the two). Jumping stresses are calculated using an assumed jumping force of 0.15 N and experimentally measured dimensions for the tibia (and the flexure formula).

Plotting the failure strength and the estimated jumping stresses experienced (Figure 5.11), reveals that the safety factor is initially less than one, meaning the leg is in serious danger of failure (in fact, failure is certain if forces of 0.15 N are applied). The safety factor increases almost linearly as the leg ages, eventually becoming greater than 6.

Another possibility is that the jumping force also increases proportionally as the insect becomes heavier in the weeks after moulting (Weis-Fogh, 1952). If this is the case, jumping in the early stages of adult life (provided the exocuticle is “fully sclerotized”) may be safer than predicted above. This would also imply that the predicted jumping stress will also increase as the insect ages, effectively reducing the safety factor for thicker legs plotted in Figure 5.11.

One may assume that if the locust is to jump early in life, it must do so with less force than usual, or risk failure of the tibia. I may have encountered one such locust during these experiments. Both of its hind tibiae were bent in such a way that the permanent deformation could only have occurred when the legs were not yet fully sclerotized or hardened. They were badly bent without

being buckled or fractured. This locust is pictured in Figure 5.12. This perhaps highlights the reason for significantly subdued activity observed in locusts in the days immediately after a moult.

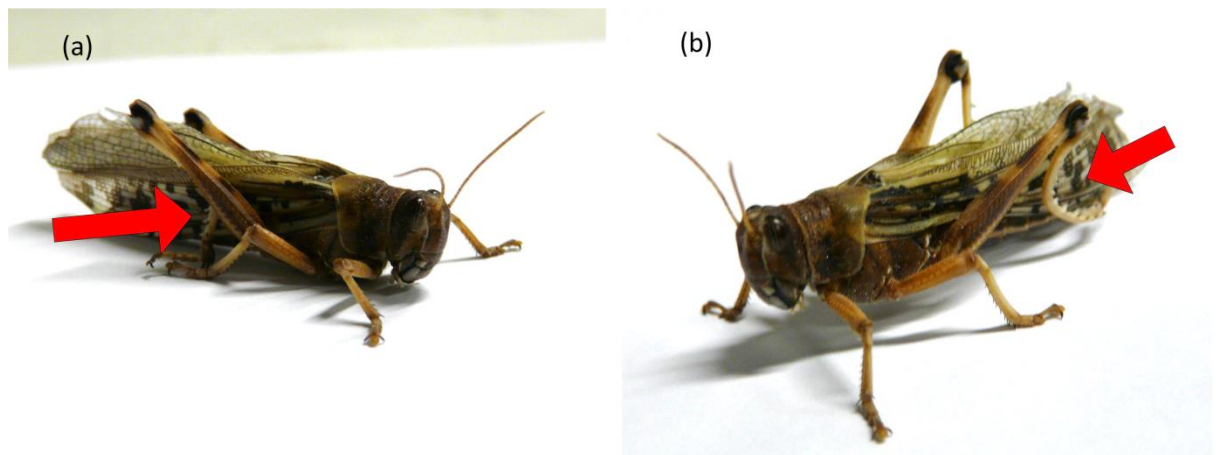


Figure 5.12: a locust with both right (a) and left (b) hind tibiae permanently deformed. These legs (highlighted with arrows) seemed to be as stable and rigid as normal hind tibia, so the bending must have been caused shortly post-moult before the leg hardened due to sclerotization, or perhaps something went wrong during the moulting process.

5.6.1 Purpose for deposition

If the initial rapid deposition of endocuticle serves to quickly increase the strength of the leg until failure occurs due to tensile or compressive yielding rather than buckling, then what is the purpose of the continued deposition of endocuticle after this point, when it does not serve to increase the material strength? Properties like strength (and stiffness) – basically “force per unit area” – are independent of thickness, so it is no surprise that the additional deposition of cuticle does not contribute to increasing the material strength (or stiffness). I have shown (in Figure 5.4) that it does lead to an increase in the bending moment required to cause failure. The relationship between bending moment to failure and cuticle thickness is almost constant across all thicknesses. The addition of material later in life could serve to offset the increased weight of the insect. Greater forces may be required for jumping, so the addition of endocuticle may counteract the greater induced stresses in the tibiae – keeping the safety factor for jumping balanced. This would certainly make for some interesting research in the future.

5.6.2 Stimulus for deposition

There is another interesting question arising from this study. I have observed two significantly different cuticle deposition rates, and have established possible reasons why these rates are required. But what is the nature of the stimulus for these two rates of deposition? How does the insect “know” when to deposit cuticle rapidly, and when to do so more slowly?

It is quite possible that there is a process occurring that is similar to that of modelling in the bones mammals. As mentioned in the Introduction (Section 1.10), bone modelling and remodelling are processes of adaptation in mammal bone in response to loading which involves mechano-sensing cells. Modelling involves targeted deposition of bone matrix, where remodelling involves simultaneous resorption and deposition (also in a targeted manner) in response to micro-damage. As resorption is absent in adult insects, any targeted deposition would therefore be a modelling process.

Also mentioned earlier (Section 1.4.1) are the sensory capabilities of the insect tibia. Locusts and other insects are furnished with deformable oval structures called campaniform sensilla. These monitor loads in the legs of insects and are particularly sensitive to bending. The purpose of this load sensing (which is coupled with muscles in the legs via the nervous system) is to respond to forces and strains experienced *in vivo* (resulting in the “postural position reflex”). The sensilla are derived from and in constant contact with the epidermis – the only living part of the insect integument, from which all cuticle is deposited. Is it possible that these so called “strain gauges” present in locust tibia cuticle may be somehow signalling to the epidermis to deposit cuticle more rapidly when the legs are thin (and therefore experiencing relatively high strains when jumping / walking)? This could account for the sudden stop or slowing down of cuticle deposition. Once the sensilla recognise that strains in the cuticle have reached acceptable levels, they may signal to the epidermis to return to “normal” or “slow” levels of cuticle deposition.

If this is true, it would mean that the sensory feedback coming from the campaniform sensilla is not just used for control and adjustment of locomotion, but for the fine tuning and control of the structural properties of the insect’s exoskeleton, similar to the modelling process seen in mammal

bones. It may even be possible that this feedback system is used for transient control of cuticle properties (e.g. plasticization by hydration) when required.

Another possibility is that the epidermal cells themselves are responding to the applied strains, inducing them to deposit material rapidly when experiencing large strains, and more slowly when experiencing smaller (acceptable) strains. This target of “acceptable levels” of strain may actually be reached when the tibia cuticle transitions through the optimal r/t value outlined earlier. Cells can sense strain. The process of mechanotransduction – how mechanical loading applied to bodies is translated onto the living cells – is an important process which affects cell behaviour. This is not yet well understood for mammals, let alone arthropods.

This theory may also explain the varied geometries and stiffness values seen across the different tibiae and species observed in Chapter 3 where each leg seemed to be “built for purpose” in so far as having similar safety factor for emergency situations (ranging from 1.7 to 4). Many more experiments would be required to test this hypothesis, some of which may include inducing extra strains (or reduced strains) in the locust’s tibia – perhaps by adding to the weight of the locust (increasing the forces and strains experienced while jumping) – this may stimulate further deposition. It would certainly make for some interesting experiments in the future.

When conducting these tests, I removed both hind legs from an individual insect and tested them one after another. I also conducted a batch of tests where I first removed and tested one hind leg from an individual, doing the same for its remaining hind leg some days later. This was done across many age ranges. The purpose of these experiments was primarily for comparison purposes – how much thicker and stronger had the second leg become compared to the first in the intervening time? There was a possible artefact of this test that I did not initially consider. Could removing one leg from the locust cause the remaining leg to be loaded to a greater extent than normal (and hence become stronger)?

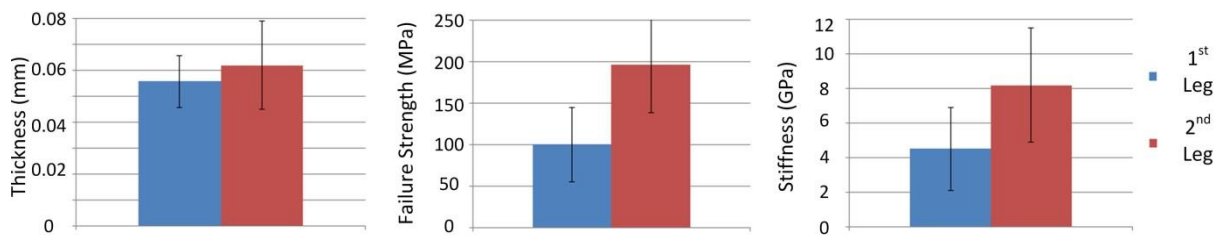


Figure 5.13: thickness, failure strength and stiffness of 1st leg removed compared to the 2nd (remaining) leg

T-tests conducted showed that while the thickness of the legs did not differ significantly ($p = 0.25$), the failure strength and stiffness did ($p = 5 \times 10^{-5}$, $p = 0.0025$ respectively). Comparing this to the results outlined above, it is not clear whether this is due to normal growth or a strengthening of the remaining leg in response to losing the first. Bennet-Clark (1975) noted that a locust with one leg removed will only jump half as far as an uninjured locust, implying that both legs contribute equally to the overall jump. Presumably these tests were carried out shortly after removing the first leg, leaving no opportunity for the second leg to become stronger in compensation.

Only two groups of samples shed any light on the situation. Both are from “fully mature” legs. One is a group where the *first leg* was removed on day 27. These show an average thickness of 0.06mm, failure strength of 142 MPa and stiffness of 5.5 GPa. Compared to a group whose *second leg* was removed on day 27 (the first being removed on days 8 or 12). These show an average thickness of 0.04mm, failure strength of 258 MPa, and stiffness of 9.9 GPa. So although *thinner* than the “first legs”, they are two thirds as strong and almost twice as stiff despite both groups being the same age. Each group only contained 4 samples so this data could be due to natural scatter, but it could also suggest that some strengthening and stiffening of the tibia is occurring possibly due to overloading and compensation in response to the insect losing a leg.

This would seem to support the theory that some modelling of the cuticle is occurring in insect tibiae. Another possible explanation could be that the removal of one leg caused the other to dry out – hence becoming stiffer, stronger, but also thinner. Again, this requires much more in depth investigations beyond the scope of this study.

5.7 Conclusions

I have shown that the thickness of a locust hind tibia increases rapidly for the first 21 days post-moult. This increase in thickness (accompanied by an increase in material stiffness) results in an increase in buckling strength for the tibia. The long slender structure of the locust hind tibia is particularly vulnerable to buckling failures as high loads are applied almost exclusively in bending when the insect jumps. The fitness of the insect depends on its ability to reinforce its leg as quickly as possible in order to endure these high loads. The predictive models complement the theory that the tested legs initially fail due to buckling, but once they are above a certain thickness experience a different type of failure due to the material strength being reached during the test. I have also shown that it may be possible that the buckling failure and material failure modes may be to some extent interacting or competing to bring about failure of the leg.

The initial rapid deposition of cuticle is stopped (or at least slowed down to negligible levels) once the leg has transitioned over a certain thickness (or a particular r/t value). This indicates an intelligent system. The initial resource investment needed for rapid deposition of cuticle is essential to increase the leg's buckling strength. Once local buckling is no longer an issue, the thickness, the failure strength and the stiffness all remain relatively constant. A failure beyond this point will be due to applying loads which the material itself (not necessarily the tibia structure) cannot endure, and which could not be avoided by the addition of more cuticle. The triggers that control these deposition rates remain a mystery, but it is possible that the campaniform sensilla – strain sensitive structures in the tibia itself – may be somehow signalling or stimulating the epidermis to deposit cuticle at different rates when required in a sensory feedback system similar to that seen in mammal bone modelling.

5.8 Future Work

Although it was necessary to perform my calculations as if the tibia contained only one material, it may be possible to model the graded structure using FEA models, and to compare these models to what I found experimentally in this study. A “tube within a tube” model made from two similar materials (with varying stiffness estimated from the literature) could go some way to revealing

the contribution of the endocuticle to the overall material stiffness of the tibia structure, and also to showing how the stress is distributed throughout this graded structure. This, coupled with our ongoing staining work could shed some light on whether the properties of the layers change as the insect ages. It would also be interesting to carry out similar experiments as outlined above on different tibiae and different insects.

Chapter 6: Bridging the gap: targeted cuticle deposition restores mechanical strength to wounded insect tibiae

6.1 Abstract

Animals of every kind must be capable of healing wounds in order to survive and thrive. Insects and arthropods display an injury response that is similar in many ways to that of mammals. Blood coagulation effectively seals the wound, followed quickly by a migration of epidermal cells to restore epidermal continuity, after which they begin to secrete new cuticle. The biological, cellular and genetic processes involved have been studied and compared to those of mammals and vertebrates. Mammalian tissues such as skin, bone and muscle can be fully restored by tissue regeneration and remodelling, restoring their original functional integrity (Li, Chen et al., 2007; Taylor, Hazenberg et al., 2007). Damage to the insect integument cannot be fully healed in adult insects, and to date, no study has been published as to the effectiveness of the wound repair mechanisms of the insect at restoring the structural functionality that existed before injury. I examined the effect of the “patch” of new cuticle deposited under an incision, and found that it almost doubles the mechanical strength of the injured tibia cuticle. The repair process is not a passive phenomenon, but is targeted to specifically reinforce the injured area. The cuticle deposition rates post-injury are more than 4 times that of similarly aged uninjured control samples, but only in the area adjacent to the injury. Other areas of the tibia do not experience any change to normal growth rates, indicating that the localised accelerated growth rate is stimulated by the presence of the injury. If the insect is unsuccessful at reinforcing the area, the tibia strength will remain at 33% of that of an intact specimen, even up to 30 days after the injury. This capacity for repair will depend on the type and severity of the injury.

6.2 Introduction

A summary of the insect's cuticle layers, their constituents and function in relation to protecting the insect are summarized in Table 6.1:

	Epicuticle	Procuticle
Immune Function	Physical barrier	Physical barrier
	Hydrophobic, waxy	Protection against prey / attack
	Prevents adhesion of pathogens	Determines the structural stability, shape, size of the insect
	Impregnated with antibacterial & antifungal peptides and lipids	Connected to the hemolymph via a network of pore canals and wax canals

Table 6.1: Summary of constituent layers of an insect exoskeleton and their immune functions (Chapman, 2013)

As mentioned in Section 1.8, cuticle is not vascularised. Insects have an open circulatory system – organs and cells are “bathed” in hemolymph which flows freely around them, not being contained in vessels as is the case for mammals. The extracellular cuticle of the exoskeleton is separated from the hemolymph by the epidermis and the basement membrane – a selectively permeable membrane which determines what substances are transported, secreted or absorbed into the epithelium and beyond, into the cuticle via a network of pore canals (Lai-Fook, 1966). The epidermis and pore canals are most active before, during and after the moulting process (outlined in Section 1.3), but are also used in response to wound healing.

Table 6.2 summarizes the four main stages of insect wound healing in chronological order (more detail in Section 1.9):

	Coagulation	Melanization	Cell Migration	Cuticle Growth
Purpose	Prevent bleeding Prevent invasion of pathogens Provide structural stability Provide scaffold for cell migration	Encapsulates foreign bodies and parasites Increase stability Can occur without epidermis breach (pinch wound) Area close to scab can also be melanized / sclerotized	Cells migrate from all sides Cell movement and division continues until continuity of epidermis is restored.	New layers of Endocuticle secreted from epidermis once it is continuous Clot & wound remain until next moult
If Absent	Chronic wound ensues	Only 15% of insects survive past 24hrs	Chronic wound ensues	Chronic wound ensues

Table 6.2: the four stages of wound healing, their purpose, and what happens if any one stage is absent. Information gathered from Wigglesworth (1937), Lai-Fook (1966); Lai-Fook (1968), Locke (1966), Rowley and Ratcliffe (1976); Rowley and Ratcliffe (1978), Dillaman and Roer (1980), Wright (1987), Lai, Chen et al. (2001), Galko and Krasnow (2004), Dushay (2009) and Belacortu and Paricio (2011)

The timings of these various stages can vary dramatically from insect to insect; an example of these timings for *Drosophila* is outlined in Figure 6.1.

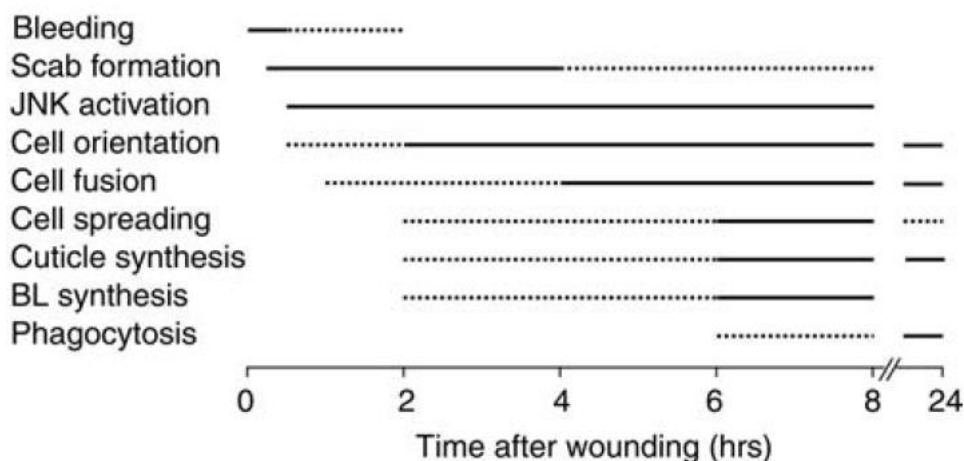


Figure 6.1: From Galko and Krasnow (2004): timing of wound responses for *Drosophila* larvae following a puncture wound. Solid line = time response most often observed, dashed line, occasionally observed, BL = basal lamina.

The hind leg of the adult desert locust provides an ideal specimen to examine the insect injury repair mechanism and its effectiveness at restoring structural integrity. Locusts use their hind legs

to jump in order to take flight, to escape prey, and to fight, and as such it is a crucial appendage. Although a locust can survive and endure for weeks in captivity without both hind legs, it is undoubtedly a severe disadvantage for evading predators and competing against rivals for food and / or mates in the wild. It is therefore highly important for the fitness of an individual to maintain the leg's functionality by recovering from sustained injuries.

The insect's physical response to injury has been summarized in Table 6.2 (and detailed in Section 1.9), but several questions remain unanswered. The primary objectives of this study are to shed light on such questions as:

- Is the response effective at restoring the original strength and stiffness to the material (as is the case for mammal tissue healing (Broughton and Rohrich, 2005; Li, Chen et al., 2007)?
- Is the response effective at stopping cracks from growing from the wound?
- Is the deposition of new endocuticle under the wound a response that is triggered by the injury, or just the result of normal endocuticle growth (a natural occurrence throughout the life of the insect)?
- Is this deposition specifically localised to the wounded area?
- What is the composition of this new material?
- How quickly is the new material deposited?

6.3 Materials and Methods

6.3.1 Insects

Mature (> 30 days post final moult) adult female locusts were used (kept and cared for as outlined in Section 2.2)

6.3.2 Experimental Procedure

In the first iteration of these tests, I bound the wounded femur and tibia together using some fine wire in order to prevent jumping and hence eliminate crack growth from the incision. This yielded some interesting results in so far as these wounded and bound legs appeared to be much stronger and stiffer than they were initially before wounding (approx. 14 days previously). Unfortunately, I discovered that this was an artefact of the binding procedure. Legs that were bound and not wounded showed the same increase in stiffness and strength, implying that the change in material properties was due to binding, and not the wound healing processes. The binding process was perhaps cutting off the circulation of the hemolymph to tibia of the insect, causing it to dry out, becoming more brittle (and hence much stronger and stiffer). This would be an interesting study to carry out in the future, but was a setback for this particular study.

It was decided that instead of binding, the locusts should be housed in individual small tubs after injury in order to minimize kicking and jumping. Trial and error was used to find an “ideal” cut depth – that is, an incision that breached the epidermis which would not lead to further crack propagation from the incision during normal locomotion. A miniature cutting rig (see Figure 6.2) was manufactured for performing these incisions.

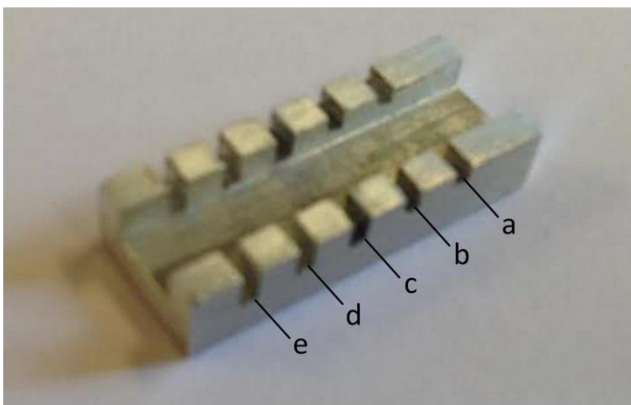


Figure 6.2: the cutting rig for performing incisions. The tibia was placed along the trough in the middle and incisions were made with a scalpel using slots a-e, whose distance above the bottom of the rig were 1.5 mm, 1.25 mm, 0.75 mm, 0.5mm and 0 mm (a-e respectively).

This rig ensured the geometry of the injury and the uninjured section was relatively constant across all samples. To find this “ideal cut depth”, cuts of various depths were performed on locust tibiae using the various slots on the cutting rig, and the insects were left for a period of 14 days to

recover. After this time period, the tibiae were removed and stained, using Acid Fuchsin which would reveal if any cracks had grown from the incision in the intervening time.

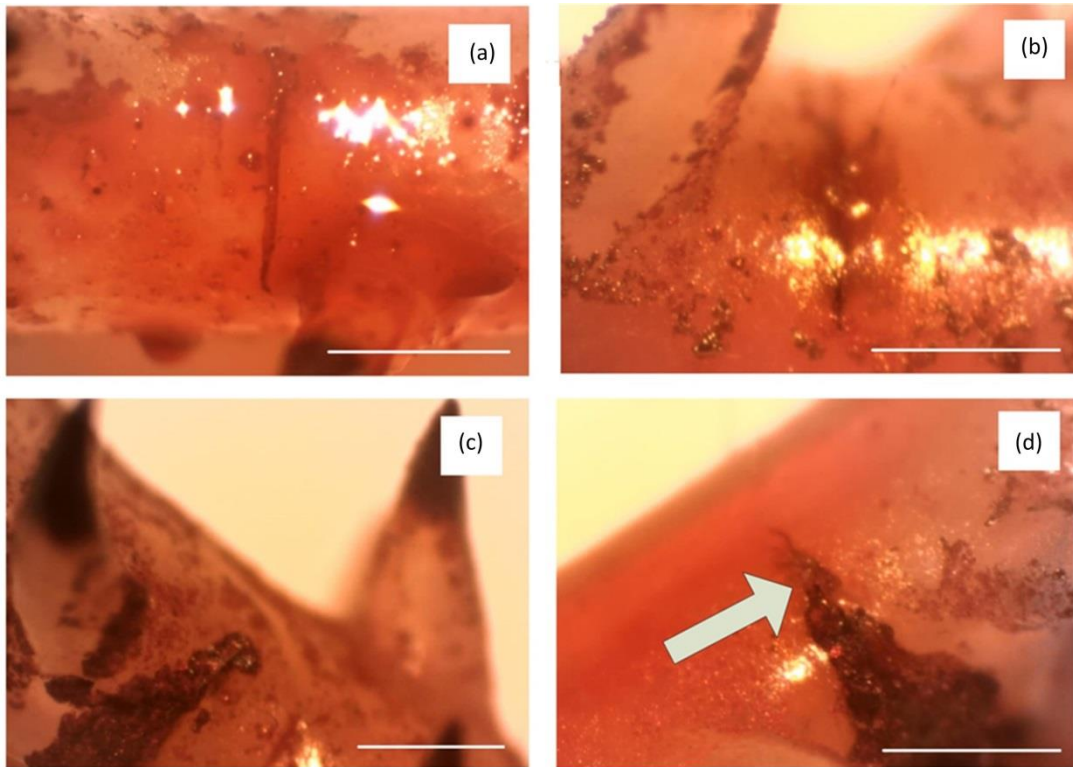


Figure 6.3: Photos of samples showing incremental cut depths used. Scale bars show approx. 0.5mm (a), (using slot a) only superficially scratched the surface, (b) (using slot b) damaged the Procuticle as can be seen from the melanization surrounding the incision, (c) (using slot c) penetrated the epidermis. The melanised clot is visible, and no crack growth is visible beside the incision. (d) (using slot d) leads to crack propagation from the tip of the incision (arrow). This crack propagation occurred under normal locomotion while the locust was housed in isolation in a small tub. This was therefore deemed too deep. This was the deciding factor in choosing cut depth (c) for use in all experiments.

Some cuts did not breach the epidermis (Figure 6.3 (a) and (b)). Other cut depths resulted in significant crack growth from the incision (Figure 6.3 (d)). Neither of these would be suitable for determining the ability of the insect to restore a wounded leg to its original strength or stiffness. The “ideal” cut depth was the largest possible cut depth that did not result in cracks propagating from the incision during normal locomotion (Figure 6.3 (c)).

To perform incisions for the experiments, the insects were sedated and a small incision perpendicular to the tibia axis was made with a scalpel on the dorsal side of the hind tibia (just below the 3rd spine proximal to the femur) such that the epidermis was breached. These

transverse incisions were of average length $L = 780 \pm 60 \mu\text{m}$ (see Figure 6.5). After incision, the locusts were separated into individual small tubs to discourage excessive use of their hind tibia (jumping, kicking, and fighting). Each locust was allowed to recover for up to 40 days in the same environmental conditions as outlined in Section 2.2.1.

6.3.3 Testing

After this period of recovery, the injured legs were removed from the insects under sedation by cutting just below the tibia-femoral joint (the knee). These specimens were tested, measured and stored as before. A measurement (x) specific to this study was taken; the distance from the point of contact to the incision (shown in Figure 6.4) was required for my calculations.

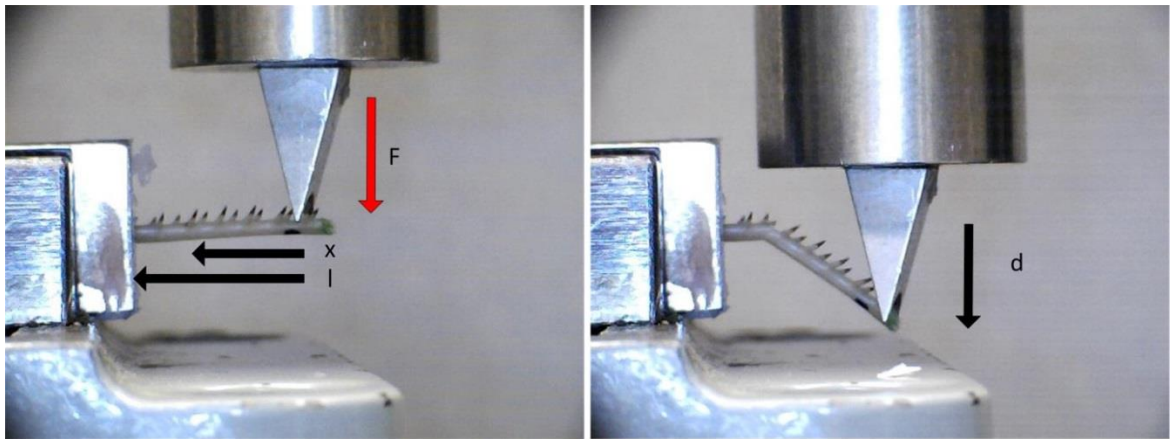


Figure 6.4: The testing rig used with locust tibia secured with dental cement in an aluminium cube for testing, and dimensions relevant in making calculations. (b) shows a failure occurring at the point of incision.

In order to determine if there was targeted repair in any particular area of the tibia, further thickness measurements were taken for each sample at the site of injury using photographs taken in an SEM and Fiji image processing software. The cross section of each tibia was divided into 4 zones as outlined in Figure 6.5. On each sample, an average of several thickness measurements was taken for each zone:

- T1 – the cuticle thickness of the injured area (the dorsal spiny side)
- T2 – the cuticle thickness of the area opposite to the injury (the ventral side)

- T3 – the cuticle thickness of the sides (lateral / medial) of the tibia, which were averaged, as no differences were found between sides.

For comparison purposes, similar measurements were carried out on several uninjured locust hind tibiae from SEM photographs taken during previous studies (Chapter 5). These are the uninjured control samples referred to later.

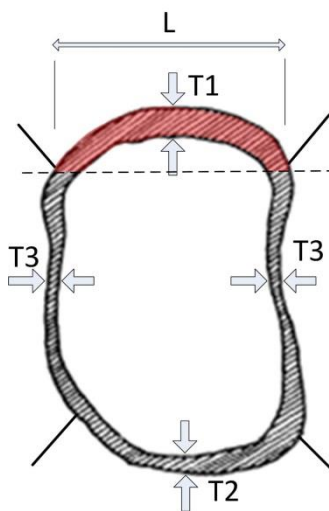


Figure 6.5: Cross section of the tibia separated into wounded dorsal area (T1), the ventral (T2) and sides (T3) of the tibia, also showing the cut length (L) and the injured area (shaded red).

Again, the flexure formula (6.1) was used to calculate the bending stress:

$$\sigma = \frac{Fxr}{I} \quad (6.1)$$

Dirks and Taylor (2012a) examined the fracture toughness of locust cuticle. They performed incisions to locust tibiae in much the same way as this study, doing so after the leg was removed from the insect (so healing was not possible). They assumed the incision to be a sharp crack in the tubular tibia structure, calculating the fracture toughness using the formula:

$$K_{ic} = F_b \sigma_f \sqrt{\pi a} \quad (6.2)$$

Where:

F_b = the shape factor

σ_f = the stress to cause failure (using the flexure formula (6.1))

a = half the crack length

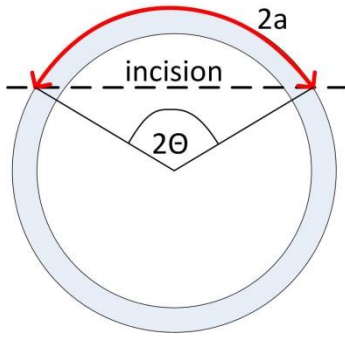


Figure 6.6: Shown are the incision, the arc length of the incision (2a) used in my calculations for apparent fracture toughness, and the included angle.

The arc length of the incision (2a) shown in Figure 6.6 was calculated thus:

$$2a = 2\theta \times r \quad (6.3)$$

The shape factor (F_b) is estimated using the same technique as Takahashi (2002) who examined the fracture of thin walled tubes.

$$F_b = 1 + A_b \left(\frac{\theta}{\pi}\right)^{3/2} + B_b \left(\frac{\theta}{\pi}\right)^{5/2} + C_b \left(\frac{\theta}{\pi}\right)^{7/2} \quad (6.4)$$

$$A_b = -3.26543 + 1.527840.072698 \left(\frac{R_m}{t}\right)^2 + 0.0016011 \left(\frac{R_m}{t}\right)^3 \quad (6.5)$$

$$B_b = 11.36322 - 3.91412 \left(\frac{R_m}{t}\right) + 0.18619 \left(\frac{R_m}{t}\right)^2 - 0.004099 \left(\frac{R_m}{t}\right)^3 \quad (6.6)$$

$$C_b = -3.18609 + 3.84763 \left(\frac{R_m}{t}\right) - 0.18304 \left(\frac{R_m}{t}\right)^2 + 0.00403 \left(\frac{R_m}{t}\right)^3 \quad (6.7)$$

I performed my analysis using a similar protocol, looking at the “apparent” fracture toughness, as my tests are not strictly speaking fracture toughness tests. By the time of testing, the incision or crack (which was an open defect for Dirks and Taylor (2012a)) would be somewhat sealed up by a clot and perhaps reinforced by new cuticle depending on the progress of the healing experienced by the leg.

6.4 Results

Table 6.3 shows the general trend is an increase in the average of failure strength, apparent stiffness, bending moment to failure and apparent fracture toughness the longer the insect is allowed to heal from its injuries over periods from 1 to 40 days. There is also considerable variation among samples, with standard deviations ranging between 50-75% of the mean in some cases.

Days Since Injury	Failure Stress (MPa)	Stiffness (GPa)	Bending Moment to Failure (Nmm)	Fracture Toughness (MPaVm)
1	60.9 ± 32.0	0.81 ± 0.06	2.80 ± 1.63	3.40 ± 1.89
2	70.5 ± 16.0	1.14 ± 0.86	3.19 ± 0.36	3.63 ± 0.54
10	90.3 ± 37.8	2.31 ± 1.47	3.83 ± 0.89	5.07 ± 3.36
20	64.7 ± 37.0	3.09 ± 1.11	3.95 ± 2.22	3.84 ± 1.94
30	89.0 ± 27.3	4.16 ± 2.06	3.79 ± 1.11	5.12 ± 1.78
40	120.6 ± 7.1	4.73 ± 1.66	4.71 ± 0.52	7.45 ± 0.39

Table 6.3: Average values for failure stress, (apparent) stiffness and BM to failure for each time period. Values show mean ± 1 s.d.

Examining the SEM photos in more detail allowed me to visually determine which of the samples had experienced new cuticle deposition after injury.

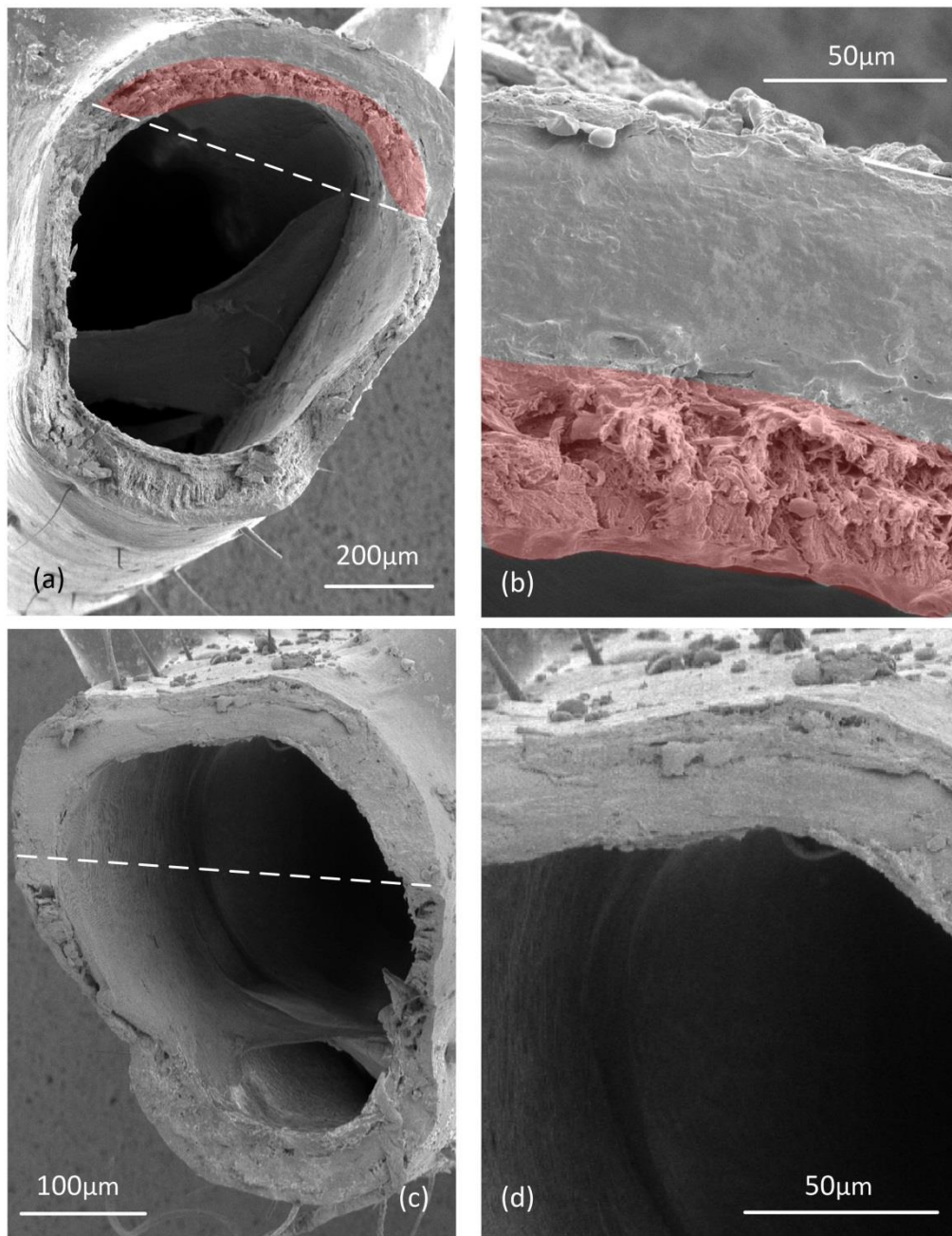


Figure 6.7: Cross sections of tibia at the point of incision (original incision shown by the dashed line). (a) and (b) show an area of new cuticle formation beneath the incision (shaded in red). The smooth area of the fracture surface was caused by the initial scalpel incision. Jagged areas (seen everywhere else) indicate separation of normal fibrous cuticle. The area shaded in red must therefore be new cuticle that was laid down by the insect after the incision was made. (c) and (d) show no such repair. The plane of incision has left a smooth fracture surface, and no new cuticle has grown beneath this.

This allowed me to separate the sample population into two distinct categories; those showing no repair (such as those in Figure 6.7 (c) and (d)), and those showing significant growth of new cuticle

(such as those in Figure 6.7 (a) and (b)). Samples showing minimal repair or samples where the state of repair was unclear were eliminated:

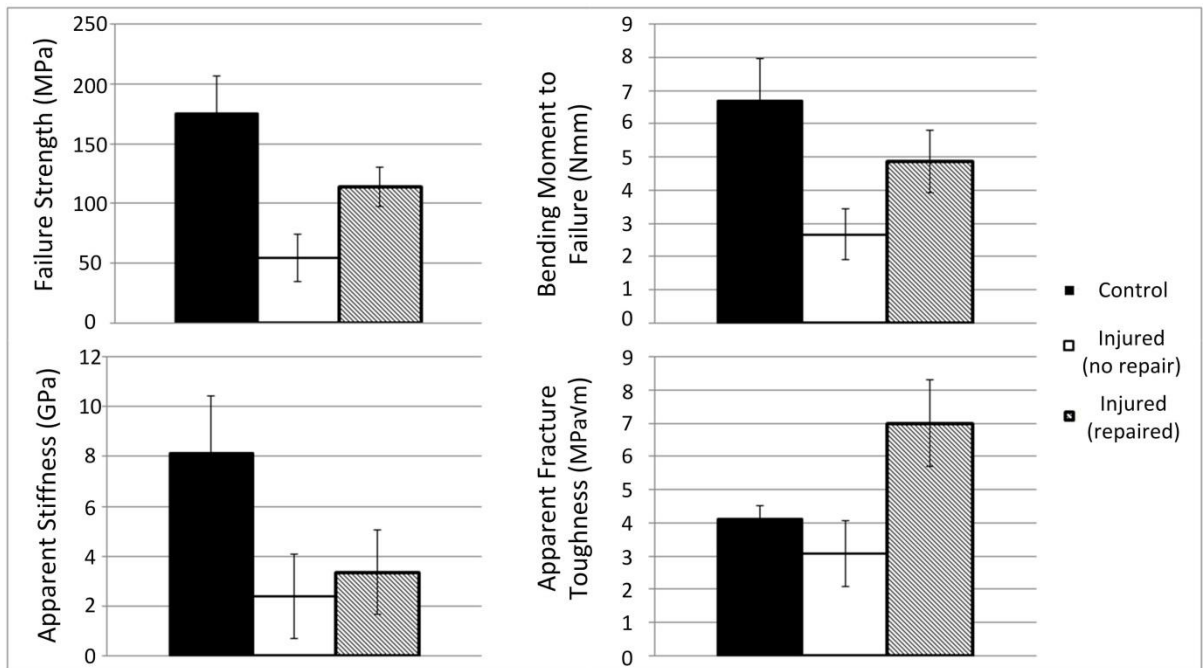


Figure 6.8: Results for failure strength, bending moment to cause failure, apparent stiffness and apparent fracture toughness. Plotted are mean values (error bars show ± 1 s.d.) of the three groups: injured tibiae for which no repair occurred (tested 20-50 days after injury), injured tibiae for which repair did occur (tested 20-50 days after injury) and uninjured controls (tested 20-63 days after moult). Control value for apparent fracture toughness (4.12 MPavm) is taken from Dirks and Taylor (2012a) – the value for fracture toughness of fresh locust tibia cuticle.

Figure 6.8 shows the effect of injury and repair on several mechanical properties. T-tests showed that failure strength, bending moment, apparent stiffness and apparent fracture toughness all differed significantly for the injured (no repair) samples compared to the uninjured controls. When comparing the injured (no repair) to the injured (repaired) groups, t-tests indicated that repaired samples display significantly greater failure strength ($p = 9.57 \times 10^{-6}$), bending moment to failure ($p = 0.00074$), and apparent fracture toughness ($p = 5.66 \times 10^{-6}$). Apparent stiffness of the two groups does not differ significantly ($p = 0.23$).

6.4.1 Thickness Results:

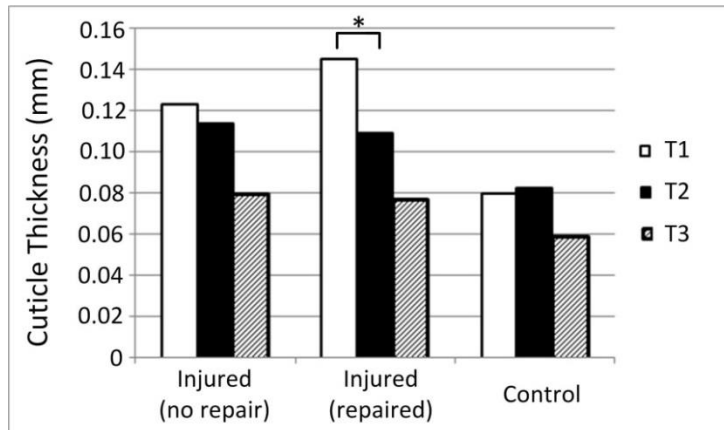


Figure 6.9: A plot of the cuticle thickness on the dorsal (injured) side (T1), the ventral side (T2), and the average thickness of the side regions (T3) for the three groups of samples: injured and not repaired, injured and repaired, and uninjured control legs from a previous study. * indicates significance.

T1 is significantly larger than T2 ($p=0.003$) for the injured (repaired) group, but not so for the others ($p = 0.13$ for injured (no repair) and $p = 0.45$ for control group). The side thickness (T3) is almost constant for both of the injured categories. Average thickness values for the uninjured samples are slightly smaller as some of these samples were not as old (20-30 days) as the injury repair specimens (all > 30 days). Absolute difference between T1 and T2 averaged 33.2% for the injured-repaired group, 14.9% for the injured-no-repair group, and 12.3% for the uninjured control set.

6.4.2 Cuticle Deposition Rates:

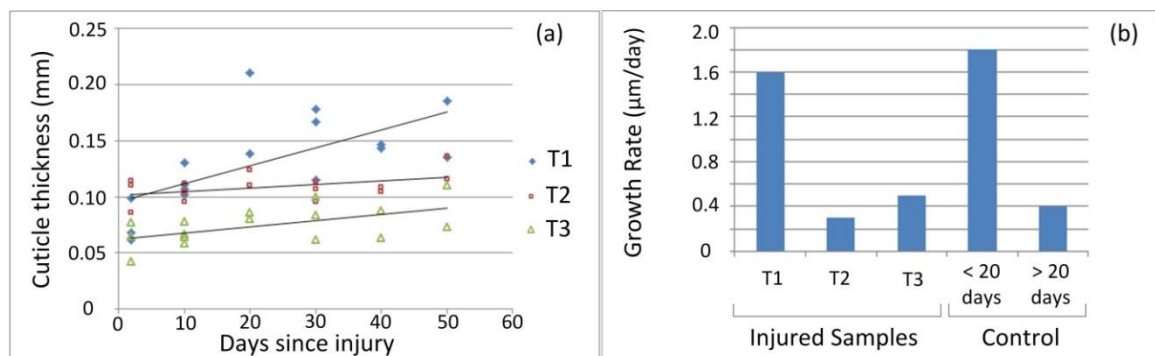


Figure 6.10: (a) cuticle thickness as a function of time since injury for various zones T1 (dorsal injured zone), T2 (ventral), T3 (average side thickness) for all samples displaying repair. (b) plots the cuticle deposition rates post injury (figures obtained from linear trend-lines in (a)) compared to deposition rates observed in the uninjured control samples in the immediately post moult modelling period, and the later dormant period.

Figure 6.10 shows an increase in thickness for T1 of approximately 1.6 μm per day, with T2 and T3 showing an increase in thickness of 0.3 μm and 0.5 μm per day respectively. The growth rate of zone T1 is more similar to that seen in uninjured control samples in their first 20 days post-moult, while the other areas (T2, T3) resemble the smaller, “dormant” phase seen in older insects.

6.5 Discussion

Mammal tissue goes through a process of modelling (when growing and maturing), and remodelling in response to damage. Bones are remodelled constantly in response to micro-damage (Burr and Martin, 1993; Taylor and Lee, 2003), which involves bone resorption and deposition, and is also the final stage of the wound healing process in mammals (Broughton and Rohrich, 2005). Shortly after moulting, insects can be said to undergo a “modelling” process as their exoskeleton grows and matures, changing shape in a predetermined way as outlined in Chapter 5. Mature adult insects do not display a process of remodelling, as there is no resorption of material, but they can be induced to deposit cuticle when injured. It has previously been established that new cuticle is deposited at the wound site “where needed” (Wigglesworth, 1937) – that is, at the site of an excision, and to a lesser extent, under the cuticle adjacent to a wound (Lai-Fook, 1968), but the amount or rate of deposition has never been accurately quantified. As remodelling is absent in adult insects, wounds can never be fully healed – the cells of the insect do not absorb the scab to leave a scar as is the case in mammals. After injury, a scab stabilizes the area, providing a continuum across the incision, and acting as a scaffold for the epidermis to migrate across, after which new material is deposited to reinforce the injured area. This study has examined several factors stemming from this final stage of the injury response of a locust hind tibia. I first looked at its effect on the mechanical properties of the leg. The tests employed cantilever bending in order to replicate the forces applied during normal locomotion (jumping) by the locust. One important factor for the survival of the leg is its failure strength. From studies outlined in Chapter 5, I found that an uninjured tibia of similar sex and age has an average failure strength of 175 MPa, a bending moment to failure of 7.2 Nmm (and average stiffness of 8.12

GPa). The results for injured specimens averaged 84.1 MPa for failure strength, 3.85 Nmm for bending moment to failure (and 3.04 GPa for apparent stiffness).

These average values (taken across all samples) do not give a true picture of the locust's ability for healing. Figure 6.8 shows that the growth of new cuticle under an injury has a very significant effect. This deposition of new material appears to be the most important factor in restoring structural integrity to an injured insect leg. It was therefore necessary to split the data into two distinct groups and analyse them separately.

Inducing an injury in a locust leg reduces the failure strength significantly (from 175 ± 31.5 MPa to 54.3 ± 19.1 MPa). As a result of repair, this failure strength can be doubled to 113.7 ± 16.4 MPa. This implies that an injured locust can restore on average 66% (and possibly up to 75%) of its original strength if growth of new cuticle material is well established underneath the injury. The injured legs where repair was absent remained at approximately 33% of their original strength permanently, even if allowed up to 30 days to heal. The increase in strength due to repair was seen to occur over the first 10 days post injury, and then remain constant.

Results for the bending moment to failure followed a similar pattern. The repaired legs displayed a bending moment that was approximately twice as large as those with no repair (4.86 ± 0.95 Nmm compared to 2.67 ± 0.76 Nmm) – again, a restoration of approximately 68%.

The stiffness measurements of the injured specimens are not an indication of the true material stiffness, as I have assumed an intact tibia for my calculations, which is why I refer to stiffness measurements as “apparent stiffness”. Stiffness measures the ratio of applied force to deflection (or stress to strain). A tibia with an incision held together by a clot or even a small bridge of new cuticle will certainly deform more per unit of applied force than an undamaged one, so these figures cannot really be compared to the original stiffness value. The effect of repair on apparent stiffness was therefore not as pronounced as other properties (3.34 ± 1.7 GPa for repaired legs compared to 2.38 ± 1.7 GPa). Although this is a slight increase, it is not significant ($p = 0.23$). The initial drop in stiffness (from 8.12 ± 2.3 GPa) caused by the injury could not be restored. The major

deterioration of how the tibia deflects under applied force is expected, but not really quantifiable by this analysis.

It should be also noted that the injury does not cause the actual material strength to be decreased – only the failure strength of the tibia as a structure. When considering the failure mode of these specimens (indeed, any specimen with a defect), there are two distinct possibilities shown in Figure 6.11:

Mode 1: Failure by stressing the material beyond its ultimate strength (solid line)

Mode 2: Failure by “brittle fracture” due to a crack or flaw in the material (dotted line)

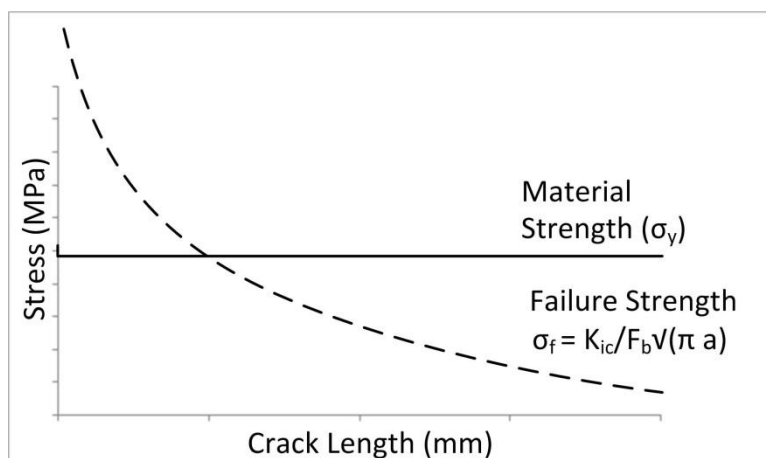


Figure 6.11: two possible failure modes for a specimen with a defect, yielding and fracture as a function of flaw or crack size.

When analysing brittle failures, one can consider the fracture toughness formula (6.2), rearranging to isolate the failure stress:

$$\sigma_f = \frac{K_{IC}}{F_b \sqrt{\pi a}} \tag{6.8}$$

As fracture toughness (K_{IC}) is a material constant, the stress to cause failure (σ_f) is inversely proportional to the (square root of the) crack length (a). This predicted failure stress is plotted as a dotted line in Figure 6.11. When stressing specimens to failure, the material strength (compressive or tensile) will be reached before the predicted failure strength for those with smaller crack lengths. For this failure mode (Mode 1), one can assume that any crack present in the sample is too small to have any effect. For larger crack lengths, the predicted failure strength is reached before the material strength, so the failure mode is one of brittle fracture (Mode 2).

Essentially, the sample should always fail at the lower of the two predicted stresses. For tests carried out in this study, the crack lengths were always of length significant enough to cause a Mode 2 failure (see Figure 6.12), which in this case was always one of fracture originating from the incision.

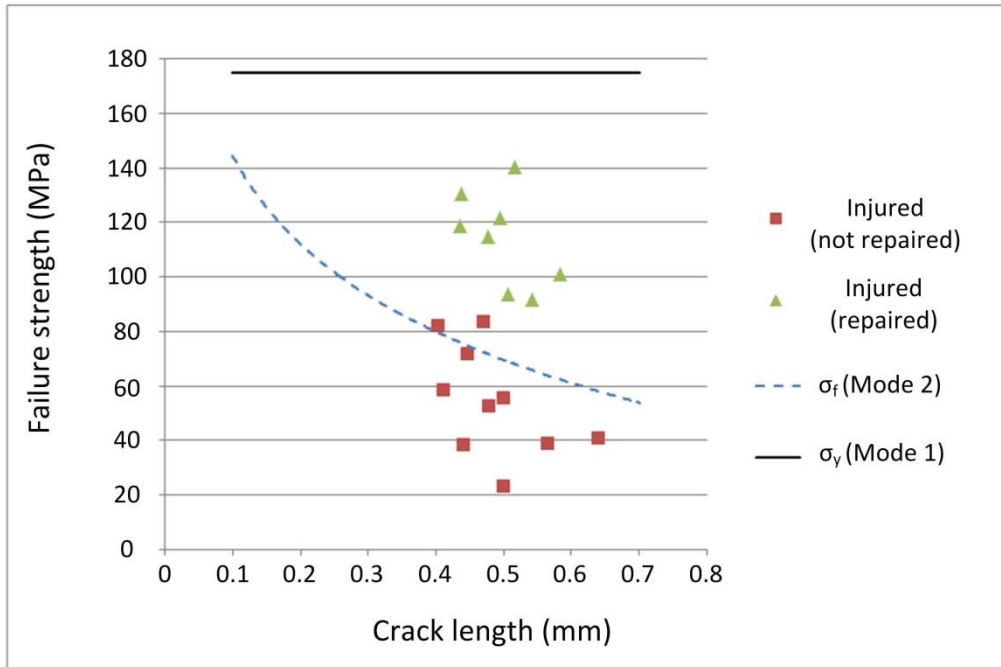


Figure 6.12: the two possible failure modes. Mode 2 is based on a fracture toughness of 4.12 MPa√m (Dirks and Taylor, 2012a) and equation (6.8), using the average value observed for the shape factor $F_b = 1.5$. Mode 1 is the average failure strength of mature adult tibiae documented in Chapter 5 (175 MPa). Plotted are the failure strengths as a function of crack length for samples showing significant repair (green triangles) and those showing none (red squares). Omitted are those showing small amounts of repair (and samples where the state of repair was unclear)

Figure 6.12 shows that samples showing no repair had failure strengths at or below the predicted brittle fracture strength. Injured repaired samples have higher failure strengths than this prediction. The repair is not significant enough to restore the strength fully (as far as the material strength, denoted by the black line), but it can restore the tibiae to on average 66% of this strength.

The significantly higher failure strength and bending moment to failure (and higher “apparent fracture toughness”) provide strong correlative evidence that the deposition of new cuticle under the incision is vital for restoring mechanical stability to the wounded tibia. The absence of this

deposition correlates to a general lack of healing and restoration of functional integrity. Previous studies (Taylor and Dirks, 2012) show that the locust hind tibia experiences stresses of 42.2 MPa during jumping. For mature adult insects with an injured leg, this stress may prove too great if the leg is not properly healed, and the leg may be lost during such a jump (which was occasionally observed during this study). The deposition of new cuticle material is critical in preventing such failures, thus restoring the fitness of the insect.

6.5.1 Apparent Fracture Toughness

Fracture toughness is a measure of a material's ability to resist crack growth under static loading. This is another important factor for the welfare of an injured leg. Previous studies (Dirks and Taylor, 2012a) found the average fracture toughness of a fresh locust tibia was 4.12 ± 0.4 MPaVm (2.06 ± 0.6 MPaVm for dry cuticle). In Dirks' tests, incisions were made to locust tibia after removal so no healing was possible. From observations made on the SEM photos, it can be assumed that samples showing no new cuticle deposition simply have their incision plugged (sometimes not even completely) by a clot or scab. These samples (Injured, no repair in Figure 6.8) had an apparent fracture toughness of 3.07 ± 0.99 MPaVm – midway between Dirk's results for fresh and dry cuticle. This suggests that these legs have a poorer defect tolerance than a freshly injured leg, possibly due to some drying out of the tibia cuticle since the time of wounding, which could lead to some embrittlement. Injury due to cuticular abrasion has been shown to correlate with higher water loss rates (Johnson, Kaiser et al., 2011), and dehydration of locust tibia cuticle has been shown to lead to a more brittle material (Dirks and Taylor, 2012a). This also shows that "plugging the gap", while necessary for biological reasons such as sealing the area to prevent invading pathogens and water / blood loss (Wigglesworth, 1937) is not mechanically effective at impeding crack growth or restoring the original properties of the fresh cuticle.

For the samples showing repair, not only has the defect been plugged, but new material has also been deposited underneath. This provides a bridge across the injury which effectively restores stability to the structure, raising its apparent fracture toughness to an average of 7.01 ± 1.32 MPaVm. This implies that repaired samples are 70% more effective at resisting the growth of a

crack from the initial wound site as a leg which is not given a chance to heal, and over 130% more so than the samples that have simply “plugged” the incision. This does not mean that the fracture toughness of the material has been increased to 7.01 MPavm, but indicates the effect that the new material has in hindering a crack from propagating from the incision by bridging the gap.

6.5.2 What stops repair?

Repair was not always observed (see Figure 6.7 (c) and (d)). From a total of 32 subjects tested, only 15 showed any repair – identified by visible growth of new cuticle underneath the incision. 12 showed none, and for the others, it was unclear, so these were discarded. Several longitudinal sections were also taken of incised (untested) specimens to see if there were any observable patterns or reasons which would determine whether or not repair could occur. The injuries fell into two distinct categories.

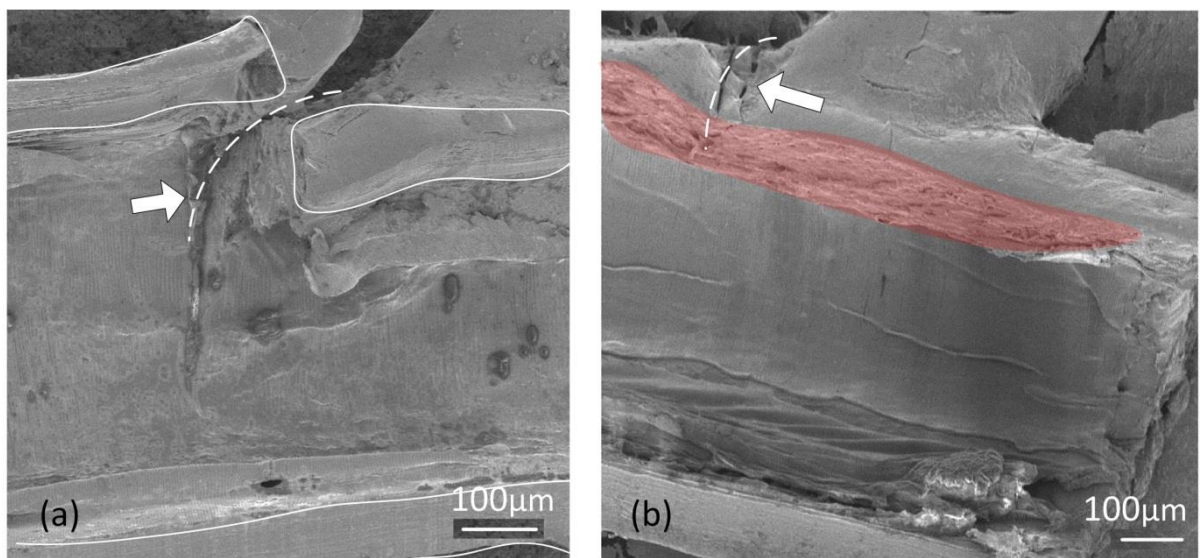


Figure 6.13: longitudinal section of untested tibiae 30 days after injury. Incision is denoted by dotted line and arrow. (a) shows no repair, possibly due to the fact that the injury is more severe. Sections outlined in white on the top surface should be lined up. Their displacement has made it impossible for the epidermis to re-join up post-injury making deposition of new cuticle impossible. (b) shows significant deposition of new cuticle (shaded in red) beneath the original injury. Although this new cuticle is somewhat lamellate in nature, it is not as homogeneous or organized as the cuticle in the opposite surface (below).

Figure 6.13 (a) shows an injured sample with no new cuticle growth visible. The two “planes” or faces of the incision outlined in white have become separated during the injury process. These

should line up, but separation and the lack of a clot bridging the two faces implies that there was no scaffold over or through which the epidermis could have migrated to re-establish a continuous layer of cells which would go on to deposit new cuticle.

Figure 6.13 (b) shows an injured sample with visible repair. New cuticle can be seen underneath the incision which is quite significant in size (shaded red). This is somewhat laminate in nature, but is not as organized as the layered structure seen on the opposite (ventral) side of the same leg. These photos indicate that for new cuticle to bridge a wound, it must be possible for the epidermis to establish a continuous layer bridging the injury site completely. Cut depths and cut lengths were standardized as outlined earlier. All cuts were carried out in the same manner, but even the slightest variation in force or angle of attack could have caused the opposing faces of the injury to be displaced from their original position (as in Figure 6.13 (a)). A blunting of the scalpel during cutting could also lead to a wider incision. If the clot cannot provide a link across a wound for the epidermis to migrate through, a “proper” wound healing response would be prevented. No brace of new cuticle could be formed under the wound to re-stabilize the area. This indicates that during the life of an insect, the manner in which a leg is injured, as well as the severity of the injury will determine whether or not the epidermis can reconnect and therefore whether or not the injury can be healed at all.

6.5.3 Thickness Results

Our t-tests revealed that for samples displaying visible repair only (not for the other groups), the cuticle was significantly thicker ($p = 0.003$) in the area adjacent to the injury (T1) than the area opposite the injury (T2). Figure 6.9 shows that the cuticle thickness at the injury site increased to $146 \pm 36 \mu\text{m}$ as a result of repair, while the dorsal side remained at $109 \pm 11 \mu\text{m}$. The uninjured control samples, in contrast showed very similar dorsal and ventral thicknesses (similarly, the injured, not repaired samples showed no significant difference between dorsal and ventral thickness). It may seem obvious that only those samples showing growth due to repair would have a thicker cuticle, but these results show that the deposition of new cuticle is specifically targeted to reinforce the injured area more so than any other. T1 is on average 33% larger than T2

for samples displaying repair (15% larger for those not) (see Figure 6.9). The side thickness (T3) is almost constant for both injury categories, suggesting that what happens at the incision is independent of what happens at the sides – again confirming specific targeting of the injury site.

6.5.4 Cuticle Deposition Rates:

After its final moult, the outer surface of the adult insect exoskeleton remains unchanged for the remainder of its life. During the course of the adult insect's life, new layers of endocuticle grow "inwards" on a daily basis. The study outlined in Chapter 5 shows that the endocuticle initially grows quite rapidly (1.8 μm daily), but the growth rate slows down over time (to <0.4 μm daily after approximately 20 days). I deliberately chose older adult insects for this study, as they are unlikely to have anything but small to negligible daily growth.

Figure 6.10 (a) plots only samples showing repair (small and significant amounts) – excluded are all samples showing none. Plotting the thickness of areas T1 (adjacent to the injury site), T2 (opposite the injury site) and T3 (average side thickness) as a function of time since the leg was injured and fitting a linear trend-line to each data set allowed me to estimate the daily increase in thickness of each area. The daily rates of increase in thickness are displayed in Figure 6.10 (b), alongside those for uninjured samples. Cuticle thickness increased at the injury site (T1) at a considerably greater rate than other areas. This rate was a close match to the 1.8 $\mu\text{m}/\text{day}$ growth rate seen in newly moulted (<20days) locusts. Ventral and medial/lateral deposition rates closely match the "normal" or "dormant" growth rate of 0.4 $\mu\text{m}/\text{day}$ seen in mature adults. This is a strong indication that the initial growth phase (seen after moulting) may have been re-initiated or that a dormant process may have been reawakened by the injury, and also that this increased growth rate is localised around the damaged area.

All cuticle is deposited from the epidermis. It has been shown that the signal triggering plug or scab formation does so exclusively at the wound site, but that the JNK pathway activator (that which influences cell migration and proliferation) influences epidermal cells up to seven cell diameters away from the wound site (Galko and Krasnow, 2004). This activation (or a similar one) could also be the stimulus for the observed rapid cuticle deposition, which would explain why it is

only present at the injury site. These activated cells are the only ones that rapidly produce the new cuticle. Cells further from the area do not experience any such activation or disturbance, and continue to deposit cuticle at the normal rate.

This study complements previous research done on the biological (Lai-Fook, 1968; Rowley and Ratcliffe, 1978), cellular (Wigglesworth, 1937; Bohn, 1975; Marmaras, Charalambidis et al., 1996) and genetic (Wright, 1987; Galko and Krasnow, 2004; Belacortu and Paricio, 2011) responses to wound healing in so far as it further underpins the similarities between insect and mammal wound healing processes. When comparing insect and mammal injury responses, (Broughton and Rohrich, 2005) there are far more similarities than differences. Both involve inflammation, cell proliferation and a maturation of sorts (Belacortu and Paricio, 2011). There are many parallels in terms of fundamental cellular and molecular responses to wound healing. I have shown another parallel – the critical purpose of these processes in restoring the original functionality and structure to the wounded area. Each stage of the overall process is a necessary stepping stone leading to the ultimate goal of restabilising and strengthening the damaged area to as close to its original state as possible.

6.6 Conclusions

This has been the first biomechanical study of injury repair in an arthropod. I have shown that while an adult insect cannot ever completely heal an injury, the growth of new cuticle can have a significant restorative effect on the structural integrity of an injured locust hind tibia. This new growth can re-establish on average 66% of the original failure strength of the leg compared to the 33% strength seen in injured samples showing no repair. I have shown the importance for the survival of an insect of not just “plugging a hole”, but being able to establish a bridge across the injury in order to deposit new cuticle. This increases the leg’s ability to resist crack propagation by 70-130% compared to freshly injured or poorly healed legs.

I have confirmed that this repair and reinforcement is not due to the passive cuticle growth seen in uninjured mature adult locusts, but the targeted growth of new cuticle specifically directed to

the area of induced injury. The injury appears to resurrect the dormant modelling process in a mature adult insect, causing cuticle deposition at rates closely matching those observed immediately post-moult. This process is confined to the injured area, placing cuticle where it can most successfully improve the tibia strength, increasing the safety factor of the injured leg. In all other areas, the growth remains at rates seen in mature uninjured specimens. This intelligent system of reinforcing only the area structurally weakened or damaged by injury is an effective strategy for the insect to ensure its survival while saving resource investment.

6.7 Future Work

It would be interesting to examine the deposition rates post-injury and compare them to the post-moult rates. How long after the injury does the deposition rate slow down to “normal” or dormant levels? It would also be very interesting to stain the new cuticle material in a similar way to that mentioned in Chapter 5. This may reveal if the new cuticle is more similar to endocuticle or exocuticle, as so far, very little is known about this, save that it does not appear to be lamellate. The effect of the severity of the injury may provide some insight in to the limits of the insects wound repair capabilities. The effectiveness of the process for different wound types and geometries (puncture wounds, longitudinal incisions, etc.) could also be examined. Modelling the repair situation using finite element analysis may also provide some valuable insights into the effectiveness of patches of material placed internally to repair cracked or damaged tubular structures (and even into the actual strength of the new cuticle material itself).

Chapter 7: Self-healing properties of insect cuticle

7.1 Abstract

Having examined the insect response to major (or macro) damage in the previous chapter, I wanted to perceive if the insect was responsive to micro or material level damage. This could include layer delamination, fibre or matrix cracking, or even bond breaking due to applied stresses close to but below the yield strength of the material.

All previous studies have examined insect tibiae after removal from the insect. If remodelling or recovery processes in response to minor damage or injury are to be examined, they would have to be examined on living cuticle material. This study takes a “before and after” approach to investigate the recovery properties of the living cuticle tissue of the adult desert locust. To replicate forces experienced by the locust when jumping, a cyclic load was applied to a living locust hind tibia until softening or plastic deformation was seen to occur. The locust was allowed a period of time to recover, after which the experiment was repeated in order to gauge whether or not the material had been permanently weakened in the preceding test. The entire procedure was then repeated on tibiae that were first *removed* from the locust. Results show that the living cuticle recovers its original stiffness after such cyclic tests. Also shown is the absence of this recovery in the “dead” cuticle, suggesting that this recovery is not entirely a passive material phenomenon. The insect may play an active part in regulating its material properties, and self-healing micro-damage experienced within the cuticle.

7.2 Introduction

While jumping, the locust tibia experiences bending forces greater than twenty times its body mass (Bennet-Clark, 1975) over a period of 20-30 ms (Bayley, Sutton et al., 2012). While kicking, the full extension of the leg can be reached in 5 ms. A locust can only jump 10-20 times consecutively before muscle fatigue (tiredness) sets in – even when stimulated to do so electrically (Bennet-Clark, 1975). A rest period is required between every few jumps. It is possible that this rest period is also an opportunity for the cuticle material to recover from any

deformation or damage experienced during the jumps. If any such recovery process was more than just a passive material phenomenon, the hemolymph and epidermis would undoubtedly play a role, so the cuticle would need to be still attached to the living insect. Jensen and Weis-Fogh (1962) observed plastic deformation in locust tibia cuticle (removed from the insect) during testing and its recovery when the material was left to rest. Was this just due to the viscoelastic nature of the cuticle? Had the integrity of the material (its stiffness) been affected?

The objective of this study is to test the hypothesis that mechanical properties of cuticle might be different when the material is still part of the living insect. In particular, I considered whether the insect could control the responses of its tibia cuticle material to cyclic loading, such as that which occurs during walking and jumping.

7.3 Materials and Methods

7.3.1 Insects

Adult female desert locusts were housed and cared for as previously outlined (Section 2.2.1)

7.3.2 Experimental Setup

The experimental rig in Figure 7.1 was designed to keep the locust as stationary and comfortable as possible, and to immobilise and secure the tibia for testing in order for consecutive tests on the same sample to be comparable.

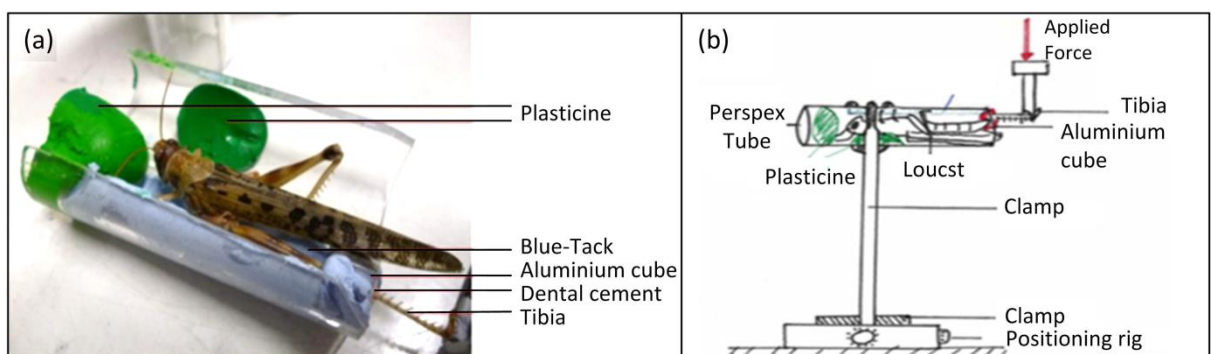


Figure 7.1: (a) rig for housing the locust for duration of the experiment, (b) how cyclic load was applied.

The locusts were housed in some Perspex tubing for the duration of the experiment as shown in Figure 7.1 (a). During handling, locusts tend to remain stationary when handled by a pincer grip to

the pronotum (saddle shaped area of hardened cuticle on their back/neck). Plasticine was used to simulate this grip, while the bottom of the tube was lined with blue tack to keep the locust stationary. The tibia was inserted through a hole in an aluminium cube, and the region of the tibia below the femoral-tibia joint was secured in place using fast hardening cold-cure acrylic dental cement. This cube was secured in the Perspex tube using another custom made aluminium part. As in previous experiments, the cement effectively eliminated the buckling region (Bayley, Sutton et al., 2012), making the sample being tested more uniform. Precise positioning of this entire setup was possible using the positioning rig shown in Figure 7.1 (b).

Bending stresses applied to the tibia during jumping and kicking can range from 30-60 MPa (Bennet-Clark, 1975; Bayley, Sutton et al., 2012). Taylor and Dirks (2012) estimated 42.2 MPa. My tests replicate these *in vivo* stresses experienced by the insect. Samples were tested in cantilever bending as before. In this study, 3-5 cycles of loading were applied to each sample. Displacement and applied force were recorded. The process was repeated approx. 20 hours after the first test, and again 4 hours later. Only the left tibia of each locust was tested.

Identical experiments were carried out on tibiae which had been removed from the locust and soaked in water for 24 hours to prevent desiccation (and to ensure no living processes were still active). Control tests carried out during previous experiments (Dirks, Parle et al., 2013) showed that soaking a tibia under water for up to 48 hours had no significant effect on its strength or stiffness. These tibiae were cycled in the same manner, left for a rest period of approx. 20 hours (in water), and tested again. In order to introduce another level of control, both the left (cycled) and the right (idle) tibiae of the living specimens were removed from the locust and tested to failure in order to gauge if the cyclic loading had any effect on the ultimate strength of the material.

7.3.3 Calculations

Assumptions regarding tibia shape and material (outlined in Section 2.2.6) were used. Stress, strain and stiffness were calculated as before. Dimensions of the tibia used for this experiment were average values calculated by Dirks and Taylor (2012a), namely:

- The radius of the tibia = 594 μm
- The thickness of the tibia = 50 μm
- I , the moment of inertia of the tibia = 0.038 mm^4

The area under the loading curve was calculated to give the “loading energy” (MJ/m^3) required in deforming the cuticle. This was done by fitting a quadratic or cubic trend-line (whichever gave the best R^2 value) to the loading curve and integrating its equation. The area under the “unloading” portion gave the elastic energy recovered during unloading. The difference between the two indicating the amount of energy absorbed by the material during loading.

7.4 Results

Cyclic softening of the tibia material was observed during all cyclic load tests (see Figure 7.2). On average, 10.3% less stress is required to reach the same displacement for cycle 2 compared to cycle 1. A further decrease in stress of 7.7% is required for cycle 3 (a total reduction of 17.3% of the original stress required).

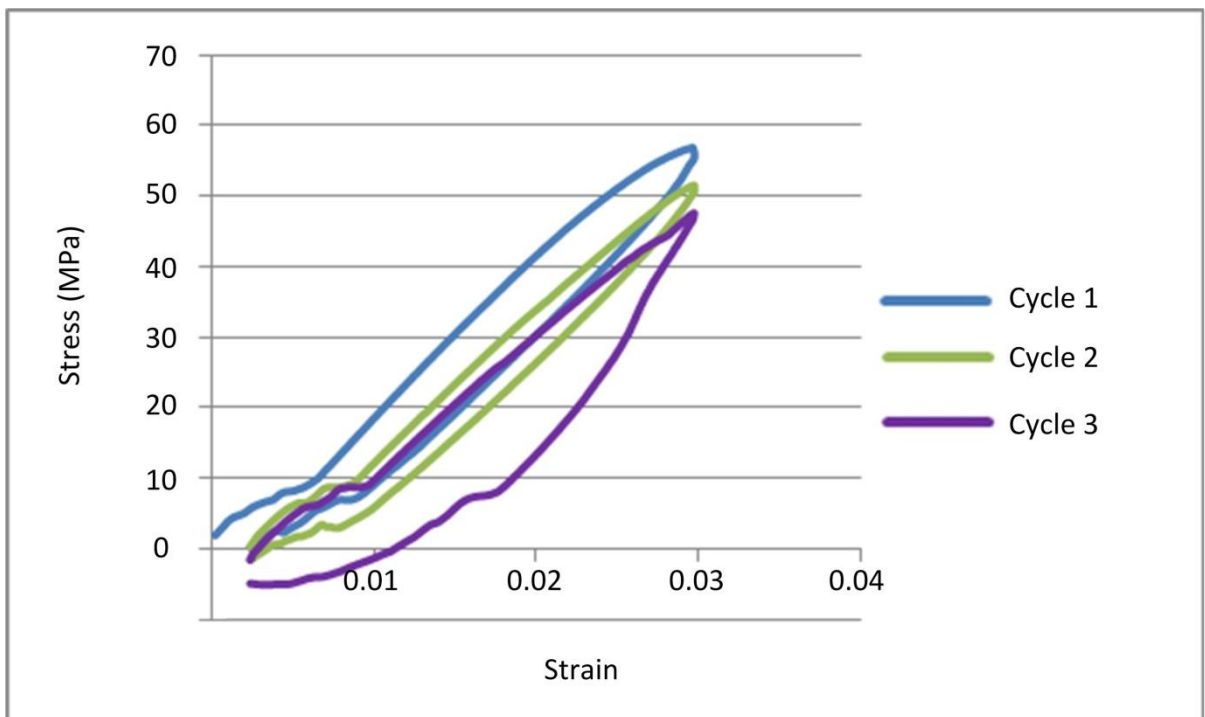


Figure 7.2: A typical test graph plotting stress (force per unit area) against strain (deflection) The slope of the linear portion of the loading curve in graphs such as this is used to estimate the material’s stiffness (Young’s Modulus, E). The areas under these curves are used in the energy calculations.

Figure 7.3 shows that the energy required in loading the tibia was seen to fall by an average of 24.4% from the first to the second cycle, and by a further 5.1% from cycle 2 to cycle 3. Subsequent tests on the same tibia showed almost identical results, indicating the material had recovered from any damage inflicted during previous tests.

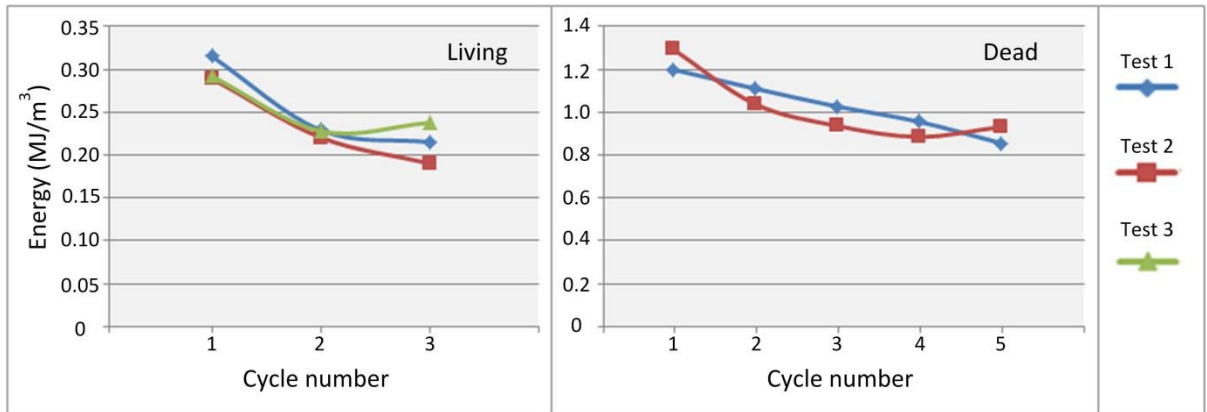


Figure 7.3: Loading Energies – plotted is the energy required to deform a tibia by 1 mm at a rate of 5 mm/min for each cycle in three consecutive tests. The energy required to achieve the same displacement falls during each cycle, again indicating some deformation and / or damage. Both living and dead cuticles show very little variation in loading energies from one test to the next.

Figure 7.4 shows that the energy for unloading was always significantly lower than that for loading, indicating that some of the applied energy had been absorbed. The difference between loading and unloading energies averaged 49.5% for the living material, and 35.6% for tibia which were tested post removal.

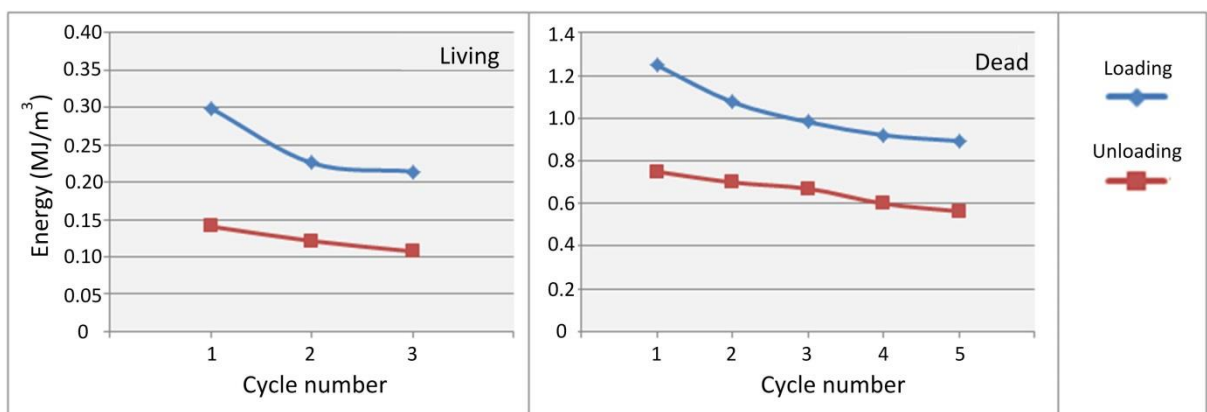


Figure 7.4: Plotting the average energies required for loading and unloading all tibiae for each cycle of the tests. Although the batch of locusts used for the “dead” tests were much stiffer, they absorbed proportionally less energy.

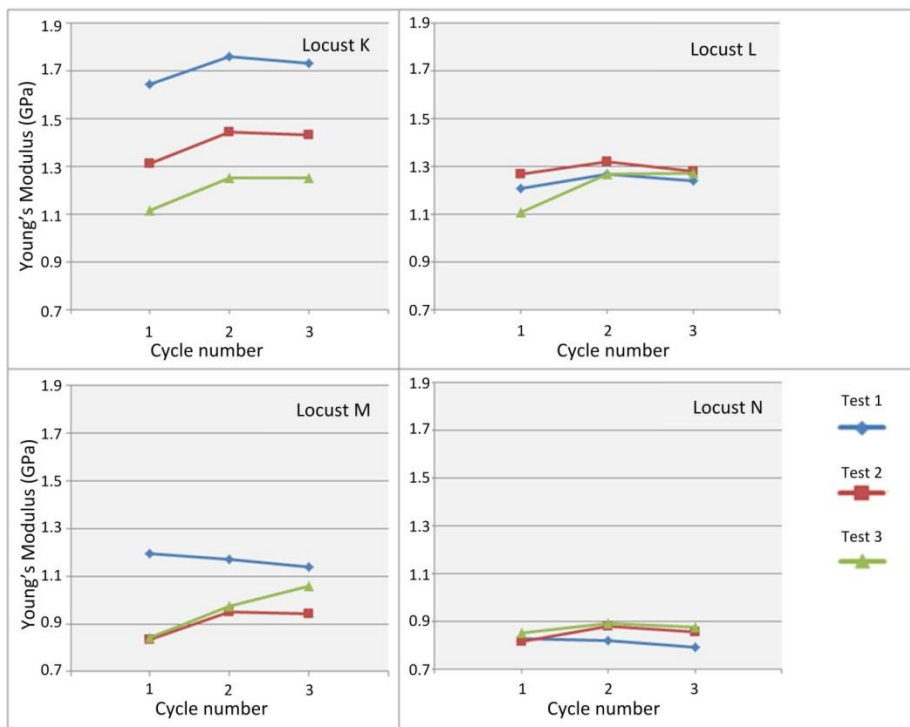


Figure 7.5: Sample of individual stiffness values for living cuticle. Data points show stiffness values for each cycle for three consecutive tests - the second test being carried out approx. 20 hours after the first, and the third being carried out 4 hours after this. Stiffness values were calculated from the slope of the linear portion of the loading curve for each cycle.

Stiffness values for individual locusts were seen to vary slightly from test to test (Figure 7.5). Some showed a decrease in stiffness for subsequent tests (Locust K, M), while some remained almost constant (Locust L, N). On average (Figure 7.7 (a)), there was a drop in stiffness of 9.8% from test 1 to test 2. 83% of specimens showed an increase in stiffness from cycle 1 to cycle 2 – the average increase being 12.5% of the original stiffness.

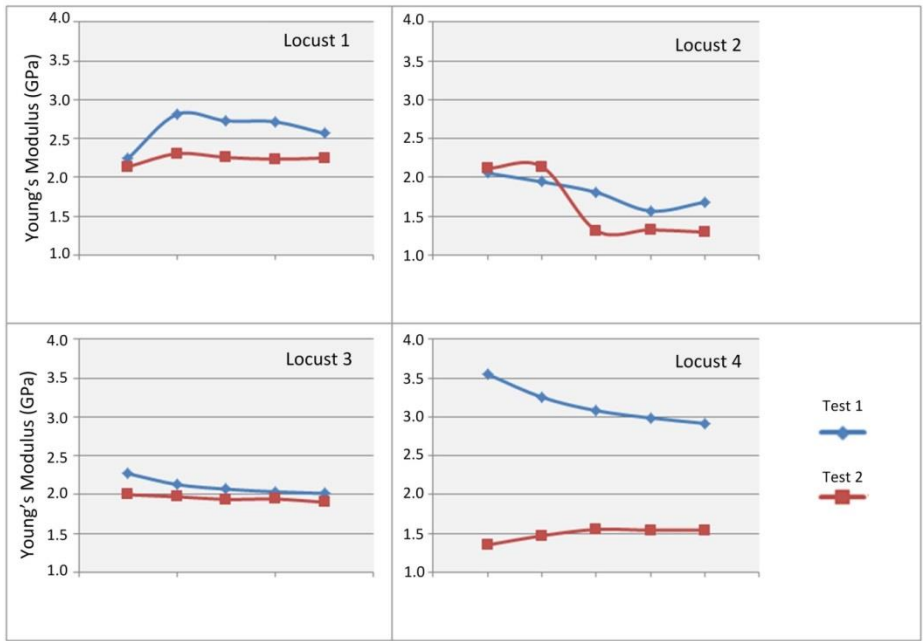


Figure 7.6: Sample of individual Young's Modulus values for cuticle post removal. Data points show stiffness values for each cycle for two consecutive tests - the second test being carried out approx. 20 hours after the first. Stiffness values were calculated from the slope of the linear portion of the loading curve for each cycle. All specimens show a decrease in stiffness from test 1 to test 2 (the exception being Locust 2 which shows a slight increase for cycle 1 and 2). Only 50% of tests showed an increase in stiffness from cycle 1 to cycle 2.

Stiffness results for the "dead" cuticle (Figure 7.6) showed a more noticeable trend, with over 80% of samples showing a significant drop in stiffness from test 1 to test 2 (averaging 24.5% - Figure 7.7 (b)).

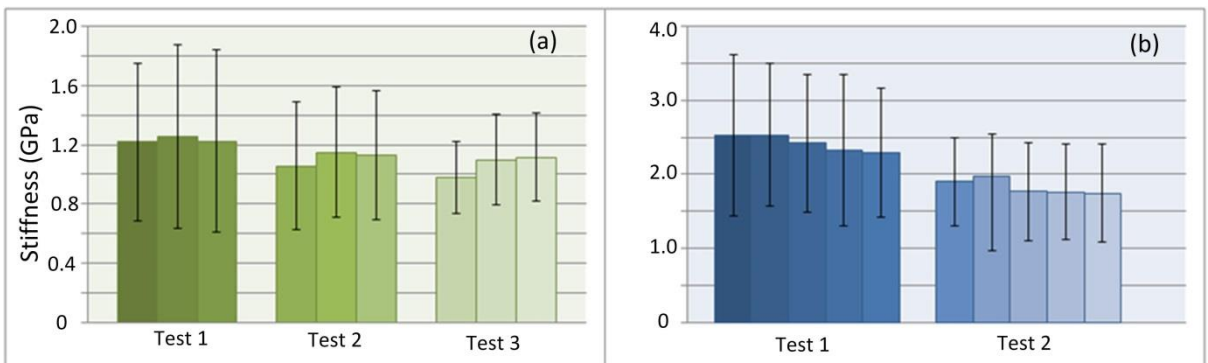


Figure 7.7: (a): average stiffness results for living cuticle for three consecutive tests, with three cycles per test. (b): average stiffness results for dead cuticle for two consecutive tests, with five cycles per test. All values are averages of 5 locusts, error bars calculated using Student t-distribution based on a sample size of 5. The error bars (showing the standard error) do not indicate a wide variation of stiffness occurring in any individual locust tibia during testing, but rather encapsulate the range of stiffness encountered across all samples due to natural scatter.

Figure 7.7 shows that on average, there is initially a slight increase in stiffness (comparing cycle 1 and 2 in each test). Also shown is a slight average decrease in stiffness from test 1 to test 2 for the living specimens which is more pronounced for the dead cuticle.

7.5 Discussion

The first thing to notice in these tests is that the “dead” tibiae are much stiffer than the living ones. This is an artefact of the testing procedure. Living locusts tested were much younger than those from which I removed tibiae for the “dead” tests. This study was carried out before I discovered the effect that aging and growth could have on tibia cuticle properties and dimensions. Using average values for radius and thickness of the tibia is another reason for the large difference in stiffness values and loading energies seen between the two categories. Younger legs will be more slender (same radius, smaller thickness) leading to higher stresses than those calculated from average values. This would also yield higher values for stiffness and loading energies due to an increase in the slope of the loading curve. It is less likely that the living leg, while attached to the locust acts much less stiff than outlined in previous chapters, or that the removed legs increased in stiffness in the 24 hours post-removal when they were stored in water. While further testing in this area would be required to make accurate comparisons (preferably using the actual tibia dimensions for calculations for each sample instead of averages), I believe that these tests go some way to shedding light on the differences between the recovery of the living and dead cuticle in a proportional sense, if not in terms of actual magnitudes. For this reason, I have analysed all data in terms of percentages of the initial values (loading energies, stiffness, and strengths). In the future, it would be interesting to repeat this study on fully mature similarly aged adult locusts and see how the scale of these properties compares between living and dead cuticle.

7.5.1 Energy

Insect cuticle softens and deforms during testing. This is done by absorbing some of the energy applied during loading. When left to rest, the material fully recovers. Cyclic softening of the

material can be observed in the stress strain curve (Figure 7.2). 10.3% less stress is required to reach the same displacement for cycle 2 compared to cycle 1. A further decrease in stress of 7.7% is required for cycle 3 (a total reduction of 17.3% of the *original* stress required). This shows that the material is softening significantly. The loading energy (Figure 7.3) required in deforming the cuticle also decreases for subsequent cycles – averaging a 24.4% drop from cycle 1 to cycle 2, and a 5.1% drop from cycle 2 to 3. This drop was seen to occur for both the living cuticle and the tibiae removed from the insect (though was more pronounced in the living). Almost identical energy values for loading and unloading were observed for subsequent tests on each sample (Figure 7.3), showing that the tibia has recovered fully during the rest period. This data is in agreement with that of Bayley, Sutton et al. (2012) who showed the cuticle's potential for absorption and release of energy when kicking and jumping. My results show this potential for the entire tibia, not just the specialised buckling region studied by Bayley.

Figure 7.4 shows that the loading and unloading curves differ considerably. On average, 49.7% less energy is required for unloading compared to loading. This indicates that approx. 50% of the energy applied to the tibia is actually absorbed during the test. The loading rate for these tests was 5 mm/min – slower than the actual locust jump by orders of magnitude. Each test took 12 seconds to deform the leg by 1mm, while the insect jump takes 20-30 msec to apply the same stress levels. Nonetheless, these tests show the tibia's ability for absorbing energy. This is effectively energy lost that cannot be used for jumping. Katz and Gosline (1992) showed that the substantial deflection in the hind leg observed when the locust jumps may account for 10% of the total kinetic energy of the jump. This suggests that the legs behave more like flexible springs instead of rigid levers. The ability of cuticle to absorb energy is also favourable in terms of its resilience for running insects such as cockroaches. Leg resilience has been shown to range up to 90% in terrestrial insects (Blickhan, 1986; Katz and Gosline, 1992; Sensenig and Shultz, 2003; Dudek and Full, 2006) – this could aid in absorbing energy (acting like a damper) while running, leading to a self-stabilizing effect when perturbed.

The “dead” cuticle is not as efficient at absorbing energy as the living – only absorbing 35.6% of the applied loading energy. It is possible that the dead cuticle has lost some of its elasticity post mortem. The exact mechanism at work here is unclear, but this is not an unusual phenomenon for a natural material.

Figure 7.2 shows that plastic deformation is present. As well as the reduction in stress to reach the same strains, the stress remains at zero on cycles 2 and 3 until a strain of 0.0025 is reached, as the tibia has lost contact with the testing machine due to plastic deformation. Plastic strain (deformation) accounts for 8.33% of the total applied strain. Jensen and Weis-Fogh (1962) noticed this plastic deformation visually and also its recovery once the material was left to rest. They theorised that as secondary bonds seem to be absent in the material, deformation that does not break any primary bonds should have no permanent effect. Cuticle is a viscoelastic material, which means the imposition of a stress results in an instantaneous elastic strain (true for all materials) which is followed by a time dependant viscous strain (which is a form of an-elasticity) (Callister, 2005). The rate of strain applied determines the response of the material. A higher applied strain rate would result in an apparently stiffer material, less energy absorption and less viscoelastic deformation. The strain rate (5 mm/min) used in these experiments is much slower than those experienced when jumping (Bayley, Sutton et al., 2012), so the plastic deformations observed (due to viscous strain), and the amount of energy absorption observed would be much less *in vivo*.

7.5.2 Stiffness

The stiffness of a material is a measure of how easily it deforms or deflects under a given stress. Figure 7.5 shows a sample of Young’s Modulus values for individual locusts during testing. The general pattern seems to be that the stiffness either decreases, or stays approximately the same (an insignificant increase is noted in some cases). The decrease is usually less significant between test 2 and test 3. Figure 7.7 (a) plots the averages of all these stiffness values. On average, there is a decrease in stiffness of 9.8% between test 1 and test 2, and a further reduction in stiffness of 4.3% between test 2 and test 3. It appears that applying a small number of high load cycles does

not stimulate the insect to make any significant changes to the stiffness of the cuticle material. One would assume that during natural locomotion, the tibiae of the locust could be cycled in a fashion similar to the tests carried out here. Bennet-Clark (1975) showed that the locust can only endure <20 jumps before a rest period is required. Small (<10) numbers of high load cycles can be endured on a regular basis so long as regular rest periods are also taken.

Figure 7.6 and Figure 7.7 (b) show that this recovery is absent for “dead” cuticle. On average, the decrease in stiffness between test 1 and test 2 is 24.5% for dead cuticle - more than double that of the corresponding value for living cuticle. Figure 7.6 shows that unlike the living cuticle samples, all “dead” samples showed a drop in stiffness between test 1 and test 2 (the exception being a slight increase for cycles 1 and 2 for Locust 2). These results suggest that the recovery of the cuticle is not purely due to the viscoelastic or time dependant properties of the material itself, but may be somehow regulated by the insect. It is possible that the cuticle experiences some micro-damage (in the form of tiny cracks in its fibres or protein matrix, or some delamination) when loaded. The insect may be actively repairing this damage. Lai-Fook (1968) and Johnson, Kaiser et al. (2011) have shown the ability of the insect to detect minor damage to its surface caused by abrasions. The response to this damage may be the release of substances from the hemolymph via the basement membrane, epidermis and pore canals to the injured area, often resulting in localised melanization at and adjacent to the damaged areas, or possibly a signal to catalyse or activate certain substances already present (but dormant) in the injured area. It is possible that this may be occurring at some small level internally due to micro-damage caused by the applied cyclic loads. This offers one explanation why the living material shows more pronounced recovery than the dead, and requires many further tests to confirm. Interestingly, the recovery is also present comparing test 2 and 3, between which there was only a 4 hour gap. The speed of this recovery is unknown. This would also be an interesting topic for future study.

7.5.3 Control Experiments

Both the cycled (left) and idle (right) tibiae were loaded to failure after the above tests were conducted. These showed no significant differences between the legs in failure strength or stiffness, confirming that the applied cyclic loads had little or no effect on the living cuticle tissue.

7.5.4 Applying a load increases the stiffness

An increase in stiffness between the first and second cycle is apparent in 83% of live tests (Figure 7.5) and over 50% of dead tests (Figure 7.6). This increase is statistically significant, averaging 12.5% of the original stiffness. This indicates that the material stiffens somewhat after initial loading. The material's fibre-matrix laminar structure offers an explanation for this. In the locust tibia, fibres are predominantly oriented parallel to the long axis (alternating with helicoidally arranged layers as outlined in Section 1.2). When stressed, fibres in off-axis layers or slightly misaligned fibres in 0° layers can reorient themselves slightly in the viscoelastic matrix to be parallel to the applied force (Harris, 2003). This realignment of fibres to best resist the applied stress can slightly increase the strength and stiffness of the material. When straining the locust tibia, plastic deformation was observed. This may be due to fibre and layer realignment, leading to a stronger, stiffer material. When left to rest, these fibres and layers return to their original position in the viscoelastic matrix, releasing any residual strains. The first cycle is the only one that leads to this increase in stiffness (see Figure 7.5), as this fibre realignment would only occur once and not incrementally for each cycle.

7.5.5 Hydration regulation mechanism of the locust is controlled centrally

Dirks and Taylor (2012a) showed in a previous study that desiccation or dehydration of a sample can lead to embrittlement of the material, essentially increasing its strength and stiffness, but lowering its toughness, and making it more vulnerable to crack propagation. When cementing the live tibia samples, it was important not to cement the knee-joint itself, as this was seen to cause a gradual but significant stiffening of the tibia cuticle over time. The harder Exocuticle is absent at joints such as this to allow articulation. The waxy water-resistant layer (Epicuticle) may also be

absent here, allowing absorption of fluid (or in this case, dental cement) into the joint. This shows that the hydration-regulation mechanism which is so important in maintaining homeostasis (constant material properties) for each region of the cuticle is centrally regulated, and can be interrupted if a barrier is introduced. Even a thin film of cement could cause significant damage upon hardening. Perhaps other mechanisms than hydration are also centrally regulated, such as those which enable the insect to regulate its material properties. This will require further study.

7.6 Conclusion

Living insect cuticle was seen to absorb 49.5% of the applied energy during loading; this caused deformation which, when left to rest, was seen to recover fully. This was expected, as the insect would endure countless such cycles (and rest periods) in a lifetime while jumping. Although residual deformation was observed during the cyclic tests, minimal changes in stiffness were observed in subsequent tests, suggesting that any damage caused had been recovered from. Control tests showed the cycled legs had strengths comparable to the idle (contralateral) legs, again suggesting no permanent damage had been caused by the cyclic loads. Cuticle *removed* from the insect absorbed much less (35.6%) of the energy applied during loading, and the recovery of its original stiffness was absent. The reduction in stiffness between test 1 and test 2 for dead cuticle averaged at 24.5% compared to 9.8% reduction for the living material. This implies that the recovery process is more than just a passive material phenomenon, and may be actively controlled by the insect in some way.

Conclusions

This work has focused on a single limb segment, the tibia, and how its mechanical properties can be influenced by several different factors.

Biomechanical factors seem to have influenced properties such as stiffness and geometry of insect legs between species and from one leg to another on a single insect. Insects are an extremely diverse group of animals, and various body parts are subjected to different applied forces during daily activities. It is logical that not all parts of the insect (and not all insect tibiae) need have the same stiffness and strength, but that these properties should be balanced against their specific day to day requirements (within a degree of safety). The insect leg must not only be able to endure countless cycles while running and walking without succumbing to a fatigue failure, but must also withstand higher loads due to more strenuous activities experienced such as righting, jumping and wedging (activities crucial for the insect's survival in emergency situations) without fracturing or yielding. During these strenuous activities, the insect tibia is operating at quite low factors of safety (2-4), implying that the leg is operating close to its structural limit. It appears to be slightly "over-designed" for running and walking, but this is necessary to avoid failure during emergencies. The form and material properties seem to have evolved in response to the mechanical functions of the same body part in different insects.

The failure strengths of these tibiae when tested in bending were found to depend on both material quality and geometry, implying that the failure mode was local buckling. The thin-walled tubular shape of the tibia and the bending stresses experienced *in vivo* make insect legs vulnerable to this type of failure (which is difficult to predict, as it happens at less than the material's yield strength).

The experimental failure strengths of tibiae of 5 different insect species loaded in bending, were matched closely by predictions made for buckling using both finite element analysis and empirical predictions from the literature. This allowed me to deduce that most were failing due to local elastic buckling. Stick insect tibiae examined had several longitudinal ridges, which the FEA analysis suggested would protect against buckling but these legs failed due to material yielding

before the predicted buckling strength could be reached. Bees displayed a triangular cross section which was just as effective at resisting a buckling failure as a circular tube with the same cross-sectional area. The accuracy of the FE approach suggests that similar analysis could be useful for investigating the buckling of thin-walled tubes with complex geometries and specialisations such as fins.

The growth of cuticle over the life of an adult insect, and its influence on the mechanical properties of the tibia was the next factor to be investigated. I found that in the first days and weeks post-moult, when the cuticle is mostly comprised of (supposedly stiff, strong) exocuticle, that the cuticle is relatively thin, quite weak, and not very stiff. The deposition of (supposedly much softer) endocuticle in the first three weeks occurs at quite a rapid pace ($1.8 \mu\text{m}/\text{day}$). This is accompanied by a dramatic rapid increase in strength, and in stiffness. The increase in strength is without doubt linked to the increase in thickness and stiffness in these formative weeks, as the mode of failure is one of local buckling (predictions for local buckling accurately match experimental values for thinner samples). As the cuticle grows, it transitions from being poorly equipped to resist buckling, to being “over equipped” – passing through an optimal slenderness ratio (radius/thickness) for resisting bending sometime between day 12 and 25. The increase in stiffness is not as straightforward to explain, as the addition of a softer material to a stiffer one should actually reduce the overall stiffness, but the opposite is observed. I concluded that the cuticle must undergo a sclerotization process (cross-linking of its proteins) gradually and continuously for the first three weeks post-moult. This was previously thought to stop after 3 days. This is currently being investigated by our research group.

Once the tibia cuticle reaches a certain thickness, the addition of new material slows down to negligible levels ($0.3 \mu\text{m}/\text{day}$), and remains at this “dormant” phase indefinitely. The failure strength and stiffness also plateau as the thickness stops increasing. These thicker legs fail due to a material yielding (fracture / buckling) which could not be avoided by adding more material. As the cuticle grows and matures, the safety factors will also fluctuate slightly, depending on both the strength of the tibia, and the forces applied. Safety factors calculated for the locust tibia range

from just above 1 to almost 6 over this time period. It is possible that the stimuli for these deposition rates may be linked to a sensory feedback system such as the campaniform sensilla (strain monitoring structures in the tibia), or indeed the straining of the epidermal cells – the cuticle depositors themselves. Whatever the trigger, an intelligent system seems to be at work. Rapid deposition requires large initial resource investment post-moult, but is necessary to increase the leg's buckling strength (and seemingly its stiffness). Once the optimum r/t value has been reached and buckling is no longer an issue, the deposition rate is permanently reduced, and strength and stiffness remain almost constant.

Cuticle deposition rates also feature significantly in the effectiveness of the wound healing response of an adult insect. Damage to the insect integument cannot be fully healed in adult insects. When an insect suffers an injury significant enough to breach its epidermis, a clot is formed to seal the area, this is melanised to fight off bacteria, after which the epidermis can migrate across it to restore epithelial continuity. Only after this can the epidermis begin to secrete new cuticle material under the wound to reinforce the area, and restore some structural stability. I found that this deposition accounts for a restoration of 66% of the original (uninjured) failure strength to the leg – double that of a similarly wounded leg experiencing no deposition. It also has a significant effect at preventing crack growth from the incision – increasing the fracture toughness of the leg from 4.12 MPa√m (for a freshly wounded leg) to an apparent fracture toughness of 7.01 MPa√m (much higher than the 3.07 MPa√m for wounded samples showing no repair). This is the first biomechanical study of injury repair in an arthropod.

I found that this deposition of new cuticle is specifically targeted to the injured area. The deposition rate here averaged 1.6 $\mu\text{m}/\text{day}$, implying that the injury may be responsible for the reawakening of the cuticle deposition rate seen immediately post moult. Deposition rates in all other areas of the tibia (even at the sides next to the injury) remained at the normal “dormant” rates of 0.4 $\mu\text{m}/\text{day}$. Several factors could be encouraging this fast deposition rate. It is possible that the activation of the epidermal cells (causing the migration across the wound, and observed up to 7 cell diameters from the wound) could also be a stimulus for these cells to quickly deposit

new cuticle. Whatever the cause, reinforcing only the area structurally weakened by injury is an effective strategy for the insect to ensure its survival while saving resource investment.

Having examined the insect response to major (or macro) damage, I wanted to perceive if the insect was responsive to micro or material level damage. For this, I carried out stress tests on living locust tibia cuticle. I found that the living material could absorb almost 50% of the applied energy during loading (compared to 35% for dead cuticle), and that although both suffered plastic deformation or softening during cyclic loading, the living cuticle recovered its original stiffness to a greater degree than the dead. Control tests showed that cycling one tibia had no permanent effect on its strength or stiffness compared to the other (contralateral) leg. This implies that the recovery process is more than just a passive material phenomenon, and may have an active biological component.

Future Work

This research has uncovered new information about the different factors that can influence the mechanical properties of insect cuticle. Many interesting opportunities for future work were also uncovered which were beyond the scope of this study. One such opportunity is that of staining the different layers of the tibia cuticle to determine the proportions of exocuticle and endocuticle present. Does the exocuticle grow over time? Does the endocuticle become more tanned as the insect ages? Such a study could be combined with my data on how the thickness, failure strength and stiffness change over time to shed light on the contributions of each of the constituent layers of the cuticle. Staining analysis could also reveal what exactly the new cuticle deposited underneath and adjacent to an injury is composed of. Does it differ significantly from the “normal” cuticle adjacent to the wound? Is it lamellate in nature at all? Is it more similar to exocuticle or endocuticle? The staining process may also shed light on the effect of wounding on “old” cuticle next to the wound. All of these studies could focus on the locust hind tibia, but it would be also interesting to perform some staining analysis on the other insect tibiae examined – the locust mid-leg, the American and Death’s Head cockroach hind-legs, and the stick insect and

bee legs. How do the proportions of exo and endocuticle compare in these legs to that of the locust hind-leg? This could reveal interesting statistics on the biomechanical influences of the geometry and quantities of these two layers.

Finite element analysis (FEA) proved very useful in predicting buckling strengths of tubular structures. Modelling the graded structure of the tibia cuticle could also provide valuable information on the contributions of the layers to the overall performance of the tibia. Modelling the tibia as a “soft tube within a stiff tube” could give insights into the complex stress and strain distributions at work in the tibia, and the advantages of having a graded structure over one composed of a single material. FEA could also help to shed more light on the effectiveness of the wound-healing response of applying a patch of new material to the inside of a cracked or fractured surface. Using the “Large Deflections” option made it possible to predict elastic local buckling in circular and non-circular tubes, and also tubes with specialisations such as fins. This technique could prove useful in analysing complex engineering structures that may be prone to local buckling failures.

Another interesting area is that of triggers or stimuli present in the insect tibia. I have shown two different cuticle deposition rates – the quicker one ($1.6 - 1.8 \mu\text{m} / \text{day}$) is present immediately after moulting (for approx. 20 days) and after injury (for approx. 10 days), but only in the injured area. The slower rate is observed elsewhere at all other times. If the post-moult injury deposition rate is due to induced strains in the cuticle (whether sensed by the campaniform sensilla or the epidermis), it may be possible to induce strains that exceed the norm by adding weights to the insect, or stimulating it to jump more often than normal. Also – does removing one hind-leg have a significant effect on the other (in terms of forces experienced during jumping, and hence on the material properties)?

Performing various types of injuries (puncture wound, longitudinal incision, excision, etc.) on locust tibiae may shed light on the extent and the range of new cuticle deposition that the insect is capable of, and also to examine the limits of its wound-healing capacity.

Although studies have been carried out on some mechanical properties of insect cuticle in the past, none have examined what effect factors such as applied biomechanical forces, growth and development, and induced injury can have upon these properties, and how they influence the safety factors or fitness of the insect. Insect cuticle continues to yield interesting results the more it is studied. A study such as this could be combined with others to assemble a complete picture of this material and its mechanical properties. Such information could prove useful when considering the mechanical behaviour of a cuticle-inspired bio-mimetic material in the future. Its many remarkable material properties such as high fracture toughness and low stiffness, high fatigue strength and low density would certainly be desirable for fields such as aerospace engineering. Chitin derivatives such as chitosan have been used in wound dressings, anticoagulation therapies, surgical sutures and scaffolds for tissue regeneration, drug delivery systems and as a bone substitute (in combination with calcium compounds to mimic crustacean cuticle) (Khor, 2001). Chitin is biocompatible and bioresorbable – two very desirable properties, when coupled with its mechanical assets may lead to it being a major player in the bioengineering industry in the future. Establishing the mechanical properties of insect cuticle and their potential influencers may contribute in some way to realising its potential as a widely used biomaterial.

Bio-inspired materials are increasingly used by engineers. Nature is generally considered to have the advantage of millions of years of evolution to optimize structures and material properties to suit their individual function. Many natural materials (cuticle, bone, antler, etc.) have a hierarchical structure. There may be nothing remarkable about the individual building blocks (e.g. chitin, collagen, keratin, cellulose etc.), but the manner in which they are arranged lend remarkable mechanical properties to the overall material. Even more impressive is that nature must operate within strict limitations when creating such materials. The constituent compounds that make up the material itself are limited to what the living organism can produce from what it takes in from its environment, and all materials must be formed at ambient temperatures.

As engineers drawing inspiration from such materials, we may wonder how far down the hierarchical chain is it necessary for us to go in order to effectively mimic natural materials and

achieve the desired mechanical properties? The limitations mentioned above do not apply to engineers, who can pick and choose elements, compounds and manufacturing processes to fine tune material and structural properties. This comparative simplicity is a great advantage for man-made materials. Nature creates materials the only way it can – from the bottom-up. Ours is more “top-down” approach. We are limited only by our technical expertise and our imagination. We can also apply such simplifications when analysing materials. In my studies I have not analysed the properties of individual chitin fibres, their orientation and proportions, or those of the proteins within insect cuticle, instead analysing the insect tibia as one single uniform material. I have shown that such a relatively simple approach can work, at least for cuticle. As such, cuticle-inspired biomaterials may not display any similarities in microstructure, but may be very similar in terms of the material properties which I have explored during this Ph.D.

References

- Alexander, D. E., Blodig, J. and Hsieh, S.-Y. (1995). Relationship between function and mechanical properties of the pleopods of isopod crustaceans. *Invertebrate Biology* **114**(No. 2): 169-179.
- Andersen, S. O. (2010). Insect cuticular sclerotization: a review. *Insect Biochemistry and Molecular Biology* **40**(3): 166-178.
- Andersen, S. O., Peter, M. G. and Roepstorff, P. (1996). Cuticular sclerotization in insects. *Comparative Biochemistry and Physiology* **113B**(4): 689-705.
- Barbakadze, N., Enders, S., Gorb, S. and Arzt, E. (2006). Local mechanical properties of the head articulation cuticle in the beetle *Pachnoda marginata* (Coleoptera, Scarabaeidae). *J Exp Biol* **209**(Pt 4): 722-730.
- Baron, R. and Kneissel, M. (2013). WNT signaling in bone homeostasis and disease: from human mutations to treatments. *Nature Medicine* **19**: 179-192.
- Barwig, B. (1985). Isolation and characterization of plasma coagulogen of the cockroach *Leucophaea maderae* (Blattaria). *Journal of Comparative Physiology* **155**: 135-143.
- Baxter, R. M., Dai, T., Kimball, J., Wang, E., M.R., H., Weismann, W. P., McCarthy, S. J. and Baker, S. M. (2013). Chitosan dressing promotes healing in third degree burns in mice: gene expression analysis shows biphasic effects for rapid tissue regeneration and decreased fibrotic signaling. *Journal of Biomedical Materials Research Part A* **101** (2): 340-348.
- Bayley, T. G., Sutton, G. P. and Burrows, M. (2012). A buckling region in locust hindlegs contains resilin and absorbs energy when jumping or kicking goes wrong. *Journal of Experimental Biology* **215**(Pt 7): 1151-1161.
- Belacortu, Y. and Paricio, N. (2011). *Drosophila* as a model of wound healing and tissue regeneration in vertebrates. *Developmental Dynamics* **240**(11): 2379-2404.
- Bennet-Clark, H. C. (1975). The energetics of the jump of the locust *Schistocerca gregaria*. *Journal of Experimental Biology* **63**: 53-83.
- Bergner, A., Muta, T., Iwanaga, S., Beisel, H. G., Delotto, R. and Bode, W. (1997). Horseshoe crab coagulogen is an invertebrate protein with a nerve growth factor-like domain. *Journal of Biological Chemistry* **378** (3-4): 283-287.
- Bernays, E. A. (1972). Changes in the first instar cuticle of *Schistocerca gregaria* before and associated with hatching. *Journal of Insect Physiology* **20**: 281-290.
- Blickhan, R. (1986). Stiffness of an arthropod leg joint. *Journal of Biomechanics* **19**: 375-384.
- Bohn, H. (1975). Growth-promoting effect of haemocytes on insect epidermis *in vitro*. *Journal of Insect Physiology* **21**: 1283-1293.
- Brazier, L. G. (1927). On the Flexure of Thin Cylindrical Shells and Other "Thin" Sections. *Proceedings of the Royal Society of London* **116**(104).
- Breugelmans, B., Van Soest, S., Van Hoef, V., Vanden Broek, J., Franssens, V. and Simonet, G. (2008). The role of hemocytes, serine protease inhibitors and pathogen-associated patterns in prophenoloxidase activation in the desert locust, *Shistocerca gregaria*. *Pathogens* **29**: 235-241.
- Bronzino, J. D. (2006). The Biomedical Engineering Handbook, *Taylor & Francis*.
- Broughton, G. and Rohrich, R. J. (2005). Wounds and Scars. *Selected Readings in Plastic Surgery* **10**(7): Part 1.
- Burns, M. D. (1973). The control of walking in orthoptera I: leg movements in normal walking. *Journal of Experimental Biology* **58**: 45-58.
- Burr, A. and Cheatham, J. (1995). Mechanical Design and Analysis, section 5.2, *Prentice-Hall*.
- Burr, D. B. (2000). Damage detection and behaviour in bone. *12th Conference of the European Society of Biomechanics., Dublin: Royal Academy of Medicine in Ireland*.
- Burr, D. B. and Martin, R. B. (1993). Calculating the probability that microcracks initiate resorption spaces. *Journal of Biomechanics* **26**: 613-616.
- Calladine, C. R. (1983). Theory of Shell Structures, *Cambridge University Press, Cambridge, UK*.

- Callister, W. D. (2005). *Fundamentals of Materials Science and Engineering: An Integrated Approach*, John Wiley and Sons Inc.
- Candy, D. J. and Kilby, B. A. (1962). Studies on chitin synthesis in the desert locust. *Journal of Experimental Biology* **39**: 129-140.
- Carolina Nature website- <http://www.carolinanature.com/trees/litu.html> - cited 24/09/2015
- Cavagna, G. A., Heglund, N. C. and Taylor, C. R. (1977). Mechanical work in terrestrial locomotion: two basic mechanisms for minimizing energy expenditure. *American Journal of Physiology* **233**: 243-261.
- Cavagna, G. A., Saibene, F. P. and Margaria, R. (1964). Mechanical work in running. *Journal of Applied Physiology* **19**: 249-256.
- Chapman, R. F. (2013). *The insects: structure and function*, Cambridge University Press.
- Charters, A. C., Neushul, M. and Barilotti, C. (1969). The functional morphology of *Eisenia arborea*. *International Seaweed Symposia* **6**: 89-105.
- Chen, B., Peng, X., Wang, J. G., Fan, J. and Wu, X. (2004). Investigation of fiber configurations of chafer cuticle by SEM, mechanical modeling and test of pullout forces. *Computational Materials Science* **30**(3-4): 511-516.
- Chen, B., Peng, X., Wang, W., Zhang, J. and Zhang, R. (2002). Research on the microstructure of insect cuticle and the strength of a biomimetic preformed hole composite. *Micron* **33**: 571-574.
- Currey, J. D. (2002). *Bones: Structure and Mechanics*. Princeton NJ, Princeton University Press.
- Daniel, O. I. I. M. (2006). *Engineering Mechanics of Composite Materials*, Oxford University Press.
- Daily Mail: Doctor pulls inch-long cockroach from man's ear after it burrowed in while he slept and he failed to suck it out with a vacuum cleaner (www.dailymail.co.uk)
- Delcomyn, F. (1971). The locomotion of the cockroach *Periplaneta Americana*. *Journal of Experimental Biology* **54**: 443-452.
- Dillaman, R. M. and Roer, R. D. (1980). Carapace Repair in the Green Crab, *Carcinus maenas*. *Journal of Morphology* **163**: 135-155.
- Dirks, J. H. and Durr, V. (2011). Biomechanics of the stick insect antenna: damping properties and structural correlates of the cuticle. *Journal of Mechanical Behavior of Biomedical Materials* **4**(8): 2031-2042.
- Dirks, J. H., Parle, E. and Taylor, D. (2013). Fatigue of insect cuticle. *Journal of Experimental Biology* **216**(Pt 10): 1924-1927.
- Dirks, J. H. and Taylor, D. (2012a). Fracture toughness of locust cuticle. *Journal of Experimental Biology* **215**(Pt 9): 1502-1508.
- Dirks, J. H. and Taylor, D. (2012b). Veins improve fracture toughness of insect wings. *PLoS One* **7**(8): e43411.
- Dudek, D. M. and Full, R. J. (2006). Passive mechanical properties of legs from running insects. *Journal of Experimental Biology* **209**: 1502-1515.
- Dunn, P. E. (1991). *Insect antibacterial proteins in Phylogenesis of Immune Function*, Plenum Press.
- Dushay, M. S. (2009). Insect hemolymph clotting. *Cellular and Molecular Life Sciences* **66**: 2643-2650.
- Enders, S., Barbakadse, N., Gorb, S. N. and E., A. (2004). Exploring biological surfaces by nanoindentation. *Journal of Materials Research* **19**: 880-887.
- Engineering_Toolbox_Website. (2015). "Engineering Toolbox Website." Elastic properties and modulus for some common materials, from www.engineeringtoolbox.com.
- Fabritius, H.-O., Sachs, C., Triguero, P. R. and Raabe, D. (2009). Influence of Structural Principles on the Mechanics of a Biological Fiber-Based Composite Material with Hierarchical Organization: The Exoskeleton of the Lobster *Homarus americanus*. *Advanced Materials* **21**(4): 391-400.
- Fernandez, J. G. and Ingber, D. E. (2012). Unexpected strength and toughness in chitosan-fibroin laminates inspired by insect cuticle. *Advanced Materials* **24**(4): 480-484.

- Fontaine, A. R., Olsen, N., Ring, R. A. and Singla, C. L. (1991). Cuticular metal hardening of mouthparts and claws of some forest insects of British Columbia. *Journal of the Entomological Society of British Columbia* **88**: 45-55.
- Full, R. J. and Ahn, A. N. (1995). Static forces and moments generated in the insect leg: comparison of a three-dimensional musculo-skeletal computer model with experimental measurements. *Journal of Experimental Biology* **198**: 1285-1298.
- Full, R. J., Blickhan, R. and Ting, L. H. (1991). Leg design in hexapedal runners. *Journal of Experimental Biology* **158**: 369-390.
- Full, R. J. and Tu, M. S. (1990). The mechanics of six-legged runners *Journal of Experimental Biology* **148**: 129-146.
- Full, R. J. and Tu, M. S. (1991). Mechanics of a rapid running insect: two-, four- and six legged locomotion. *Journal of Experimental Biology* **156**: 215-231.
- Full, R. J., Yamauchi, A. and Jindrich, D. L. (1995). Maximum single leg force production: cockroaches righting on photoelastic gelatin. *Journal of Experimental Biology* **198**: 2441-2452.
- Galko, M. J. and Krasnow, M. A. (2004). Cellular and genetic analysis of wound healing in *Drosophila* larvae. *PLoS Biology* **2**(8): E239.
- Geng, C. and Dunn, P. E. (1988). Hemostasis in larvae of *Manduca sexta*: Formation of a fibrous coagulum by hemolymph proteins. *Biochemical and Biophysical Research Communications* **155**: 1060-1065.
- Greenhalgh, D. G. (1998). The role of apoptosis in wound healing. *International Journal of Biochemistry and Cell Biology* **30**: 1019-1030.
- Harris, B. (2003). Fatigue in Composites, *Woodhead Publishing Ltd*.
- Hashin, Z., and Shtrickman, S. (1963). A variational approach to the theory of elastic behaviour of multiple materials. *Journal of the Mechanics and Physics of Solids*. **11**: 127-140
- Haslett, C. (1992). Resolution of acute inflammation and the role of apoptosis in the tissue fate of granulocytes. *Clinical Science (London)* **83**: 639-648.
- Heitler, W. J. (1977). The locust jump II: structural specializations of the metathoracic tibiae. *Journal of Experimental Biology* **67**: 29-36.
- Heitler, W. J. (2012). "How Grasshoppers Jump." (<https://www.st-andrews.ac.uk/~wjh/jumping/>)
- Hepburn, H. R. and Chandler, H. D. (1976). Material properties of arthropod cuticles: the arthroidal membranes. *Journal of Comparative Physiology* **109**: 177-198.
- Hepburn, H. R. and Joffe, I. (1974). Locust solid cuticle: a time sequence of mechanical properties. *Journal of Insect Physiology* **20**: 497-506.
- Hillerton, J. E. (1984). Biology of the Integument. Chapter 32: Cuticle mechanical properties, *Springer Verlag*.
- Hillerton, J. E., Reynolds, S. E. and Vincent, J. F. V. (1982). On the hardness of insect cuticle. *Journal of Experimental Biology* **96**: 45-52.
- Hinz, B. (2007). Formation and function of the myofibroblast during tissue repair. *Journal of Investigative Dermatology* **127**: 526-537.
- Jayaram, K., Springthorpe, D., Haldane, D., DiRocco, A., McKinley, S. and Full, R. (2013). Challenges of confined space locomotion - a case study using the American cockroach A1.42, 6 July. *Society of Experimental Biology Annual Meeting*. Valencia, Spain.
- Jensen, M. and Weis-Fogh, T. (1962). Biology and physics of locust flight v strength and elasticity of locust cuticle. *Philosophical Transactions of the Royal Society of London, Series B, Biological Sciences* **245**(721): 137-169.
- Johnson, R. A., Kaiser, A., Quinlan, M. and Sharp, W. (2011). Effect of cuticular abrasion and recovery on water loss rates in queens of the desert harvester ant *Messor pergandei*. *Journal of Experimental Biology* **214**(Pt 20): 3495-3506.
- Jones, H. H., Priest, J. D., Hayes, W. C., Tichenor, C. C. and Nagel, D. A. (1977). Humeral hypertrophy in response to exercise. *Journal of Bone and Joint Surgery* **59-A**: 204-208.
- Kaae, R. (2015). "Expert Witness / Entomology."(insectexpertphd.com)

- Katz, S. L. and Gosline, J. M. (1992). Ontogenetic scaling and mechanical behaviour of the tibiae of the African desert locust (*Schistocerca gregaria*). *Journal of Experimental Biology* **168**: 125-150.
- Katz, S. L. and Gosline, J. M. (1994). Scaling modulus as a degree of freedom in the design of locust legs 1. *Journal of Experimental Biology* **187**: 207-223.
- Ker, R. F. (1977). Some structural and mechanical properties of locust and beetle cuticle, Oxford University, UK.
- Khor, E. (2001). Chitin: Fulfilling a Biomaterials Promise, *Elsevier*.
- King, J. W., Brelsford, H. J. and Tullos, H. S. (1969). Analysis of the pitching arm of the professional baseball player. *Clinical Orthopaedics and Related Research* **67**: 116-123.
- Klocke, D. and Schmitz, H. (2011). Water as a major modulator of the mechanical properties of insect cuticle. *Acta Biomaterialia* **7**(7): 2935-2942.
- Koehl, M. A. R. (1977a). Effects of sea anemones on the flow forces they encounter. *Journal of Experimental Biology* **69**: 87-105.
- Koehl, M. A. R. (1977b). Mechanical organization of cantilever-like sessile organisms: sea anemones. *Journal of Experimental Biology* **69**: 127-142.
- Lackie, A. M. (1988). Haemocyte behaviour. *Advanced Insect Physiology* **21**: 85-178.
- Lai-Fook, J. (1966). The repair of wounds in the integument of insects. *Journal of Insect Physiology* **12**(2): 195-198.
- Lai-Fook, J. (1968). The fine structure of wound repair in an insect (*Rhodnius prolixus*). *Journal of Morphology* **124**(1): 37-77.
- Lai, S. C., Chen, C. C. and Hou, R. F. (2001). Electron microscopic observations on wound-healing in larvae of the mosquito *Armigeres subalbatus* (Diptera: Culicidae). *Journal of Medical Entomology* **38** (6): 836-843.
- Lee, T. C. and Taylor, D. (1999). Bone Remodelling: Should We Cry Wolff? . *Irish Journal of Medical Science* **168**(2): 102-105.
- Li, J., Chen, J. and Kirsner, R. (2007). Pathophysiology of acute wound healing. *Clinical Dermatology* **25**(1): 9-18.
- Locke, M. (1966). Cell interactions in the repair of wounds in an insect (*Rhodnius prolixus*). *Journal of Insect Physiology* **12**: 389-392.
- Marmaras, V. J., Charalambidis, N. D. and Zervas, C. G. (1996). Immune Response in Insects: The Role of Phenoloxidase in Defense Reactions in Relation to Melanization and Sclerotization *Archives of Insect Biochemistry and Physiology* **31**: 119-133.
- Martin, P. (1997). Wound healing—Aiming for perfect skin regeneration. *Science* **276**: 75-81.
- McCullough, E. L. (2014). Mechanical limits to maximum weapon size in a giant rhinoceros beetle. *Proceedings for the Royal Society Series B: Biological Sciences* **281**(1786).
- Moorehouse, J. E., Fosbrooke, I. H. M. and Kennedy, J. S. (1978). "Paradoxical driving" of walking activity in locusts. *Journal of Experimental Biology* **72**: 1-16.
- Mori, T. and Tanaka, K. (1973). Average stress in a matrix and average elastic energy of materials with misfitting inclusions. *Acta Metallurgica*. **21**: 571-574.
- Mortensen, A. (2006). Concise encyclopedia of composite materials, *Elsevier Science*.
- Muller, M., Olek, M., Giesrig, M. and Schmitz, H. (2008). Micromechanical properties of consecutive layers in specialized insect cuticle: the gula of *Pachnoda marginata* (Coleoptera, Scarabaeidae) and the infrared sensilla of *Melanophila acuminata* (Coleoptera, Buprestidae). *Journal of Experimental Biology* **211**: 2576-2583.
- Nakamura, S., Iwanaga, S., Harada, T. and Niwa, M. (1976). A clottable protein (coagulogen) from amoebocyte lysate of Japanese horseshoe crab (*Tachypleus tridentatus*). Its isolation and biochemical properties. *Journal of Biochemistry (Tokyo)* **80**: 1011-1021.
- NASA (1968). Buckling of thin-walled circular cylinders (NASA SP-8007). *NASA (USA)*.
- Neville, A. C. (1963). Daily growth layers for determining the age of grasshopper populations. *Oikos* **14**(Fasc. 1): 1-8.
- Neville, A. C. (1965). Chitin lamellogenesis in locust cuticle. *The Quarterly Journal of Microscopical Science* **106**(3): 269-286.

- Neville, A. C. (1983). Daily cuticular growth layers and the teneral stage in adult insects: A review. *Journal of Insect Physiology* **29**(3): 211-219.
- Palmer, R. A., Taylor, G. M. and Barton, A. (1999). Cuticle Strength and Size-Dependence of Safety Factors in Cancer Crab Claws. *The Biological Bulletin* **196**: 281-294.
- Parle, E. and Taylor, D. (2013). The self-healing properties of insect cuticle. *Journal of Postgraduate Research, Trinity College Dublin*. Volume XII, 90-111
- Pryor, M. G. M. (1940). On the hardening of the cuticle of insects. *Proceedings of the Royal Society B: Biological Sciences* **128**(852): 393-407.
- Rees, D. W. A. (1997). Basic Solid Mechanics.
- Reinhardt, L., Weihmann, T. and Blickhan, R. (2009). Dynamics and kinematics of ant locomotion: do wood ants climb on level surfaces? *Journal of Experimental Biology* **212**(Pt 15): 2426-2435.
- Reuss, A., (1929) Berechnung der Fliegengrenze von Mischkristallen auf Grund der Plastizitätsbedingung für Einkristalle. *Z. Angew. Journal of Applied Mathematics and Mechanics*. **9**: 49-58, .
- Roux, W. (1881). Der kempf der teile im organismus, *Engleman*.
- Rowley, A. F. and Ratcliffe, N. A. (1976). The granular cells of *Galleria mellonella* during clotting and phagocytic reactions in vitro. *Tissue and Cell* **8**: 437-446.
- Rowley, A. F. and Ratcliffe, N. A. (1978). A Histological Study of Wound Healing and Hemocyte Function in the Wax-moth *Galleria mellonella*. *Journal of Morphology* **157**(2): 181-199.
- Sabick, M. B., Torry, M. R., Kim, Y.-K. and Hawkins, R. J. (2004). Humeral torque in professional baseball pitchers. *American Journal of Sports Medicine* **32**: 892-898.
- Scherfer, C., Karlsson, C., Loseva, O., Bidla, G., Goto, A., Havemann, J., Dushay, M. S. and Theopold, U. (2004). Isolation and characterization of hemolymph clotting factors in *Drosophila melanogaster* by a pullout method. *Current Biology* **14**: 625-629.
- Schoberl, T. and Jager, I. L. (2006). Wet or dry hardness, stiffness and wear resistance of biological materials on the micron scale. *Advanced Engineering Materials* **8**: 1164-1169.
- Sensenig, A. T. and Shultz, J. W. (2003). Mechanics of cuticular elastic energy storage in leg joints lacking extensor muscles in arachnids. *Journal of Experimental Biology* **206**: 771-784.
- Sewell, M. T. (1955). Lipo-protein cells in the blood of *Carcinus maenas*, and their cycle of activity correlated with the moult. *The Quarterly Journal of Microscopical Science* **96**: 73-83.
- Singer, A. J. and Clark, R. A. (1999). Cutaneous wound healing. *New England Journal of Medicine* **341**: 738-746.
- Snodgrass, R. E. (2015). Insects, their ways and means of living, *Dover Publications*.
- Sun, J. Y., Tong, J. and Ma, Y. H. (2008). Nanomechanical behaviours of cuticle of three kinds of beetle. *Journal of Bionic Engineering* **5**: 152-157.
- Sutton, G. P. and Burrows, M. (2008). The mechanics of elevation control in locust jumping. *J Comparative Physiology A: Neuroethology, Sensory, Neural and Behavioural Physiology* **194**(6): 557-563.
- Takahashi, Y. (2002). Evaluation of leak before break assessment. *International Journal of Pressure Vessels and Piping* **79**: 385-392.
- Taylor, D. (2011). What we can't learn from nature. *Materials Science and Engineering: C* **31**: 1160-1163.
- Taylor, D. and Dirks, J. H. (2012). Shape optimization in exoskeletons and endoskeletons: a biomechanics analysis. *Journal for the Royal Society Interface* **9**(77): 3480-3489.
- Taylor, D., Hazenberg, J. G. and Lee, T. C. (2007). Living with Cracks: Damage and Repair in Human Bone. *Nature Materials* **2**: 263-268.
- Taylor, D. and Lee, T. C. (2003). Microdamage and mechanical behaviour: predicting failure and remodelling in compact bone. *Journal of Anatomy* **203** (2): 203-211.
- Taylor, G. M., Palmer, A. R. and Barton, A. C. (2000). Variation in safety factors of claws within and among six species of Cancer crabs (*Decapoda: Brachyura*). *Biological Journal of the Linnean Society* **70**: 37-62.

- Telewski, F. W. and Jaffe, M. J. (1986). Thigmomorphogenesis: field and laboratory studies of *Abies fraseri* in response to wind or mechanical perturbation. *Physiologia Plantarum* **66**: 211-218.
- Timoshenko, S. and Gere, J. M. (1961). Theory of Elastic Stability, *New York*.
- Tychsen, P. H. and Vincent, J. F. V. (1976). Correlated changes in mechanical properties of the intersegmental membrane and bonding between proteins in the female adult locust. *Journal of Insect Physiology* **22**: 115-125.
- Vincent, J. F. and Wegst, U. G. (2004). Design and mechanical properties of insect cuticle. *Arthropod Structural Development* **33**(3): 187-199.
- Vincent, J. F. V. (1980). Insect cuticle: a paradigm for natural composites. *The Mechanical Properties of Biological Materials, 34th Symposium for the Society for Experimental Biology*: 183-210.
- Vincent, J. F. V. (2009). If it's Tanned it Must be Dry: A Critique. *The Journal of Adhesion* **85**(11): 755-769.
- Vincent, J. F. V. and Hillerton, J. E. (1979). The tanning of insect cuticle - a critical review and a revised mechanism. *Journal of Insect Physiology* **25**: 653-658.
- Voigt, W. (1928). *Lerhbuch der Kristallphysik*. Leipzig Teubner.
- Wadee, M. K., Wadee, M. A., Bassom, A. P. and Aigner, A. (2006). Longitudinally inhomogeneous deformation patterns in isotropic tubes under pure bending. *Proceedings of the Royal Society A* **462**(2067): 817-838.
- Wainwright, S. A., Biggs, W. D., Currey, J. D. and Gosline, J. M. (1976). Mechanical design in organisms, *Arnold, London*.
- Wegst, U. G. K. and Ashby, M. F. (2007). The structural efficiency of orthotropic stalks, stems and tubes. *Journal of Materials Science* **42**: 9005-9014.
- Weinreb, M., Rodan, G. A. and Thompson, D. D. (1989). Osteopenia in the immobilised rat hind limb is associated with increased bone resorption and decreased bone formation. *Bone* **10**: 187-194.
- Weis-Fogh, T. (1952). Fat combustion and metabolic rate of flying desert locusts *Philosophical Transactions of the Royal Society* **237B**: 1-36.
- Whalen, R. T., Carter, D. R. and Steele, C. R. (1988). Influence of physical activity on the regulation of bone density. *Journal of Biomechanics* **21**: 825-837.
- Wigglesworth, V. B. (1937). Wound healing in an insect (*Rhodnius prolixus hemiptera*). *London School of Hygiene & Medicine*.
- Wolff, J. (1870). Über die innere Architectur der Knochen und ihre Bedeutung für die Frange vom Knochenwachstum. *Virchow's Archiv* **50**: 389-450.
- Wolff, J. (1892). Das Gesetz der Transformation der Knochen.
- Wright, T. R. (1987). The genetics of biogenic amine metabolism, sclerotization, and melanization in *Drosophila melanogaster*. *Advances in Genetics* **24**: 127-222.
- Young, W. C. (1989). *Roark's Formulas for Stress and Strain, International Edition*, , *McGraw-Hill Book Company*.